EPSM 2004

REGIONAL HEALTHCARE TECHNOLOGIES
OVERCOMING THE TYRANNY OF DISTANCE
14 – 18 November 2004
Deakin University Waterfront Campus
Geelong, Victoria, Australia

Proceedings

The abstracts of all papers and posters presented at this year's Engineering and Physical Sciences in Medicine conference are published in the following pages.

The abstracts published here are intended to be exactly as printed in the conference handbook, though there may be minor editorial changes due to the different formatting requirements.

The full papers submitted with the presentations will be published in this and forthcoming issues. All conference presenters are encouraged to submit a paper to the journal for publication.

Conference Prize Winners

Engineers Australia Young Biomedical Engineers Award — **Govinda Poudel**
G.R. Poudel and H.T. Nguyen, *Bioimpedance Spectrometer for Tissue Impedance Analysis*

Varian Prize (Radiation Oncology) — **Kristie Harrison**
K. Harrison, S. Rolton, D. Cornes, J. Denham, M. Ebert, S. Howlett and C. Hamilton, *Elvis the Pelvis: A Purpose Built Anthropomorphic Phantom for an Australasian Level III Dosimetry Intercomparison*

CMS Poster Prize — **Tom Deans**
T. Deans and B. McKernan, *A Novel System for the Production of Immobilisation Face Masks for Radiotherapy*

IOP Publishing Student Poster Prize — **Ivan Williams**
I. Williams, R. Lewis, J. Whitely, et al, *The First Synchrotron Images of Tamar Wallaby Lungs*

Thank you to all presenters at EPSM 2004 and congratulations to all prize winners.

Rhonda Brown
EPSM 2004 Convenor:

Abstracts of the plenary sessions

REGIONAL HEALTHCARE TECHNOLOGIES FORUM

FROM PEDAL RADIOS TO SATELLITES: TECHNOLOGICAL TRANSFORMATIONS WITHIN THE ROYAL FLYING DOCTOR SERVICE

Peter R. Kronborg

Vice President, National Council of Australia, Royal Flying Doctor Service, Melbourne, Victoria, Australia

The Royal Flying Doctor Service (RFDS) was established at Cloncurry in Queensland by the Reverend John Flynn, and has been providing aero-medical and health services for over 75 years. The RFDS began operations with a single plane, a De Havilland DH50 aircraft chartered from the Queensland and Northern Territory Aerial Service, (Qantas). The aircraft was a single engine, fabric covered, cabin bi-plane capable of carrying a pilot and four passengers at a cruising speed of just under 80 miles per hour.

Although the tyranny of distance was slowly being overcome, one of the greatest problems faced by the Service was the lack of an extensive communications network. Early pedal radios became the initial backbone of the service. Unfortunately, problems associated with primitive 'technologies', or the lack of any, resulted in many unnecessary deaths.

With the development of advanced technologies, including 'sat' phones, the internet, and other hi-tech medical equipment on the planes, at the bases, and in the hands of the doctors and nurses, engineers and patients, the Service has progressively been able to deliver better quality health services. Interestingly, whereas a few years ago, all calls for medical assistance were received by radio, this form now accounts for only about 2% of all such calls. Despite these developments, technology continues to be the vital issue for both the patient and the RFDS.

Today, the Service has grown to become the largest dedicated aero medical, non-military fleet in the world. With over 40 aircraft spanning the nation, the RFDS services rural and remote locations from Tasmania to Cape York, Lizard Island to Christmas Island and the largest driest island continent in between.

In this keynote address, the RFDS National Vice President traces the advancements in technology throughout the Service's existence. He outlines the challenges and certain new and emerging developments in technology and telecommunications that will ensure that the RFDS continues to deliver exemplary medical health services to patients in some of the remotest places in Australia.

STATE GOVERNMENT DIRECTIONS & INNOVATIONS IN REGIONAL AND RURAL HEALTHCARE

Matt Viney

Parliamentary Secretary, Innovation and Industry, State Government of Victoria, Vic, Australia

Government has a key role to play in ensuring the health system responds to new challenges - today and into the future. That way all Victorians can reap the economic and health benefits that flow from an innovative healthcare system. The talk will examine these challenges, technology take-up, small technologies and medical devices, infrastructure integration, ICT connectivity, and the roll-out of Government programs in rural and regional areas.

KNOWING THE LIMITATIONS OF INTERNET TECHNOLOGIES

Grenville Armitage

Director, Centre for Advanced Internet Architectures, Swinburne University of Technology, Hawthorn, Vic, Australia

Various technologies underpin what we know today as "the Internet", some of them fixed (like ADSL or Cable Modems or dial-up) and others wireless (such as cellular modems and 802.11 wireless LANs). The use of Internet-based tools for document delivery is becoming an attractive proposition for de-centralised health-care service providers. However, before you roll out service it is wise to understand the security and performance limitations of the technologies your Internet service runs over. This talk will reflect on the other side of the hype - a realistic appraisal of where some of these technologies shine and where they fade.

BACK TO BASICS – MEDICAL EQUIPMENT MANAGEMENT IN A DEVELOPING COUNTRY

David A.W. Smith

PNG HSSP Pty. Ltd., Port Moresby, Papua New Guinea

THE CONTRASTS: Medical equipment is now so much a part of clinical practice that it appears there was never a time when it was not. If you have visited your GP lately, chances are your history is displayed on his PC screen in front of you. You may be diagnosed and treated on the spot or given a referral to a specialist physician who will have access to advanced technology which may assist you to return to full health. In the Emergency Department, Alotau Hospital, Milne Bay Province, Papua New Guinea, there are no computers, little in the way of technology and a minimal referral process.

THE GROWTH OF TECHNOLOGY IN DEVELOPING COUNTRIES: The introduction of medical technology into medicine is dictated by the human element – the doctors with their brochure or the community with their donation, unlike other areas of technology which through its development, change the way humans work and live[1]. It is the embrace of technology by developed countries which produces the flow-on into developing countries who may not be able to meet the whole of life costs that the technology brings[2].

THE PROBLEMS: We examine the situation of the provincial hospitals in Papua New Guinea and compare this with the difficulties which are experienced by health facilities in remote areas. The supply and cost of spare parts are typical problems of the hospitals. Maintenance providers in the local area offer little support to a health facility due to the specialised nature of medical equipment. Often the support is misdirected or woefully inadequate.

THE SOLUTIONS: The solutions to the problems of medical equipment management must be simple and cost neutral as there will be little in the way of funds left after the hospital staff are paid. Improved communication between the remote location and the nearest technical resource is required to give the staff of the hospital some chance of managing the technology. This assumes that the clinical and other users are trained in the equipment's care and operation. Training is an important resource in achieving successful medical equipment management. Communication is also important to convey the needs of users to donors, before the volunteers pack the containers of surplus equipment for shipment around the country. If the hospital is unable to support the technology that it has, the only practical solution is to reduce the reliance on the technology by reducing the inventory[3]. A harsh move but it achieves immediate relief, particularly if the equipment is a heavy consumer of disposables. The solution to the problem of medical equipment management is – Management. Good management with a comprehensive overview of the state of affairs in the health facility is the tool that clinical engineers and technologists can wield to successfully bring about a change for the better.

REFERENCES:

[1]K. Taylor, M. Frize, N. Iverson., C Paponnet-Cantat, http://www.sce.carleton.ca/faculty/frize/devcount.htm, 2001.
[2]3rd IEE Seminar on " Appropriate Medical Technology for Developing Countries ", IEE London, 2004.
[3]Medical Equipment Management Project, IDP Education Australia Ltd, 2003.

RIVERINA CANCER CARE CENTRE – "A DREAM COMES TRUE" SUCCESS AGAINST THE ODDS

Joe Schipp

Riverina Cancer Care Community Trust, Wagga Wagga, NSW, Australia

With phenomenal generosity communities throughout the wider Riverina and South West Slopes of New South Wales we now have our own privately operated regional Cancer Care Centre located in Wagga Wagga – the State's first and only rurally based Cancer Clinic established without one cent of State or Federal Government capital support.

The key to establishment of this state-of-the-art specialised medical service was the determined and resourceful partnership which developed between dedicated doctors, known locally as "The St Vincent's Doctors Group (now Riverina Cancer Care Pty Ltd), Calvary – Little Company of Mary (LCM) Hospital and an extremely generous and resolute "bush community". Remove any component of this partnership and the battle against bureaucratic obstinacy and political indifference would have been lost.

In 1994 the "St Vincent's" doctors advanced a proposal to self-fund "sister cancer clinics", with resource sharing, operating in Wagga Wagga and Albury/Wodonga. Despite protracted lobbying and negotiations at both State and Federal political levels the plan appeared to be scuttled when during the 1998 federal election campaign, Health Minister Michael Wooldridge "out of the blue" announced approval for a cancer clinic to be located in Wodonga (Vic).

In essence the shock of this announcement ignited community anger sufficient to motivate the proponents to re-energise, re-group and convene a hugely successful public meeting held on 18 August, 1999.

Two and a half years on community fund-raising had built, fitted out and furnished ($4m) Riverina Cancer Care Centre, equipped by RCC Pty Ltd doctors ($6.5m) on land provided by LCM adjacent to Calvary Hospital. Additionally a 20 unit cancer patient accommodation lodge ($2.7m) has been built in joint venture between the local community, Cancer Council of NSW and CPAS (Cancer Patients Assistance Society).

Observations to be explored
- Battling medico/bureaucratic bunker mentality
- "State owned" ideological hurdles
- City Centric political indifference
- People Power properly marshalled creates an irresistible force
- Rising above the ruck to achieve the important goals we set ourselves.

THE "VARIAN" KEYNOTE

(Sponsorship from Varian Medical Systems Australasia)

THE ASI-BASED EPID FOR ROUTINE ABSOLUTE DOSIMETRIC PRE-TREATMENT VERIFICATION OF DYNAMIC IMRT FIELDS

A. Van Esch and D. Huyskens

7Sigma, qA-team in Radiotherapy Physics

INTRODUCTION: In parallel with the increased use of intensity modulated radiation treatment (IMRT) fields in radiation therapy, flat panel amorphous Silicon (aSi) detectors are becoming the standard for online portal imaging at the linear accelerator. If IMRT is to become widely available without compromising on the quality of the IMRT plan and/or delivery, the workload related to the quality assurance of the IMRT fields must be minimised. We have therefore explored the possibility of using a commercially available aSi portal imager for absolute dosimetric verification of the delivery of dynamic IMRT fields.
METHODS: We investigated the basic dosimetric characteristics of an aSi portal imager (aS500, Varian Medical Systems), using an acquisition mode especially developed for portal dose integration during delivery of a - static or dynamic - radiation field. Measurements were performed to assess the detector saturation, linearity, memory effects and reproducibility. The field size dependence of the detector signal as well as its behaviour as a function of build-up thickness was measured for 6MV as well as 18 MV photon beams. Taking the measured characteristics into account, the dose calculation algorithm of a commercially available treatment planning system (Cadplan, Varian Medical Systems) was modified to allow prediction of the portal dose image, i.e. to compare the intended fluence distribution with the fluence distribution as actually delivered by the dynamic multileaf collimator. In order to reduce the workload connected to pre-treatment QA to a minimum, we have focussed on absolute rather than relative dose distributions, hence eliminating the need for supplementary point dose measurements. The portal dose image prediction was compared to the corresponding acquisition for several clinical IMRT fields by means of the gamma evaluation method.
RESULTS: The acquisition mode is accurate in integrating all portal doses over a wide range of monitor units, provided detector saturation is avoided. Although the dose deposition behaviour in the portal image detector is not equivalent to the dose to water measurements, it is reproducible and self-consistent, lending itself to quality assurance measurements. Gamma evaluations of the predicted versus measured portal dose distribution were within the predefined acceptance criteria for all clinical IMRT fields, i.e. allowing a dose difference of 3 % of the local field dose in combination with a distance to agreement of 3 mm.
DISCUSSION & CONCLUSIONS: Once the TPS IMRT modules have been accurately commissioned, the portal imager allows fast and easy quality assurance of individual imrt field fluences in clinical routine, reducing the time required for QA to the time needed for the actual field delivery and 5 to 10 additional minutes for data evaluation.

THE "PHILIPS" KEYNOTE

(Sponsorship from Philips Medical Systems Australasia)

TURNING THE CORNER: TOWARD AFFORDABLE TELEHEALTH IN ALASKA AND NORTHWEST USA

D. A. Lodge

Logi-Teq Consulting, Longview, WA, USA

ABSTRACT: The theoretical and practical benefits of telemedicine and telehealth technologies have long been understood and appreciated. Yet, state-of-the-art telehealth has often proven too expensive in implementation and operation or too limited in performance and functionality for adoption as a standard-of-care. To date, telehealth has been recognized as the

exception, and not the rule. Within the past decade in Alaska and Northwest USA, large government and business investments enabled development of significant regional telehealth capacity and infrastructure. New tools and technologies were formally evaluated for clinical utility within extreme environments, and linking vast distances. Standardized applications, distributed databases, redundant image archives, and fast wide-area intranet-based solutions demonstrated their practical telehealth potential. These significant capital investments created "foundations" in infrastructure upon which ***affordable*** telehealth is now "built." The author will present specific examples of how multimillion-dollar investments in telemedicine, teleradiology, and enterprise-level RIS/PACS network technologies over the past decade have enabled powerful economies-of-scale, making ***affordable*** telehealth a reality for healthcare providers. In the face of improved infrastructure, inter-organizational collaboration, creative marketing, and the continued free-fall in pricing and availability of modular, off-the-shelf hardware and software, health systems, hospitals, and physician practices are currently scrambling to embrace and participate in the location-independent, telehealth paradigm. Standardized, plug-and-play telehealth technologies have found market acceptance, and are proliferating rapidly. The minimum amount of per-site capital required to participate in telehealth has dropped significantly. Operational costs and image archive costs are falling as well. Implementing telehealth across large healthcare enterprises and connecting it up with "the last mile" (reaching the most isolated of remote healthcare providers) has never been easier or less expensive. It now appears that we are TURNING THE CORNER from embracing telehealth as state-of-the-art, to adopting it as a standard-of-care.

Figure 1. *Telemedicine Workstation.*

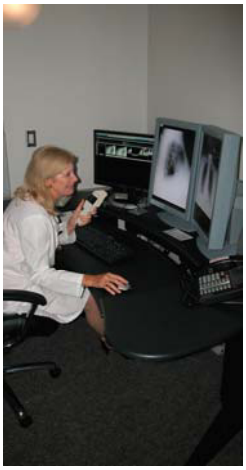

Figure 2. *RIS/PACS Workstation.*

KEYNOTE 2

REMOTE REAL-TIME EDUCATION FOR MEDICAL PHYSICS USING THE INTERNET

K-H. Ng[1] and M. Woo[2]

[1]*University of Malaya, Department of Radiology, Kuala Lumpur, Malaysia*
[2]*University of Toronto, Department of Medical Biophysics and Department of Radiation Oncology, and Sunnybrook and Women's Health Science Centre, Toronto, Ontario, Canada*

Medical Physics is a relatively small community but it spans great geographical distances, usually with a scarcity of experts whose expertise could greatly benefit students entering into the field. In addition to training, the constantly evolving field of Medical Physics with its many emerging advanced techniques and technologies require constant continuing education as well as consultation with experts.

Many continuing education courses and workshops are constantly being offered, including many web-based study courses and virtual libraries. However, one mode of education and communication that has not been widely used is the real-time interactive process. Web-based conferencing systems do exist, but these usually require a substantial amount of effort and cost to set up.

We had developed a simple-to-use, widely-accessible, and cost-effective method to allow real-time interactive education and consultation, using the World Wide Web [1-2]. The collaboration between the Department of Medical Physics at the Toronto-Sunnybrook Regional Cancer Centre in Canada and the Department of Radiology at the University of Malaya in Malaysia in using this system has been ongoing for two years. A class of Medical Physics graduate students at the University of Malaya attended lectures provided by lecturers in Toronto, using the Internet as the main tool of communication. Various topics including traditional classroom lectures as well as hands-on workshops were also delivered.

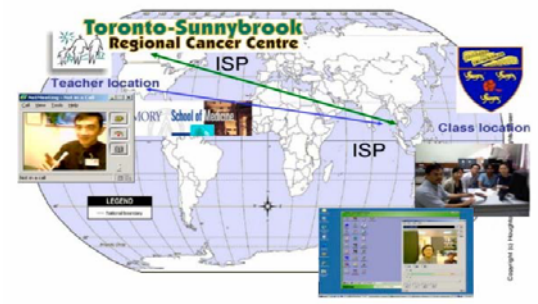

The development of the process is continuing, with connections and trials to other users in several countries. One of the features being explored is to assign different lecturers at different areas to deliver lectures. Another feature is to establish a system similar to web-conferencing, but with a much easier set-up and wider accessibility.
The concept of real-time interactive remote education is viable and holds promise for providing economical and practical tele-education to the Medical Physics community, but it depends heavily on the availability of the Internet in a lot of developing countries.

Figure 1. *Remote Real-Time Education System.*

REFERENCES:

[1]M. Woo and K-H. Ng., *A* Model for Online Interactive Remote Education for Medical Physics Using the Internet J Med Internet Res., March, 31; 5(1):e3. http://www.jmir.org/2003/1/e3/index.htm, 2003.
[2]Remote Real-Time Learning Web Site http://members.rogers.com/rrtl/index.htm

KEYNOTE 3

(Speaker support from Crazy John's)

VENTRICULAR ASSIST DEVICES AND THE ARTIFICIAL HEART: THE LATEST NEWS

D. Esmore

Surgical Head & Unit Head of Heart & Lung Transplant Services, The Alfred Hospital, Melbourne, Vic, Australia

The development of a reliable cardiac replacement remains at the forefront of biomedical engineering challenges. Recent trends have been towards the development of left ventricular assist systems(LVAS) rather than a total artificial heart per se, with some 30 devices currently under development worldwide. Funding trends have moved from government based to the venture capital/public sector resources with a move towards profit driven development.
The three main R&D trends are as follows:

1) Continued refinement of the more conventional first generation volume displacement devices,
2) Further development of the smaller 2nd generation axial flow, left ventricular assist devices and
3) The evolution of third generation "bearingless" centrifugal pump systems.

Currently some 1500 ventricular assist devices are implanted around the world each year, the majority of these being what is termed the "bridge" to transplantation application, the latter resulting in a 60% successful transplantation rate. The application where the greatest need indeed resides, is so called "destination therapy" for the ageing Class1V CHF population for whom transplantation is not an option. Market projections suggest 100,000 to 150,000 patients worldwide per annum would benefit from implantation of a LVAS as destination therapy. A 'forgettable' destination therapy LVAS would demonstrate inherent reliability, avoiding the serious adverse advents that have plagued previous devices, namely pump thrombosis, thromboembolism, mechanical failure and infection. A 5 year device life is the engineering standard .
The Australian designed and produced Ventra-Assist LVAS is one of very few third generation devices currently under clinical trial. Early results have proven promising with three destination therapy patients surviving 16, 11 and 9 months in NYHA Functional Class I to II. A further patient has recently been successfully bridged to cardiac transplantation. An international pivotal trial is planned in the latter half of 2004 towards achieving a CE mark and subsequent FDA approval.
If current projections are correct, the availability of a forgettable LVAS would see some 1000 implants performed annually in Australia, the impact of which will be discussed.

THE VentrAssist™ LEFT VENTRICULAR ASSIST DEVICE

J. Woodard

Business Development and Clinical Director, Ventracor Ltd, Sydney, NSW, Australia

INTRODUCTION TO THE VentrAssist™ LVAS: The VentrAssist™ Left Ventricular Assist System (LVAS) incorporates a "third generation" centrifugal pump featuring hydrodynamic suspension of an 'open-flow' rotor (Fig. 1).
Thrombosis risk has been minimized by the use of diamond-like carbon coatings on the blood contacting surfaces of the pump and the blood flow path has been designed to ensure all areas within the pump receive full flow. This ensures that there are no areas of stasis or backflow. Connection to the left ventricular apex is made using a silicone cannula with a bell-

shaped inflow and the pump outflow is connected to the ascending aorta via a 10mm reinforced Vascutek Gelweave™ gelatin-impregnated polyester graft. The pump is implanted in a subdiaphragmatic pocket (Fig. 2). Two externally-worn batteries and a controller provide power to the implanted pump via a thin percutaneous lead (Fig 3). The batteries and controller are worn in a backpack that can also be configured as a shoulder bag.

PILOT TRIAL DESIGN AND OBJECTIVES: The pilot trial provides left ventricular assistance for up to 10 patients with end stage heart failure. The trial is a sequential non-randomized design used to establish confidence in the safety of the system prior to initiation of multicentre trials. The trial has concluded at the Alfred Hospital, Melbourne. Both destination and "niche" bridge-to-transplant (BTT) indications have been included.

OUTCOMES:

- 9 patients implanted (4 deaths)
- 2 of the 4 destination patients are long-term survivors (at home 17 mo. 11mo., NYHA II)
- 3 of the 4 bridge patients are awaiting transplant
- No device failures
- One bleeding episode (2 take backs)
- No device related thrombus
- Negligible hemolysis
- Minimal infections
- Functional improvement
- Improved quality of life
- Minimal levels of anticoagulation are currently being employed: INR of 2 – 2.5 and aspirin 100 mg/day

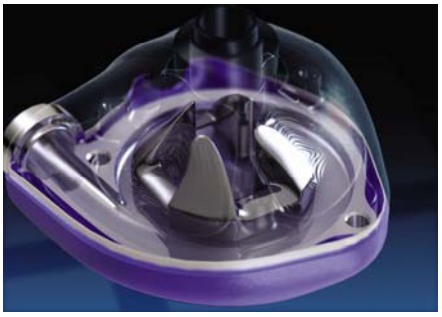

Figure 1.

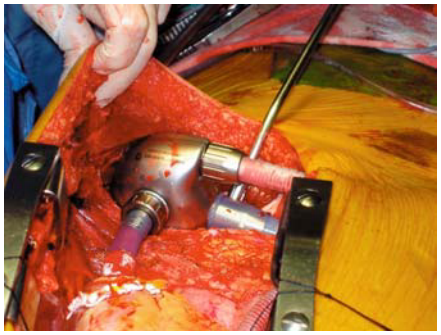

Figure 2.

Figure 3.

NOVEL TECHNIQUES

(Speaker support from Victorian Department of Innovation, Industry and Regional Development)

BIOPHOTONICS: A BRIDGE BETWEEN PHOTONICS AND LIFE SCIENCES

Min Gu

Centre for Micro-Phonics, Faculty of Engineering and Industrial Sciences, Swinburne University of Technology, Hawthorn, Vic, Australia

In last century the invention of lasers has revolutionised the optical sciences. Lasers have opened up numerous opportunities for photonics, information technology and biomedical sciences. Today a new frontier of photonics, biophotonics, is opening a horizon to a new generation of non-invasive and cost-effective biomedical technologies that have a significant impact on healthcare. Biophotonics represents a new fusion of photonics and biomedical sciences, contributing to the growth of novel devices for the early detection of diseases and new modalities of light-guided and light-activated therapies [1]. The concept of biophotonics will be illustrated by a spectrum of applications with detailed examples concentrating on optical microscopy in life sciences, laser tweezers and photonic crystals for biosensing.

Laser scanning microscopy is a basic approach for optical bioimaging, which allows multidimensional image and applications to a broad range of live biological species. The power of modern microscopy lies in its ability to collect images in optical sections with enhanced spectral accessibility from biological specimens [2]. Discussion will include confocal microscopy, two-photon fluorescence microscopy, fluorescence resonance energy transfer, fluorescence lifetime imaging microscopy, and second harmonic generation microscopy. Nonlinear fibre-optic endoscopy utilizing two-photon

fluorescence and second harmonic generation and aiming to achieve optical biopsy for cancer diagnosis will also be presented.
Focused laser beams can be used as laser tweezers designed to trap, micromanipulate and diagnose biological specimens. Basic principles and techniques used for single photon and two-photon laser trapping will be explained. Two-photon fluorescence excitation of morphology dependent resonance effects can provide sensitivity and multimodality because of its highly localized nature. Near-field trapping based on total internal reflection is a new technology in this area.
Introduced a few years ago, photonic crystals are now being used in sensing. Photonic-bandgap devices are sensitive to PH level, glucose concentration, and ionic strength. The photonic crystal can be important in bio-hazardous material identification.

REFERENCES:

[1]P. N. Prasad., *Introduction to biophotonics.*, John Wiley & Sons New Jersey, 2003.
[2]M. Gu., *Principles of Three-Dimensional Imaging in Confocal Microscopes,* World Scientific Singapore, 1996.

VIRTUAL REALITY SURGICAL SIMULATOR (VRSS). A VIRTUAL REALITY-BASED ENDOSCOPIC SURGERY SIMULATOR FOR TRAINING ENDOSCOPIC SURGEONS. THE TECHNOLOGY

Ian T. H. Brown

Director, Centre for Biomedical Engineering, Monash University, Clayton, Vic, Australia

This system is to be designed for virtual reality simulation of endoscopic surgical procedures. It allows the user to wield actual surgical tools and manipulate them as if performing surgical procedures. The aim is to create virtual reality simulation of medical procedures that both look and feel like the actual surgery or procedure. The system consists of a workstation and high-resolution visual display, simulation software to produce a gynaecological virtual environment, haprascopic instruments and a haptia interface. The main novel aspects of this system are the virtual gynaecological environment including realistic virtual resistance forces and the integration of video for realistic scenario introduction.
The research team have engaged in a project to develop a virtual reality based obstetric and gynaecological surgery simulator for training obstetric and gynaecological surgeons in complex key-hole surgical procedures.
The essential elements of the system are:

- A set of rigid endoscopic instruments
- A multichannel rigid endoscopic movement transducer system
- A computer with graphics software and high definition monitor
- A virtual 3D Gynaecology field
- Video integration using video on demand (Monash based technology)
- Systems design and integration
- Development of tactile sensory haptics
- Development of dynamic virtual field (objects that move when contacted)
- Scenario Programs

In the presentation Associate Professor Brown will discuss:

1. System requirements
2. The decomposition of this complex system into do-able tasks.
3. Visual graphics tasks
4. Haptic rendering tasks
5. Training tasks.
6. Systems validation.
7. IT platforms
8. Unique solutions, IP and publications.
9. Project management in a research environment.
10. Keeping the medical collaborators happy.

SYNCHROTRONS AND THEIR APPLICATIONS IN MEDICAL IMAGING AND THERAPY

Rob Lewis

Director, Monash Centre for Synchrotron Science, Monash University, Clayton, Vic, Australia

Australasia's first synchrotron is being built on the campus of Monash University near Melbourne. Is it of any relevance to the medical imaging and radiation therapy communities? The answer is an unequivocal yes.

Synchrotrons overcome many of the problems with conventional X-ray sources and as a result make it possible to demonstrate extraordinary advances in both X-ray imaging and indeed in radio-therapy. Synchrotron imaging offers us a window into what is possible and the results are spectacular. Specific examples include lung images that reveal alveolar structure and computed tomography of single cells. For therapy treatments are being pioneered that seem to be effective on high grade gliomas.
An overview of the status of medical applications using synchrotrons will be given and the proposed Australian medical imaging and therapy facilities will be described and some of the proposed research highlighted.

REFERENCES:

[1]R. A. Lewis., Medical phase contrast X-ray imaging: current status and future. Phys. Med. Biol. 49, 3573-3583, 2004.
[2]R. A. Lewis., C. J. Hall., A. P. Hufton., S Evans., R. H. Menk., F. Arfelli., L. Rigon., G. Tromba., D. R. Dance., I. O. Ellis., A. Evans., E. Jacobs., S. E. Pinder., K. D. Rogers., X-ray refraction effects: application to the imaging of biological tissues. British Journal of Radiology 76: 301-308, 2003.
[3]Kan-Cheung Cheung., Khalid Fayz., David Laundy., Rob Lewis., Barry Dobson. and Chris Hall., First test pictures from X-ray diffraction enhanced imaging camera for high contrast medical imaging at SRS. Nuclear Instruments and Methods in Physics Research A 513: 32–35, 2003.

INVITED SPEAKERS

TRS 398 DOSIMETRY PROTOCOL FOR RADIOTHERAPY

(Speaker support from Oxford Scientific)

H. Palmans[1] and V. Smyth[2]

[1]National Physical Laboratory, Teddington, England, UK
[2]National Radiation Laboratory, Christchurch, New Zealand

In recent years, international codes of practice based on absorbed dose to water standards have been published for the clinical reference dosimetry of external beams[1-4]. It has become widely accepted that dosimetry of radiotherapeutic beams should be based on these standards. These codes of practice are a major improvement over earlier ones that used air kerma calibration factors as they are based on a calibration directly in a phantom in terms of the quantity of interest. The previous codes begin with calibration in air in terms of air kerma, then use theoretical and generic conversion factors to obtain dose to water that do not take account of chamber-to-chamber variation. Other good reasons for implementing the new codes are that they are conceptually simpler, include improved physical data and improve the consistency for various ionisation chamber types as well as between different beam types.
TRS-3982,3 is a new Code of Practice (CoP) for reference dosimetry of external radiotherapy beams based on absorbed dose to water calibrations and was published by the IAEA in a joint effort with the WHO, PAHO and ESTRO. It is the first CoP of its kind comprehensively covering all external radiotherapy beams except neutrons. The Radiotherapy Interest Group (RIG) of the ACPSEM has recommended that radiotherapy centres in Australia and New Zealand implement this CoP by the end of 2004.
In this workshop, the general philosophy of the CoP will be outlined which will provide a framework for each of the individual subcodes. Although it represents just one of the potential implementations of the CoP, this workshop will deal only with dosimetry based on a cylindrical ionisation chamber with an absorbed dose calibration factor in 60Co from the standards laboratory. With the framework of the code in mind, it is straightforward to identify the basic steps that are required for measuring absorbed dose under reference conditions in a high-energy photon beam. The same is true for high-energy electron beams. However, the necessity of having an electron beam calibration factor for plane-parallel chambers and how to obtain it will be explained. Emphasis will be on practical aspects of implementing the CoP and the changes with respect to TRS-277 and TRS-381. Published experimental information4 on the expected differences to dosimetry based on the old codes will be discussed.

REFERENCES:

[1]Huq, M. S. and Andreo, P., Advances in the determination of absorbed dose to water in clinical high-energy photon and electron beams using ionization chambers, Phys Med Biol 49 (4) R49-104 Review, 2004.
[2]Andreo, P., Burns, D. T., Hohlfeld, K., Huq, M. S., Kanai, T., Laitano, F., Smyth, V. and Vynckier, S., IAEA INTERNATIONAL ATOMIC ENERGY AGENCY, "Absorbed Dose Determination in External Beam Radiotherapy. An International Code of Practice for Dosimetry Based on Standards of Absorbed Dose to Water", Technical Report Series no. 398, Vienna, 2000.
[3]Worksheets for the IAEA Code of Practice TRS-398 based on standards of absorbed dose to water (version 1.06), http://www-dmrp.iaea.org/nahu/dmrp/codeofpractice.shtm.
[4]Palmans. H., Nafaa, L., de Patoul, N., Denis, J-M., Tomsej, M. and Vynckier, S., A dosimetry study comparing NCS report-5, IAEA TRS-381, AAPM TG-51 and IAEA TRS-398 in three clinical electron beams, Phys Med Biol 48(9) 1091-107, 2003.

CT TECHNOLOGY UPDATE

S. Edyvean

ImPACT, St. George's Hospital, London, England, UK

The capabilities of CT scanning as a diagnostic imaging medium increased dramatically with the introduction of four slice scanners in the second half of 1998. The ability to acquire four sets of scan projection data per revolution of the scanner gantry can be exploited by imaging a scan volume faster, or with greater z-axis resolution than a single slice scanner, or scanning larger volumes in the same total time. This has improved the quality of a number of clinical applications, as well as enabling new techniques that were not previously possible.
This workshop will review the advances in CT scanning that have lead to modern multi-slice scanning. The operation of scanners will be explored looking at the hardware required and the changes in reconstruction techniques necessary with the higher number of imaged slices. The advantages and disadvantages of multi-slice scanners over their single-slice equivalents will be investigated, and image quality and dose issues will be discussed. An overview of the clinical applications that benefit from multi-slice technology will be given. The talk will end with a glimpse into the future where we have 64 and 256 slice, as well as flat panel, systems currently being trialled.

COMMISSIONING AND QUALITY CONTROL OF CT SCANNERS (DIAGNOSTIC RADIOLOGY AND RADIOTHERAPY)

S. Edyvean

ImPACT, St. George's Hospital, London, England, UK

Testing of CT scanners is undertaken for a variety of purposes whether type testing, acceptance (commissioning) or for quality control. Type testing identifies the features of a particular model and is of use in assistance in the purchase process, acceptance ensures that the scanner is operating to the purchase specification, and within that, commissioning ensures that the scanner is fit for use for all its purposes. Quality control ensures that the scanner continues to operate at its required performance. The purpose of the use of the scanner needs to be considered, particularly with the increasing use of scanners for simulation in radiotherapy, and now for attenuation corrections in PET-CT.
This workshop describes the various tests that can be carried out for acceptance and quality control, and how to perform them. It mainly covers image quality and dose issues with some other mechanical and alignment tests also discussed. It also explores practical approaches for undertaking different testing protocols. Attention is paid to particular aspects of multi-slice scanners which need to be addressed. Reference is also made to the UK and USA Physics professional bodies (IPEM and AAPM), and their recommendations. Specific issues relating to scanners used in radiotherapy is also covered.

Abstracts of oral presentations - radiation therapy

AN IMRT DOSE DISTRIBUTION STUDY USING COMMERCIAL VERIFICATION SOFTWARE

M. Grace[1], G. Liu[1], W. Fernando[1] and K. Rykers[1]

[1]*Austin Health, Melbourne, Vic, Australia*

INTRODUCTION: The introduction of IMRT requires users to confirm that the isodose distributions and relative doses calculated by their planning system match the doses delivered by their linear accelerators. To this end the commercially available software, VeriSoft™ (PTW-Freiburg, Germany) was trialled to determine if the tools and functions it offered would be of benefit to this process.
METHODS: The CMS Xio (Computer Medical System) treatment planning system was used to generate IMRT plans that were delivered with an upgraded Elekta SL15 linac. Kodak EDR2 film sandwiched in RW3 solid water (PTW-Freiburg, Germany) was used to measure the IMRT fields delivered with 6 MV photons.
RESULTS: The isodose and profiles measured with the film generally agreed to within ± 3% or ± 3 mm with the planned doses, in some regions (outside the IMRT field) the match fell to within ± 5%. The isodose distributions of the planning system and the film could be compared on screen and allows for electronic records of the comparison to be kept if so desired.
DISCUSSION & CONCLUSIONS: The features and versatility of this software has been of benefit to our IMRT QA program. Furthermore, the VeriSoft™ software allows for quick and accurate, automated planar film analysis.

IMPACT OF MARGIN ON TUMOUR AND NORMAL TISSUE DOSIMETRY IN PATIENTS TREATED WITH IMRT USING AN ENDORECTAL BALLOON FOR PROSTATE IMMOBILIZATION

Salahuddin Ahmad[1] and Maria Vlachaki[2]

[1]*The University of Oklahoma Health Science Center, Department of Radiological Sciences, Oklahoma City, USA*
[2]*New York University Medical Center-School of Medicine, New York, USA*

INTRODUCTION: In treatment of prostate cancer with IMRT (Intensity Modulated Radiation Therapy), clinical target volume margin is determined by organ motion and set-up error. However, the margin width that achieves the desired dose escalation while minimizing normal tissue exposure is dependent upon the patient immobilization and/or organ localization techniques. In this study, we compare the impact of margin width on the dosimetry of tumour and normal tissues using the endorectal balloon for prostate immobilization.
METHODS: IMRT plans were generated for ten patients using margin widths of 0, 3, 5, 8 and 10 mm. Patients had a planning CT scan in the prone position with an endorectal balloon filled with 100 cc of air for prostate immobilization. The Corvus version 3.0.11 was used for treatment planning. The dose for the prostate and seminal vesicles was 70 Gy in 2 Gy per fractions, prescribed at the 83% isodose line. Dose restrictions to normal tissues were as follows: 33% of bladder was allowed to receive above 65 Gy, 15% of rectum above 68 Gy and 10% of femurs above 45 Gy. Analysis of Variance was used to compare the target and normal tissue doses. Tumour control probability and normal tissue complication probability calculations are currently being performed and will be presented.
RESULTS: The mean doses ranged from 73.93 to 75.31 Gy for the prostate and from 73.71 to 75.31 Gy for the seminal vesicles. A 10 mm margin produced significantly lower mean doses compared to 0 or 5 mm for both targets (prostate $p<0.038$, seminal vesicles $p<0.015$). Percent target volumes below 70 Gy ranged from 1.48% to 5.25% for prostate and from 0.7% to 4.02% for seminal vesicles ($p>0.062$). For bladder and rectum the mean doses ranged from 18.49 to 22.30 Gy ($p=0.605$) and from 29.34 to 31.33 Gy ($p=0.135$), respectively, while the percent rectal volumes above 68 Gy were significantly higher for margins of 5, 8 and 10 mm ($p<0.006$) ranging from 10.72% to 15.81%. Mean doses to the femurs and pelvis were significantly higher for 8 and 10 mm margins, ranging from 20.9 to 29.39 Gy for femurs ($p<0.015$) and from 15.05 to 19.98 Gy for pelvis ($p<0.0005$). Also the percent femoral volume above 45 Gy significantly increased with higher margins ($p<0.0005$).
DISCUSSION & CONCLUSIONS: Margin width above 5 mm results in increased dosing of rectum, femurs and pelvic tissues, and may have significant impact on early and late normal tissue toxicities especially in cases of dose escalation. Minimizing set-up uncertainty as well as prostate motion using the endorectal balloon will allow safe delivery of higher, more effective radiotherapy doses with tighter margins.
ACKNOWLEDGEMENTS: This work was partly done at the Veterans Affairs Medical Center and the Baylor College of Medicine in Houston, Texas, USA.

HYPERBOLIC PROJECTIONS OF SIEMENS 3D-MLC LEAF PATHS

N. Menzies

Riverina Cancer Care Centre, Wagga Wagga, NSW, Australia

INTRODUCTION: The Siemens Primus linear accelerator has the option of being fitted with a multi-leaf collimator (3D-MLC) that is marketed as having "double focus", to achieve a constant dose penumbra for all leaf settings. This is achieved by moving the leaves through arcs (similar to some conventional collimator jaws), as well as shaping the leaf side-faces as divergent planes from the x-ray source.
One consequence of the mechanical design of the 3D-MLC is that as individual leaves are moved, their projections from the light / x-ray source to the treatment plane follow paths that are hyperbolic, as shown in the figure below. (The eccentricity of the hyperbola is a function of leaf number / distance from centre.)

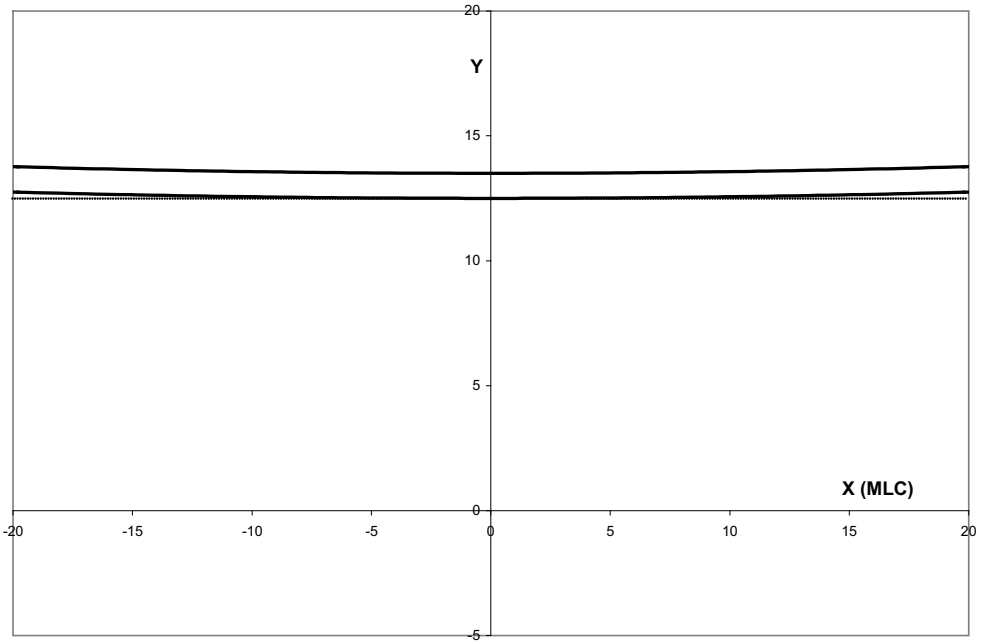

METHODS: The trajectories of the MLC leaves were modelled (in a spreadsheet) using geometrical projections of the MLC leaves to the treatment plane, with construction details provided in Siemens documentation. The results were checked against the image of the leaf in the linac light field.
RESULTS: This problem belongs to the class of conic sections in mathematics, where the intersection of a plane with both nappes of a double right circular cone results in a hyperbola. The good agreement between the model and the light field image provided confirmation of the MLC construction details.
DISCUSSION & CONCLUSIONS: AS/NZS 4434.1:1996 (reproduced from IEC 976:1989)[1] provides specifications for maximum deviation from orthogonality of adjacent edges, which can be interpreted for MLC collimators to parallelism of the direction of leaf travel and the adjacent collimator edge (e.g. Elekta ATS[2]). However for the Siemens "double focused" MLC, it is demonstrated that the geometrical construction of the MLC militates against the leaf image being used for this kind of test. It is also demonstrated that at last one commercial treatment planning system[3] models the Siemens leaf trajectories linearly. The clinical significance of the error in this model is shown to be negligible.
REFERENCES:
[1]AS/NZS 4434.1:1996 Medical electrical equipment – Medical electron accelerators – Part 1: Functional Performance Characteristics (Standards Australia / Standards New Zealand) - Test 8.3.1.
[2]Customer Acceptance Test Schedule 1.3.2.2/3 Elekta Oncology Systems Pty Ltd 2000.
[3]PLATO Sunrise (Nucletron Pty Ltd).

INVERSE IMRT WORKFLOW PROCESS AT AUSTIN HEALTH

K. Rykers, W. Fernando, M. Grace, G. Liu, A. Rolfo, A. Viotto, C. Mantle, M. Lawlor, D. Au-Yeung, G. Quong, M. Feigen, D. Lim-Joon and M. Wada*Radiation Oncology Centre, Austin Health, Melbourne, Vic, Australia*

INTRODUCTION: The work presented here will review the strategies adopted at Austin Health to bring IMRT into clinical use. IMRT is delivered using step and shoot mode on an Elekta Precise machine with 40 pairs of 1cm wide MLC leaves. Planning is done using CMS Focus/XiO. A collaborative approach for RO's, Physicists and RTs from concept to

implementation was adopted. An overview will be given of the workflow for the clinic, the equipment used, tolerance levels and the lessons learned.

DISCUSSION:

1. Strategic Planning for IMRT
2. Training
    a. MSKCC (New York)
    b. ESTRO (Amsterdam)
    c. Elekta (US & UK)
3. Linac testing and data acquisition
    a. Equipment and software review and selection
    b. Linac reliability/geometric & mechanical checks
    c. Draft Patient QA procedure
    d. EPI Image matching checks and procedures
4. Planning system checks
    a. export of dose matrix (options)
    b. dose calculation choices
5. IMRT Research Initiatives
    a. IMRT Planning Studies, Stabilisation, On-line Imaging
6. Equipment Procurement and testing
    a. Physics & Linac Equipment, Hardware, Software/Licences, Stabilisation
7. Establishing a DICOM Environment
    a. Prescription sending, Image transfer for EPI checks
    b. QA Files
8. Physics QA (Pre-Treatment)
    a. Clinical plan review; DVH checks
    b. geometry; dosimetry checks; DICOM checks
    c. 2D Distance to agreement; mm difference reports; Gamma function index
9. Documentation
    a. Protocol Development
        i. ICRU 50/62 reporting and prescribing
    b. QA for Physics
    c. QA for RT's
    d. Generation of a report for RO/patient history

IMPLEMENTATION OF IMRT FOR HEAD AND NECK TUMOURS

P. Engstrom, J. Crosbie, R. Smith, F. Gagliardi, R. M. Millar and S. Davis

The William Buckland Radiotherapy Centre, The Alfred Hospital, Melbourne, Vic, Australia

INTRODUCTION: Intensity modulated radiation therapy (IMRT) is regarded as perhaps the most significant development in radiation delivery over the last thirty years. Head and neck tumours lend themselves to IMRT as the beam modulation can more precisely deliver radiation to irregular target volumes and avoid critical structures. The clinical implementation of IMRT poses a number of challenges to a radiation oncology department. We present our initial experience, focussing on the commissioning and quality assurance issues.

METHODS: A research physicist with IMRT experience spent 12 months assisting with the implementation of IMRT at The William Buckland Radiotherapy Centre (WBRC). The protocol developed was based largely on the IMRT program at Copenhagen University Hospital and the Danish National Head and Neck Cancer Protocol (DAHANCA). Optimisation and inverse planning was initially carried out using the Nucletron Plato ITP planning system employing dynamic MLC IMRT. We were not able to treat using the dynamic MLC technique due to stability issues, and subsequently employed the step and shoot technique (segmental MLC IMRT). The treatments were delivered on two Varian 2100C linear accelerators one equipped with an 80-leaf, and the other with a 52-leaf MLC. For patients with disease in the nasopharynx, tonsil or upper pharyngeal nodes, parotid sparing was a key planning objective. The MLC was modelled extensively using physical and geometrical parameters in the configuration files. For the purposes of commissioning and treatment verification, the treatment plans were delivered to a perspex phantom in which were placed an ion chamber and radiographic films. Ion chamber readings of a high dose region (isocentre) and a low dose region (e.g. spinal cord) were taken. The measured ion chamber doses and intensity patterns of the film were compared to the equivalent from the treatment planning system by extracting the 3-dimensional dose grid of the phantom. Analysis of the films and planned doses was performed using RIT© software tools. Independent dose verification was performed on patients by inserting a TLD filled naso-oesophageal tube during their first fraction

RESULTS: It has taken us approximately nine months from the commencement of the IMRT commissioning project to the treatment of our first patient. To date (July 2004) we have treated four Ca. tonsil patients and one patient with a nasopharyngeal tumour using step-and-shoot IMRT. The measured ion chamber doses at the isocentre and in a region of low dose have agreed with the planned dose to within approximately 3.0% for all patients. Typically, the measured doses are less than the calculated dose. The measured film intensity patterns plotted as isofluence contours agreed with calculated patterns to within approximately ± 3%. The doses as recorded by TLD in-vivo dosimetry have come within the range of doses on the plan.
DISCUSSION & CONCLUSIONS: A significant amount of training was required for key staff in order that they would have confidence in their role in the planning and treatment process. IMRT for head & neck tumours has proven deliverable but time consuming for physics and clinical staff. The aim of reducing dose to normal tissue appears to have been achieved to date with less acute toxicities noted by the limited series of patients treated thus far. Our QA program gives us confidence in our ability to deliver such complex treatments accurately and effectively to our patients.

COMMISSIONING AND DOSIMETRIC VERIFICATION OF A COMMERCIAL ELECTRON MONTE CARLO PLANNING ALGORITHM

R. Tummers[1,2], K. Harrison[1,3] and P. Ostwald[1,3]

[1]*Newcastle Mater Hospital, Newcastle, NSW, Australia*
[2]*Eindhoven University of Technology, Netherlands*
[3]*Mathematics and Physical Sciences, Newcastle University, Newcastle, NSW, Australia*

INTRODUCTION: Electron pencil beam based planning algorithms, have well demonstrated lack of accuracy under complex conditions [1]. Electron Monte Carlo algorithms can show an improvement in dose calculation for these conditions, but must be able to deliver the dose calculation in a timely manner for the algorithm to be useful in a clinical environment. The Newcastle Mater Hospital has begun preliminary testing of a clinical electron Monte Carlo Planning Algorithm, for dosimetric accuracy and ease of use.
METHODS: The ADAC Pinnacle[3] Electron Monte Carlo (EMC) module (Philips, USA) has been commissioned for use with an electron beam based on a 16 MeV beam from the Varian 21EX linear accelerator in the Department. The beam has been commissioned using both the beam modelling software supplied in Pinnacle[3], and a phase space file generated by the BEAMnrc Monte Carlo beam modelling code (National Research Council, Canada). Results have been compared with the standard Hogstrom based electron algorithm (Pinnacle[3]) commissioned used clinically in the Department.
Accuracy of electron beam modelling was compared for the EMC model, the BEAM phase space model and the standard pencil beam model. Comparison plans were made for standard pencil beam, for a variety of simple test cases. Tests include elongated fields (4 x 10 cm), surface irregularities and the presence of inhomogeneities (bone, air). Comparison plans were also calculated for complex anatomical cases using a KSS/Capintec head phantom, with inset bone and air cavities.
Dosimetric verification of the simple test cases was performed using a Wellhofer CC13 ion chamber in a water tank and LiF:Mg,Ti TLDs (ribbons 4.5 mm diameter x 0.9mm thick and microcubes 1 mm^3) in solid water.
RESULTS: For an elongated field (4x10cm) the EMC model is more accurate than the pencil beam model. For a small missing tissue surface irregularity measured at a depth of 3cm, the EMC model and the pencil beam appear to have similar inaccuracies. In an inhomogeneity test using a small piece of bone analogy in solid water, dose distributions generated using both models show calculation differences of up to 20% directly beneath the bone. For the EMC model, the uncertainty in dose distribution calculations was set to 2%, and calculated using an average of 5 million histories. Each of the simple tests took approximately 45 minutes for the EMC to calculate.
DISCUSSION & CONCLUSIONS: The clinical Electron Monte Carlo module indicates an improved accuracy for complex electron treatment fields and anatomies. The algorithm delivers an isodose plot in a timely manner. Beam modelling is more time consuming and complex than the standard electron model, putting it on par with photon modelling, but more clinical experience should make the process easier.
REFERENCES:
[1]P. M. Ostwald, P. E Metcalfe, J. W Denham, C. S. Hamilton, (1994), *Int J Rad Oncol Biol Phys*, 28:731-740.

EVALUATION OF COMMERCIAL MU CALCULATION SOFTWARE

P. Lanzon[1] and J. Clarke[2]

[1]*Sir Charles Gairdner Hospital, Perth, WA, Australia*
[2]*Ipswich Hospital, Suffolk, UK*

INTRODUCTION: In radiotherapy, independent checking of the monitor units used to deliver the prescribed patient dose is an essential quality assurance procedure. In-house software has previously been used for this purpose, however, such

software has significant limitations particularly with complex treatment procedures. A commercial program, RadCalc®, produced by LifeLine Software Inc, has recently been implemented for this purpose.
METHODS: RadCalc calculates MUs and point doses for photon and electron beams, including in-vivo dose calculation. It enables all field details, including MLCs, to be entered or imported in DICOMRT format from a treatment planning system. Plan export is also available. Other features include photon IMRT MU calculations. The dataset used by RadCalc includes PDD/TPR and profile data for all wedged fields, except in the unwedged direction, field size dependent wedge factors and collimator and scatter phantom correction factors. Beam data can be imported from beam data acquisition systems.
RESULTS: To date RadCalc has only been implemented for non-IMRT photon beam treatments. Extensive comparison with the results of a CMS XiO treatment planning system and measured data has shown general good agreement. The user interface for the software is good and it has been accepted well in clinical use. This is partly due to the ability to configure many parameters to the department's equipment and procedures and to features such as the beam graphical display. Applications software support from LifeLine has been prompt.
DISCUSSION & CONCLUSIONS: RadCalc is a useful tool for independent photon MU calculation and has considerable advantages over the previous in-house software.
ACKNOWLEDGEMENTS: Radiation therapists at Sir Charles Gairdner Hospital.

ENHANCED DYNAMIC WEDGE AND INDEPENDT MONITOR UNIT VERIFICATION

S. J. Howlett[1,2]

[1]*Department of Radiation Oncology, Newcastle Mater Misericordiae Hospital, Newcastle, NSW, Australia*
[2]*Faculty of Health Sciences, University of Newcastle, Newcastle, NSW, Australia*

INTRODUCTION: Some serious radiation accidents have occurred around the world during the delivery of radiotherapy treatment. The regrettable incident in Panama clearly indicated the need for independent monitor unit (MU) verification. Indeed the International Atomic Energy Agency (IAEA), after investigating the incident, made specific recommendations for radiotherapy centres which included an independent monitor unit check for all treatments. Independent monitor unit verification is practiced in many radiotherapy centres in developed countries around the world. It is mandatory in USA but not yet in Australia. The enhanced dynamic wedge factor (EDWF) presents some significant problems in accurate MU calculation, particularly in the case of non centre of field position (COF). This paper describes development of an independent MU program, concentrating on the implementation of the EDW component. The difficult case of non COF points under the EDW was studied in detail.
METHODS: A survey of Australasian centres regarding the use of independent MU check systems was conducted. The MUCalculator was developed with reference to MU calculations made by Pinnacle 3D RTP system (Philips) for 4MV, 6MV and 18MV X-ray beams from Varian machines used at the Newcastle Mater Misericordiae Hospital (NMMH) in the clinical environment. Ionisation chamber measurements in solid water™ and liquid water were performed based on a published test data set. Published algorithms combined with a depth dependent profile correction were applied in an attempt to match measured data with maximum accuracy. The principal equation utilized is that of Gibbon[1]

$$EDWF = \frac{W_0 S_G(0) + W_{60} S_G(Y_0) + W_{60} a_1 b_1 \alpha e^{\beta Y_0} \left(\frac{e^{b_- Y_{FJ}} - e^{b_- Y_0}}{b_-} + e^{2 b_1 Y_0} \frac{e^{-b_+ Y_{FJ}} - e^{-b_+ Y_0}}{b_+} \right)}{W_0 S_G(0) + W_{60} S_G(Y_{FJ})} \quad (1)$$

RESULTS: The survey results are presented. Substantial data is presented in tabular form and extensive comparison with published data. Several different methods for calculating EDWF are examined. A small systematic error was detected in the Gibbon equation used for the EDW calculations. Generally, calculations were within $\pm$2% of measured values, although some setups exceeded this variation.
DISCUSSION & CONCLUSIONS: Results indicate that COF equations may be used in the non COF situation with similar accuracy to that achieved with profile corrected methods. Further collaborative work with other centres is planned to extend these findings, with a view to recommending the most accurate algorithm and method for both COF and non COF EDWF determination for use in independent MU calculations.
ACKNOWLEDGEMENT: Helpful discussions and suggestions from Tomas Kron, London Regional Cancer Centre, Canada, are gratefully acknowledged.
REFERENCES:
[1]Gibbons, J. P. *Calculation of enhanced dynamic wedge factors for symmetric and asymmetric photon fields*, Med. Phys. 25(8), 1411-1418 (1998).

A PRACTICAL SEQUENCE AND INHOMOGENEITY CORRECTION METHOD FOR USE IN BLOCKED EQUIVALENT SQUARE CALCULATIONS IN CONSIDERATION OF REDUCING THE DISCREPANCY RATES FOR 3D PLANNING MONITOR UNIT CHECKS

Y. Wang[1], X. Deng[2], S. Huang[2] and Z. Qi[2]

[1]*East Coast Medical Physics, St. Vincent's Clinic, Sydney, NSW, Australia*
[2]*Radiation Oncology, Sun Yet-Sen University Cancer Centre, China*

INTRODUCTION: In 3D planning checks the BEQS (Blocked Equivalent Square) calculation is sometimes the most challenging part of the work [1], as geometric size estimation does not always reflect real tissue volume involved in a 3D treatment field. This is especially so for the tangent field with obliquity. This study attempts to develop a practical method in order to more easily handle the estimation for BEQS in 3D clinical planning checks to reduce the discrepancy caused by a simple geometric BEQS estimation.
METHOD AND MATERIAL: A combined BEQS estimation procedure involving Geometric + Inhomogeneity + Irregular Skin Surface correction is presented. This procedure is sequentially managed by an in-house developed software as:
A blocked field shape (MLC or shielding blocks) is loaded from planning system export or directly drawn in the screen picture box by user;
Clarkson calculation or Irregular Rectangular Shape estimation [2] can be performed as an option by selecting the functions to receive the geometric BEQS for the shape;
Inhomogeneity Correction for the tissues involved at the level of the beam weight point depth;
Irregular Skin Surface correction is then processed for the surface level of the beam entry point.
RESULT AND DISCUSSION: The BEQS calculated by this procedure sometimes shows a very different result compared with the BEQS simply calculated by geometric estimation, especially for the tangent beam entry fields or the field involved with significant inhomogeneity tissues. The different result causes different TPR and Sp values to be selected in the planning monitor unit check. In comparison, by using this BEQS correcting sequence, the planning check result discrepancy could be reduced on average by 1.5% - 2.0% for the tangent beam entry fields such as breast or head and neck cases.
CONCLUSION: The BEQS calculation in 3D planning is not a simple geometric size estimation but is an integration, voxel by voxel, for inhomogeneity tissues distributed in the field volume. If these corrections are incorporated into 3D monitor unit checking, then there will be reduction in discrepancy between simple geometric estimation methods and the method presented by this study.
REFERENCES:
[1]J. Chan (2002) *Comparison of monitor unit calculations performed with a 3D computerized planning system and independent "hand" calculations: Results of three years clinical experiences*, Journal of Applied Clinical Medical Physics, vol. 3, No. 4.
[2]F. M. Khan (2003 Third Edition) *The Physics of Radiation Therapy*, Lippincott Williams & Wilkins.

SOFTWARE FOR VARIAN ENHANCED DYNAMIC WEDGE FACTOR (EDWF) CALCULATION

T. Ravichander

The Canberra Hospital, Canberra, ACT, Australia

INTRODUCTION: Manual MU calculation is a recommended QA for Treatment Planning Systems. The EDWF is used in the manual MU calculation of the treatment fields. The aim of this work was to write basic software, which provides EDWF at any position for all possible clinical treatment fields.
METHODS: Two models the MU fraction model [1] and the Gibbons model [2] were tested for all possible circumstances. The accuracy of each model and subsequent EDWF calculation output under the various circumstances were confirmed by measurement. The Marcus chamber and solid water were used in all of the EDWF measurements.
The program was written in MATLAB to allow the use of the two models. The appropriate model for the EDWF calculation will be chosen based on the entered input parameter (as shown in the fig.1).

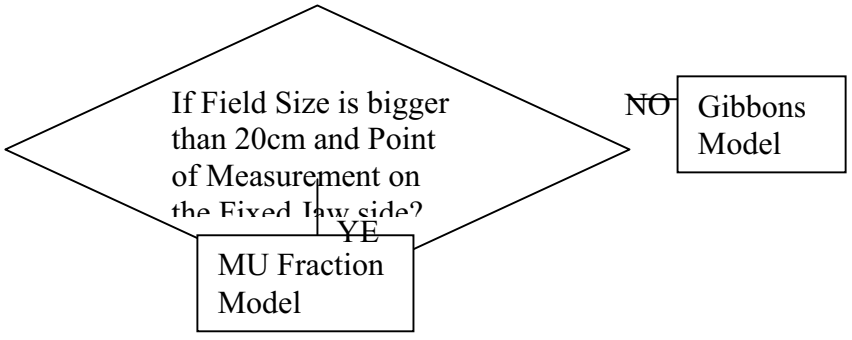

Figure 1. *Flow chart for selection of the model.*

RESULTS: In all routine clinical circumstances calculated EDWF was <2% of the measured values.
DISCUSSION & CONCLUSIONS: Only under extreme circumstances i.e. 60^0 wedge and a maximum field size (Y1=20, Y2=10) and the point of measurement >3cm from the centre of the field the calculated EDWF was found to be >2% to the measured value. Generally MU calculation points are chosen closer to the centre of the Enhanced Dynamic wedge field.
One feature of this program is that it gives warning messages whenever the entered parameters exceed the Varian EDW limitations.
ACKNOWLEDGEMENTS: The author would like to thank Brendan Hill (Chief Physicist, Canberra Hospital) for his valuable contribution in compiling and installing this program in PCs.
REFERENCES:
[1]Varian Medical Systems (1996) *C-Series Clinac Enhanced Dynamic Wedge Implementation Guide*, Palo Alto, CA..
[2]J. P. Gibbons, (1998) *Med.Phys.* ,25(8):1411-18.

REAL-TIME VERIFICATION OF HDR BRACHYHERAPY SOURCE LOCATION: IMPLEMNTATION OF DETECTOR REDUNDANCY

T. Nakano[1], N. Suchowerska[1,2], D. R. McKenzie[1] and M. M. Bilek[1]

[1]*School of Physics, The University of Sydney, NSW, Australia*
[2]*Royal Prince Alfred Hospital, Camperdown, NSW, Australia*

INTRODUCTION: HDR brachytherapy is a highly customized treatment procedure, in which a small radioactive source is dynamically placed in close proximity to the tumour cells using catheters placed within the patient. Independent treatment verification is needed for this to ensure that the treatment proceeds as prescribed
We investigated the feasibility of a proposed real-time source position verification process. This process provides immediate confirmation of the source position during the treatment, so that the treatment can be aborted and modified if necessary. We show that an array of dosimeters placed on the patient's skin can independently verify the position in three-dimensions.
METHODS: A mathematical algorithm was constructed to estimate the location of the source given a measured data set in the presence of tissue inhomogeneity. The data set consisted of dosimeter readings taken at up to twelve locations on the surface of an anthropomorphic phantom. The dosimeter used for this application were the diamond detector type 60003 (PTW Freiberg) and MOSFET dosimeter RD-502 (Thomson & Nielsen). The radiation source (Ir-192) was delivered to 5 dwell positions in a catheter located inside the phantom, using a Nucletron MicroSelectron HDR brachytherapy afterloader.
RESULTS: The accuracy of the source localization was found to increase with the number of detectors used to compute the estimation of the source position. The resolution to which the twelve detectors can identify the location of the source was 3 mm.
DISCUSSION & CONCLUSION: The investigation of detector redundancy in source localization provided a proof of concept that the array of detectors can be used to localise the HDR brachytherapy source accurately. The mathematical algorithm constructed in this work has successfully identified the compromised detectors due to inhomogeneity and weighted the contribution of these detectors to the source localisation accordingly.
This study offers the opportunity to verify complex brachytherapy application in vivo on line. In addition the technique of detector redundancy is generally useful for all detectors capable of real-time readouts.
REFERENCES:
[1]J. Duan, D. J. Macey, P. N. Pareek, and I. A. Brezovich, (2003) *Med. Phys*., 28, 167-173.
[2]T. Nakano, N. Suchowerska, M. M. Bilek, D. R. McKenzie, N. Ng, and T. Kron, (2003) *Phys. Med. Biol*., 48, 2133-2146.

DOSIMETRIC COMPARISON OF SEED STRENGTH FOR I-125 PROSTATE IMPLANTS

S. Elliott, J. Droege and C. Beaufort

WilliamBuckland Radiotherapy Department, The Alfred Hospital, Melbourne, Vic, Australia

INTRODUCTION: The strength of I-125 seeds for prostate brachytherapy has been a topic of increasing popularity in the literature over the last few years. Recent reports, which include planning and clinical studies, compare dosimetry between plans and implants using higher (0.5 – 0.8 U, where 1 U = 1 μGym^2h^{-1}) or lower (0.3 – 0.4 U) seed strength. The majority of these studies support higher seed strengths for obtaining optimal dosimetry. At the WBRC, a seed air kerma strength of just under 0.4 U is currently used for seed implants. The purpose of this work is to investigate the use of higher strength seeds for our prostate implants.
METHODS: Twenty-four patients were selected according to prostate size, and re-planned using a seed strength of 0.5 U or 0.6 U. Planning was performed following our standard preplanning guidelines as closely as possible; that is, manual

planning using a modified Seattle approach and dosimetry limits for the target volume of D_{100}: > 95 Gy, V_{100}: > 98 %, V_{150}: 52 – 62 % and V_{200}: 11 – 16 %. Dosimetry from the original preplans was then compared to the dosimetry from the re-planned cases.

RESULTS: Satisfactory dosimetry was obtained using 0.5 U or 0.6 U strength seeds. Seed placement was typically around the periphery of the target on all slices, to avoid overdosing the urethra. The mean D_{100} (Gy) is marginally improved with the higher seed strength. As expected, the V200 (%) is also higher. The mean number of seeds required per implant decreased by 16 % and 28 % for 0.5 U and 0.6 U seeds respectively. The mean number of needles decreased by 7 needles for 0.6 U seeds, however only by 3 needles for 0.5 U seeds. Rectal doses, when using the higher strength seeds, were easily constrained to less than the original preplan doses.

Although there was no apparent trend in dosimetry statistics with volume size, as a function of seed strength, it was noted that the reduction in needle and seed number was most significant for medium and large target volumes.

DISCUSSION & CONCLUSIONS: A large number of pre-plans were investigated in this study and show some advantages of using a higher strength seed for our manually planned prostate implants. Apart from a minimal increase in target coverage, the main benefits were of a practical rather than clinical nature. The mean number of seeds used per implant was substantially decreased with higher seed strength, hence the total cost of seeds and physics seed loading time would subsequently be reduced. For a seed strength of 0.6 U there was a significant reduction in the total number of needles used for the implantation. Therefore for this seed strength, theatre time would be reduced, as well as the extent of injury to tissue.

RELOCATION OF A NUCLETRON MICROSELECTRON-HDR BRACHYTHERAPY SYSTEM

T. Bartrum[1], T. Tran[1], N. Freeman[1] and J. Morales[1]

[1]*St Vincents Hospital, Darlinghurst, Sydney, NSW, Australia*

INTRODUCTION: For a period of four weeks, our clinical Nucletron microSelectron high dose rate (HDR) brachytherapy system was pulled out of clinical use and relocated to a new building. During this period decommission tests, de-wiring of the treatment unit and its associated safety system (such as radiation detector, emergency off circuits and door interlocks), transportation of all equipment, re-wiring of this equipment in the new location and recommission tests were carried out. The decommission and recommission test program was designed upon consultation with the manufacturer's (Nucletron) acceptance test procedures and work carried out by others[2]. The ACPSEM tolerances[1] for remote afterloaders was used as a guideline.

In addition to mandatory dosimetry, positional, workstation database and safety tests, two *Australian Standard* compliance tests were carried out. The compliance tests involved one for remote afterloaders[5] and another for treatment room design[6]. This testing program was designed and implemented with the aim of ensuring ongoing safe delivery of brachytherapy doses to the patient.

METHODS: The testing program consisted of two parts. The first involved a series of decommissioning tests that consisted of dosimetry tests such as source and check cable positional accuracy and source calibration tests. In addition to these tests an inventory of standard plans, patient records and system configuration information was catalogued.

The second part involved a series of recommission tests and involved carrying out dosimetry tests on the brachytherapy system (positional accuracy and calibration tests), simulating common treatment scenarios (prostate, cervical, vaginal and bile duct) and checking standard plans; patient records and system configuration had remained unchanged. During this period, other tests were carried out. These included Nucletron acceptance and preventative maintenance tests, *Australian Standards*[5, 6] compliance testing and integrity of network transfer of brachytherapy plans tests.

RESULTS: There were no identifiable changes to the mechanical performance of the treatment unit. Correct functional performance of the workstation database, safety interlocks and network transfer of treatment plans was demonstrated. Standard treatment simulations indicated no unusual outcomes. The Nucletron microSelectron HDR remote afterloader meets *Australian Standard* compliance. The treatment suite meets *Australian Standards* compliance except for radiation signage, which is currently being addressed.

DISCUSSION & CONCLUSIONS: The relocation of the Nucletron MicroSelectron-HDR brachytherapy unit did not introduce any changes to the system. Compliance with the relevant *Australian Standard* was determined. The system was successfully released for clinical use within the planned time frame.

REFERENCES:

[1]Millar, M., Cramb, J., Das, R., Ackerly, T., Brown, G., Webb, D. *ACPSEM Position paper recommendations for the safe use of external beams and sealed sources in radiation oncology* APESM 20 (3) (1997) 1-35.

[2]Wallace, A.B. *Technical note. Acceptance testing, commissioning and quality assurance for a 370GBq ^{192}Ir HDR Brachytherapy Afterloader,* APESM 20 (2) (1997) 112-116.

[5]AS/NZS 3200.2.17:1994 Australian/New Zealand Standard. Approval and test specifications – *Medical electrical equipment. Part 2.17: Particular requirements for safety – Remote-controlled automatically-driven gamma-ray afterloading equipment*.

[6]AS/NZS 3824:1998 Australian/New Zealand Standard. *Guidelines for radiotherapy treatment room designs*.

PHOTO-DYNAMIC THERAPY (PDT) FOR SKIN CANCER USING A XENON ARC LAMP WITH INTERFERENCE FILTERS

J. Hagekyriakou

Peter MacCallum Cancer Centre, East Melbourne, Vic, Australia

INTRODUCTION: Phototherapy involves the production of photochemical reactions in cells by the direct action of light, including Ultra Violet, leading to biological effects, including cell death. Photo Dynamic Therapy involves the application of light, at wavelengths and intensity which has no biological effects, in combination with a photosensitizing compound, which is biologically inert in the absence of light, which once located in cells, can produce cellular damage when activated by light of certain wavelengths. The active compound produced during PDT is singlet Oxygen which has a half life of 3 microseconds. This necessitates the use of very powerful light sources, such as lasers, in order to achieve treatment delivery within a reasonable time, say minutes. Even though PDT is very effective in the treatment of skin cancer using topically applied photosensitizing drugs, the cost of powerful lasers, required to produce light in the red part of the spectrum, has been prohibitively expensive for widespread application of the above technique.
METHODS: A 300 Watt Xenon arc light source, with tuneable wavelength and bandwidth, used predominantly for Forensic Science applications, manufactured by Rofin Australia Pty, Ltd, has been modified by the manufacturer, boosting the power to 500 Watts. A group of Interference filters have been specifically made to facilitate irradiation at 670nm, 620nm and 600 nm, at relatively narrow bandwidth, typically 50 nm. This would provide adequate penetration of the light, for a variety of skin cancers, depending on the thickness of the lesion and the skin type involved. A relatively broad band Ultra Violet interference filter has also been inserted in the instrument for observation of Fluorescence of the lesion prior to treatment, as an indicator of photosensitizing drug uptake by the lesion involved.
Patients with skin cancers such as Basal Cell Carcinoma (BCC) and Paget's Extramammary disease were treated at the Peter MacCallum Cancer Centre, using the above light source in combination with Methyl Aminolevulinate (Metvix, by Galderma) as the photosensitizing agent. The patient's tumours were scraped using a small curette, in order to remove loose crust and debris from the surface. The photosensitizing drug, in a cream base, was then applied to the lesion and covered with a transparent occlusive dressing (Tegaderm, 3M) for a period not less than 3 hours, to allow the drug to diffuse throughout the lesion in question. The patient subsequently returned to the clinic whereupon the dressing was removed, excess cream wiped from the surface, and light irradiation was administered to a dose of 40 Joule/cm^2. The light beam was delivered from the lamp using an 8mm diameter Liquid Light Guide, whose light transfer and coupling efficiency is greater than that of a glass or plastic optical fibre, for this type of application; including transmission in the UV.
RESULTS: On application of the UV light following the 3 hour drug uptake, visible fluorescence was observed in patients with superficial BCC and Paget's Extramammary disease, with minimal (if any) fluorescence present in the neighbouring normal skin (to which drug was also applied). The fluorescence demonstrates that the photosensitizing drug has stimulated the accumulation of Hematoporphyrins within the diseased area, indicating that subsequent photo irradiation will be potentially beneficial. Excellent cosmetic results were obtained for superficial BCCs, even at 2 weeks post-treatment, for the patients evaluated thus far. Longer follow-up, typically 4 to 6 weeks, is required for a more quantitative evaluation of the procedure using the above technique.
CONCLUSION: A Xenon arc lamp is capable of producing sufficient power at narrow bandwidth within the red part of the spectrum, selectable with interference filters, and be delivered to the skin surface in a flexible manner using a liquid light guide, in order to facilitate PDT for a variety of skin cancers. This type of technique eliminates the use of expensive, high powered lasers, and can provide treatment outcomes cosmetically superior to surgery and radiotherapy, without the scars and hazards associated with such treatments.

INVESTIGATION OF THE DOSIMETRIC PROPERTIES OF AN a-Si FLAT PANEL EPID

A. L. Fielding[1], S. T. Jahangir[1], D. Cassidy[2] and R. Fitchew[2]

[1]*School of Physical and Chemical Sciences, Queensland University of Technology, Brisbane, Qld, Australia*
[2]*Royal Brisbane and Women's Hospital, Brisbane, Qld, Australia*

INTRODUCTION: Electronic portal imaging devices (EPIDs) are primarily used as an electronic replacement for film to verify the set-up of radiotherapy patients based on imaged anatomy. There has recently been much interest in the use of amorphous silicon (a-Si) flat panel EPIDs for dosimetric verification in radiotherapy[1]. The work presented here has been carried out to determine their suitability for dosimetric applications by investigating some of the basic response characteristics and the implications these might have.
METHODS: The measurements reported in this paper were performed using 6-MV photon beams from an Elekta Precise linear accelerator fitted with Elekta iViewGT amorphous silicon flat panel EPIDs. Measurements were performed to investigate the response of the EPID as a function of exposure and field size. Similar measurements were made with an

ionisation chamber for comparison. Further measurements were carried out to investigate the response of the EPID to multiple low dose exposures (e.g. 5 x 2 MU) such as might be encountered in Intensity Modulated Radiotherapy (IMRT). This was compared with the response to a single high dose exposure (e.g. 10 MU) and repeated for a range of exposures.
RESULTS: The results show the response of the EPID, to a good approximation, to be linear with dose over the range of 1 – 200 MU. However, 'under-responses' in the EPID of up to 5% were seen at the lowest exposures. For multiple low dose segments the sum of the EPID responses was found to be less than the response to the same total exposure in a single large segment. This effect reduces with increase in the magnitude of the low dose segments. The variation in EPID response with field size was found to be greater than that indicated by the ionisation chamber.
DISCUSSION & CONCLUSIONS: The results show that the a-Si detector responds to dose, to a good approximation, in a linear manner. The EPID under-response at low doses is thought to be related to the so called ghosting effect[2]. Each image frame has a residual component of signal from previous frames, the magnitude of which is influenced by the dose delivered in the previous frames. The variation of detector response with exposure has implications for the verification of IMRT treatments that consist of a combination of multiple short and long dose segments. The difference in EPID response to different field sizes compared to ionization chamber dose measurements may be partly due to variations in the energy spectrum of the photon beam with field size and partly due to inadequate build-up above the EPID detector layer.
REFERENCES:
[1]P. B. Greer and C. C. Popescu, (2003) *Med. Phys*., 30; 1618-1627.
[2]J. H. Siewerdsen and D. A. Jaffrey (1999) *Med. Phys*., 26; 1624-1641.

TRANSMISSION DOSIMETRY IN PINNACLE[3] 3D TREATMENT PLANNING SYSTEM

P. Reich[1, 2], E. Bezak[1, 2] and L. Fog[2]

[1]*School of Chemistry and Physics, University of Adelaide, Adelaide, SA, Australia*
[2]*Medical Physics Department, Royal Adelaide Hospital, Adelaide, SA, Australia*

INTRODUCTION: Transmission dosimetry plays an important role in radiotherapy treatment verification. Electronic Portal Imaging Devices (EPIDS) record transmitted radiation in 2D, the images are acquired in real time, and are stored electronically, allowing for easy archiving and image processing. However, EPIDs do not record true dose and therefore need to be calibrated, usually with an ionisation chamber. Calculation of transmitted dose using modern 3D Treatment Planning Systems (TPSs) has been investigated recently [1]. In the current work a solid water phantom and EPID were modelled in Pinnacle[3] TPS to calculate transmission doses in the EPID. Transmission dose calculations have been performed in for various phantom thicknesses and phantom-to-EPID distances.
METHODS: A homogeneous solid water phantom and EPID, based on a realistic clinical setup were modelled in Pinnacle[3] TPS. The 3D-dose distribution was calculated throughout the phantom-EPID region for a 2 Gy dose (6 MV beam from Varian 600CD linac) prescribed to the phantom centre, positioned at the isocentre. The corresponding dose matrix was extracted from Pinnacle[3] and processed in Matlab. A 2D dose matrix at the EPID level was obtained. Dose distributions for two experimental setups were modelled. In the first case, the phantom thickness was varied from 5 to 30 cm, while the phantom-EPID distance was fixed. In the second setup, the phantom thickness was varied, while the EPID was kept at fixed SSD; i.e. the phantom-EPID distance was varied. In each setup, the mean dose on the central axis was calculated and the noise level near the central axis was investigated. The data was compared with doses obtained from EPID images acquired for an equivalent experimental setup, using Varian 600CD linac and 6 MV beam. The pixel values in the EPID were converted to dose using an empirical calibration curve.
RESULTS: The Pinnacle[3] calculations in setup (i) show an exponential attenuation of dose for increasing phantom thicknesses. The standard deviation in the dose was less than 0.2% (1 sd) at the central axis for any given phantom thickness. The pixel to pixel variation was at most 0.5% in a 10x10 pixel region centred on the central axis for the 30 cm thick phantom and 1% for the 3 cm thick phantom. There is no correlation between the noise level in the thin solid water layer and phantom thickness. In setup (ii), the curve shows the additional effect of the inverse square law for large airgaps on the dose.

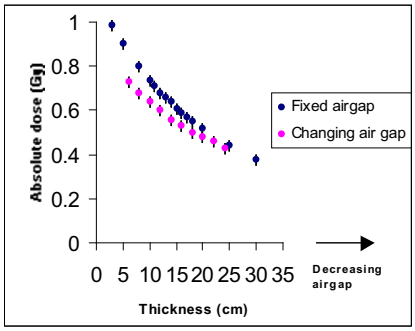

Figure 1. *Variation of dose with phantom thickness.*

DISCUSSION & CONCLUSIONS: A phantom and EPID assembly was successfully set up in Pinnacle[3] treatment planning system. Transmission dose calculations can be performed in Pinnacle[3] with a noise level less than 1% in the EPID layer. The dose calculations compare with experimental EPID measurements. In the future, the calculated EPID images and measured EPID images will be compared pixel by pixel to obtain 2 D dose maps and more EPID- phantom setups will be investigated for more complicated phantoms.

REFERENCES:

[1]T. R. McNutt *et al* (1996) *Med. Phys.* 23:1381-1392.

PREDICTION OF TRANSMITTED PORTAL DOSE FOR IN-VIVO DOSIMETRY BY A SUPERPOSITION-CONVOLUTION PLANNING SYSTEM

Peter Greer[1,2]

[1]*Newcastle Mater Hospital, Newcastle, NSW, Australia*
[2]*University of Newcastle, Newcastle, NSW, Australia*

INTRODUCTION: Verification of the dose delivered to a patient during radiotherapy is an important quality assurance procedure, however this is rarely performed due to the extra time involved. Electronic portal images (EPIs) are currently acquired at many centres during radiotherapy treatment for positioning verification. These could be utilised for dose verification provided 1) an accurate prediction of the dose transmitted through the patient to the EPID can be produced for the patients' radiotherapy beams, and, 2) the EPID image can be converted to an accurate measured dose. Ideally, the radiotherapy planning system (RTPS) would be used to produce the predicted dose as part of the planning procedure. The aim of this project is to investigate whether the convolution-superposition model of the Pinnacle RTPS can accurately calculate dose transmitted through a patient and deposited in a phantom at a large source to surface distance.

METHODS: The dose transmitted through a uniform ("patient") phantom (PP) placed at 100 cm source-surface distance (SSD) and deposited in a uniform ("EPID") phantom (EP) placed 35 cm beneath the PP was simulated with Pinnacle. The dose to the EP phantom was recorded with 200 monitor units (MU) prescribed to d_{max} on the central axis of the PP. As the Pinnacle d_{max} dose with 200 MU under these calibration conditions was less than 200 cGy all doses were increased accordingly. Open fields with field sizes at isocentre of 5×5, 10×10 and 20×20 cm^2 were simulated as well as a 60° dynamically wedged field. Two thicknesses of the PP of 15 and 25 cm, were used with the distance to the EP of 150 and 160 cm respectively to maintain the 35 cm air-gap. The EP was 5 cm thick and the dose at 3 cm depth within this phantom on the central axis was recorded. The energy was 6 MV.

Experimental measurements were made of the dose at 3 cm depth in a solid water (EP) phantom with an ionisation chamber, and a solid water PP, with the geometry of the simulations reproduced. The measurements were referenced to the readings at d_{max} in the PP where 200 MU (200 cGy) was delivered, to yield the dose to the EP.

RESULTS: The following table gives the results of the comparison of predicted and measured doses from the beam transmitted through the PP and deposited in the EP.

PP Thickness	Field size (cm^2)	Predicted dose to EP (cGy)	Measured Dose to EP (cGy)	Difference (cGy)
15 cm	5×5	40.2	39.2	+1.0
	10×10	43.4	42.4	+1.0
	20×20	48.3	47.7	+0.6
	10×10, 60° EDW	28.5	27.9	+0.6
25 cm	5×5	23.0	22.1	+0.9
	10×10	25.0	24.3	+0.7
	10×10, 60° EDW	16.3	16.0	+0.3

Table 1. *Accuracy of Pinnacle prediction of transmitted dose to the EPID phantom.*

DISCUSSION & CONCLUSIONS: The transmitted doses are in reasonable agreement, being within 1.0 cGy, and this shows promise for the use of this system to predict doses to the EPID. The Pinnacle prediction of dose is consistently high, and if this is consistent, then a correction factor could be incorporated into the predicted doses. As the Pinnacle system had a reference dose at 10 cm depth, future work will assess whether prescribing the dose to this depth in the PP rather than d_{max} gives more accurate results. Furthermore, non-homogeneous phantoms will be investigated, along with comparison of predicted and measured beam-profiles.

THE USE OF A UNIFORM FLOOD FIELD FOR RELATIVE DOSIMETRY USING THE AMORPHOUS-SILICON EPID

J. Crosbie, S. Elliott, P. Engstrom and R. Smith

William Buckland Radiotherapy Centre, The Alfred Hospital, Melbourne, Vic, Australia

INTRODUCTION: The amorphous silicon electronic portal imaging device (a-Si EPID) has been investigated by several researchers as a means of performing relative and absolute dosimetry measurements, in particular dosimetric verification of IMRT fields. It has been suggested that a uniform (flat) flood field calibration plays an important role in subsequent image acquisition for ensuring accurate dose response[1]. The aims of this paper are (i) to determine the conditions required to obtain a uniform flood field, and (ii) to investigate the dosimetric response of the EPID when uniform and non-uniform flood field calibrations are applied, in the context of a comparison between EPID acquired IMRT fields, radiographic film and the treatment planning system.

METHODS: Flood-field (FF) calibrations were performed on the a-Si EPID using 0 cm, 2 cm, 5 cm, 7 cm and 10 cm of solid water build-up material placed directly onto the vinyl protective cover of the EPID. Source-EPID distance of 155 cm and 105 cm were used for these calibrations. The FF calibration was also performed by placing 0 cm, 1 cm, 2 cm, 3 cm and 4 cm solid water build-up material close to the gantry head in the applicator holder. After each FF calibration an open field test image was acquired with no build-up on the EPID. Images of wedged fields with differing FF calibrations were also acquired. A 45 degree physical wedge was used on a Varian 600C linac and a segmental MLC step wedge used on a 2100C linac. Images of open and wedged fields were acquired under similar conditions using XOmat-V radiographic film. Relative dosimetric scans were obtained in a Wellhofer water tank using a PTW IC10 ionisation chamber. In addition, a segmental MLC IMRT field was delivered and a continuous frame-averaging mode image of the IMRT field was acquired. The open-field and IMRT images therefore, had the previous FF calibration applied. In addition, the fluence map of the field was acquired from the treatment planning system. Inplane and crossplane profiles along the central axis were obtained to assess the uniformity/flatness of the FF images using Image-J freeware. RIT V4© software was used to register the EPID IMRT images, and the fluence map from the planning system.

RESULTS: In the absence of build-up, the cross-plane profile of the FF resembles a parabola in shape for a SDD of 155 cm. The cross-plane profiles of the FF images become flatter with the addition of solid water build-up material placed directly on the EPID. In particular, the central portion of the FF was flat to within approximately 2% for the profile with 10 cm build-up. This behaviour was not observed when build-up material was placed in the applicator tray. The crossplane profiles for a SDD of 105 cm were significantly different, suggesting an additional physical effect such as glare. Profiles of the open field test images and the wedged images showed that the uniformity/flatness of the field varied depending on the amount of build-up in the FF calibration. Similarly, for the IMRT fields, the agreement between the acquired EPID image, radiographic film and the treatment planning system varied depending on the calibration of the flood field. Our analysis shows that a FF calibration performed with 5 cm of solid water build-up material improves the agreement slightly, between measured EPID image, film and the TPS

DISCUSSION & CONCLUSIONS: The ideal flood field for image acquisition would display a uniform profile. In practice, the FF image is generated from an open photon beam, which contains 'energy horns'. Subsequent FF correction removes the 'horns' from EPID image, affecting the EPID's ability to act as a dosimeter. During the calibration of the FF, the uniformity can be made to vary by the addition of build-up material. Our preliminary results show that a reasonably flat flood field is obtainable with the addition of between 7 and 10 cm of solid water build-up material. This has implications for EPID dose response, which were manifest when we obtained slightly improved agreement between the EPID IMRT field and the planned fluence map for the case of the 5 cm FF calibration.

REFERENCES:

[1]P. Greer. C. Popescu. *Dosimetric properties of an amorphous silicon electronic portal imaging device for verification of dynamic intensity modulated radiation therapy*. Med. Phys. 30(7), July 2003.

AN INVESTIGATION OF DOSE AND BEAM PROFILE DOSIMETRY WITH AN AMORPHOUS SILICON EPID

Peter Greer[1,2]

[1]Newcastle Mater Hospital, Newcastle. [2] University of Newcastle, Newcastle, Australia.

INTRODUCTION: There is much current interest in the use of electronic portal imaging devices (EPIDs) for dosimetric applications such as accelerator quality assurance, in-vivo dosimetry, and verification of IMRT. However, the use of EPID for these purposes requires that the images can be used to obtain accurate dose measurements. The aim of this work is to investigate the accuracy and reproducibility of dose and beam profile measurements with an amorphous silicon EPID.

METHODS: The Varian aS500 detector produces a "frame-averaged" image that is the image pixel values are the average of all acquired frames. By averaging frames throughout the delivery and then multiplying the result by the number of frames,

an integrated pixel value can be obtained. The reproducibility of EPID response to the same incident dose was assessed by weekly measurement of the mean value of a 9×9 pixel region at the central axis, for a 100 monitor unit irradiation of a 10×10 cm field under the same set-up conditions. At each session, three images were acquired. The EPID dose response was obtained by multiplying the pixel value by the number of acquired frames. Images were acquired for both 6 MV and 18 MV at 105 cm to the EPID detector surface with 4 cm added solid water build-up. The linearity of the EPID response with linear change in dose was measured. Images were acquired for MU settings of 5, 10, 25, 50, 100, 200 and 300 MU for both 6 and 18 MV. Three images were acquired for each MU setting and the pixel values multiplied by the number of frames acquired. The reproducibility of open field profiles measured with the EPID with dose (MU) settings of 20, 50, 100, 200 and 300 MU was investigated. Additional solid water build-up of 0.5 cm and 2 cm was used for 6 and 18 MV to give d_{max} build-up. The field size was 30×30 cm. Open field profiles were compared to water-tank measurements with and without flood-field corrections to the EPID image. A correction image was developed to convert EPID profiles to dose-to-water profiles.

RESULTS: The standard deviation of the EPID response to 100 MU for repeated irradiation within the same session was within 0.2%. The standard deviation of the response for weekly measurements was within 0.3%. The EPID response was found to be linear with linear change in dose. The frame-averaged pixel value decreased with decreasing MU setting. However the number of frames acquired per MU increased correspondingly to result in a linear dose response. The decrease in pixel value is therefore due to the lower average dose-rate and hence dose per frame for shorter MU irradiations. The linearity of the EPID response to change in dose was within 0.2%. Variation in the EPID measured beam profile for different irradiations was found. The variation was largest in the inplane direction but was always less than 1%. Variation was found particularly for small MU settings, however two profiles recorded with the same MU setting (e.g. 100 MU) also exhibited differences. The EPID was found to over-respond to the change in the incident beam profile off-axis, compared with water-tank measurements, and the response was non-uniform in the inplane direction. This over-response is largely removed with a flood-field acquired under the same conditions.

DISCUSSION & CONCLUSIONS: The highly reproducible response of the EPID suggests that it is well suited to dosimetric applications such as quality assurance, in-vivo dosimetry, and verification of IMRT. There was no evidence of ghosting or detector memory effect compromising the dose measurements. The reason for the beam profile variation is unclear, however this is likely to be due to the frame-averaging, and possibly dose ramp-up during imaging. This does not appear to be a major impediment to accurate beam profile measurements as the variation is small. The over-response of the EPID with distance off-axis must be accounted for to obtain good agreement between EPID measured profiles and water-tank measurements.

SHAPING THE FUTURE: PHYSICS FOR RADIATION ONCOLOGISTS

N. Suchowerska[1,2,3], A. Miller[1,4] and R. Brown[1]

[1]*RANZCR Radiotherapeutic Physics Panel of Examiners*
[2]*Royal Prince Alfred Hospital, Sydney, NSW, Australia*
[3]*School of Physics, University of Sydney, Sydney, NSW, Australia*
[4]*QEII Health Sciences Centre, Halifa,x NS, Canada*

New technologies, directly resulting from rapid advances in medical physics have stimulated large changes in radiation therapy practice[1,2,3,4]. In response considerable international activity has focused on establishing and implementing new standards and guidelines to improve the **quality** of training and assessment of professionals in radiation oncology [5,6,7,8,].

A recent review commissioned by the Royal Australian and New Zealand College of Radiologists into the validity and reliability of the examinations processes makes recommendations, which may ultimately influence the process of assessment of registrars' competence in radiation oncology. A summary of the critical approach taken in reviewing the examination in radiotherapeutic physics will be presented. This is of particular relevance to radiation oncology medical physicists who are, or may be called upon, to prepare registrars for this assessment.

The principal matters considered include:

- The choice of an appropriate measuring instrument [method of assessment]
- Assessment of content validity to ensure adequacy and representative sampling of the syllabus, via a 'Blueprint for Examination'
- Development of explicit performance standards, improving inter-examiner reliability
- Development of feasible performance standards for each examination papers as an entity
- Formalisation of procedures by which standards are applied in reaching a final judgement about the competence of a candidate on the Radiotherapeutic Physics paper.

A draft assessment procedure has been developed, addressing each of the above, building on the existing solid foundation established by previous Examiners.

REFERENCES:
[1]W. Tome et al (2001), *Radiother Oncol,* 61[1]:33-44.
[2]N. Wachter-Gerstner et al (2003), *Radiother Oncol,* 68[3]:269-76.
[3]M. Braaksma et al. (2003), *Radiother Oncol,* 66[3]:291-302.
[4]S. Das et al (2004), *Med. Phys.* 31[6]:1452-1480.
[5]M. Baumann et al (2004), *Radiother Oncol,* 70[2]:103-105.
[6]R. Hunter et al (2001), *Radiother Oncol,* 70[2]:117-122.
[7]E. Rottinger et al (2001), *Radiother Oncol,* 70[2]:123-124.
[8]T. Eudaldo et al (2001), *Radiother Oncol,* 70[2]:125-136.

NEW RADIOCHROIC FILM DENSITOMETRY SYSTEM

T. Tran[1,2], N. Freeman[1] and P. Johnston[2]

[1]St Vincents Hospital, Darlinghurst, NSW, Australia
[2]Royal Melbourne Institute of Technology, Melbourne, Victoria, Australia

INTRODUCTION: The advantages of radiochromic film in radiation dosimetry are well known. They include dosimetry with high spatial resolution, response less dependent on incident beam energy than common radiotherapy films (such as the Kodak XV films), tissue equivalence and the ability to be handled and developed in room light[1].
This study entails the design and testing of a new radiochromic densitometry system. The system consists of a single light emitting diode (LED), opaque "diffuser" and digital camera. Customised software was developed to analyse images obtained from the digital camera.
METHODS: Standard characteristics of a commercially available super bright red LED (peak wavelength 625nm) was analysed in order to determine the voltage, current and intensity settings. Various methods in diffusing the single LED light source were investigated and it was determined that an opaque transmission "diffuser" was the best alternative. While the intensity of the LED was kept constant, the digital camera exposure times were varied in order to determine a setting which would produce the best image exposure. The system was designed and built and preliminary tests were carried using the standard radiochromic film GafChromic MD-55-2.
RESULTS: LED current vs. voltage curves were characteristically exponential for positive voltage. Studies into LED intensity versus camera exposure produced an unexpected result. At high exposures the camera saturates and if even higher exposures are used the LED intensity apparently decreases. This was thought to be due to the pixels in the charge couple device (CCD) saturating and eventually electronically "bleeding" into adjacent pixels. Using the opaque transmission "diffuser" enabled successful use of the single LED light producing an area of homogenous light intensity in which images of radiochromic films can be obtained.
Preliminary results from radiochromic film characteristic studies show no unusual results.
DISCUSSION & CONCLUSIONS: The single LED, diffuser and digital camera densitometer system provides a practical radiochromic film densitometer.
REFERENCES:
[1]Niroomand-Rad A, Blackwell C, Coursey B, Gall K, Galvin J, McLaughlin W, Meigooni A, Nath R, Rodgers J, Soares C, (1998) *Radiochromic Film Dosimetry: Recommendations of AAPM Radiation Therapy Committee Task Group 55,* Med Phys, 25(11), pp 2093-115.

MEDICAL RADIATION DOSIMETRY WITH RADIOCHROMIC FILM

Martin J. Butson[1,2], Tsang Cheung[1] , Peter K.N. Yu[1] and Peter Metcalfe[2]

[1]Department of Physics and Materials Science, City University of Hong Kong, Tat Chee Avenue, Kowloon Tong, Hong Kong
[2]Department of Medical Physics, Cancer Services, Crown St, Wollongong, NSW, Australia

Photon, electron and proton radiation are used extensively for medical purposes in diagnostic and therapeutic procedures. Dosimetry of these radiation sources can be performed with radiochromic films, devices that have the ability to produce a permanent visible colour change upon irradiation. Within the last ten years, the use of radiochromic films has expanded rapidly in the medical world due to commercial products becoming more readily available, higher sensitivity films and technology advances in imaging which have allowed scientists to use two-dimensional dosimetry more accurately and inexpensively. Radiochromic film dosimeters are now available in formats, which have accurate dose measurement ranges from less than 1 Gy up to many kGy. A relatively energy independent dose response combined with automatic development of radiochromic film products has made these detectors most useful in medical radiation dosimetry.
ACKNOWLEDGEMENTS
This work has been fully supported by a grant from the Research Grants Council of Hong Kong Special Administrative Region, P.R. China (Project No. CityU 100603).

VIRTUAL FILM TECHNIQUE USED IN 3D AND STEP-SHOT IMRT PLANNING CHECK

Y. Wang[1,2], W. Zealey[2], X. Deng[3], S. Huang[3] and Z. Qi[3]

[1]*East Coast Medical Physics, St. Vincent's Clinic, Sydney, Australia*
[2]*University of Wollongong, Wollongong, NSW, Australia*
[3]*Radiation Oncology, Sun Yet-Sen University Cancer Centre, China*

INTRODUCTION: A virtual film technique developed and used in segmented field dose reconstruction for IMRT planning dose distribution check. Film dosimetry analysis is commonly used for the isodose curve comparison but the result can be affected by film dosimetry technical problems, and the film processing also takes a significant amount of workload. This study is focused on using digital image technique to reconstruct dose distribution for a 3D plan by mapping water-scanning data on screen in black and white intensity value, and by simulating the film analysis process to plot equivalent Isodose curve for the planning Isodose comparison check.
METHODS: In-house developed software is used to select the TPR (Tissue-Phantom Ratio) and OCR (Off Central-Axis Ratio) data for different beam field types and sizes; each point dose of the field is interpolated and converted into the greyscale pixel value. The location of the pixel is calculated by the triangular function according to the beam entry position and gantry/collimator angles. After each segment field is processed, the program gathers all the segments and overlays the greyscale value pixel by pixel for all the segments into a combined map. The background value is calibrated to match the water scan curve background level. The penumbra slope is adjusted by an interpolated divergent angle according to the OAD (Off Central-Axis Distance) of the field. A normal film dosimetry analysis can then be performed to plot the Isodose curves.
RESULT AND DISCUSSION: By comparing some typical fields with both single beam and segmented IMRT fields, with the point dose checked by ionization measurement, the central point dose discrepancy is within ±2% and the maximum 3-5% for a random point using TLD technique. Compare the Isodose overlaying result to planning curves for both perpendicular and lateral beam. Although the curve shape for the virtual film viewed is more artificial compared with real film, the results are easier to compare for the quantity analysis with less signal noise, without film processing artefact, no depth dependents and no beam to film entry angle dependences. This creates a more consistent result. The virtual film technique is currently tested in clinical planning check. By using water scanned curve data to build the intensity map of dose distribution for a radiotherapy field, all film processing artifacts can be removed from the analysis results. As the quality assurance, mapped intensity data can be compared with water scanned curve routine based work.
CONCLUSION: Although the intensity map build by virtual film technique given more artificial viewing result compared with real film process, further improvement and further development are obviously to be continued. By using the virtual film technique, an IMRT plan can be checked by one process with the central point dose MU check plus a lateral film shape digital analysis overlay with planning calculated curves, the clinical QA time for IMRT can be saved by simplified procedure with more a consistent result.

SURFACE DOSES UNDER HEAD AND NECK IMMOBILISATION DEVICES

E. Baveas[1]

[1]*Cancer Care Services, Royal Brisbane and Women's Hospital, Brisbane, Qld, Australia*

Methods using ion chambers, TLDs and film were developed to measure the skin-sparing properties of three head and neck immobilisation devices used in radiation therapy, viz. Sinmed multi-perforated and micro-perforated posicast thermoplastic masks (used with a supporting carbon fibre back support), and a Kablite vacuum-formed shell plastic mask (used with a Perspex back support). All measurements were performed with 6 MV beams from Elekta Precise linear accelerators.
Two situations have been considered in this study. In the first situation, phantom surface doses under the flat unmoulded mask and back-support materials lying on the surface of a "solid water" phantom were measured with parallel plate ion chambers and correlated with the physical properties of the materials. In the second situation a particular head and neck treatment technique was adopted and the treatment planned on an anthropomorphic tissue-equivalent phantom. The clinical setup consisted of a wedged pair to the right parotid, planned to deliver a reference dose of 63 Gy to the isocentre, plus an anterior supraclavicular field planned to deliver a reference dose of 50 Gy at a depth of 2 cm. The 3 immobilisation masks were each moulded to the anthropomorphic tissue-equivalent phantom. TLD chips were used to measure the phantom skin dose at a set of 18 locations under each of the 3 immobilisation masks and also without an immobilisation device.
The results clearly demonstrate the extent to which the various immobilisation devices increase the surface dose. Results for the first situation are summarised in Table 1.
The averages of the doses recorded by the TLDs in three separate regions for the second situation are shown in Table 2.
The combined results show that the areal density of the unmoulded mask materials correlates with the surface dose these

Materials on Surface	Physical Thickness (mm)	Areal Density (g/cm^2)	Surface Doses as % of Dmax
None	-	-	12 %
Multi-perforated posicast	2.3	0.18	50 %
Micro-perforated posicast	2.3	0.20	55 %
Shell plastic	1.9	0.25	60 %

Table 1. *Skin-sparing properties of various head and neck immobilisation materials before moulding.*

	Parotid Region (upper neck)	Parotid Region (lower neck)	Supraclavicular Region
No mask	40 Gy	37 Gy	31 Gy
Multi-perforated	49 Gy	47 Gy	38 Gy
Micro-perforated	54 Gy	52 Gy	43 Gy
Shell plastic	48 Gy	46 Gy	39 Gy

Table 2. *Anthropomorphic phantom skin doses from the investigated treatment technique.*

materials produce before moulding, but this correlation is lost after moulding for the clinical situation considered. This change upon moulding is attributed to differences in the amount and spatial variation of the stretching which occurs in the three materials in the moulding process. Film was used to demonstrate qualitatively the distinct spatial variation of the skin dose under the two posicast masks. For a posterior beam passing through the back support used with the Sinmed masks, the surface dose was measured as 68 % of Dmax, which provided an explanation for the observed erythema on the posterior skin when parallel opposed anterior and posterior supraclavicular fields were used clinically with this system.
The results from this study and due consideration of other factors relevant to the clinical use of these devices led to the adoption of the multi-perforated posicast immobilisation mask as the preferred system for routine head and neck treatments at the Royal Brisbane and Women's Hospital.

COMMISSIONING OF A MOSFET IN-VIVO PATIENT DOSE VERIFICATION SYSTEM

G. O.Jenetsky and R L. Brown

Andrew Love Cancer Centre, Geelong Hospital, Geelong, Vic, Australia

INTRODUCTION: TLD dosimetry has long been used for in-vivo measurements in estimating absorbed dose to critical structures on patients. Preparing TLDs for measurement, and then obtaining the results is a time consuming process taking many hours. The Thomson-Neilson "MOSFET 20" (Metal Oxide Semiconducting Field Effect Transistor) dose assessment system, allows for in-vivo measurements (preparation and results) within minutes. Before being used clinically for dose verification, the MOSFETs were tested against the manufacturer's technical specifications, and compared with results from TLDs measured under controlled experiments and patient measurements.
METHODS: Standard sensitivity MOSFETs (TN-502RD) were used with the bias supply set to High sensitivity range. MOSFETs were tested for linearity (5-100cGy) and their calibration factors obtained for all energies (6MV, 18MV, 6MeV, 12MeV, 16MeV, 20MeV) using the method described by Ramani[1]. MOSFETs and TLDs were exposed to a 6MV beam for 50MU at various depths (RW3 solid water phantom) and field sizes and compared to results taken with an ion chamber. Measurements using both systems were also taken at beam edge and 5mm and 10mm out of the field. Eleven patients, who had lens dose assessment requests were measured with both TLDs and MOSFETs and a paired t-test was performed on the results. On two patients, multiple (nine and four) MOSFET measurements were taken and the range of results compared to the range obtained from the TLDs. (See *Table 1*)
RESULTS: MOSFET linearity obtained co-efficients of $R^2 \geq 0.996$ for all energies, this compared to $R^2 \geq 0.996$ recorded by both Ramani and Chaung[2]. The y-intercept values varied from 0 to -2.0mV. Greatest variation between calibration factors, measured for each energy, was 7.5%, this is substantially greater than 3.8% quoted by the manufacturer. For the measurements taken at varying depths and field sizes both TLDs and MOSFETs agreed with the ion chamber results ±1cGy. Measurements taken at beam edge varied ±6cGy. 5mm and 10mm out of the field MOSFETs and TLDs recorded the same dose. The paired t-test performed on the data taken from 11 separate lens measurements did not show any significant difference between the means at the 95% level of significance (left lens p=0.13, right lens 0.67)

	MOSFET total dose Gy	TLD total dose Gy
Left lens	2.5 – 3.0	2.5 – 2.8
Right lens	3.0 – 3.6	3.0 – 3.5
Right Outer Canthus	3.7 – 4.4	3.8 – 4.2

Table 1. *Dose range estimated by MOSFET and TLD measurement.*

DISCUSSION & CONCLUSIONS: The negative y-intercept suggests that they should be added to the raw reading before being converted to dose, this is important when measuring in low dose regions. The problem with a larger than expected variation between energies, can easily be overcome by using individual calibration factors for each energy. For central beam and scatter doses results between TLDs and MOSFETs varied by 1cGy. The greatest variation of 6cGy occurred at beam edge where the dose gradient is greatest. This can be attributed to TLD chips measuring over a 9mm^2 area while a MOSFET measures over 0.04mm^2. Multiple readings per patient are now being performed relying on slight positional changes to provide a larger area for the MOSFETs to record "point" measurements. After a careful commissioning procedure, the MOSFET 20 dose verification system provides reliable, consistent and accurate measurements equal to that of a TLD system. However, the MOSFETs can be prepared for use within seconds, and give results of total dose within minutes, and can be re-used instantaneously making them a far more efficient method of patient dose verification.

REFERENCES:

[1]R. Ramani, S. Russell, P. O'Brien (1997) *Int. J. Radiation Oncology Biol. Phys.*, 37(4): 959-964.
[2]C. Chuang, L. Verhey, P. Xia (2002) *Med. Phys*., 29(6): 1109-1115.

UNCERTAINTIES IN MEGAVOLTAGE PHOTON CALIBRATIONS WHEN ADOPTING TRS-398

D. Butler and D. Webb

Australian Radiation Protection and Nuclear Safety Agency, Yallambie, Vic, Australia

INTRODUCTION: The Australian primary standards of air kerma and absorbed dose are realized using Co-60 qualities. To calibrate megavoltage photon beams from linear accelerators, radiotherapy centres have their ionization chamber calibrated in a Co-60 beam, and then use a protocol to transfer this calibration to the higher energy. At present, there are two protocols in use: the ACPSEM protocol[1] (an adaptation of the IAEA's TRS-277 Code of Practice), based on an air kerma calibration, and the IAEA's TRS-398 Code of Practice[2], based on an absorbed dose to water calibration. In 2004, several centres have either recently adopted the new protocol, or are about to make the change. We calculate the changes to be expected when an Australian therapy centre changes protocols to TRS-398. These differences are discussed in the light of the uncertainties which are inherent in the primary standards and the protocols.

RESULTS: We review the uncertainties in the primary air kerma and absorbed dose standards for Co-60 radiation. These are currently given as 0.3% and 0.2%, respectively, at the 1 sigma level. However, it has been suggested that the overall uncertainty may be underestimated by a factor of about 2. This does not affect the reproducibility of a chamber calibration, which for NE2571 chambers owned by ARPANSA is of the order of 0.2%. The uncertainties in the theoretical k_Q correction factors in TRS-398 are also reviewed. These values have a standard uncertainty of about 1%.

In adopting the new protocol, it is helpful to separate changes arising from the protocol itself from changes which arise from the use of a different primary standard for the chamber calibration. To this end, the theoretical ratio between the absorbed dose to water and air kerma calibration coefficients has been calculated using equation 1:

$$\frac{N_{D,W,Q_0}}{N_{K_{Co}}} = \left[(1-g)k_{att}k_m k_{cel}\right]_{Co}\left(S_{w,air}\right)_{Q_0}\left[p_{cav}p_{wall}p_{cel}\right]_{Q_0}\left(p_{dis}\right)_{Q_0}. \qquad (1)$$

The meanings of the symbols are explained in reference 2, and numerical values come from the ACPSEM protocol, except for p_{dis} which is estimated from depth dose data, and k_{cel} which is set to 1. At Co-60, this ratio is calculated to be 1.094 for an NE2571 chamber. At ARPANSA, the ratio has been measured to be 1.095 with a standard deviation of 0.2% (average of 40 measurements using 4 chambers). Hence, we expect only a small change to come from the difference between ARPANSA's air kerma and absorbed dose to water standards. The absorbed dose will be 0.1% higher using the new protocol. For qualities other than Co-60, Equation 1 gives k_Q factors which differ by a maximum of a further 0.2% – 0.4% between the protocols, above the 0.1% which derives from the primary standards. Hence, users can expect a linac calibration to change by 0.3% - 0.5%, the absorbed dose always being higher when TRS-398 is used. When Type A standard uncertainties associated with ionization chamber measurements are included, we estimate this range to expand to 0.0 % - 0.8 %.

REFERENCES:

[1]Australian College of Physical Scientists and Engineers in Medicine, *Absorbed Dose Determination in Photon and Electron Beams: An Adaptation of the IAEA International Code of Practice*, 2nd Edition, 1998, ACPSEM.
[2]P. Andreo, D. T. Burns, K. Hohlfeld, M. S. Huq, T. Kanai, F. Laitano, V. Smythe and S. Vynvkier, (2000) *Absorbed Dose Determination in External Beam Radiotherapy: An International Code of Practice for Dosimetry based on Standards of Absorbed Dose to Water*, IAEA Technical Reports Series No 398, Vienna, International Atomic Energy Agency.

THE ADOPTION OF TRS 398 AS A MEGAVOLTAGE CODE OF PRACTICE (CoP) AT WILLIAM BUCKLAND RADIOTHERAPY CENTRE, ALFRED HOSPITAL, MELBOURNE, AUSTRALIA

F. Gagliardi, R. M. Millar, J. Droege, R. Smith and S. Elliott

William Buckland Radiotherapy Centre, The Alfred Hospital, Melbourne, Vic, Australia

INTRODUCTION: The Radiotherapy Interest Group (RIG) of the Australasian College of Physical Sciences and Engineering in Medicine (ACPSEM) has recommended that physicists in Australia and New Zealand adopt the IAEA TRS 398 CoP by the end of 2004.
The TRS 398 CoP is an absorbed dose to water protocol which covers most radiation types used in radiotherapy, including megavoltage photons and electrons and kilovoltage photons.
For TRS 398, the standards laboratory is required to provide $N_{D,wQ0}$ for a suitable range of energies and likewise a set of correction factors $k_{Q,Q0}$ which correct for differences between the calibration energy Q_0 and the user's energy Q. If Q_0 is ^{60}Co then TRS398 provides a table of $k_{Q,Q0}$.
For megavoltage photons, the user's energy Q is determined by measuring $TPR_{20,10}$. For megavoltage electrons, the user's energy Q is determined from R_{50}. This paper reviews the differences between the Air Kerma based CoPs and TRS398 and discusses the differences in the data measured at William Buckland Radiotherapy Centre using the two different methods.
CONCLUSION: The use of TRS398 is straight forward for megavoltage photons and electrons and the difference in the absorbed dose to water using the two different methods is 1.1% for both 6MV photons and 18MV photons.
For electrons the maximum difference was 1.2 % for a 6 MeV beam and the mean difference for five electron energies between 6 and 18 MeV was 0.8 %.
REFERENCE:
Technical Report Series 398, Absorbed Dose Determination in External Beam Radiotherapy, IAEA, Vienna (2000).

CALIBRATION OF PHOTON BEAMS USING TRS398 AT RECOMMENDED DEPTH MAKING 1mu = 1cGY (GOODBYE TO d_{max} AND ALL THAT!)

S.J.Howlett and M.P.Barnes

Department of Radiation Oncology, Newcastle Mater Misericordiae Hospital, Newcastle, NSW, Australia

INTRODUCTION: For many years now absolute dose determination protocols using ionization chambers have recommended calibrating dose at depth beyond the depth of dose maximum (d_{max}). However by tradition and because of machine design, the relationship between dose and monitor units have been normalized at depth of d_{amx}. This seems somewhat outdated since the vast majority of treatments are delivered isocentrically to a prescription point at a depth much closer to the recommended calibration depth than to d_{max}. Indeed d_{max} can be a troublesome creature and is rarely used as a prescription point for dose delivery in photon beam treatment. This work looks at the process of changing from a 100cm SSD, 10cm x 10cm field, d_{max} depth mu normalization to a 100cm SCD, 10cm x 10cm field, d_{cal} depth mu normalization for photon beams.
METHODS: An email query was sent out via the ACPSEM list server to determine the current methods used by centres in Australia and New Zealand. Our centre uses Varian linacs and contact was made with Varian Australia to seek their recommendations on changing our calibration setup. Preliminary work was conducted on our 4MV Clinac 600 linac since this would involve the largest change in mu adjustment. Data was acquired under the new system and a new machine modelled on our Pinnacle RTP system. The other two linacs in the department are 21EX with 6MV and 18MV photon beams. We intend to investigate and implement the same technique in these machines and systems
RESULTS: Most centres reported they still use the traditional setup. Simple calculation reveals a required increase in output of 9%, 6% and 5% for 4MV, 6MV and 18MV respectively, when 100cm SCD, d_{cal} is used. The 4MV was tested for operation after changing the calibration values. The 600C performed as normal under the 250 mu/min clinical dose rate. The calibration depth for this energy is 5cm and all relative output data was acquired here so that a new machine could be commissioned for our Pinnacle RTP computer. At the time of writing the 4MV beam data is being used to alter our Pinnacle RTP for thorough verification. We intend to implement the new system on this machine and proceed to alter our remaining two linacs in a similar way.
DISCUSSION & CONCLUSIONS: The method of changing calibration setup and MU/dose relationship described here is achievable with Varian linacs. Changeover requires a systematic and careful approach with proper verification procedures. The disruption to clinical treatment is minimal with adequate forward planning
ACKNOWLEDGEMENT: The author gratefully acknowledges helpful discussion with Ole Hagen of Varian Australia and ACPSEM respondents to the email inquiry regarding calibration setup.
REFERENCES:
[1]*Technical Report Series 398: Absorbed Dose Determination in External Beam Radiotherapy. An International Code of Practice for Dosimetry Based on Standards of Absorbed Dose to Water*. IAEA, Vienna. 2000.

A TLD THERAPY DOSIMETRY QUALITY ASSURANCE PROGRAM FOR AUSTRALIA-RESULTS 2002-2003

M. Cox, R. Huntley and D.Webb

Australian Radiation and Nuclear Safety Agency (ARPANSA), Melbourne, Vic, Australia

INTRODUCTION: Australia has developed a TLD Quality Assurance program traceable to the national primary standard of absorbed dose to water. The service is based on IAEA procedures so that previous results can be compared. In addition to the nominal 2 Gy exposure evaluation, ARPANSA also offers beam quality evaluations. A pilot study was undertaken by ARPANSA during May to June 2002 involving 6 Australian radiotherapy centres. After assessing the pilot study and obtaining positive results, the full Australian TLD Quality Assurance Program began in March 2003.
METHODS: IAEA standard capsules and jigs were sent to each of the centres involved, along with several capsules filled with LiF powder. Each centre used 1, 2 or 3 different beam energies to expose their capsules to 2 Gy at D_5 position. Another 2 capsules were exposed to 2 Gy in a water phantom, with either a $TPR_{20/10}$ or $D_{20/10}$ beam specification for each beam used. Centres were given a 'window' in which to irradiate their capsules, while calibration capsules were exposed at ARPANSA to a nominal absorbed dose to water of 2Gy.
RESULTS: 36 beams were surveyed in batches of 4-6 centres. The difference between centre stated dose D_s and ARPANSA measured dose D_m for all 36 beams tested was within ±3%.

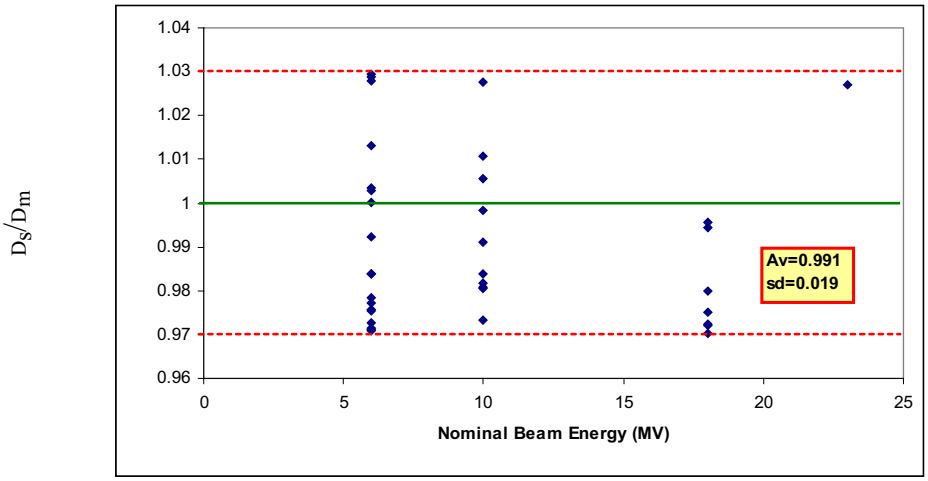

Figure 1. *Results of the Australian TLD Quality Assurance Program 2002-2003.*

DISCUSSION & CONCLUSIONS: ARPANSA's national TLD dosimetry audit program provides an important check on medical linear accelerators. It also provides assurance that protocols are being applied uniformly and appropriately. There are approximately 33 Australian radiotherapy centres and 17 of these centres have taken part to date. Of those centres not participating, some cited lack of funding, while others did not believe the audit necessary for their centre. Despite the program being supported by the ACPSEM, participation needs to improve to develop full value. While the program cannot be cost free, ARPANSA will ensure that costs are as low as reasonably possible so as to allow centres to budget for the service.
ACKNOWLEDGEMENTS: The IAEA is gratefully acknowledged for their previous audits on Radiotherapy Centres in Australia, and for their guidance in developing Australia's own program.
REFERENCES:
[1]J. Izewska (1998) *IAEA DMRP-9809.*
[2]M. Cox (2002) *International symposium on standards and codes of practice in medical radiation dosimetry Vienna (Austria) 25-28 Nov 2002 Book of extended synopses,* 209-210.

ELVIS THE PELVIS: A PURPOSE BUILT ANTHROPOMORPHIC PHANTOM FOR AN AUSTRALIASIAN LEVEL III DOSIMETRY INTERCOMPARISON

K. Harrison[1], S. Rolton[2], D. Cornes[1], J. Denham[1], M. Ebert[1], S. Howlett[1] and C. Hamilton[1]

[1]*Collaboration between the Centre for Clinical Radiation Research and the Trans-Tasmin Radiation Oncology Group (TROG), Newcastle Mater Misericordiae Hospital, Newcastle, NSW, Australia*
[2]*Wysiwig 3D P/L, Sydney, NSW, Australia*

INTRODUCTION: In a previous Level III dosimetry intercomparison, phantom design and recommendations were made to improve dosimetric reproducibility and accuracy[1]. These recommendations have been addressed for an additional Level III dosimetry intercomparison with the design and manufacture of a specifically designed anthropomorphic phantom. It is anticipated that this 'anatomically correct' phantom will provide this study with clinically relevant results relating to regions of interest for both tumour control and normal tissue tolerance. These results may benefit analysis of outcome for prostate and rectal cancer treatments, especially the clinical trial environment.

METHODS: The phantom was based on the organ outlines generated from a human CT and contains structures to simulate bowel, skeletal structure, seminal vesicles, prostate and bladder. Points of interest were located throughout the dataset to identify where point-dose values could be measured with TLD materials. The centre of the prostate was identified as the location for point-measurement with a small-volume ionization chamber. The materials used in this phantom were tested against water to determine relative attenuation, density and CT numbers. Three materials were chosen to mimic bone, organs, and a backfill material.
RESULTS: The phantom has been manufactured in five slices with 30 TLD locations and one cavity matched to accommodate a Wellhofer cc13 chamber. The phantom CT scans show good matching of densities and organ geometries. Due to heat release during manufacture, tiny air-gaps are present throughout the phantom which produce artifacts on lateral images, but have minimal implications on the dosimetry. Initial measurements indicate the reproducibility to be within 0.1% for the chamber measurement and within 2% for TLDs.

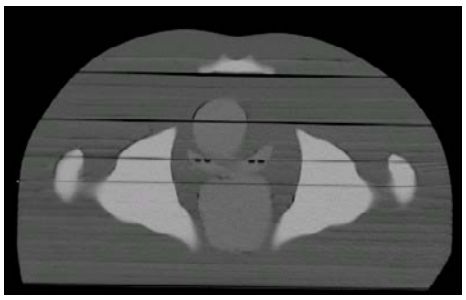

Figure 1. *CT Image of Phantom - ELVIS.*

DISCUSSION & CONCLUSIONS: The phantom incorporates the recommendations made by Kron et al[1], and will be a effective tool for an intercomparison of prostate and rectal treatments in Australasia.
ACKNOWLEDGEMENTS: Department of Health and Aged Care, Health Technology and Evaluation Centre and P-Type P/L, Blackburn, Melbourne
REFERENCES:
[1]T. Kron, C. Hamilton, M. Roff, J. Denham (2002), *Int J Radiation Oncology Biol Phys*, 52, 2:566-579.

DOSE MEASUREMENT IN THE LEVEL I SECTION OF THE NATIONAL DOSIMETRY PILOT PROJECT

S. J. Howlett[1], M. A. Ebert[1], Kristie Harrison[1], Chris Hamilton[1], Deidre Cornes[2] and J. W. Denham[1]

[1]*Department of Radiation Oncology, Newcastle Mater Misericordiae Hospital, Newcastle, NSW, Australia*
[2]*Trans-Tasman Radiation Oncology Group Operations Office, Newcastle Mater Hospital, NSW, Australia*

INTRODUCTION: The National Dosimetry Pilot Project commenced in 2004. It will be the largest dose intercomparison study conducted in Australasia, involving some 32 centres. It extends on the work of Kron *et al*[1]. The project involves the use of a purpose built anthropomorphic phantom in a level III dosimetry study for prostate and rectal treatments. Additionally a compact water phantom will be used for a level I absolute dose comparison. The use of a small volume ionization chamber is included for accurate absolute dose and prescription point dose measurements. Thermoluminescent Dosimeters (TLD) will be used as relative dosimeters to map doses to points of interest in the treated volumes. The particulars of the Level I study are presented here.
METHODS: A 30cm cubic acrylic phantom was constructed to hold a cc13 Wellhofer chamber and allow absolute dose measurement for reference conditions. The empty system is light weight and easily transportable to various centres, at which water filling can occur. The cc13 is waterproof and hence can be directly inserted in to the water phantom. It is connected to a Dose 1 Wellhofer electrometer. This measuring assembly was intercompared with our ARPANSA calibrated department standard assembly (Farmer 2571 0.6 cc chamber and NE 2560 meter) for 4MV, 6MV and 18MV beams according to IAEA TRS277 and TRS398 protocols. It also came with its own calibration from Germany (Scanditronix Wellhofer GMBH). Dose can be measured at depths from 1cm to 20cm as well as the TPR^{20}_{10}. Once the absorbed dose to water calibration factor ($N_{D,w,Qo}$) was determined, calibrations in clinical megavoltage photon beams can be performed at the various participating centres. Initial calibrations and comparisons will be performed at several Sydney sites to determine an average $N_{D,w,Qo}$ which can then be used for all further calibrations. This improves the reliability of the calibration factor. A special solid water holder for TLD relative dosimeter calibration was made. This holder sits at the calibration depth in water and is irradiated immediately after the absolute dose determination, thus providing an accurate reference for the various point measurements made throughout the anthropomorphic phantom irradiated volume.

RESULTS: The $N_{D,w,Qo}$ using a 4MV (TPR^{20}_{10}= 0.628) beam was found to be within 0.4% of the PTW documented value. Calibrations for our 5 clinical photon beams were made with both assemblies and agreement was within 0.3%. It is anticipated that several centres will have been visited by November and preliminary results will be presented at the conference.

DISCUSSION & CONCLUSIONS: A portable, accurate method for conducting a precise Level 1 dosimetry intercomparison has been developed. This will represent the largest and most accurate study yet conducted in Australasia. Earlier TLD audits conducted by IAEA through ARPANSA, while effective and useful, cannot achieve the accuracy inherent in the use of ionization chambers as outlined in this work. Combined with the overall level I/III study, it is hoped that this pilot scheme will lead to a permanent National Dosimetry facility which will improve and then maintain the quality of dose delivery to radiotherapy patients in Australia and New Zealand.

ACKNOWLEDGEMENT: We gratefully acknowledge the equipment contribution of the cc13 chamber and Dose 1 electrometer from Oxford Scientific, 64 Derby St, Silverwater. NSW.

REFERENCES:

[1]Kron et al, *Int J Radiation Oncology Biol Phys*, Vol 52, No 2, pp 566-579, 2002.

AUSTRALIASIAN LEVEL III DOSIMETRIC INTERCOMPARISON USING A PURPOSE BUILT ANTHROPOMORPHIC PHANTOM

C. Hamilton[1], M. Ebert[1], K. Harrison[1], D. Cornes[1], S. Howlett[1] and J. Denham[1]

[1]Collaboration between the Centre for Clinical Radiation Research (CCRR) and the Trans-Tasmin Radiation Oncology Group (TROG), Newcastle Mater Misericordiae Hospital, Newcastle, NSW, Australia

INTRODUCTION: Comparison of the absolute dose given at a reference point is defined as a level I dosimetric intercomparison. Level III dosimetry methodology will verify radiotherapy treatment from patient data acquisition through to planning and treatment (figure 1). The CCRR (Centre for Clinical Radiation Research) at the Department of Radiation Oncology, Mater Hospital, Newcastle, in collaboration with TROG (Trans-Tasmin Radiation Oncology Group), is undertaking a combined level I/III dosimetry intercomparison project as a follow up to a previous study performed in 1999[1], which involved 19 Australian and New Zealand centres.

METHODS: A purpose-built anthropomorphic pelvic phantom has been designed and constructed for anatomical accuracy and dosimetric reproducibility. Clinically-relevant points were located throughout the phantom for TLDs to be placed and the centre of the prostate was identified as the location for point-measurement with a small-volume ionization chamber.

RESULTS: Radiotherapy centres throughout Australia and New Zealand were invited to voluntarily participate and 32 sites expressed an interest. After initial testing and development of study protocol in mid-2004, site visits will commence. The phantom will be transported to each department and accompanied by a physicist and additional member of CCRR staff. The study requires CT, simulation, planning and treatment of the phantom for prostate and rectal treatments. The project will require one day at each treatment centre with (in addition to access to equipment) the time of one local radiation oncologist, radiation therapist and physicist. Protocols for performing phantom irradiations have been developed, as well as a protocol for the undertaking of a Level I dosimetry measurement (basic accelerator output) at each centre. Plans are underway for the use of the SWAN software for analysis of treatment plans collected at each centre.

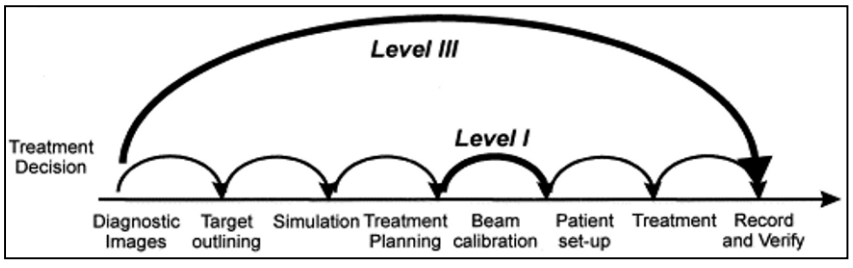

Figure 1. *The role of Level I and III dosimetry intercomparisons within the radiotherapy treatment chain.*

DISCUSSION & CONCLUSIONS: This study will provide substantial clinical and dosimetric information regarding structure outlining, local irradiation techniques, geometric and dosimetric accuracy, dose distributions in realistic phantom, the accuracy of different treatment planning systems as well as the feasibility of multi-centre dosimetry studies. Each centre will receive an individual dosimetry report but cumulative results will only be reported and published in an anonymous form.

ACKNOWLEDGEMENTS: Project jointly funded by the Department of Health and Aged Care, Health Technology and Evaluation Centre and the CCRR. The equipment contribution of the cc13 chamber and Dose 1 electrometer from Oxford Scientific, 64 Derby St, Silverwater, NSW.

REFERENCES:

[1]T. Kron, C. Hamilton, M. Roff and J. Denham (2002), *Int J Radiation Oncology Biol Phys*, 52, 2:566-579.

PRACTICAL PERFORMANCE FOR CT SIMULATOR SET UP AND COMMISSIONING FOR 3D RADIOTHERAPY

Y. Wang[1,2], A. Rinks[1] and W. Zealey[2]

[1]*East Coast Medical Physic, NSW, Australia*
[2]*University of Wollongong, Wollongong, NSW, Australia*

We present a summary of the protocol used to commission two GE LightSpeed and One Siemens CT-Sim for 3D radiotherapy in early 2004. The protocol defined was based on AAPM TG-66 and ACPSEM 1997 position paper.

Scanning Med-TEC Iso-align Laser Alignment Device for three-D isocentre alignment

1. *Couch Movement Accuracy* for both manual and scanning movement checked before isocentre alignment, as the reference distance is required for the external isocentre setup.
2. *Gantry scan rotation circle vertical and tilted angle alignment* checked by overlaying the vertical and horizontal image coordinate lines using the aligned ball-bearings in the phantom to determine the gantry cross plane image vertical accuracy and tilt angle accuracy.
3. *Zero scan position* determined by scanning the horizontally set Med-Align phantom, and adjusting the phantom position forward and backward to match the image scanning centre.
4. *Internal lasers position* determined by the position of aligned Med-Align phantom after the scanning centre determined.
5. *Couch top to Gantry Perpendicular* checked by matching the couch axis in the longitudinal and lateral direction to the position of the laser lines determined according to the CT scanning orientation.
6. *Couch Central Axis* aligned to ensure the couch travels though the internal isocentre for the full range of longitudinal of movement.
7. *External isocentre and laser focus* can be determined by moving the couch back a set distance (50cm or 60cm normally) from the internal isocentre.

Planning image transfer and DRR image alignment

1. *Scanning Centre* indicated on the planning image depends on the functionality of the planning system. Some planning systems load the image with the scanning centre at zero position, others load up the image with the absolute distance.
2. *Zero Slice position* aligned to the centre of the phantom using the external laser.
3. *Orientation and Distance* were checked by scanning the Iso-align in both vertical and horizontal directions with the slice thickness less than the diameter of ball-bearing size, and the orientation and distance are measured over the slice images and DRR images.

Electron Density Calibration

1. *Tube Voltage kV* – the electron density depends on the voltage setting (kV). Calibrations are carried out for different kV settings and separate electron density tables are generated.
2. *Tube Current mA* – experimental results show that change of HU's is not significant, but low mA scans produce higher Standard Deviation and noise.
3. *Scan speed* – made no noticeable differences if scan setup is unchanged (e.g. kV or collimation)
4. *Collimation* – experimental results show that the same slice thickness with different collimation, e.g. 1x5 or 5x1 in the reconstructed image, will cause electron density values to vary. It is suggested that the slice thickness in different collimation settings should be calibrated separately.
5. *Sample Area* – the readings taken from close to the phantom surface can be different compared with the readings taken from a deeper position in the phantom due to different scanning scatter effects. Calibration tables for the body and head-neck were performed separately.

CONCLUSION: For a new CT installation the scanning isocentre is determined first before setting up the couch and external lasers. This routine assists the engineer during installation and commissioning to ensure the CT scanner meets specifications required for a therapy scanner. The electron density should be calibrated for each kV used. Collimation also affects electron density values. Separate tables for different volumes such as body and head and neck may be warranted.

IMPLEMENTATION OF VIRTUAL SIMULATION WITH A WIDE-BORE MULTISLICE HELCALCT SCANNER

Peter Greer[1,2] and John Kenny[1]

[1]*Newcastle Mater Hospital, Newcastle, NSW, Australia*
[2]*University of Newcastle, Newcastle, NSW, Australia*

INTRODUCTION: Multislice large-bore CT scanners specifically designed for radiotherapy have very recently become available. The issues relating to these type of scanners in radiotherapy and the implementation of virtual simulation are

therefore of much current interest. A GE LightSpeed RT 4-slice helical CT scanner with a 80 cm bore size was installed in the radiation oncology department of the Newcastle Mater Hospital. This replaced our only simulator, a conventional unit. Specific issues relating to the imaging performance, and virtual simulation process with the large-bore multislice scanner were studied to ensure an accurate radiotherapy process.

METHODS: The detector array fully samples a 50 cm diameter scan circle. The reconstructed diameter can be increased to 65 cm with partial sampling of the extra volume. The GE Advantage Sim (ASim) virtual simulation software was commissioned, with transfer of CT images and DICOM RT plans to the Pinnacle radiotherapy planning system (RTPS) for dose calculation. Some specific issues investigated were: 1) The image quality performance for image reconstruction with the 65 cm area compared to 50 cm was measured with a line-pair phantom. 2) The accuracy of CT numbers with lateral position was assessed with a commercial electron density phantom. 3) Couch lateral movement and sag during acquisition were measured with the couch weighted with 86 kg. 4) The accuracy of the transfer of plans from ASim to Pinnacle was verified with known plan geometries.

RESULTS: 1) Image resolution throughout the entire CT image was found to be significantly lower when scan reconstruction was performed with 65 cm scan circle compared to 50 cm. The 0.3, 0.38 and 0.5 lp/mm bars were clearly distinguishable with the 50 cm reconstruction compared to only the 0.3 lp/mm bars in the 65 cm reconstruction. 2) CT numbers varied significantly outside the 50 cm reconstructed area (see Fig).

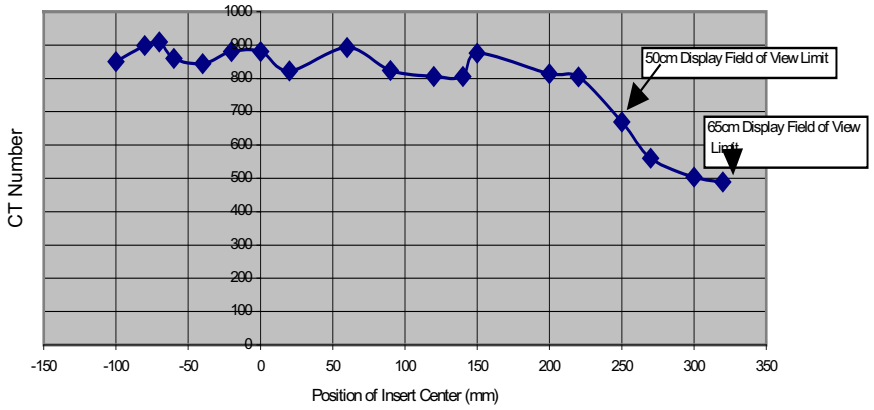

Figure 1. *Variation in CT number of a bone insert with lateral position.*

3) Couch lateral movement during scanning was within 1 mm. Couch sag was 4 mm at the imaging plane relative to the laser plane. 4) Offsets in the CT and isocentre coordinates occur during the transfer to Pinnacle, however the anatomical locations of the beams are transferred correctly. Plan names and identifiers are not imported into Pinnacle making plan identification problematic.

DISCUSSION & CONCLUSIONS: Scanning should wherever possible be performed within the 50 cm diameter fully sampled region due to inferior quality and large variation in CT number. The isocentre defined in CT coordinates within the patient during virtual simulation is ~4 mm above the tattoos marked using the external lasers without patient sag, therefore couch-height set-up must be used for virtual simulation patients. The GE scanner and ASim software export the DICOM standard patient-specific coordinate system, while the Pinnacle RTPS currently does not. It is advisable to print hard-copies of plan details and isocentre location as transfer of the correct plan to Pinnacle is otherwise difficult to verify. No major problems resulting from the lack of a conventional simulator within the department have arisen to date.

A METHOD FOR DETERMINING ANGLES TO ACHIEVE IMPROVED CT IMAGES WITH LIMITED DATA

R. Widita[1] and L. Holloway[2]

[1]*School of Physics, University of New South Wales, Sydney, NSW, Australia*
[2]*Department of Radiation Oncology, Liverpool Hospital, Liverpool, NSW, Australia*

INTRODUCTION: In radiotherapy planning, margins are used to account for the uncertainties due to internal organ and patient motion as well as set-up error. Improvement in radiotherapy treatments may be achieved by reducing the set-up uncertainty and thus treatment margins allowing a higher dose to be delivered to the target volume. It is important to be able to verify the success of the treatment by determining the position of patient and the dose deposited in the patient at each fraction. One possibility for achieving this would be to collect limited information while the patient is on the treatment couch. Ideally, data for the images would be collected at the same angles as those used for treatment. Several algorithms have been proposed in the literature to generate an image from limited projections [1-2]. These methods have investigated

the development of good quality images with a given set of limited data, often approximating the missing data. The aim of this study is to develop a method for determining intelligent angles to use to reconstruct an image for dose verification.

METHODS: A method optimising the angles based on an objective function is required. The methods developed here are based on image correlation and projection correlation. Two optimisation methods, deterministic and stochastic (simulated annealing), were also assessed. The effectiveness and practicality of each of these combinations were compared. The image correlation is considered here to assess the accuracy of projection correlation.

RESULTS AND DISCUSSION: Based on previous authors work, 7 beams were considered to give acceptable results [3]. We consider 12 projection data equally spaced at 30^0 angular increments as the angles to be initially selected from to compare all possible combinations. The best result is achieved with image correlation. However, this algorithm is very time consuming, especially when it is applied to the stochastic optimisation. Projection correlation images have similar quality with image correlation images. This method is much faster than the image correlation. Deterministic and simulated annealing optimisation using projection correlation (fig.1d & e) produces no significant differences.

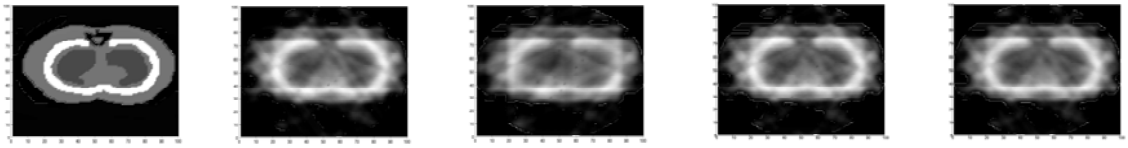

(a) (b) (c) (d) (e)

Figure 1. *Reconstruction using 7 angles with 12 projection data (a). Original Image (b). Image Correlation (c). Projection Correlation (d) Deterministic algorithm (e) Simulated Annealing algorithm*

CONCLUSION: All methods considered improved the image quality by selecting 'intelligent' beam angles. The image achieved with angles selected by simulated annealing using projection correlation gives similar quality with image correlation images. This method presents several advantages. It can be applied without any iterations, and it produces a fast algorithm. Together with more advanced image reconstruction software this could potentially be used in a clinical environment.

REFERENCES:

[1]Brunetti, A. and B. Golosio (2001). "A new algorithm for computer tomographic reconstruction from partial view projections." Med. Phys. 28(4): 462-468.

[2]Peng, H. and H. Stark (1992). "Image recovery in computer tomography from partial fan-beam data by convex projection." IEEE Trans. Med. Imag. 11(4): 470-478.

[3]Thomas Bortfeld, J. B., R. Boesecke, Wolfgang Schlegel (1990). "Methods of image reconstruction from projections applied to conformation radiotherapy." Phys. Med. Biol. 35(10): 1423.

EFFECT OF CONTRAST ON TREATMENT PLANNING SYSTEM DOSE CALCULATIONS IN THE LUNG

J. Lees, L. Holloway, M. Fuller and D. Forstner

South Western Sydney Cancer Services, Liverpool, NSW, Australia

INTRODUCTION: Contrast-enhanced x-ray computed tomography is utilised in the planning of radiotherapy lung treatments to allow greater accuracy in defining tumour volume and nodal areas. The use of contrast results in increased density in the region of the tumour and may result in an overall increased density in the lung volume.

It is possible that this change in density may affect the accuracy of any dose calculations based on this CT data. As yet, the effect of the contrast agent on the calculations performed by the treatment planning computer is unclear. Ideally, a study would be undertaken using pre- and post- contrast patient data, however this may be considered unethical as an extra CT scan would be required. For this reason, the following study was undertaken to assess the possible impact in a simulated environment.

The object of this study was to explore the effect of the contrast agent upon the isodose curves and the monitor units calculated by the treatment planning system.

METHODS: Two investigations were made. Initially, pre- and post-contrast images were acquired using an anthropomorphic phantom. Contrast-enhancement was simulated by replacing cylindrical sections of the lung with lengths of drinking straw containing contrast agent. The effect of increased density in the tumour volume was considered in this comparison.

Secondly, block density corrections were used in an existing patient dataset to simulate an increase in lung density and compared with the original dataset.

In the two investigations, a treatment was generated using both datasets. Fields were placed on the non contrast-enhanced scan, and then transferred onto the contrast-enhanced scan. The numbers of monitor units calculated in each of the plans were compared, as were the resulting isodose curves.

RESULTS: In the first investigation, the relative electron density in the contrast-enhanced scan varied between 0.523 and 1.705 within the tumour volume. This resulted from the presence of undiluted contrast agent and the associated artifacts, which is unlikely to occur in a clinical situation. The relative electron density within the tumour volume ranged from 0.966 to 0.987 in the non contrast-enhanced dataset. No significant differences were apparent in the resultant isodose curves, and the number of monitor units calculated was comparable however this may be due to the averaging of the densities from the contrast and the artefact.

In the second investigation the numbers of monitor units calculated before and after altering the electron density in the existing patient dataset were consistent. Differences however, were apparent in the isodose curves. These may influence the acceptability of a plan.

DISCUSSION & CONCLUSIONS: No significant discrepancies between plans generated from non contrast-enhanced and contrast-enhanced phantom datasets were observed.

The contrast agent was found to have a minimal dosimetric impact upon the treatment plans generated.

THE ADOPTION OF TRS 398 AS A KILOVOLTAGE CODE OF PRACTICE IN HOSPITALS FOR HVL's LESS THAN 3 mm Al

R. M. Millar[1], F. Gagliardi[1], D. Butler[2] and D. Webb[2]

[1]*William Buckland Radiotherapy Centre, The Alfred Hospital, Melbourne, Vic, Australia*
[2]*Ionizing radiation standards, ARPANSA, Yallambie, Vic, Australia*

INTRODUCTION: The Radiotherapy Interest Group (RIG) of the Australasian College of Physical Sciences and Engineering in Medicine (ACPSEM) has recommended that physicists in Australia and New Zealand adopt the IPEM (1996) Kilovoltage Code of Practice[2] (CoP) for the calibration of Kilovoltage units and has also recommended that radiotherapy centres change over to the IAEA TRS 398[1] CoP by the end of 2004.

The IPEM CoP is an Air Kerma protocol and breaks the kilovoltage range into three categories, Medium energy X-rays (0.5-4 mm Cu HVL), Low energy X-rays (1.0-8 mm Al HVL), and Very Low energy X-rays (0.035-1.0 mm Al HVL).

The TRS 398 CoP is an absorbed dose to water protocol and uses two categories, Medium energy X-rays with an HVL > 3 mm Al, 100 kV, and Low energy X-rays with an HVL < 3 mm Al, 100 kV.

This paper will concentrate on the lowest energy range for both CoP's. These energy groups both require the use of a parallel plate chamber in a full scattering phantom.

For TRS 398, the standards laboratory is required to provide $N_{D,wQ0}$ for a suitable range of HVL's and likewise for $k_{Q,Q0}$. A majority of Standards laboratories including ARPANSA have taken the view that they will provide N_k and then convert to $N_{D,wQ0}$ using section 1.2 in Appendix 1 of TRS 398.

DISCUSSION: The problem with the above procedure is that the parallel plate chamber used by most hospitals for kilovoltage photons is the PTW chamber which has significant backscatter associated with it, hence the backscatter factors to be used in the relationships in Appendix 1are uncertain.

Most standards laboratories can provide N_k for a suitable range of HVL's but not in a full scatter phantom.

Measurements have been carried out at WBRC and ARPANSA using a PTW parallel plate chamber both in air and in a full scattering phantom to attempt to determine the best method of calculating $N_{D,wQ0}$ and review the uncertainties in doing this. These results and uncertainties will be presented.

One method that a hospital physicist can use to obtain information on the appropriate backscatter factor to use, or $N_{D,wQ0}$ is to do measurements in or close to the overlap regions of 2-3 mm Al HVL using an in-water technique with a cylindrical chamber and in a full scatter phantom with a parallel plate chamber as required by TRS 398. The results from comparing the in-water and in phantom measurements in the overlap region will be presented.

REFERENCES:

[1]*Technical Report Series 398, Absorbed Dose Determination in External Beam Radiotherapy*, IAEA, Vienna (2000).

[2]Klevenhagen, S.C. et al, *The IPEMB code of practice for the determination of absorbed dose for x-rays below 300 kV generating potential (0.035 mm Al – 4 mm Cu HVL; 10 – 300 kV generating potential)*, Phys.Med.Biol. 41 2605-2625 (1996).

DOSIMETRY OF VARIOUS TREATMENT CONES ON THE PANTAK SXT 150 KILOVOLTAGE X-RAY TREATMENT UNIT

B.J. Healy and K.N. Nitschke

Southern Zone Radiation Oncology Services – Mater Centre, Princess Alexandra Hospital, Brisbane, Qld, Australia

INTRODUCTION: In commissioning a Pantak SXT 150 kilovoltage treatment unit, the IPEMB 1996 protocol [1] was used for absolute calibration in the 1 mm Al to 13 mm Al beam quality range. Absolute calibration with a Farmer 2571 chamber

was performed on the 5 cm diameter treatment cone (15 cm FSD), and the calibration was transferred to other treatment cones with an in-phantom output factor measured with a parallel plate chamber. This method of calibration was compared to a direct calibration with the Farmer chamber and the IPEMB protocol for the 10 cm and 15 cm diameter (25 cm FSD) cones. Discrepancies in dose rates between the two methods of up to 3% warranted further investigation.
METHODS: A secondary standard Farmer 2571 ionisation chamber and a NE 2532/3 low energy chamber were used for ionisation measurements. Polyethylene sheets were used above the low energy chamber to maintain the active volume beyond the range of contaminating electrons [2]. The low energy chamber was used in a water-equivalent solid water block on top of a water tank.
RESULTS: Output factor and percentage depth dose (PDD) measurements were performed on the 5 cm, 10 cm, and 15 cm treatment cones. The 5 cm cone is a cylindrical stainless steel and acrylic end window design, while the 10 cm and 15 cm cones are tapering stainless steel applicators. The output factors for the 10 cm and 15 cm cones demonstrated a depth-dependence for sub-millimetre depths, with changes in the output factor of the order of 2% for changes in depth of 0.5 mm. Also the PDD fall off with depth was more rapid for the 10 cm and 15 cm cones than for the 5 cm cone, again for sub-millimetre depths.
DISCUSSION & CONCLUSIONS: Both sets of results indicate a significant low energy photon component at the end of the 10 cm and 15 cm stainless steel cones. These low energy photons may be generated from scatter off the applicator walls. In the IPEMB protocol, dose conversion factors such as the energy absorption coefficient ratio (water to air) and backscatter factor are not modified for photon spectrum changes [3,4], but are determined from HVL measured under narrow beam conditions.
REFERENCES:
[1]IPEMB (1996) *Phys. Med. Biol.* **41**: 2605-2625.
[2]S. C. Klevenhagen, D. D'Souza, and I. Bonnefaux, (1991) *Phys. Med. Biol.* **36**: 1111-1116.
[3]A. E. Nahum, (1999) in *Kilovoltage x-ray beam dosimetry for radiotherapy and radiobiology* C–M Ma and J P Seuntjens (Eds.) Proceedings, Medical Physics Publishing, Madison.
[4]L. Ma, C-M. Ma, J.F. Nacey, A.L. Boyer, (1999) in *Kilovoltage x-ray beam dosimetry for radiotherapy and radiobiology* C–M Ma and J P Seuntjens (Eds.) Proceedings, Medical Physics Publishing, Madison.

BACKSCATTER OF SUPERFICIAL RANGE X-RAYS FROM PROTECTIVE LEAD SHIELDS

Wasantha Fernando[1], Guilin Liu[1], Michael Grace[1], Peter Johnston[2] and Kym Rykers[1]

[1]*Radiation Oncology Centre, Austin Health, West Heidelberg, Vic, Australia*
[2]*Applied Physics, RMIT University, Melbourne, Vic, Australia*

INTRODUCTION: The use of superficial x-ray beams is an important modality in radiation therapy. For some clinical superficial x-ray applications, internal shields commonly made with lead are used to protect structures beyond the planned treatment volume. However, dose to tissue upstream from a shield is enhanced due to backscattered radiation from the shield. This can lead to uncertainty in the dose calculation if the backscatter from the lead shield is not included correctly, particularly where small tissue thicknesses are irradiated. Several published protocols are available for standard dosimetry for these beams but there is a scarcity of information available on dosimetry due to backscatter from internal shielding with variable tissue thicknesses upstream of the shield. This work was undertaken to determine the dose contribution from these protective shields to the prescription point for the treatment volume. The results of the investigation will be presented.
METHODS: The study used superficial range x-ray beams generated by an MXT 225 Therapax Pantak unit. Dose measurement with Gafchromic films was found to be unsuccessful due to its limited sensitivity. Dose measurements were then performed with a PTW Markus and a PTW soft x-ray parallel plate chambers. Monte Carlo calculations were also generated to mimic the experimental set-up.
RESULTS: The preliminary results show that backscatter from the lead shield can penetrate up to 10 mm upstream in tissue. At 5 mm and 3 mm upstream from the lead shield in tissue, scatter contribution from the lead shield is about 2% and 4% respectively of the total dose (primary and scatter from irradiated tissue).
DISCUSSION & CONCLUSIONS: Results suggest that an effective tissue thickness should be used in dose calculation process that incorporates the physical thickness of the tissue to the lead shield and an additional tissue thickness based on backscatter from the protective lead shield.

SPREADING THE FRUITS OF INNOVATION IN RADIOTHERAPY: THE LITTLE STORY OF 7SIGMA

D. P. Huyskens[1] and A.Van Esch[1]

[1]*7Sigma, qA-team in Radiotherapy Physics*

INTRODUCTION: New techniques in radiotherapy are mostly developed, tested and implemented in large (university) centres. Medical physicists in smaller centres are immerged in clinical routine and often do not have the time nor the know-

how to confidently implement new technologies, even if well described in literature and even though manufacturers go through a lot of effort to make the equipment user friendly and widely available.
During our careers as medical physicists at a university hospital, we were involved in clinical routine, in research and development and in quality assurance across multiple centres. Seeing many of our external colleagues struggle, trying to re-invent the wheel without the proper resources, the concept of a QA-team grew. We have now set it our goal to facilitate the spread of new treatment techniques, while maintaining high standards for quality assurance.
METHODS: In order to achieve our goal, we have subdivided our activities in three interconnected categories: research and development, on-site implementation of new techniques and quality control of radiotherapy trials.
In collaboration with companies and a network of clinical partners we perform clinical testing and guiding of hardware and software products developed in the field of radiation therapy. For radiation therapy centres of varying sizes and staffing we go on-site to implement these new techniques together with the local physicists and oncologists. For clinical trials in radiation therapy, we perform the quality control of the involved radiotherapy centres and/or patient data included in these trials.
RESULTS: We will present some results for each of the above mentioned categories. In the research and development area, we are currently testing the new dose calculation algorithm of Varian Medical Systems, the so-called AAA algorithm. Some preliminary results will be shown. We have implemented IMRT (with the Varian solution) in a few centres now and will present some general conclusions on the ease of implementation as well as on the practical applicability of IMRT in clinical routine. Regarding the quality assurance of clinical trials, surprising results have shown up in the subgroup of centres entering patients with IMRT treatments, ranging from reassuring to very alarming.
DISCUSSION & CONCLUSIONS: Although our story has just started, the results so far are encouraging. The on-site implementations of IMRT have been rewarding for both parties. The availability of a network of clinical partners not only allows us to stay in touch with a diversity of routine practices, it also increases the efficiency for testing of new techniques. The knowledge and experience gained during the testing is spread through later on-site implementations. It is also translated into QA procedures, designed to intercept possible causes of errors or inaccuracies.

MONTE CARLO MODELLING OF THE EFFECT OF AN ABSORBER ON AN ELECTRON BEAM

L. Li[1,2], A. T. Stewart[2] and W. H. Round[1]

[1] *Electrical and Electronic Engineering, University of Waikato, Hamilton, New Zealand*
[2] *Oncology Service, Auckland Hospital, Auckland, New Zealand*

INTRODUCTION: The electron beam from a linear accelerator is essentially spatially uniform in energy and intensity. Hence it may not be suitable for treating a patient where it is desirable for the treatment depth to vary across the field. Using an absorber to shield the part of the beam where a shallower treatment depth is required may provide a solution. But the absorber will cause energy degradation, spectrum spreading and scattering of the incident beam. This situation was investigated using Monte Carlo simulation to determine the changes in the incident beam under, and near the edge of, a sheet absorber made of a low atomic number material.
METHODS: The EGSncr system, along with user code written in Mortran, was used to perform the Monte Carlo simulations.
A situation where a thin absorber was placed in a pure 15 MeV 10 cm wide electron beam from a point source was modelled. The absorber was placed to cover half of the beam. This was repeated for different thicknesses of aluminium. It was further repeated for absorbers where the edge on the middle of the beam is chamfered. The dose distributions were plotted, and compared to measured distributions from a clinical accelerator.
In addition, the effects of energy degradation, spectrum spreading and scattering were also investigated. This was done by analysing the energies and angles of the simulated electrons after passing through the absorber. Knowledge of energy loss versus scattering angle for different thicknesses of different materials allows for a better choice of absorber.
RESULTS: The simulations predicted that at the edge of the shadow of the absorber a hot spot appeared outside the shadow and a cold spot inside the shadow. This was confirmed by measurement. Chamfering the edge of the absorber was seen to reduce this effect with the significance of the effect being dependent in the absorber thickness and the shape of the chamfer.
DISCUSSION & CONCLUSIONS: The choice of thickness of the absorber should take into account the effects of energy spectrum change, angular spread and the reduction in fluence. With a careful choice of absorber material, thickness and shaping of the edge of the absorber, a satisfactory dose distribution can be achieved.

ASSESSMENT OF AN AMORPHOUS SILICON EPID FOR QUALITY ASSURANCE OF ENHANCED DYNAMIC WEDGE

Peter Greer[1,2]

[1]*Newcastle Mater Hospital, Newcastle, NSW, Australia*
[2]*University of Newcastle, Newcastle, NSW, Australia*

INTRODUCTION: Routine quality assurance (QA) of enhanced dynamic wedge (EDW) is usually performed weekly to monthly. Wedge factors are measured with ion-chamber, and profiles usually with diode-arrays such as the Profiler. The use of an electronic portal imaging device (EPID) for these measurements would combine these into a single rapid set-up and measurement. Currently the Varian EPID in standard imaging mode will not acquire integrated images during EDW treatments, and therefore has not been utilised for EDW dosimetry. Modification to image acquisition was made to enable imaging for EDW, and the performance of the EPID for suitability for quality assurance of EDW was investigated.
METHODS: The accuracy of EDW profiles measured with the EPID were assessed by comparison to Profiler measurements. The EPID was positioned at 105 cm to the detector surface, with 4 cm of additional solid water build-up to give total build-up including EPID inherent build-up of 5 cm. Images of EDW fields were acquired with continuous frame-averaging throughout the delivery. Field sizes of 10×10 cm, and 20×20 cm were used for 30° and 60° wedge angles for both 6 MV and 18 MV x-rays. Profiler measurements of the same fields were made with 5 cm of solid water build-up with 105 cm to the detector. Profiles in the wedged direction along the central axis of the beam were then compared. The reproducibility of the EPID measured profiles was assessed by three measurements made at weekly intervals.
The accuracy of EPID measured wedge factors was investigated with the same experimental set-up. Three images of a 10×10 cm open field were acquired, and the mean pixel value in a 9×9 pixel region at the central axis was found. As the pixel value is the average of all acquired frames, this was multiplied by the number of frames to yield an integrated pixel value. This was repeated for three 10×10 cm 60° wedge irradiations. The wedge factor measured with the EPID was then compared to routine weekly measurements made with an ionisation chamber under the same conditions. The reproducibility of the EPID measured wedge-factors was determined by comparing three weekly measurement results.
RESULTS: EPID profiles measured were in good agreement (within 5%) of Profiler measurements for both wedge angles and all field sizes. The EPID profiles had flood-field corrections removed to give the raw-response of the EPID system. Normalised EPID 60° wedge profiles measured at weekly intervals were within 0.5% of each other excluding the penumbra region.
The EPID measured wedge-factors are shown in Table 1. These were all within 0.6% of the mean result from routine weekly ion-chamber measurements. The standard deviation of the three measurements was 0.27% which is similar to the standard deviation of the routine ion-chamber measurements of 0.4%.

Energy	Wedge Factors			
	Ion-Chamber	EPID Week 1	EPID Week 2	EPID Week 3
6X	0.659	0.663	0.657	0.660
18X	0.728	0.729	0.723	0.725

Table 1. *Accuracy and reproducibility of EPID measured EDW factors.*

DISCUSSION & CONCLUSIONS: The amorphous silicon EPID is highly suited to routine quality assurance of EDW. Measurements of both wedge-factors and wedge profiles are accurate and reproducible. The quality assurance measurements can be made in a matter of a few minutes, with virtually no experimental set-up time.

CHARACTERISATION OF A DIGITAL FILM SCANNER TO CHECK CALIBRATION OF LINEAR ACCELERATOR JAW POSITION

P. Fogg and J. Cramb

Peter MacCallum Cancer Centre, East Melbourne, Vic, Australia

INTRODUCTION: A quality assurance program is required for linear accelerator jaw calibration analysis procedures. These procedures incorporate the use of x-ray film and a film scanning system for the measurement and analysis applications. Two scanning systems were studied, a Therados analogue and a Vidar charge coupled device 12 bit digital scanner.
METHODS: A number of tests were carried out on the scanners to characterise their performance. These tests included geometric, reproducibility, hysteresis, linearity, base plus fog removal, contrast, signal to noise ratio, film slippage, filtering, alignment and normalisation. Jaw setting methods and jaw calibration techniques were compared. Radiation/light field congruence films were scanned for field size and the junction magnitude, comparisons were made between the two scanners' results. Film, ion chamber and radiotherapy treatment planning system (XiO) profiles were compared for offset jaw junctioning at the central axis, 1cm, 5cm and 8cm from the central axis. Simulated gaps and overlaps were also performed using film and XiO for simulated $\pm$1mm jaw errors.
RESULTS: The Vidar scanner indicated a larger range of detectable density levels, finer spatial resolution, superior geometrical accuracy, reproducibility, signal to noise ratio and contrast detection over the Therados scanner.

There was excellent agreement between film and XiO for the simulated junction measurements. The widely accepted jaw tolerance of ±1 mm each jaw produced approximately a ±40% junction magnitude. The Peter Mac dip and peak tolerance of –15% to 5% corresponded to a tighter jaw pair range than the accepted tolerance.

DISCUSSION & CONCLUSIONS: The Therados scanner was found to measure both parameters of the film quality assurance test less accurately by overestimating the field size and underestimating the junction size. The Vidar scanner is therefore more suitable for quality assurance film analysis procedures.

REFERENCES:

P. Kemp (2003*), Characterisation of a Digital Film Scanner to Check Calibration of Linear Accelerator Jaw Position*, Thesis, Queensland University of Technology, Brisbane.

SHIELDING PROVISION IN AN OLD 6MV BUNKER FOR A NEW 18MV LINAC

S. J. Howlett, M. A. Ebert and J. W. Kenny

Department of Radiation Oncology ,Newcastle Mater Misericordiae Hospital, Newcastle, NSW, Australia

INTRODUCTION: In October 2003 the Newcastle Mater Hospital commenced clinical use of a new Varian 21EX which replaced it's 14 year old Varian Clinac1800. The 1800 had only been enabled for 6MV X-ray beam for most of its clinical use but was enabled for 18MV for a period in 2000. This was to make up for the loss of an 18MV beam from another Clinac 1800 which was being replaced in a bunker designed for that higher energy. The new 21EX would provide both 6MV and 18MV beams for routine clinical use. The original bunker had been designed for the lower energy and hence additional shielding was required to meet radiation dose limits recommended in ICRP 60[1] and adopted in ARPANSA RPS6[2].

METHODS: A general radiation survey was conducted around the bunker area when the 18MV beam was available on the older linear accelerator. This rather unique situation provided data which would normally be impossible to obtain. Photon activation in the neutron door was a source of increased dose levels in the control area. Commercial design was contracted for the additional barrier calculations and supply. Additional shielding was required on one primary barrier and the neutron door. Post installation surveys were conducted and the R&V system was used for usage figures. Using dose constraints for public and occupational exposure, various survey points were measured around the bunker. This data was assessed in terms of calculated requirements, actual requirements and the ALARA principle for radiation shielding design. Review of staff dose histories was also performed.

RESULTS: The final survey calculations showed the additional shielding more than adequate for the usage of 18MV and 6MV photon beams. The availability of the R&V data gives supporting evidence for design of barriers to be adjusted on usage values as has been reported in an earlier work at this centre[3]. The issue of occupancy arises in this work as dose histories indicate.

DISCUSSION & CONCLUSIONS: Typically barrier design is always conservative and survey results on properly constructed barriers return significantly lower dose readings than required to meet recommended levels for public and occupational exposure. There are reasonable reductions in shielding achievable for bunker construction based on real data of beam usage and personnel dose histories as evidence of occupancy. Indeed many radiotherapy centres possess dose level survey results and personnel dose histories, such as those discussed in this work, which could form a reference data base for future design. ARPANSA holds a national database on dose histories. We propose that such information would lead to a cost reduction in equipment provision for radiotherapy leaving funds available that could be better utilized in the stressed health budget.

ACKNOWLEDGEMENT: Helpful discussion with Mr Kevin Fitzsimmons of Radiation Services is gratefully acknowledged.

REFERENCES:

[1]ICRP Publication 60, *1990 Recommendations of the International Commission on Radiological Protection*, Pergamon Press, 1991.

[2]National Directory for Radiation Protection (Edition 1) *Radiation Protection Series No. 6*, Australian Radiation Protection And Nuclear Safety Agency (ARPANSA). Yallambie, Vic. August 2004.

[3]Kron T, Aldrich B, Jovanovic K, Howlett S and Hamilton C. *Workload and use factor of medical linear accelerators in radiotherapy*, (1995) Health Physics, 69(6):971-975.

GENERATION OF LOW KV X-RAY PORTAL IMAGES WITH MEGA-VOLTAGE ELECTRON BEAMS

J. Kenny[1,2], M. Ebert[1,3] and P. Greer [1,3]

[1]*Newcastle Mater Hospital, Newcastle, NSW, Australia*
[2]*Queensland University of Technology, Brisbane, Qld, Australia*
[3]*University of Newcastle, Newcastle, NSW, Australia*

INTRODUCTION: The increasing complexity of radiation therapy plans and reduced target margins, have made accurate localization of patients at treatment a crucial quality assurance issue. Mega-voltage portal images, the standard for treatment

localization, are inherently low in contrast because x-ray attenuation at these energies is similar for most body tissues. Thus anatomical features are difficult to distinguish and match to features on a reference diagnostic image. This project investigates the possibly of using x-rays created by an *external* target placed in the path of a clinical mega-voltage electron beam. This target is optimised to produce a higher proportion of useful imaging x-rays in the range of 50-200kV. It is thought that a high efficiency Varian aSi500 amorphous silicon EPID will be sufficient to compensate for the very low efficiency of x-ray production.

METHODS: The project was undertaken with concurrent theoretical and experimental components. The former involved Monte Carlo models of low Z target design while in the later, experimental data was gathered to validate the model and explore the practical issues associated with electron mode image acquisition.

A 6 MeV electron beam model for a Varian Clinac 21EX was developed with EGS4/BEAMnrc User Code[1] and compared to measured beam data. Phase space data scored at the secondary collimator then became the input for simulations of a target placed in the accessory tray. Target materials were predominately low atomic number (Z) because a) production of high energy x-rays is minimized and, b) fewer low energy x-rays produced will be absorbed within the target[2]. Photon and electron energy spectrums of the modified beam were evaluated for a range of target geometries. Ultimately, several materials were used in combination to optimise an x-ray yield for energies <200kV while removing electrons and very low energy x-rays, that contribute to patient dose but not to image formation.

Low energy images of a PIPs EPID QA phantom and a purpose built contrast phantom were evaluated for contrast enhancement using purpose written MATLAB code. Information from these images was implemented in the Monte Carlo model to refine the target construction. Electron mode image acquisition was achieved using the clinical (R&V) and service interfaces however the EPID was activated using an internal trigger rather then a trigger pulse from the linac, since it does not recognise the linac pulses for electron modes.

RESULTS: Images could be acquired in as little as 5 monitor units (MU), with reasonable quality images generated with ~20MU. Doses of this magnitude indicate that such images could be acquired in a clinically viable amount of time, especially if higher dose rates was used e.g. 1000MU/min. Image quality is affected because the EPID is not synchronised to the linac pulses. Furthermore a flood-field correction image for the low energy beam is difficult to acquire and a "standard" one has been applied.

DISCUSSION & CONCLUSIONS: Although not optimal for efficient x-ray production, the low Z target maximises the content of low energy x-rays in the imaging beam, leading to portal images with improved contrast. Using a high efficiency EPID, images could be acquired in clinically practical times. This method of low energy portal imaging is relatively simple, inexpensive to construct and easy to install. Image quality would benefit from a special imaging mode that maximizes EPID performance under these conditions.

REFERENCES:

[1]Rogers, D.W.O. et al (1995) *BEAM: A Monte Carlo code to simulate radiotherapy treatment units.* Med. Phys., 22(5):503-524.

[2]Mah, D.W. et al (1993) *Low-energy imaging with high-energy bremsstrahlung beams: Analysis and scatter reduction.* Med. Phys., 20(3):653-665.

A TWO-SHIFT OPTIMISATION OF THE "NO ACTION LEVEL" SETUP CORRECTION PROTOCOL

C. Fox[1] and R. Fisher[2]

[1]*Physical Sciences, Peter MacCallum Cancer Centre, Melbourne, Vic, Australia*
[2]*Statistical Centre, Peter MacCallum Cancer Centre, Melbourne, Vic, Australia*

INTRODUCTION: As electronic portal imaging equipment becomes more common, many radiotherapy centres now have the ability to collect patient treatment position deviation values. One commonly used off-line set-up correction protocol for calculating patient setup corrections is the "no action level" (NAL) protocol. This paper proposes a two-shift approach and calculates the number of images required for minimum systematic error. Patient data is used in a simulation to confirm this approach.

METHODS: Patient treatment position deviations were available for all treatment sessions for a large group of patients undergoing radiation therapy for prostate. Thirty of these patients were selected. The patient position at treatment and all isocentre shifts made were recorded in the treatment notes. These were used to simulate the effect of the NAL protocol using a range of image numbers as the basis of the set-up correction. As Bortfeld et al[1] noted, there is an error minimum that can be observed beyond which the mean radial systematic set-up error increases slowly with an increase in the number of images used.

An enhancement to the NAL was proposed in which the patient's position is corrected on two occasions; once early in the treatment schedule, and again after more images have been collected. The expectation value of the set-up error for this two-shift NAL was found and minimised.

RESULTS: The optimum staging for the two-shift NAL for the prostate patients was to image for a total of 9 sessions and to shift the patient after 3 sessions and 9 sessions. The thirty patients showed an uncorrected mean radial setup error of

0.65cm. In this simulation this was corrected to 0.26cm by application of the NAL using 5 images and to 0.17 cm using the two shift NAL with shifts after three and nine images.

DISCUSSION AND CONCLUSIONS: In situations where staff can manage the workload of collecting and analysing portal images for nine sessions for each patient, the two-shift NAL will result in a high level of set-up accuracy.

REFERENCE:

[1]Bortfeld T, van Herk M, Jiang S, (2002) *Phys Med Biol N297-N302.*

Abstracts of oral presentations - radiation safety and medical imaging

CT REFERRAL RATES AND THE POTENTIAL IMPACT IN PRODUCING DETERMINISTIC EFFECTS OF THE EYE

L. Wilkinson[1] and J. Heggie[2]

[1]*Medical Imaging Department, St Vincent's Hospital, Fitzroy, Vic. Australia*
[2]*Medical Engineering and Physics, St. Vincent's Hospital, Fitzroy, Vic. Australia*

With the recent advances in CT technology, the popularity of this imaging modality is appearing to be increasing with referring doctors. Historically concern has been raised regarding the possibility of cataract formation from CT of the head. The aim of this paper is to examine recent CT referral rates for patients in a 350 bed, adult teaching hospital to determine referral rates for CT of the head, and from these rates assess the potential to produce radiation induced opacities/cataracts.
A review of data from the hospital's Radiology Information System for the period 1998 to 2003 was conducted. Data shows that the number of CT scans referred per year has increased by 28% over the monitoring period. However the proportion of patients being referred for multiple CT examinations has not changed. During the monitoring period, of those patients referred for head scans, 20% had multiple scans. Approximately 2% of the patients referred had 5 or more head scans during any two year period.
Radiation dosimetry for the CT Brain protocol used at the hospital was calculated using the ImPACT CT dosimetry spreadsheet. This dosimetry was performed for an older spiral CT scanner and a newer multi-slice CT scanner. These results showed that though the effective dose to the patient was relatively low, the eye lens dose could be as high as 100 mGy per examination.
For protracted exposures ICRP 60 suggests a possible dose rate threshold of 100 mGy/yr for the production of radiation-induced eye lens opacities. On this evidence the possibility of exceeding the threshold for producing deterministic effects in the eye lens cannot be dismissed, for those patients returning for multiple CT Brain scans.

PATIENT DOSES IN MULTI-SLICE CT – OPTIMISATION IS THE KEY TO REDUCING THEM

John C. P Heggie

Dept Medical Engineering & Physics, St. Vincent's Hospital, Fitzroy, Vic, Australia

INTRODUCTION: There have been a number of articles in the literature[1,2] recently raising concerns about the magnitude of patient doses from CT and the potential risks that may arise from the increasing use of CT scanning as a diagnostic tool. These concerns have only been heightened with the increasing implementation of the latest generation of multi-slice CT scanners. Certainly, these scanners offer superior image quality and diagnostic capability, when compared with their single-slice predecessors but there are a number of reasons, including some technical ones[3], why they may lead to even higher patient doses and associated potential risks for patients. With this in mind we decided to undertake a prospective survey of patient doses for our most common CT examinations using a single slice scanner (Siemens Somatom Plus 4) before it was decommissioned. This exercise was repeated immediately following installation and commissioning of a multi-slice scanner (Siemens Sensation 16) and then again once we had undertaken some optimisation of our scanning protocols.

METHODS: Technical data (kVp, mAs, scan time per rotation, collimated beam width, scan range and pitch as indicated) were recorded for large numbers of patients embracing most of the common CT procedures undertaken at our institution. For the Sensation 16 scanner *CareDose* was implemented where appropriate as an aid in reducing doses. A Radcal pencil chamber and dosimeter was utilised to measure the weighted CT dose index ($CTDI_w$) in standard head and body phantoms made from Perspex. These measurements were combined with the patient specific technical data to generate Dose Length Product (DLP) estimates on an individual patient basis.

RESULTS & CONCLUSION: Some of the results of our surveys are provided in the accompanying table. All dose numbers represent median values from typically 50 or more adult patients. A key finding is that the patient doses were invariably significantly higher immediately after commissioning the multi-slice scanner. However, by astute adjustment (optimisation) of our acquisition protocols over a number of months, we were able to achieve comparable or even lower doses with the multi-slice scanner when compared with its single-slice predecessor.

	DLP (mGy.cm)		
Procedure	Plus 4	Sensation (early)	Sensation (optimised)
Brain without contrast	715	960	660
Chest with contrast	320	440	315
Chest/upper abdo with contrast	320	430	340
Pulmonary angio (Query PE)	310	230	230
Chest/abdo/pelvis with contrast	610	730	530
Abdo/pelvis with contrast	500	555	330
Abdo/pelvis triple phase	860	1100	730
Lumbar spine	450	560	460

Table. *Summary of dose measurements for the single slice and multi-slice CT scanners.*

REFERENCES:

[1]DJ Brenner, CD Elliston, EJ Hall & WE Berdon (2001). *Estimated Risks of Radiation-Induced Fatal Cancer from Pediatric CT*, AJR, 176: 289-296.
[2]KN Wise (2003). *Solid cancer risks from radiation exposure for the Australian population*, Austral Phys Eng Sci Med 26: 53-62.
[3]MK Kalra, MM Maher, TL Toth et al (2004). *Strategies for CT Radiation Dose Optimization,* Radiol 230: 619-628.

RADIATION MONITORING OF PET STAFF

A. Trang

Department of Medical Technology & Physics, Sir Charles Gairdner Hospital, Perth, WA, Australia

INTRODUCTION: Positron emission tomography (PET) is becoming a common diagnostic tool in hospitals, often located in and employing staff from the Nuclear Medicine or Radiology departments. Although similar in some ways, staff in PET departments are commonly found to have the highest radiation doses in the hospital environment due to unique challenges which PET tracers present in administration as well as production.

The establishment of a PET centre with a dedicated cyclotron has raised concerns of radiation protection to the staff at the WA PET Centre and the Radiopharmaceutical Production and Development (RAPID) team. Since every PET centre has differing designs and practices, it was considered important to closely monitor the radiation dose to our staff so that improvements to practices and design could be made to reduce radiation dose.

METHODS: Electronic dosimeters (MGP DMC 2000XB), which have a facility to log time and dose at 10 second intervals, were provided to three PET technologists and three PET nurses. These were worn in the top pocket of their lab coats throughout a whole day. Each staff member was then asked to note down their duties throughout the day and also note the time they performed each duty. The duties would then correlate with the dose with which the electronic monitor recorded and an estimate of radiation dose per duty could be given. Also an estimate of the dose per day to each staff member could be made.

RESULTS: PET nurses averaged approximately 20 μSv per day getting their largest dose from caring for occasional problematic patients. Smaller doses of a 1-2 μSv were recorded for injections and removing cannulas. PET technologists averaged approximately 15 μSv per day getting their largest dose of 1-5μSv mainly from positioning of patients and sometimes larger doses due to problematic patients. Smaller doses of 1-2 μSv were again recorded for injections and removal of cannulas.

DISCUSSION & CONCLUSIONS: Following a presentation given to staff, all WA PET Centre and RAPID staff have now a greater awareness of the radiation doses associated with different duties. Close monitoring of staff radiation doses will continue, and changes to practices and design will be implemented in accordance with ALARA.

ACKNOWLEDGEMENTS: All staff of the WA PET Centre and RAPID Team, in particular Julie Crouch and Dr John De Roach.

THE AUSTRALIAN CENTRE FOR RF BIOEFFECTS RESEARCH (ACRBR) - AN NHMRC CENTRE OF RESEARCH EXCELLENCE

A. Wood[1], M. Abramson[2], V. Anderson[3], I. Cosic[3], R. Croft[1], J. Finnie[4] and R. McKenzie[5]

[1]*Swinburne University of Technology, Hawthorn, Vic, Australia*
[2]*Monash University, Clayton, Vic, Australia*
[3]*RMIT University, Melbourne, Vic, Australia*
[4]*IMVS, Adelaide, SA, Australia*
[5]*Telstra Research Laboratory, Vic, Australia*

INTRODUCTION: The Australian Centre for Radiofrequency Bioeffects Research (ACRBR) is a newly established multi-institutional research centre which seeks to research questions pertaining to possible health effects of exposure to radiofrequency devices, such as mobile phones and which is funded under the Australian National Health and Medical Research Council (NHMRC) Centres of Research Excellence funding program. The Centre of Research Excellence in Electromagnetic Energy is combining the efforts of engineers, epidemiologists, physicists, psychophysiologists and veterinary pathologists from RMIT University, the Institute of Medical and Veterinary Science in South Australia (IMVS), Monash University, Swinburne University of Technology and Telstra Research Laboratories (TRL). The centre is funded at $2.5 M over five years and will undertake a program of research to address the issue of exposure to radiofrequency (RF) devices and health. It will also train new scientists, keep the community informed of ongoing developments and help the development of government policies in this area of considerable public concern.
METHODS: The 5-year program has the following components:
Neurobiology: One important area where there is a perceived research gap is in the area of potential neurological effects, which will hence be a major focus of this Centre. The proposed studies range from *in vitro* and *in vivo* research studies of RF effects on neuron and neural system functioning in rodents, to that of RF effects on simple neural function, cognition and subjective report in humans. The latter series of studies have been developed to account for the consensus view that more emphasis needs to be placed on possible differences in RF population sensitivity (e.g. youth versus aged, and 'electromagnetic hypersensitives').
Epidemiology: Epidemiological studies are an important tool in studying the impact on public health from exposure of whole populations to modern radio technologies. Cancer outcomes in this area of research are already adequately covered the internationally based IARC study. However, epidemiological research investigating associations of mobile phone exposure and non-malignant health outcomes in the general community is less well treated. A cohort study of teenage school children, an age group identified as a priority research area, will be monitored for an initial period of three years.
Dosimetry: Technical reviews consistently identified rigorous dosimetry as a key issue for ensuring the validity of results within a given study and consistency of results between studies. This requires that a well-characterised standard methodology and suite of tools be utilised for the provision of dosimetry to research programs that are run within the Centre. The technical reviews have also raised concerns regarding the application of compliance techniques in RF human exposure standards, based on adult models, to children. Further, there remain questions as to applicability of current compliance techniques to the rapidly changing new communications technologies, particularly as they relate to nonhandset issues (wireless LANs, mobile data enabled palmtops and laptops etc[9]). The Centre will undertake both physical and computational studies to improve the understanding of dosimetric sensitivity to normal population variations such as size, ethnicity, and age and how these impact on current compliance techniques employing standard human models cited in many protocols
DISCUSSION & CONCLUSIONS: The Centre will not only advance the international body of knowledge on this subject, but also train new scientists in this multifaceted area of research. Outcomes of the research will be input into public policy and standards setting and regulatory processes. The Centre will also act as a publicly accessible information resource centre on this highly sensitive issue for the general community.

INDUCED CURRENT DENSITY IN THE FOETUS OF PREGNANT WORKERS IN HIGH MAGNETIC FIELD ENVIRONMENTS

C. Xue[1], A.W. Wood[1] and T. Dovan[2]

[1]*School of Biophysical Sciences and Electrical Engineering, Swinburne University of Technology, Melbourne, Vic, Australia*
[2]*SPI PowerNet, Melbourne, Vic, Australia*

INTRODUCTION: There are moves to limit by legislation the amount of electric and magnetic fields that workers and the general public are exposed to. In work locations near wiring, cables & equipment carrying high electric currents, there are situations in which the proposed magnetic field limits could be exceeded. Since the limits for the general public are more conservative than those for workers and since the foetus or a pregnant worker should be afforded the status of a member of the general public, it is important to assess a worst-case scenario for the purposes of a general code of practice.
METHODS: Three different magnetic field exposures are modelled, which include the worst case – the body of a pregnant woman at a smallest distance of 30 cm to the conductor. All computations were done by using Multiple Multipole Program (MMP), which is based on the Generalized Multipole Technique (GMT) from ETH (Swiss Federal Institute of Technology), Zurich, Switzerland[1,2].
RESULTS: The torso was modelled as a capped cylinder containing concentric placental and amniotic fluid layers containing a foetus. Appropriate values for conductivity and permittivity were applied to these layers and the Maxwell Equation solver applied for the situations of: cable beneath, alongside perpendicular and alongside parallel to the long axis of the body. Induced current density values were computed for cable distances of 0.3 and 0.5 m from the body and compared to the recommended limit values of 10 and 2 mA/m^2 for Occupational and General Public populations respectively. Regions where these values would be exceeded have been identified in this analysis.

CONCLUSIONS: In a worst-case scenario the proposed basic restrictions would be exceeded slightly in both maternal and foetal tissue. With appropriate pre-placement assessment, these over-exposures can be avoided.

REFERENCES:

[1]Hafner, Ch., (1999): *Post-modern electromagnetics: Using intelligent Maxwell solvers,* John Wiley and Sons, Chichester.
[2]Hafner, Ch., Bomholt, L., (1993): *The 3D electromagnetic wave simulator,* John Wiley and Sons, Chichester.

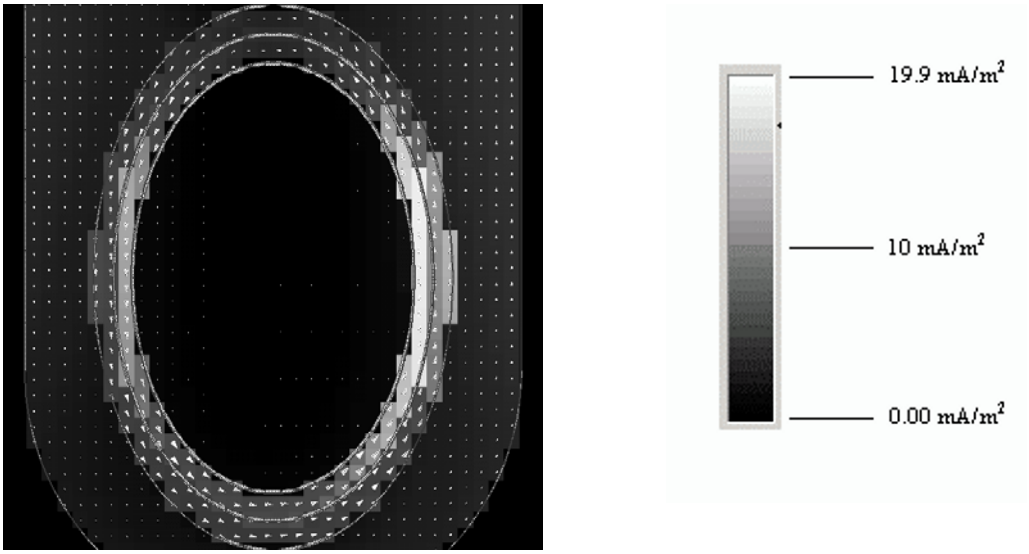

Figure 1. *Representation of a lower abdomen of a pregnant worker 0.3 m from a cable carrying 1000A. Induced current density distribution (Z=0 plane) for cable parallel to long axis of body.*

A SUGGESTED PROTOCOL FOR THE INTERCOMPARISON OF MULTI-VENDOR, MULTI-SLICE, HELICAL CT PLATFORMS FOR DOSE AND LOW CONTRAST RESOLUTION

A. B. Wallace[1]

[1]*Medical Engineering & Physics, Austin Health, Heidelberg, Vic, Australia*

INTRODUCTION: The comparison and evaluation of various contemporary CT platforms is inherently problematic on a point-by-point and like-with-like basis. This is primarily due to the inbuilt complexity and technological variety in the way that each manufacturer and system accomplishes the goals of best image quality and lowest dose – something which they all offer. The variables that each manufacturer may use to obtain the best outcome are numerous and may include kVp, filtration, slice width, detector array, acquisition kernel, field-of-view, reconstruction matrix, reconstruction algorithms, etc. As all of these variables may differ from manufacturer to manufacturer a simple intercomparison of system against system is non-trivial. A comparative protocol is suggested that may assist with this task.

METHODS: System performance was assessed using the following tests;

1. CTDI free-in-air – Axial
2. CTDI weighted – Axial
3. CatPhan Surface Dose – Axial
4. CatPhan Image Noise – Axial
5. CatPhan Limiting Low Contrast Resolution –Axial
6. CatPhan Surface Dose Using Manufacturer Chosen Helical Acquisitions
7. CatPhan Limiting Low Contrast Resolution Using Manufacturer Chosen Helical Acquisitions

RESULTS: As most manufacturers have now superseded the tested models that made up this investigation individual comparisons will not be presented. However anonymous comparative data will be shown to exemplify the strengths and weaknesses of the proposed comparative schema.

DISCUSSION & CONLCUSIONS: This assessment was a simple snapshot of the performance of 4-16 slice volume CT scanners. It was not meant to be an exhaustive evaluation of all aspects of the various systems.

However, it was assumed that as these systems were established units, their owners were happy with their performance and any data that they provided could be assumed to be indicative of that performance.

Low contrast image performance and dosimetry was assessed using scanning protocols favoured and recommended by the various applications experts provided for the assessments.

INVESTIGATION INTO THE OPTIMAL USE OF AUTOMATIC OPTIMISATION OF PARAMETERS (AOP) FOR MAMMOGRAPHY

J. Herley[1] and W. Tan[1]

[1]*Biomedical Technology Services, Queensland Health, Qld, Australia*

Automatic Optimisation of Parameters (AOP) is an AEC function offered on GE Medical Systems mammography units. It optimizes x-ray exposure to give optimal image quality by automatically selecting kVp, target/filter and mAs according to the thickness and density of the breast.
The Medical Physics group of Biomedical Technology Services (BTS) has conducted an investigation into the optimal use of the AOP modes for the GE Senographe 800T and GE Senographe DMR mammography units located in several BreastScreen Queensland (BSQ) clinics. Variation of image quality and dose using the three AOP modes were studied. The planned outcome is to develop a recommendation for the optimal use of AOP modes based on various breast thickness and composition.
Both GE Senographe 800T and GE Senographe DMR have 3 AOP mode selections: CNT (contrast), STD (standard) and Dose. Various thickness of perspex ranging from 2cm to 8cm was compressed for each mode to determine the selection of kVp, target/filter and mAs for each apparatus.
Image quality was evaluated using a Tor[Mam] phantom for various thicknesses in each AOP mode. The scoring system implemented for image quality was that recommended by Leeds X-ray Imaging (Lxi) where a numerical scale from 0 to 3 is used to denote the level of visibility of details perceived in the phantom image.
Results confirmed that mean glandular dose (MGD) increases with breast thickness. Increasing image contrast will increase dose to breast due to lower energy radiation spectrum used. The GE Senographe DMR has the advantage of utilising a Rhodium target thus giving a lower MGD than the GE Senographe 800T at thickness above 4cm.
Film image quality decreases with increasing thickness of perspex. A breast thickness of 2cm yields similar image quality in all 3 AOP modes as the selected kVp value and target filter (Mo/Mo) was similar. There was no significant difference in image quality for the GE Senographe DMR apparatus between 2cm and 4cm for all AOP modes. At greater than 4cm the CNT mode gave better image quality than both the STD and Dose modes.
ACKNOWLEDGEMENTS: BreastScreen Queensland
REFERENCES:
X. Wu, E. L.Gingold, G. T. Barnes, D. M. Tucker (1994) *Radiology*, 193: 83-89.
A. R.Craig, J. C. P. Heggie, I. D. McLean, K. S. Coakley, J. J. Nicoll (2001) APESM, 24:107-131.

AEC TESTING IN A CR ENVIRONMENT

Rob McLeod

Medical Physics and Bioengineering Department, Christchurch Hospital, Christchurch, New Zealand

Introduction: Testing of x-ray machine automatic exposure control (AEC) functionality for varying kVp and patient thickness is a fundamental health physics check. Current test protocols tend to be based on testing in a film environment using film optical density as the measure of conformance. With the move into the digital x-ray image age with the use of computed radiography (CR) and digital radiography (DR) equipment and its associated image storage and retrieval system (PACS) a new AEC testing protocol is required.
All CR systems provide a dose assessment tool (called Exposure Index or EI by Kodak) that could be used as a surrogate for optical density. However this work aims to derive an efficient means of assessing the functioning of the AEC of x-ray machines in a CR environment using dose measurement alone. This would eliminate the need to process the many image plates normally required for AEC testing in order to obtain and analyse the exposure measure from the CR system.
Methods: The EI, and other brand's equivalents, is calibrated for a given condition (for Kodak 80kVp 0.5mmCu + 1mmAl). In order to use dose measurement alone the relationship between EI and dose must be known for varying kVp and patient thicknesses (represented by a perspex phantom). This will depend on the response of the CR plate to varying beam energies. This was assessed using a series of paired exposures at various kVp and perspex thicknesses. In the first exposure of each pair a Kodak CR plate was used, processed in the normal way, and the EI noted. In a second identical exposure an Innovision 35050A pancake ionization chamber was placed in the bucky tray within a specially modified film cassette and the dose measured.
Results: Over the 50-125kVp range of clinical use the kV response of the Kodak PSP's shown below is essentially flat for a set dose to the image plate and filtered using the standard Kodak method of 0.5mmCu + 1mmAl. Similar data will be presented showing this relationship using a perspex phantom and also for EI with varying Perspex phantom thickness.

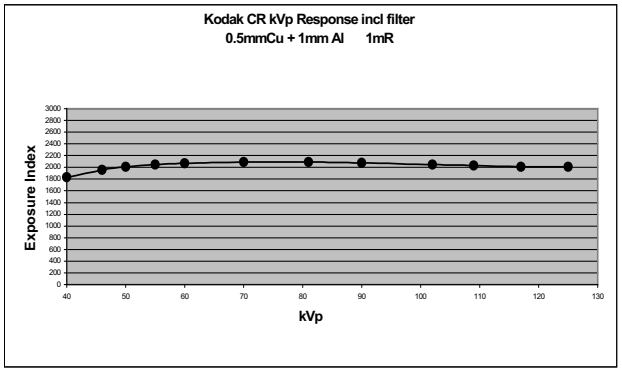

Conclusion: A correctly operating AEC system in a CR environment should result in consistent image quality over the clinical range. This can presumably be represented by minimal variation in Exposure Index reported by the CR system. Given the measured relationship between dose and Exposure Index it may be possible to use dose measurement as a direct measure of AEC performance. Setting appropriate tolerances for dose means considering the EI-dose relationship (EI $\propto$ log (dose)), the calibration accuracy of EI, and traditional tolerances accepted as reasonable in a film environment. These considerations will be discussed in detail during the presentation.

DEVELOPMENT AND DESIGN OF A BONE-EQUIVALENT CORTICAL SHELL PHANTOM TO DETERMINE ACCURACY MEASURES ON DXA AND PQCT SCANNERS

B. C. C. Khoo [1,2], T. J. Beck [3], B. Turk[1] and R. I. Price[1]

[1]*Medical Technology & Physics, Sir Charles Gairdner Hospital, Perth, WA, Australia*
[2]*School of Surgery & Pathology, The University of WA, Perth, WA, Australia*
[3]*Johns Hopkins University, Baltimore, MD, USA*

INTRODUCTION: Hip Structural Analysis (HSA) [1], is an algorithm that computes bone-structural geometry from dual energy X-ray absorptiometry (DXA) derived hip images and may be used in a complementary manner to DXA areal bone mineral density (BMD) for bone strength interpretation. DXA is normally used to facilitate the diagnosis and management of bone metabolic diseases such as osteoporosis. HSA provides a biomechanical interpretation of BMD, using its mass profiles to compute cross-sectional structural geometry. In essence, HSA provides insight into bone structural and biomechanical properties, particularly of long bones, which BMD alone cannot.
While conventional (vendor-provided) phantoms calibrate DXA machines for densitometric precision, analogous phantoms for calibrating structural geometry are lacking. This paper describes the design and preliminary testing of a densitometric bone-equivalent cylindrical phantom with "cortical" shells and "cancellous" core, and the use of this phantom to do a performance test of structural geometry variables such as cortical thickness, bone width and section modulus derived, from pQCT and DXA scan data.
METHODS: Powdered calcium-sulphate (CSC) was water-mixed in vacuum and cured. This mixture exhibited hydroxyapatite-like DXA photon-attenuation properties with density monotonically related to added water-mass. Its mass and BMD maintained temporal stability (CV%=0.03%, n=4 specimens over 321 d). Using CSC designed for a BMD=1.04g/cm^2, (for plate-thickness 10mm), a cylindrical phantom with cortical shell thicknesses of 0.5, 1.0, 2.0, 4.0mm, an acrylic-based internal core diameter of 26mm, and an acrylic surrounding "soft-tissue" were constructed. The phantom was scanned using a DXA scanner (Hologic QDR1000W) and pQCT (Stratec XCT2000, pixel resolution 0.15mm).
RESULTS: Selected cortical structural-geometric variables, derived from calculated geometry; pQCT mass-projections, and DXA HSA, were:

Variable	Calc. Geom.	pQCT	DXA HSA
Cortical Thickness (mm)			
"0.5 mm shell"	0.50	0.50	0.96
"4 mm shell"	4.00	4.04	4.87
Bone Width (mm)			
"0.5 mm shell"	27.00	27.34	27.92
"4 mm shell"	34.00	34.44	30.75
Section Modulus (mm^3)			
"0.5 mm shell"	271	360	97
"4 mm shell"	2539	2722	2131

CONCLUSIONS: In conclusion, dimensions of this novel cortical-shell phantom were fairly accurately rendered by pQCT, less accurately by DXA HSA. These encouraging results provide impetus towards the design of an anthropometric hip phantom, using this CSC mixture as a cortical-bone equivalent material, for more clinically realistic accuracy measures of structural geometry derived from pQCT, DXA HSA and CT.

REFERENCE:

Beck, T. J. et al. (2000) J Bone Miner Res. 15: 2297-2304.

ONE YEAR'S EXPERIENCE OF THE WA MEDICAL CYCLOTRON AND RADIOPHARMACEUTICAL PRODUCTION FACILITY

J. DeRoach, T. Tuchyna, C. Jones and R. Price

Department Medical Technology & Physics, Sir Charles Gairdner Hospital, Perth, WA, Australia

INTRODUCTION: The WA PET Centre Medical Cyclotron, a facility novel in Western Australia, produced its first bolus of FDG for patient injection for PET scanning in August 2003. This paper describes the methodology and practices employed during the past 12 months for ensuring that reliable routine provision of FDG is maintained, in parallel with facilitating the development and production of achievable new radiopharmaceuticals.

METHODS: An FDG production team of six staff and, a maintenance and development team of 4 staff were created from the 3.4 staff specifically recruited for this service and from incumbent staff. Teams were also set up to carry out development projects related to the service. Training procedures were created under the department's ISO9001:2000 accreditation system for the certification of production and maintenance staff. Practices and documentation systems were put in place in anticipation of a pending cGMP audit. Several unplanned major changes to equipment and infrastructure were necessary post commissioning. These changes included purchase of a different FDG synthesis module from that originally supplied, and modifications to engineering services, including changes to air conditioning, changes to supply of vacuum and upgrading of drainage in the laboratory area. A device for the measurement of end of bombardment yield was built, so that the efficiencies of the various synthesis modules could be accurately determined. Strict radiation protection procedures were put in place. All staff were provided with luxels and finger TLDs for monthly reporting of their radiation levels, as well as electronic monitors for real-time monitoring.

RESULTS: From August 2003 to June 2004 (11 months) 2229 FDG patient doses were produced and dispensed by this facility. An average of 8.0 patient doses per available working day were dispensed during the 2003 period, rising to 11.1 patient doses per day in 2004. Several $^{11}NH_3$ doses were also delivered. The cyclotron was unavailable for 9 days owing to scheduled maintenance, and a total of 35 (1.6%) patients were cancelled owing to unscheduled maintenance on 7 days.

The following major initiatives are now in place for the further development of this facility:

- Development of a solid targetry facility for the production of ^{123}I, ^{124}I, ^{64}Cu, and other isotopes. Two prototype external beam lines have been developed and trialled. Experiments designed to measure the beam profile at the end of the external beam line are underway.
- A synthesis module for the production of ^{18}FMISO and ^{18}FLT is being developed in-house in collaboration with the cyclotron manufacturer.
- A module for the synthesis of ^{18}F-Choline has been installed.
- A prototype synthesis module is under development which will allow experimentation in the production of novel radiopharmaceuticals based on isotopes produced from liquid targetry.

Normalised over 12 months, production staff received on average 3.28 mSv whole body effective dose, with the worst case being 8.46 mSv. Finger doses were 35.6 mSv on average, 70.6 mSv worst case. (Note that production staff also dispense patient doses into individual syringes). Similarly, maintenance staff received 1.41 mSv (avg), 2.56 mSv (max) whole body effective dose, and 33.0 mSv (avg), 124.3 mSv (max) finger dose.

CONCLUSION: A facility for the production and development of short-lived PET radiopharmaceuticals has been created with a capacity that is expected to satisfy Western Australian demands for the next ten years. This facility reliably and routinely produces FDG, and incorporates a well supported and vigorous radiopharmaceutical development function.

ACKNOWLEDGEMENTS: This presentation is based on the work of all members of the WA PET Centre Radiopharmaceutical Production and Development Team.

PERFORMANCE BENCHMARKING IN CARDIAC IMAGING

D. Schick[1], D. Thiele[1] and I. Smith[2]

[1]*Biomedical Technology Services, Qld Health, Qld, Australia*
[2]*St Andrew's War Memorial Hospital, Brisbane, Qld, Australia*

INTRODUCTION: Diagnostic and interventional procedures performed in a cardiac catheter laboratory while demanding high image quality may also result in high patient radiation dose depending on the length or complexity of the procedure.

Clinicians using the X-ray equipment require confidence that the system is operating optimally to ensure maximum benefit to the patient with minimum risk.
METHODS: 17 cardiac catheterisation laboratories have been surveyed using a phantom based on the NEMA XR 21 – 2000 standard. The testing protocol measures spatial resolution, low contrast detectability, patient dose rate, dynamic range and motion blur for modes of operation and simulated patient sizes applicable to a diagnostic left heart catheter study.
RESULTS: The combined results of the assessed laboratories are presented. The latest generation systems with flat-panel detectors exhibit better spatial resolution than older systems with image intensifiers. Phantom measurements show up to a 6 fold variation in dose rate across the range of systems assessed for a given patient size. As expected, some correlation between patient dose rate and the low contrast detectability score is evident. The extent of temporal filtering and pulse width is reflected in the motion blur score. The dynamic range measurements are found to be a less sensitive measure in evaluating system performance.
DISCUSSION & CONCLUSIONS: Examination of patient dose results in the context of low contrast detectability score indicates that dose reduction could be achieved without compromising diagnosis on some systems.

COMPLEX WAVELET TRANSFORM FOR MRI

P. Junor and P. Janney

Department of Electronic Engineering, La Trobe University, Bundoora, Vic. Australia

INTRODUCTION: There is a perpetual compromise encountered in magnetic resonance (MRI) image reconstruction, between the traditional elements of image quality (noise, spatial resolution and contrast). Additional factors exacerbating this trade-off include various artifacts, computational (and hence time-dependent) overhead, and financial expense. This paper outlines a new approach to the problem of minimizing MRI image acquisition and reconstruction time without compromising resolution and noise reduction.
BACKGROUND: The standard approaches for reconstructing magnetic resonance (MRI) images from raw data (which rely on relatively conventional signal processing) have matured but there are a number of challenges which limit their use. A major one is the "intrinsic" signal-to-noise ratio (SNR) of the reconstructed image that depends on the strength of the main field. A typical clinical MRI almost invariably uses a super-cooled magnet in order to achieve a high field strength. The ongoing running cost of these super-cooled magnets prompts consideration of alternative magnet systems for use in MRIs for developing countries and in some remote regional installations.
The decrease in image quality from using lower field strength magnets can be addressed by improvements in signal processing strategies. Conversely, improved signal processing will obviously benefit the current conventional field strength MRI machines. Moreover, the "waiting time" experienced in many MR sequences (due to the relaxation time delays) can be exploited by more rigorous processing of the MR signals. Acquisition often needs to be repeated so that coherent averaging may partially redress the shortfall in SNR, at the expense of further delay.
DISCUSSION: Wavelet transforms have been used in MRI as an alternative for encoding and denoising for over a decade[1]. These have not supplanted the traditional Fourier transform methods that have long been the mainstay of MRI reconstruction, but have some inflexibility. The dual-tree complex wavelet transform (DTCWT)[2] is an example of an over-complete or expansive wavelet transform. Compared with the Discrete Wavelet Transform it has the advantage of spatial invariance and directional selectivity though with greater computational burden. This processing load can be redressed by hardware approaches if necessary[3]. It has recently been used for diffusion tensor imaging, but it has yet to be determined if it is optimal for the particular noise characteristics encountered in MRI[5] (typically Rician-distributed amplitude distribution at low SNR, and with a *1/f,* rather than exclusively white, spectral density suggested for some modalities).
CONCLUSIONS: The complex wavelet transform offers a new possibility for MRI processing: the improved spatial invariance and directional selectivity promising both shorter overall acquisition time and improved image quality.
ACKNOWLEDGEMENTS: We gratefully acknowledge the support of Dr. G. Deng, Dr. R. Kirsner and Dr. D. Tay.
REFERENCES:
[1]D. Healy, J. Weaver (1992) *IEEE Trans. Inform.Theory* 38:840.
[2]N. Kingsbury (2001) *J. Applied & Computational Harmonic Analysis* 10: 234.
[3]B. Das, S. Banerjee (2001) *11th Great Lakes Symposium on VLSI (GLSVLSI 2001):* 79
[4]N. Kingsbury, A. Zymnis (2004) *Proc. EURASIP Biosignal Conference, Brno Czech Rep.*
[5]A. Wink, J. Roderink (2004) *IEEE Trans. Medical Imaging* 23:374.

QUANTITATIVE ASSESSMENT OF BREAST DENSITY FROM MAMMOGRAMS

N. Jamal[1], K.H. Ng[1], L.M. Looi[2] and D. McLean[3,4]

[1]*Department of Radiology, University of Malaya, Kuala Lumpur, Malaysia*
[2]*Department of Pathology, University of Malaya, Kuala Lumpur, Malaysia*
[3]*Westmead Hospital, Sydney, NSW, Australia*
[4]*University of Sydney, Sydney, NSW, Australia*

INTRODUCTION: It is known that breast density is increasingly used as a risk factor for breast cancer. This study was undertaken to develop and validate a semi-automated computer technique for the quantitative assessment of breast density from digitised mammograms.

METHODS: A computer technique had been developed using MATLAB (Version 6.1) based GUI applications. This semi-automated image analysis tool consists of gradient correction, segmentation of breast region from background, segmentation of fibroglandular and adipose region within the breast area and calculation of breast density. The density is defined as the percentage of fibroglandular tissue area divided by the total breast area in the mammogram. This technique was clinically validated with 122 normal mammograms; these were subjectively evaluated and classified according to the five parenchyma patterns of the Tabar's scheme (Class I- V) by a consultant radiologist.

RESULTS: There was a statistical significant correlation between the computer technique and subjective classification ($r^2 = 0.84$, $p<0.05$). 71.3% of subjective classification was correctly classified using the computer technique.

DISCUSSION & CONCLUSION: We had developed a computer technique for the quantitative assessment of breast density and validated its accuracy for computerized classification based on Tabar's scheme. This quantitative tool is useful for the evaluation of a large dataset of mammograms to predict breast cancer risk based on density. Furthermore it has the potential to provide an early marker for success or failure in chemoprevention studies such as hormonal replacement therapy.

Abstracts of oral presentations - clinical and biomedical engineering

VENTILATOR FLOW MONITORING UNDER HYPERBARIC CONDITIONS

C. Akalanli[1], I. Millar[2] and P. Junor[1]

[1]*Electronic Engineering, LaTrobe University, Melbourne, Vic, Australia*
[2]*Hyperbaric Service, The Alfred Hospital, Melbourne, Vic, Australia*

INTRODUCTION: Hyperbaric oxygen therapy is a medical treatment in which a patient breathes pure oxygen while under pressure in a hyperbaric chamber. Many of the patients undergoing this therapy are from the intensive care unit and require support from a ventilator. However, few ventilators are designed for hyperbaric conditions and those that do operate under pressure often display disturbed functioning. Examination of publications from the past three decades indicates that there has been no significant advancement regarding ventilator use in the hyperbaric chamber.[1,2,3] Accurate measurement of minute volume under hyperbaric conditions is an important parameter used to optimise assisted ventilation in a hyperbaric chamber. We describe the development of an independent electronic device which can be connected to the patient circuit of a ventilator to provide pressure compensated measurements of minute volume.
METHODS: A proprietary flowmeter with the potential to operate under hyperbaric conditions was identified[4] and its performance was tested in the chamber with a three-litre syringe used to deliver known volumes of oxygen or air at various pressures. The empirical data obtained from these tests enabled a description of the flowmeter's functioning under hyperbaric conditions: this information is required to compensate for the effects of pressure. A microcontroller system was constructed to calculate volume as a function of time from the flowmeter's analogy output, corrected by our empirically-determined calibration factor for pressure in the chamber.
RESULTS: Statistical analysis of the results obtained from the calibration tests conducted on the flowmeter revealed a linear response for air and oxygen flow with changes in pressure. The physical dimensions of the flowmeter permit it to be directly connected to the patient circuit of a ventilator, and the flowmeter is connected to the custom-designed, battery powered microprocessor unit. Results are presented on a liquid crystal display. The unit has proven functional under pressure inside the chamber.
DISCUSSION & CONCLUSIONS: The developed device offers hyperbaric medical and nursing staff a simple and accurate means of assessing the minute volume delivered to a patient without the time consuming and error-prone use of pressure correction charts or the starting and stopping of a mechanical volumeter. We have been unable to identify any such device available commercially at this time.
REFERENCES:
[1]J. A. S. Ross, H. J. Manson (1977) *Aviat Space Environ Med*, 48: 26-28.
[2]P. B. Blanch, D.A. Desautels, T.J. Gallagher (1991) *Respiratory Care*, 36: 803-814.
[3]W. Stahl, P. Radermacher, E. Calzia (2000) *Intensive Care Medicine*, 26: 442-448.
[4]TSI (2004) *Mass Flowmeters Design Guide* (TSI 4022).

MEASURING CARDIAC OUTPUT DURING ANAESTHESIA

K. K. Deo[1], P. J. Peyton[2], G. J. B. Robinson[3] and P. Junor[1]

[1]*Department of Electronic Engineering, La Trobe University, Melbourne, Vic, Australia*
[2]*Austin Health, Heidelberg, Vic, Australia*
[3]*The Alfred Hospital, Melbourne, Vic, Australia*

INTRODUCTION: It is vital to monitor cardiac output in patients undergoing anaesthesia. There are several methods and techniques used to measure or determine cardiac output. They are, however, either highly accurate but invasive, or non-invasive but relatively inaccurate or imprecise. A new system and technique has been developed for the measurement of gas exchange in two lungs independently during anaesthesia using carbon dioxide as an extractable marker gas[1]. Here we describe further enhancements that automate the measurement of CO_2 flow, gas concentrations and solenoid switching for gas sampling, temperature and pressure and improve the reliability and robustness of the system.
METHODS: Gas exchange is calculated by measuring the uptake of each gas sample; the difference between the inspiratory and expiratory flow rate of that gas. Ventilation of each lung is achieved using a dual-lumen endo-bronchial tube. The extractable marker gas allows measurement of gas exchange with any inspired gas mixture. Integrated pressure transducers with inbuilt signal conditioning, temperature compensation and calibration are used to monitor pressure downstream from the patient, and thus help to determine CO_2 flow. A linearized thermistor-based nasal probe measures patient temperature; a

Datex Capnomac Gas analyser measures anaesthetic gas concentrations: N_2O, O_2, CO_2, and AA (anaesthetic agent). Gas sampling at multiple points along the breathing circuit is achieved with solenoid switching under software control from a PC which also acquires the data from all sensors.

RESULTS: The temperature measurement was accurate within ± 1°C, and pressure measurement with the transducers used was within 2.5% of full-scale span. Washout times consistent with previous experience were observed when anaesthetic gas mixtures were passed through the solenoids and plotted for those particular gases.

DISCUSSION & CONCLUSIONS: The advantage of this new method of gas exchange is the automation of gas sampling and temperature, pressure and gas concentration measurements, and is potentially a "hands-free" system: minimally invasive, cheaper, less complex and allowing accurate continuous measurements of exchange of all gases. The modifications described here extend the automation of this novel approach.

REFERENCE:

[1]P. J. Peyton, G. J. B. Robinson, D. Terry, P. Junor (2004) *Physiological Measurement* 25:1-14.

A COMPLIANCE DEVICE FOR POSITION MONITORING IN PATIENTS WITH POSITIONAL OBSTRUCTIVE SLEEP APNOEA

E. Mackie[1], M. Barnes[2], R. Pierce[2] and P. Junor[1]

[1]*Department of Electronic Engineering, La Trobe University, Melbourne, Vic, Australia*
[2]*Institute of Breathing and Sleep, Austin Health, Heidelberg, Vic, Australia*

INTRODUCTION: Obstructive sleep apnoea (OSA) is a common disease of repeated cycles of breathing pauses during sleep with consequent fall in blood oxygen levels followed by arousals. It affects 2% of adult males and 4% adult females. The health consequences of OSA range from daytime sleepiness, reduced cognitive performance, high blood pressure, stroke and heart attacks. Some patients have positional sleep apnoea, which means they experience at least twice as many breathing pauses (apnoeas and hypopnoeas) while lying on their back than on their side. The 'tennis ball in back pack' device encourages patients to lie in a lateral rather than supine orientation. To assist in determining the effectiveness of this therapy, an at-home monitoring device is needed to monitor patient sleep position and compliance to the therapy.

METHODS: The device contains a triaxial sensor in the form of two orthogonally mounted accelerometers. They are used to determine the patient's 360-degree orientation with respect to gravitational pull and are used to in determining patient compliance. The system contains processing software for deducing patient orientation as supine, prone or lateral positions. The device is a fully self-contained system that will be incorporated into a case of similar properties to a tennis ball. It is rugged, tamperproof and capable of gathering and storing patient data collected over more than a week. Data can then be easily downloaded to a PC for analysis.

RESULTS: Previous prototypes have been capable of sensing tilt in both the X and Y-axis with accuracy of within ±4° of actual angle. Software for successfully determining patient sleep position has been developed and trialled with promising results. With the devices proven feasibility for measurement of patient compliance and the efficacy of sleep position modification, a comprehensive device to be used in clinical trials has now been designed and constructed.

DISCUSSION & CONCLUSIONS: We have proposed and designed a system for assessing both patient compliance and effectiveness of sleep position modification for the treatment of positional sleep apnoea. By covertly monitoring patient usage, we hope to determine the effectiveness of position modification as well as patients' willingness to comply with the therapy. It is hoped that position modification can become an alternative treatment for patients with mild to moderate OSA.

REFERENCES:

[1]R. Cartwright, S.Lloyd, et al. (1985) *Sleep*, 8:87-94
[2]P. Freebeck, D. Steward, (1995) *Sleep Research,* 24: 236.

INSTRUMENTATION FOR RESUSCITATION TRAINING

R. Hendry[1,2], C. Morley[2] and P. Junor[1]

[1]*Department of Electronic Engineering, La Trobe University, Melbourne, Vic, Australia*
[2]*Royal Women's Hospital, Melbourne, Vic, Australia*

INTRODUCTION: Neonatal resuscitation is an important procedure in neonatal wards and is currently assessed visually. Ten percent of newborns require some kind of assistance and one percent needs major resuscitative measures to survive[1,2]. Resuscitation has a very high success rate when performed correctly. The device being developed will improve resuscitation skills and assessment by providing the assessment officer and trainee resuscitator with an accurate recording of the resuscitation. This can then be evaluated to determine the effectiveness of lung inflation and chest compression received by a baby manikin.

METHODS: The device is designed for installation inside a Laerdal "Resusci Baby"™. It is fitted with circuitry to detect the depth of compression, and the differential and absolute pressure in the airway so that concrete results can be reviewed for accuracy, consistency and timing of resuscitation. The differential measurement is based around a 0-14.5psi pressure sensor which measures the difference between air pressure at point 'A', and point 'B' (see Fig. 1) allowing the mask leak to be calculated. Absolute sensors will also take distinct measurements from point 'A' and 'B'. The depth of chest compression 'C' is measured linearly with a sliding potentiometer. These parameters are then suitable for display and statistical evaluation under LabView™ after conversion to a digital reading using a Data Translation USB Module Data Acquisition Unit™.

RESULTS: A test circuit has been developed which eliminates mask leak; the standard Laerdal baby lung has been replaced with two Drager bellows to provide a simulation lung having the compliance of a newborn. The basic absolute pressure sensor circuitry has been tested with this test circuit and shows a change of 45.5cm H_2O, consistent with the value expected due to the pop-off valve in the self-inflating bag.

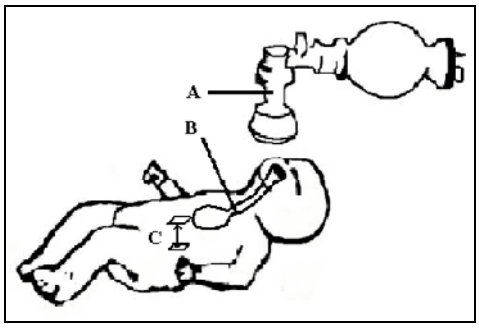

Figure 1. *Experimental setup (diagram adapted from 3,4).*

DISCUSSION & CONCLUSIONS: At present, purely visual methods are used for evaluating resuscitation. Preliminary tests have shown the potential for the new device described here to enable the evaluation of resuscitation methods using solid data and evidence.

REFERENCES:

[1]Zaichkin J., *Neonatal Resuscitation Instructors Manual*, American Academy of Paediatrics and American heart Association, 3rd edition 2000, USA, p. 2.25

[2]Goldsmith J., *Assisted Ventilation of the Neonate*, WB Saunders Company, 3rd edition 1996, USA

[3]www.who.int/reproductive-health/publications/French_MSM_98_1_reanimation_du_nouveau_ne/ MSM_98_1_chapter1.fr.html

[4]www.create-a-lab.com/ als/images/nrb-1000b.jpg

MONITORING ENDOTRACHEAL TUBE PATENCY WITH ULTRASOUND

W. H. Round[1], B. Manikkam[2], L. M. O. Jaudo[1] and J. W. Sleigh[2]

[1]*Electrical and Electronic Engineering, University of Waikato, Hamilton, New Zealand*
[2]*Auckland Medical School, Auckland University, Auckland, New Zealand*

INTRODUCTION: Endotracheal tubes are known to block with mucus when in situ. It is valuable to know whether or not the tube is patent or if mucus is building up to a level where the tube will be blocked. In this study the use of ultrasound was investigated as a means of testing patency.

METHODS: Pulses from 50 kHz electrostatic ultrasonic transducer were introduced into an endotracheal tube. Electrostatic transducers were chosen over other technologies because of their high output and sensitivity, and because they have quite a broad band. As the electrostatic transducer was of a much larger diameter than the tube, it was necessary to construct a horn to channel the ultrasound into the much smaller diameter tube. Circuitry to drive the transducer and received echoes reflected off blobs of mucus in the tube was developed.

RESULTS: Echoes from obstructions inside the tube could be readily detected using this method. It is also possible to estimate the size and position of the obstruction in the tube. However, the lengths of the echoes from the obstructions are relatively long and this can make it difficult to determine if an echo is due to single or multiple obstructions.

DISCUSSION & CONCLUSIONS: This technique shows promise, but further investigation is required to optimize the driving and receiving circuitry. Also, there is a need to construct a purpose-built transducer with a smaller diameter and a higher resonant frequency than the commercially-available transducer used.

THE EFFECTS OF ANAESTHESIA ON CORTICAL STIMULATION IN RATS: A FUNCTIONAL MRI STUDY

M. Dashti[1,2] and M. Geso[1]

[1]*Division of Medical Radiations, School of Medical Sciences, RMIT-University, Bundoora, Vic, Australia*
[2]*College of Allied Health Sciences, University of Kuwait, Kuwait*

PURPOSE: To investigate the affects of two different anaesthetic agents (Equithesin and Isoflurane) on cortical neural activations in the rat using fMRI.
METHODS: Eight healthy male Sprauge-Dawley rats were anaesthetised with isoflurane and equithesin separately with one week between anaesthesias. Functional EPI images were acquired to demonstrate neuronal activity in the sensory cortex. EPI images were acquired in axial and sagittal orientations on a Bruker 47/30 Biospec system. Each experiment included repetitive air puffs over the right face region and was divided into 4 OFF (no stimulation) and 3 ON (repeated air puffs) periods. Changes in the BOLD-fMRI signal response were analysed using a box-car response function (SPM99) correlated against each voxel to determine regions of activation (p Corrected <0.0001, Z score>3.54).
RESULTS: All eight rats showed no neural activations of any kind when equithesin was used except with one compared to consistent activations with isoflurane. 16 functional EPI scans were acquired with each anaesthetic, showing cortical activations in all isoflurane functional scans compared to only 1 out of 16 when equithesin was used.
CONCLUSION: Equithesin appears to have effectively reduced brain activity in response to sensory stimuli and this may be due to its influence on blood flow coupling. Isoflurane anaesthesia (1.6%) showed consistent, robust neural activations. It is therefore recommended that equithesin should not be considered as an anaesthetic agent for functional MRI studies and should be further investigated with other functional modalities or behavioural tests.

SYSTEMATIC PARAMETER VARIATION OF ELECTRIC PULSES USED FOR USCLE STIMULAION – AN OVERVIEW

H. E. R. Rudolph[1], D. K. Kumar[1] and Z. Deng[2]

[1]*Electrical & Computer Engineering, RMIT University, Melbourne, Vic, Australia*
[2]*formerly of: Electrical & Computer Engineering, RMIT University, Melbourne, Vic, Australia*

INTRODUCTION: This paper reports research conducted in systematically varying major parameters of electrical pulse waveforms used for muscle stimulation in order to attain maximum force and duration while minimising muscle fatigue and discomfort. The purpose of this research was to:

1) Develop a map of the boundaries of the major parameters for electrical pulse waveforms that are commonly used for surface electrode muscle stimulation with respect to the force generated by the muscles. Pain and discomfort were also considered as boundary conditions for electrical muscle stimulation.
2) Develop a starting point for a theoretical muscle model that can be used to simulate the behaviour of skeletal muscles.

METHODS: A purpose built programmable surface electrode muscle stimulator was used to vary the parameters of stimulation pulses one at a time (Frequency, Pulse width, Intensity, Number of pulses per burst). The forces and sensations produced were recorded over a range of values on 5 human subjects.
RESULTS: An optimal range of parameters for maximizing force using surface electrode stimulation was found. Increasing the pulse parameters beyond this optimum resulted in unsustainable discomfort and excessive muscle fatigue. The results provide a map of the effects of varying pulse width, intensity, frequency, pulses per burst, all at low and high frequencies. The results obtained lay the basis for developing an electrical equivalent muscle model.

PARAMETER	OPTIMIZED FOR FORCE	SENSATION THRESHOLD (START OF DISCOMFORT AND PAIN)
Pulse width W (μs)	100 to 500μs	> 600μs (F=5) > 500μs (F= 20)
Intensity I (mA)	10mA to 25mA	> 30 mA (F=5) > 22 mA (F=20)
Number of pulses N per burst	1 to 3 Pulses / burst	Max N=6 caused no discomfort for F=5 or F=25
Frequency range F (Hz)	15 to 25 Hz	
Total charge to muscles	- - -	> = 7 micro coulombs per 200ms

Table 1. *Optimal ranges for pulse width, intensity, pulse number, frequency (r=100Hz).*

DISCUSSION & CONCLUSIONS: The best balance between discomfort and maximum force with the least amount of ripple was found to be a frequency of 15 to 25 Hz with a pulse width of 100 to 500μs and current in the range of 10mA to 25mA. The number of pulses per burst N can be used to shift between different force ranges and the effective value is one to three. In the higher frequency bands (F =25) the number of pulses per burst have less effect than in the lower frequency range (F=5). As these results are based on 3 to 5 human subjects, larger trial numbers are required for verification. It is interesting to note that pain is directly related to the amount of electrical charge that is driven into the muscle. The threshold for surface electrode stimulation appears to be approximately 7 micro coulombs per 200ms.

A VESTIBULAR DIAGNOSTIC RESPONSE

M. Shoushtarian and B. Lithgow

Biosignal Processing Group, Department of Electrical and Computer Systems Engineering, Monash University, Clayton, Vic, Australia

INTRODUCTION: The SP/AP ratio is a commonplace measure used in cochleography for detection of Meniere's Disease (a pathology of the vestibular system). The measure is usually an averaged response to an acoustic stimulus. Franz[1] describes a process whereby the vestibular response rather than the cochlear response is used to elicit the SP/AP ratio. This paper examines that direct process.

METHODS: Standard cochleography (ECOG) methods were employed[2]. The exceptions and specifics are:- 1. A wick electrode was placed on the tympanic membrane; 2. The responses were analysed offline; Responses were analysed for the onset (0-3 seconds after onset of head tilt), transient (3-10 seconds) and steady state (10-18 seconds), though, in this paper only the onset component is considered; 3. A head tilt was used as a drive stimulus—this was either a request for the patient to voluntarily move their head or movement was applied via a tilt chair through an angle similar to that achieved by the patient voluntarily; 4. For the Franz test the recorded waveforms were averaged at 11.5, 23 and 46 Hz periods.

To characterize the recorded signals they were wavelet decomposed. A Morlet wavelet was selected for its excellent time-frequency localisation property. Components of the decomposition were characterised where possible according to their origin (eg. Muscle artefact, eye movement, vestibular, vestibulo-cochlear).

RESULTS: Spectral peaks observed, were analysed to determine which were the result of artifacts and which could be a vestibular response. Studying the excitatory or inhibitory nature of the neural activity generated following a head tilt could help us identify the driven response. The results showed that a back tilt of the head along with an ipsilateral tilt, both showed signs of generating excitatory responses. A forward or contralateral tilt led to inhibitory neuronal activity. A consistent peak was observed at $15 \pm 2Hz$ in the onset region of 11/12 back tilt plots (See figure opposite which is a plot of averaged coefficient magnitude versus frequency once the background signal had been removed).

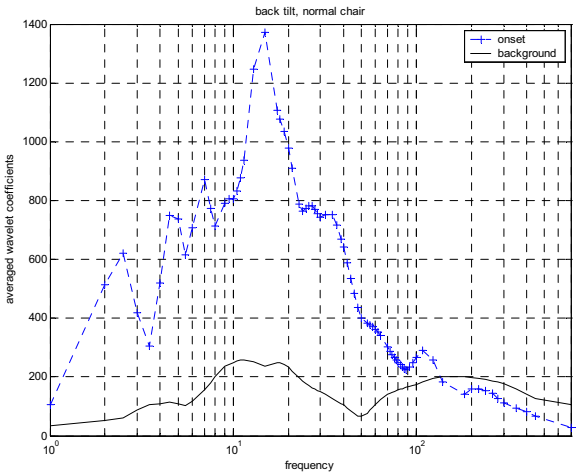

DISCUSSION & CONCLUSIONS: It is believed that this peak could show a vestibular response possibly from the semicircular canals. More data is needed to verify this. The variability of the results obtained at frequencies less than 10 Hz have led us to believe that refining the recording method could render more consistent results. Muscular and ocular artifacts exist in the recordings. Certain spectral peaks are related to these. Possible peaks have been identified however further work is needed to identify consistent frequencies or bandwidths across all subjects that are related to these artifacts. The direct process appears to detect a driven vestibular response probably from the semi circular canals at about 15Hz.

REFERENCES:

[1]Franz, B., *A method of measuring the activity of a biological system*, Patent, International publication number WO 02/47547 A1. 2002.

[2]Chung, W. H., *Clinical usefulness of extratympanic electrocochleography in the diagnosis of Meniere's disease,*. Otol Neurotol. 25: 144-149, 2004.

MODELING THE VESTIBULAR HEAD TILT RESPONSE

D. Heibert and B. Lithgow

Biosignal Processing Group, Department of Electrical and Computer Systems Engineering Monash University, Clayton, Vic, Australia

INTRODUCTION: This paper attempts to verify the existence of potentially diagnostically significant periodic signals thought to exist in recordings of neural activity[1] originating from the vestibular nerve, following a single tilt of the head. It then attempts to find the physiological basis for this signal, in particular, focusing on the mechanical response of the vestibular system.

METHODS: Simple mechanical models of the semi circular canals having angular velocities applied to them were looked at. A simple single canal model was simulated using *CFX* software. Finally, a simple model of all three canals with elastic duct walls and a moving cupula was constructed. Pressure waves within the canals were simulated using *water hammer* or *pressure transient theory.* In particular, it was investigated whether pressure waves within the utricle following a square pulse angular velocity applied to the canal(s) may be responsible for quasi-periodic oscillatory signals. The step input angular velocity was set to be 30 degrees/second, which corresponds to normal human head movements.

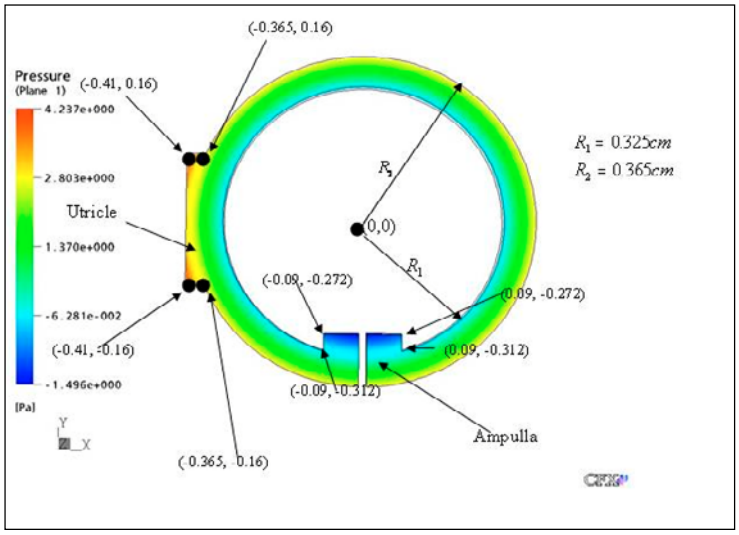

RESULTS: The upper figure shows the steady state pressure distribution in canal after a step input angular velocity is applied. The origin of the coordinate system is at the centre of the ring. Coordinates of important geometrical points are shown. R_1 and R_2 is the inner and outer radius of the ring, respectively.

The lower figure shows a plot of pressure in the utricle for k = $5.43 \times 10^{-10}\, N/m^2$ (the cupula's spring restoring moment per unit angular displacement) and Ed = $3 \times 10^5\, dyne/cm^2$ (the stiffness, or elastic modulus of the pipe walls). Only when using these unrealistic values could oscillations be made to appear in the lower plot at around 25 Hz. The pressure distribution producing these oscillations is physically unrealistic (too large). After the short time constant of 0.003 seconds, the pressure in the middle of the canal returns to its equilibrium pressure (taken as zero). In reality we know the pressure along the canal length returns to equilibrium in around 10 seconds.

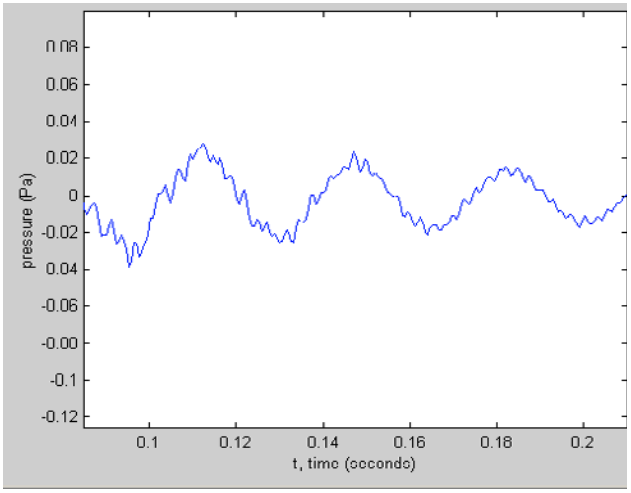

DISCUSSION & CONCLUSIONS: In summary, the simulations showed that there are no pressure waves resonating within the canals following a square pulse angular velocity applied to the canal(s). The results show that the oscillatory signals[1] are most likely not mechanical in origin. It was concluded that further investigation is required.

REFERENCES:

[1]Franz, B., *A method of measuring the activity of a biological system*, Patent, International publication number WO 02/47547 A1. 2002.

REAL-TIME RECORDING OF NEUROPSYCHOPHYSIOLOGICAL PARAMETERS DURING ELF MF EXPOSURE

H. A. Sadafi[1], P. Cadusch[2] and A. W. Wood[2]

[1]*The Walter and Eliza Hall Institute of Medical Research, Royal Melbourne Hospital, Melbourne, Vic, Australia*
[2]*School of Biophysical Sciences & Electrical Engineering, Swinburne University of Technology, Hawthorn, Vic, Australia*

INTRODUCTION: To assess the possible effects of occupational levels of 50 Hz magnetic fields (MF) on human performance it is preferable to monitor performance during rather than subsequent to MF exposure. The contamination of EEG signal by the MF exposure is clearly a problem in this type of study. Previous investigators have not reported these types of measurement concurrent with MF exposure due to the contamination difficulty; but this paper reports means of accomplishing this.

MATERIALS AND METHODS: Two categories of tests were conducted: (i) cognitive behavioural; and, (ii) neurophysiological. The apparatus, comprising a Merritt *et al*. [1] type modified two orthogonal sets of Helmholz, 4-coil system was designed and constructed at Swinburne University of Technology. A laptop was used to eliminate screen jitter. Twelve methods for reducing pickup in the neurophysiological recordings were employed: 1) Distancing instruments from the MF source; 2) Shielding the devices & wiring; 3) Proper choice of cables; 4) Grounding the instrumentation; 5) Orientation of conduits; 6) Isolation of power supplies; 7) Balancing the input impedances; 8) Using a driven shield technique; 9) Improved electronics design; 10) Analogue filtering; 11) Signal Averaging; 12) digital filtering.

RESULTS: The graphs in Fig. 1 demonstrate sample of the filtered evoked response (ER) signals superimposed on the original (unfiltered) after applying the methods listed above.

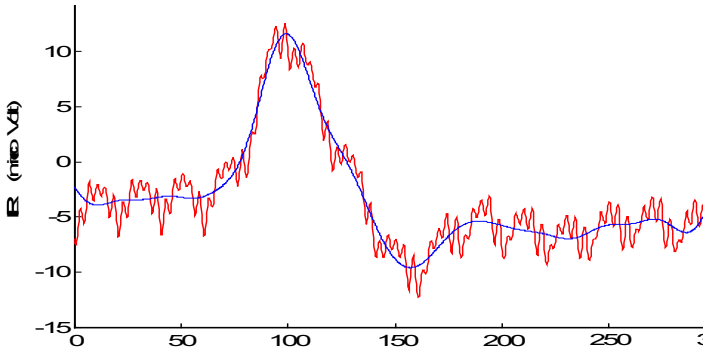

Figure 1. *Filtering the data: Horizontal axis: Time (50 msec/div); Vertical axis: ER Voltage (5 μV/div); Red plot: Pre-filter signal (noisy plot); Blue plot: Filtered signal (smooth plot).*

DISCUSSION & CONCLUSIONS: The experiments were conducted with: (i) jitter-free display of the instructions; and, (ii) reliable recording of the brain signals, concurrent with the MF exposure. Interference rejection in the neurophysiological tests was more challenging than in the cognitive behaviour tests because of the wiring needed to transmit tiny EEG signals. The experimental results on acute effect on the human brain due to 28.4 μT MF exposure will be presented in a subsequent paper.

ACKNOWLEDGEMENTS: The Electronics Workshop staff of Psychology Department in Latrobe University who assisted with the design and construction of the electronics

REFERENCES:

[1]Merritt, R., Purcell, C. and Stronik, G. *Uniform magnetic field produced by three, four and five square coils*, in *Rev Sci Instrum*. 1983, American Institute of Physics.

BIOMEDICAL ENGINEERING: DEVELOPING AREAS

B. Lithgow

Biosignal Processing Group, Department of Electrical and Computer Systems Engineering, Monash University, Clayton, Vic, Australia

INTRODUCTION: To develop a policy on future BME funding (support) many factors must be taken into account. These include: historical perspective, current curriculum funding and policy; academic and research expertise, research funding, policy and infrastructure, government policy, overseas trends, internationalization and marketability of courses, commercialization of research, industry need, professional society accreditation, as well as, general student, industry and professional society acceptance and encouragement. One of the most impacting factors, given the rapidly evolving technology and discipline field expansion into Biotechnology, is the massive new knowledge base and the attitudes of senior BME's to change. This paper deals specifically with the problems of BME policy design in Australia. Who should steer the BME ship and where should it go?
METHODS: This paper adopts a qualitative approach, which focuses on the perception and beliefs of senior academic and industry administrators as the primary source of data. Senior academic and industry Biomedical Engineering personnel were drawn from a selection of national universities, government institutions, hospitals and private industry. Components of the responses of 10 of these interviews are analysed in relation to the question of "what areas of BME should Australia focus on for the future".
RESULTS: Participant 1 is an engineer from industry with a business focus. Participant 2 is a medical physicist, academic and researcher. Participants 3-5 are engineers, academics and researchers. Participants 6, 8 and 9 are Clinical Engineers with industry experience. Participant 7 is a research engineer with industry experience. Participant 10 is an engineer from industry with a government focus.
DISCUSSION & CONCLUSIONS: The respondents have been separated into Academics, Clinical Engineers and industry types.

- The strongest support for future focus is in the areas of Physiological Modelling and Instrumentation. This support is from academia and industry but less so from the clinical sector.
- The areas of Biomechanics, Biomaterials, Biosensors, Rehabilitation Engineering, Informatics, Imaging, Biotechnology, and Clinical engineering were well supported as a focus for future BME support.
  - Only one academic of 4 and one clinical engineer of 4 supported Biomechanics, Imaging or Rehabilitation Engineering.
  - Biomaterials were specifically excluded by two respondents.
  - Biosensors or Prosthesis development was not supported by the clinical sector.
  - Informatics, Medical & Biological Analysis or Clinical Engineering was not supported by the academic sector.
- EMF and Complimentary Medicine were poorly supported.

These data point to:

- Foci for policy development being in part determined by current employment (career). It being different for the clinical and academic sectors. Numbers preclude definitive statements. An observation by the interviewer is that this is further exacerbated by daily research or job focus. By this is meant, the informatics foci by Clinical Engineers is a consequence of their daily involvement in this area whereas for the academics their daily involvement lies within their research focus which most likely includes some , for example, simulation and modelling.
- The industry sector appears more globally focused on the need for "whole" BME approaches.
- Common to most respondents was the need to encourage existing BME strengths.

MEDICAL TECHNOLOGY HORIZON SCANNING

I. Brown, A. Smale, A. Verma and S. Momandwall

Centre for Biomedical Engineering, Monash University, Clayton, Vic, Australia

ABSTRACT: Horizon scanning is becoming particularly important in the medical industry, in the identification and evaluation of emerging technologies. This paper aims to examine the role biomedical engineers may have in horizon scanning new medical technologies, and considers whether this is a useful activity for biomedical engineers. A horizon scanning methodology for conducting studies of emerging medical technologies is introduced and a horizon scanning study of remote patient monitoring technology is be reported.
HORIZON SCANNING OF REMOTE PATIENT MONITORING (RPM) TECHNOLOGY: Monash University Centre for Biomedical Engineering (MUCBE) has undertaken a number of horizon scanning studies as internal research, however in 2003 MUCBE was contracted by the Victorian Department of Health to undertake an horizon scanning project on behalf of The Hospital Admission Risk Program (HARP) Technology working party. The objectives of this working party were to review remote monitoring technologies, and identify opportunities for the application of such technologies in relation to the home based care of patients with consumptive heart failure (CHF) and chronic obstructive pulmonary disease (COPD).
The methodology developed and used consisted of the following phases:

- Systematic literature review.
- Survey of stakeholders – reference group.
- Remote patient technologies workshop.
- Other stakeholder consultation.
- Commercial technologies search.
- Literature analysis – validation.
- Horizon Scanning Report.

In part the study concludes that a strong evidence base confirming the effectiveness and cost-effectiveness of this RPM technology is not yet available, which is the case for most telemedicine applications reviewed. However, this report identifies a number of principles, which are identified in the significant body of literature reporting on RPM and telemedicine trials. These principles are not a substitute for an established and evaluated implementation model, however, they provide guidance to those who wish to introduce RPM technologies to disease management models being trailed.

CONCLUSION: Medical technology horizon scanning is being undertaken by a number of agencies for the purpose of systematically examining the status of emerging medical technology. Such work has been successfully undertaken by biomedical engineers for the purpose of advising a Government agency on the status of remote patient monitoring technology.

A MANAGEMENT PLAN FOR MEDICAL TECHNOLOGY REPLACEMENT IN AUSTRALIAN PUBLIC HOSPITALS

I. Brown, A. Smale and M. Wong

Centre for Biomedical Engineering, Monash University, Clayton, Vic, Australia

INTRODUCTION: The management of medical technology raises a range of complex issues concerning the effective use and associated costs of technology. Biomedical engineers have an important role to play in developing and implementing medical technology management plans. There is a significant and developing interest at State, national and international levels in issues relating to the effective management of medical technology[1-5], with two main drivers: service planning and cost management.

EQUIPMENT LIFE CYCLE OWNERSHIP AND PRIORITISATION: Due to the complexities of life cycle ownership and prioritisation across specialties, we suggest it is not feasible to gather and maintain the required level of information to properly model the life cycle and replacement cost for each item of medical equipment individually. Our approach is to divide the medical equipment inventory into Major and Minor items based on their estimated replacement value, obtaining detailed planning information only for the relatively small number of major items that contribute the bulk of the value of the equipment stock.

MANAGEMENT PLAN IN 3 PHASES: A management plan can be devised consisting of 3 phases: developing the planning framework, stock survey and assessment, and assessment and prioritisation of the funding requirements (see Figure 1). A detailed view of major equipment requirements (funding and priorities) can be created, with minor equipment requirements estimated from other data sources. Completion of these 3 phases then leads to an action plan, or implementation strategy, depending on capacity to meet the identified need, and other constraints.

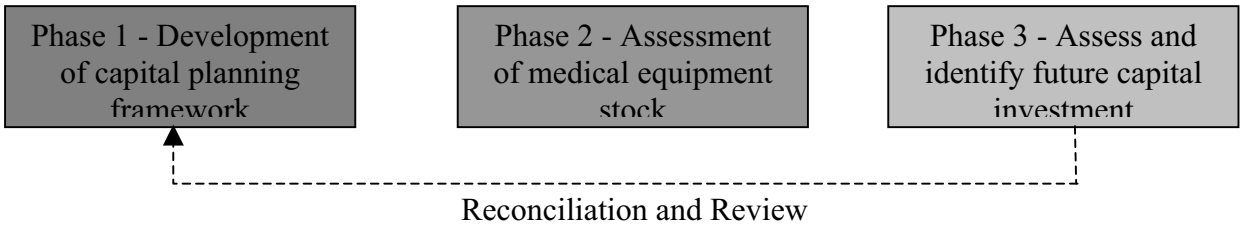

Figure 1. *The three phases of the management plan.*

SUMMARY: The management plan combines an understanding of needs (service plan), an understanding of current capability and outlook, and provides data that can be used to communicate the situation to executive management, and which they can use to validate their governance practices.

REFERENCES:

[1]Brown, I, et al, (2004) *Review of Capital Equipment Funding Strategy for WA Public Hospitals* (unpublished), Department of Health, Western Australia, June 2004.

[2]Brown, I, et al, (2001) *Review of Capital Equipment Funding Strategy for Victorian Public Hospitals* (unpublished), Department of Human Services, Victoria, March 2001.
[3]Victorian Auditor-General's Office (2003), *Managing medical equipment in pubic hospitals*, Melb., 27 March 2003. (avail. http://www.audit.vic.gov.au/reports_par/medical_report.pdf).
[4]UK National Audit Office for NHS Executive (1999), *The Management of Medical Equipment in NHS Acute Trusts in England*, HC 475 Session 1998-99, 10 June 1999. (avail. http://www.nao.gov.uk/ publications/nao_reports/9899475.pdf).
[5]Audit Scotland (2001), *Equipped to care: Managing medical equipment in the NHS in Scotland*, March 2001. (avail. http://www.audit-scotland.gov.uk/publications/pdf/01h06ag.pdf).

NOVEL SENSOR TECHNOLOGIES FOR EVALUATING PRESSURE GARMENTS

J. Wilson[1], R. Woolford[1], A. Smith[1] and C. Carati[2]

[1]Flinders Biomedical Engineering, Flinders Medical Centre, Bedford Park, Australia
[2]Dept of Anatomy, School of Medicine, Flinders University, Bedford Park, Australia

INTRODUCTION: Compression garments and bandages are often prescribed for the treatment of burns and lymphoedema. Their use is common practice but without a good method of measuring the applied pressure, efficacy studies are incomplete. Issues such as pressure perturbation, reliability, calibration and cost have limited the routine use of many pressure sensing techniques. New developments in sensor technology have shown promise for this application. We identified low cost capacitive sensors and Quantum Tunnelling Composite (QTC) material as being untested in this field.
METHOD: A range of thin pressure sensors were identified for comparative tests with the capacitive and QTC systems. These were chosen from expensive sensor systems designed for commercial applications and generic force sensing resistors. The QTC sensor was constructed from a sample of QTC material. An arrangement of interleaved electrodes enabled suitable sensitivity, thickness and the ability to slide under a garment. A variable model limb was developed for this pilot study to test the sensors for sensitivity, repeatability, the effect of curvature and effect of the compliance of underlying tissues. There is no consensus in the literature on a calibration and modelling technique that represents all of these conditions. Some sensors were excluded due to problems with range, drift or breakage.
RESULTS: Obtaining repeatable results was a problem with all of the sensors. The consistency of the interface between the applied force and sensing area is an important factor for all sensor types. Our results confirmed previous studies of pressure perturbation, reinforcing the need to minimise sensor thickness. The compliance of the underlying tissue was also shown to affect the sensor output.
DISCUSSION: The method of inserting a sensor between a garment and the tissue to measure interface pressure still has many problems to overcome. The new sensor technology has overcome some problems encountered previously but further difficulties have emerged. The consistency of the interface conditions may be further complicated by changes to the size and compliance of the limb over the treatment period. Given the importance of this application, and that similar problems are encountered with both high cost sensors and the new sensing technology, work is continuing on sensor development and measuring techniques.

AUSTRALIAN MEDICAL DEVICE INCIDENT REPORTING INVESTIGATION SCHEME AND CASE STUDY

M. Smith and J. E. Garcia

Therapeutic Goods Administration, Canberra, ACT, Australia

INTRODUCTION: The Medical Device Incident Report Investigation Scheme (IRIS) is a unit of the Therapeutic Goods Administration (TGA) that investigates adverse events and problems associated with the use of medical devices and equipment. This presentation will describe the scheme, present some statistics of adverse incidents reported in Australia and present a case study involving electrosurgical equipment. This will help to illustrate how the use of the scheme can help resolve issues related to medical device safety. The manufacturers and suppliers (sponsors) of medical devices or medical equipment are required by law to report serious events and problems that come to their attention. Participation in the scheme by clinicians and biomedical engineers is voluntary and as simple as completing a report form.[1] A panel of scientific, engineering and clinical experts assess all reports received by the TGA and recommend the level of investigation that should take place. Reports of incidents that have led or are likely to lead to serious injury are given the highest priority. All reports (even those that are not investigated) are entered into the IRIS database so that they may be easily referenced in the future. Investigations are assigned to the most appropriately qualified TGA investigator who will continue to work with the manufacturer and the reporter until the issue is resolved. Outcomes of investigation include recall, safety alert, product improvement, compliance testing, user education or an article in an appropriate journal. Australia exchanges information on significant incident investigations with other regulatory authorities.
CASE STUDY: Misconnection of electrosurgical bipolar electrodes. The TGA recently received reports of experienced operating theatre staff misconnecting bipolar electrodes to electrosurgical unit (ESU) monopolar terminals. A literature review revealed that serious adverse events associated with electrosurgical misconnection have also occurred abroad. The

incident occurs when the two connectors of the bipolar electrode are accidentally plugged into two of the three monopolar terminals. If the monopolar power output has been programmed into the ESU (eg. been left at its previous setting), serious injury can be caused to either the patient or the operator. It appears that this potential for misconnection exists with all brands of electrosurgical bipolar electrodes that have banana-type plugs mounted on flexible cables.[2]

The TGA investigation into the incident involved extensive consultation with industry and a review of current medical electrical device safety standards. Outcomes of the investigation included a published article in the TGA News and a nation wide safety alert being issued to all users. The TGA Medical Device Incident Reporting Committee (MDIRC) also recommended that ESU manufacturers ensure safety measures are in place to minimise the risk of misconnection of bipolar electrodes. Toward this end, the TGA will present its concerns to the International Electrotechnical Commission (IEC) subcommittee 62D for consideration in the current revision of the international ESU safety standard IEC 60601-2-2.[3] Comments from conference delegates on the proposed amendment(s) to the standard will be welcomed.

REFERENCES:

[1]Available at http://www.tga.gov.au/docs/doc/forms/iris_udir02.doc.

[2]Anonymous, "Misconnection of Bipolar Electrosurgical Electrodes" *Health Devices* Jan 1995; 24(1):34-5. Also available at http://www.mdsr.ecri.org/asp/dynadoc.asp?id=93&nbr=409717&search_txt=.

[3]IEC 60601-2-2: 1999 *Medical electrical equipment – Part 2: Particular requirements for the safety of high-frequency surgical equipment.*

A PEER REVIEW PROGRAM FOR CLINICAL ENGINEERING

M. Denison[1], S. Somerwil[2], D. Seymour[3] and S. Simpson[4]

[1]*Austin Health, Heidelberg, Vic, Australia*
[2]*Melbourne Health, Parkville, Vic, Australia*
[3]*Latrobe Regional Hospital, Traralgon, Vic, Australia*
[4]*Ballarat Health, Ballarat, Vic, Australia*

INTRODUCTION: A method for comparing management programs between clinical engineering departments has been established and trialled in Victoria. The program aims to provide a forum for ensuring consistency and continuous improvement in hospital-based biomedical engineering departments. It is based on a similar program developed in Canada.

METHODS: A set of Clinical Engineering Standards has been developed from an equivalent Canadian document[1]. These standards, which cover topics such as Service Management, Device Management and Risk Management and Education, have been endorsed by both, the National Clinical Panel, College of Biomedical Engineers, Institution of Engineers and the VHA Biomedical Engineering Focus Group. An assessment tool, based on these standards, was used to assess a Biomedical Engineering department in a rural hospital that services a number of facilities in the region. The assessment involved interviews over 2 days with the biomedical engineering manager, key clients of the service, and the executive director responsible for the portfolio.

RESULTS: The report on the department's performance indicates a number of strengths and weaknesses. It has enabled a development plan for the department to address the key recommendations. The review also identified a number of modifications to the assessment tool that would improve ease of use.

DISCUSSION & CONCLUSIONS: Currently the only assessment tools for biomedical managers in Australia to measure their performance are ACHS (Equip), ISO 9000 and AS 3551. The capacity of a manager to review the performance of his department is limited by the limitations of each of these tools. The peer review program offers to fill some of the gaps. Biomedical engineers who know the business perform the review (different to ACHS and ISO). Someone from outside the department does the review (as opposed to self-assessment). Further, the clinical standards set the framework for the review, and these have been developed specifically in relation to hospital based biomedical engineering departments, and endorsed by the peak engineering body – the National Clinical Engineering Panel, College of Biomedical Engineers, IEAust.

ACKNOWLEDGEMENTS: This work has relied heavily on work completed in Canada by CMBES, in particular by Dr Tony Easty and Dr Bill Gentles who were unexpectedly unable to attend this conference as Key Note speakers.

REFERENCES:

[1]Clinical Engineering: Standards of Practice for Canada, Canadian Medical and Biological Engineering Society (CMBES), 1998.

COMBINED DETERMINISM, LAMINARITY AND RECURRENCE RATE MEASURES FOR HEART RATE INTERVAL SERIES ANALYSES

H. Ding, S. Wilson and S. Crozier

The School of Information Technology and Electrical Engineering, University of Queensland, Brisbane, Qld, Australia.

INTRODUCTION: The recurrence Plot (RP) is a relatively new tool for analysing nonlinear dynamic systems. Though it has been applied to the analysis the heart rate variability (HRV), most of the studies have focused on quantitative measures. Few studies have been undertaken concerning structural analysis of the RP of HRV due to its complexity. To simplify structural analyses, our study is focused on the two dimensional distribution of the determinism (DET), laminarity (LAM)

and recurrence rate (REC). The DET, LAM and REC (DLR) in a local area are converted into RGB colours and displayed on a two dimensional collared plot. In this paper, DLR RP is applied on two segments of Lorenz series and three real HR series, including a typical ventricular tachycardia (VT) subject.

METHODS: The DLR RP can be expressed as following

$$DLR(i, j)=RGB[RD(i, j),GR(i, j), BL(i, j)] \quad (1)$$

Where $RD(i, j) = 255* DET_{2D}$; $GR(i, j) = 255*LAM_{2D}$; $BL(i, j) = 255*REC_{2D}$ (2)

DET_{2D}, LAM_{2D} and REC_{2D} denote the two dimensional DET, LAM and REC derived from a meta window, which moves at the point of (i,j). If the RP dimension is N by N, then i,j = 0, 1, 2, … N-1.

RESULTS: Our simulations and applications show that DLR RP can reveal dynamic evolution trends and states, which could not be easily observed and extracted using the conventional RP methods. The DLR RP of a typical VT subject clearly illustrates the process of decreasing HRV before VT events.

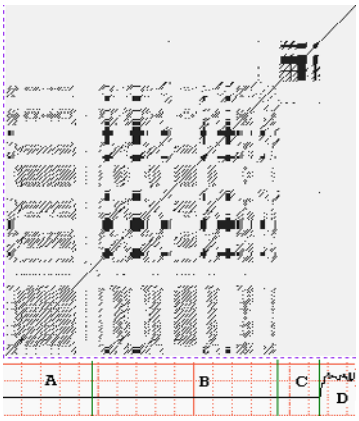

Figure 1

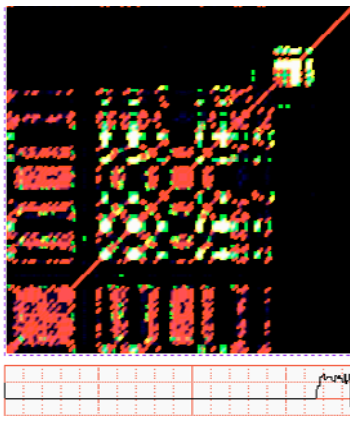

Figure 2

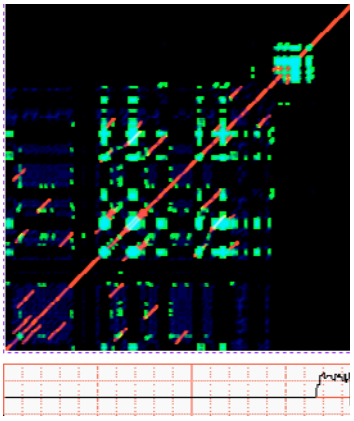

Figure 3

Figure 1. *The conventional RP of a typical VT subject. Figure 2:DLR RP of the VT subject, where the distribution and density of the laminar states can be observed more easily than in figure 1. Figure 3:Increased minimum diagonal line length to extract the long recurrences and laminar states. The increased laminar states in sections B and C indicate a decrease of HRV dynamics.*

DISCUSSION & CONCLUSIONS: Sections B and C may last less than 100 RR intervals. Conventional clinical HRV analysis methods does not capture these dynamic properties efficiently. DLR RP has the same challenging problem of configuration as conventional RP, especially for very short period series. There are a number of possibilities about how to choose parameters for RP, such as mutual information, autocorrelation etc and these will be the subject of future work. Our study shows the RP is a powerful tool to analyse the HRV and its performance and analysis can be enhanced and extended by DLR RP method.

PHYSIOLOGICAL EFFECTS OF DIFFERING ACUPUNCTURE DELIVERY MODES

M. Strudwick[1], R. Hinks[2] and S. Wilson[3]

[1]*Centre for Magnetic Resonance, University of Queensland, Brisbane, Qld, Australia*
[2]*Australian College of Natural Medicine, Brisbane, Qld, Australia*
[3]*School of Information Technology & Electrical Engineering, University of Queensland, Qld, Australia*

INTRODUCTION: The use of point injection (PI) as an acupuncture treatment method is documented, but there has been no formal assessment of PI against traditional acupuncture (TA) with respect to its physiological effects. Yang *et al* [1] outlined the use of PI to control post surgical vomiting, reaching the conclusion that PI is simple, convenient, timesaving and effective. Comparing the physiological effects of the two methods is a first step in investigating the mode of action of PI and validation of the technique as a clinical tool.

METHODS: 19 healthy subjects were studied. Personal details, biometric data, and physiologic data obtained before, and physiologic data during and after stimulation, as well as subjective measures of the stimulation. Comparative analysis was made of systolic blood pressure (SBP), heart rate (HR) and mean arterial pressure (MAP).

RESULTS: Analysis of SBP, HR and MAP pre and post stimulation is presented in Tables 1 and 2.

	MEAN	SD	SE MEAN	SIG (2-TAILED)
Pre/Post SBP	.47	8.085	1.855	NS
Pre/Post HR	.37	.37	6.751	NS
Pre/Post MAP	1.175	1.175	4.8488	NS
Pre/Initial HR	-4.00	-4.00	4.978	<0.05

Table 1. *Traditional Acupuncture*

	MEAN	SD	SE MEAN	SIG (2-TAILED)
Pre/Post SBP	6.79	9.970	2.287	<0.05
Pre/Post HR	-.11	5.021	1.152	NS
Pre/Post MAP	1.035	6.9326	1.5904	NS
Pre/Initial HR	-5.84	8.288	1.901	<0.05

Table 2. *Point injection.*

Self-report data (not presented in this abstract) demonstrated no significant difference (paired t-test, $p > .1$) with respect to subjective stimulation effects. A significant difference was found for both TA ($p = .003$) and for PI ($p= .007$) between the prestudy heart rate and the rate recorded immediately on stimulation ("Initial" in the above Tables). The findings are comparable to Sugiyama *et al* [2]

DISCUSSION & CONCLUSIONS: While marked inter-subject variability was demonstrated, especially in SBP, there appears little difference in the manner in which PI and TA elicits a physiological response. The SBP variability needs further investigation and suggests a need to modify the way the experiments are conducted. The current markers are too variable to provide a robust physiological measure of the effect of acupoint stimulation. Power spectral analysis of instantaneous heart rate variation (HRV) or non-linear measures may improve the statistical value of the physiologic data by examining changes in autonomic response [3,4]. This was not a true crossover design as all subjects were stimulated with TA first followed by PI, so session/order effects may have occurred.

ACKNOWLEDGEMENTS: Mr T Wolsky and ACNM for assistance and facilities in conducting this pilot study.

REFERENCES:

[1]L. C. Yang, B. Jawan, et al. (1993) *Acta Anaesthesiol Scand,* 37:192-4.
[2]Y. Sugiyama, et al. (1995) *Japanese Journal of Physiology,* 45:337-45.
[3]E. Haker, et al. (2000) *Journal of the Autonomic Nervous System.* 79:52–59.
[4]B. Sayers, (1973) *Ergonomics*, 16(1):17-32.

CORONARY ARTERY WALL THICKNESS DETECTION USING INTRAVASCULAR ULTRASOUND

R. L. G. Kirsner[1], A. V. Samuel[1], D. B. H. Tay[1], I. T. Meredith[2] and J. D. Cameron[1,2]

[1]*Department of Electronic Engineering, La Trobe University, Bundoora, Vic, Australia*
[2]*Cardiovascular Research Centre, Monash Medical Centre, Clayton, Vic, Australia*

INTRODUCTION: Intravascular Ultrasound (IVUS) is used to image the walls of coronary arteries and identify vulnerable atherosclerotic plaques.[1,2]. Plaque analysis using IVUS has not been very successful and we intend to utilise the raw backscattered RF IVUS signal rather than the processed ultrasonic image as it contains significantly more information about arterial wall thickness. We have developed a system that can capture the RF signal along any particular scanning angle. The system gates the patient's ECG signal with the IVUS timing signal and hence can acquire the RF signals during the systolic or diastolic phases of the cardiac cycle.

METHODS: The vector imaging data acquisition system consists of a HP SONOS Intravascular Ultrasound machine, high speed precision analogy to digital converter (A/D) (Acqiris Digitizer DP105), Vector Imaging software, RF filter, electrocardiogram (ECG) simulator and trigger circuitry. The IVUS machine also includes a vector position control box, enabling the vector cursor to be activated and positioned along the desired line of the cross section of the vessel being scanned. The ECG delay and trigger section detects the R and T waves of the ECG signal allowing the acquisition of RF data during systole or diastole. The User Interface for the Vector Imaging data acquisition system designed using Microsoft Visual C++ (Version 6.0), controls the synchronized trigger signals to the A/D card as well as data acquisition and storage.

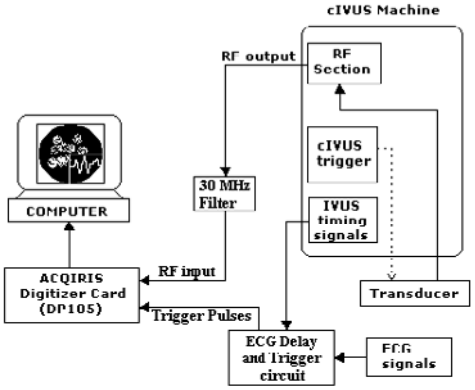

Figure 1. *Block diagram of the system.*

RESULTS: Figures 2 & 3 show the IVUS image of a diseased coronary artery and the corresponding RF signal data. The white line from the centre of the IVUS image represents the current vector along which the RF signal is being acquired.

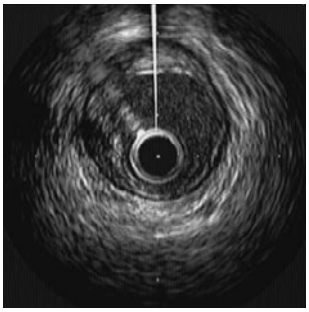

Figure 2. *IVUS image.*

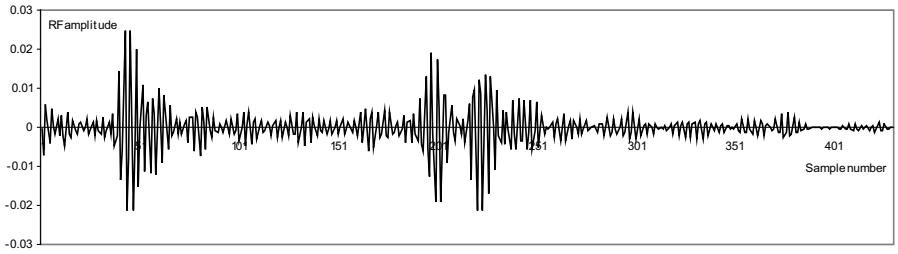

Figure 3. *The RF signal along the vector shown in Fig 2.*

CONCLUSIONS: The raw IVUS backscattered RF signal can be acquired and used in coronary artery wall analysis. Given the relative affordability of coronary artery stents, and given their potential to prevent serious illness and hospitalisation, any technique that can help to refine and target their effective use is clearly cost-effective.

REFERENCES

[1]Nissen S.E. (2001) *The American Journal of Cardiology*, 87, 4, 15A-20A.
[2]Nissen S.E., Yock P., (2001) *Circulation*, 103, 604-616.

HEART RATE VARIABILTY AND SEDATION

A. L. Smith[1,2], K. J. Reynolds[2], H. Owen[3] and C. Fahy[4]

[1]*Flinders Biomedical Engineering, Flinders Medical Centre, Bedford Park, SA, Australia*
[2]*School of Informatics and Engineering, Flinders University, Bedford Park, SA, Australia*
[3]*School of Medicine, Flinders University, Bedford Park, SA, Australia*
[4]*Department of Anaesthesia, Flinders Medical Centre, Bedford Park, Australia*

INTRODUCTION: This pilot study investigates the effect fentanyl has on heart rate variability (HRV) in the operating theatre. HRV uses changes in heart rate to indirectly observe changes in the activity of the autonomic nervous system and in particular, the changes in activity of the parasympathetic and sympathetic branches. Anaesthetics are known to affect the autonomic nervous system and HRV provides an indirect window on this activity. HRV indexes, such as respiratory sinus arrhythmia, have been used to provide a convenient and objective indication of lightening anaesthesia [1] (with propofol and isoflurane).

METHODS: Consenting patients scheduled for minor surgical procedures were studied in the 10 minutes before anaesthesia was induced. Baseline ECG was recorded for 5 minutes then a standard dose of midazolam was given, followed by a randomly selected bolus of fentanyl (50, 75, 100 or 150 microgram). A further 5 minutes of ECG was then recorded. The R-wave intervals were analysed with a range of techniques to elucidate information on changes caused by the sedative.

RESULTS: Procedural issues that affected the HRV were identified including intrusions by clinical staff, loud noises, and application of the oxygen mask. A reduction in all frequencies occurred when the oxygen mask was applied (arrow on figure). Fentanyl produced a short increase in the high frequency range (0.35 – 0.45 Hz) and a prolonged reduction in the sympathetic low frequency peak (0.1 – 0.15 Hz).

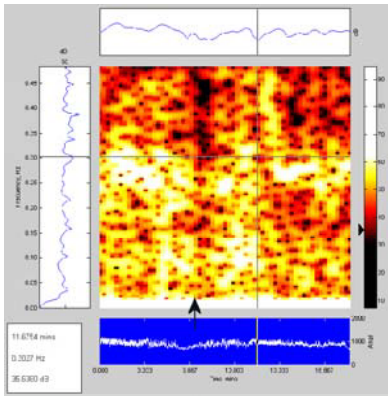

Figure 1. *Time dependent frequency analysis (MatLab spectrogram) Fentanyl administration at vertical line. Oxygen mask applied at arrow.*

DISCUSSION & CONCLUSIONS: The pilot study identified larger changes of HRV associated with procedural issues rather than with the drug being investigated. These sources of 'noise' will need to be minimised in subsequent studies. Fentanyl caused a reduction in the sympathetic low frequency peak in agreement with other studies of drug effects.

REFERENCES:

[1]Pomfrett, C. J. (1999) *Br J Anaesth* 82 (5), 659-662.

HAPTIC RENDERING IN A VIRTUAL REALITY BASED ENDOSCOPIC SIMULATOR

I. Brown, C. Seligman, Z. Mayooran and D. Healy

Centre for Biomedical Engineering, Department of Electrical & Computer Systems Engineering, Monash University, Clayton, Vic, Australia

INTRODUCTION: The Monash University Centre for Biomedical Engineering (MUCBE) and the Faculty of Medicine Department of Obstetrics & Gynecology (O&G) have together developed a new VR based simulator for training advanced endoscopic procedures in gynaecological surgery. The simulator is based on a segmental graphical model that enables the simulator to exhibit a complex anatomical field to an acceptable degree of realism. It can accommodate multiple operators and a wide range of surgical instruments, pathologies, and procedures. It also has provision for force feedback, giving the surgeons operating the simulator a sense of feeling.

METHODS: The haptic system has been implemented using a Pentium class desktop PC as a development platform. The virtual endoscopic instruments are fitted with high resolution optical encoders to give four degrees of freedom (left-right, forward-back, in-out and handle rotation) and DC motors to present force feedback to the user. Two such instruments and a virtual endoscopic camera have been fitted into a domed housing to approximate an insufflated abdomen and lend some realism to the layout. The spatial resolution of the system is better than 0.5mm in each axis, and the force motors sufficient to provide forces approximately equivalent to a 200gram weight. One small DC motor and capstan is fitted to provide force feedback along the in-out axis, whilst larger motors are fitted to the left-right and forward-back axes to generate sufficient torque at the handle. The three dimensional force feedback models are transformed to the polar representation required by the hardware, and applied to the motors to generate arbitrary forces in any direction. Computationally efficient haptic models can then be combined to varying degrees, giving a wide variety of force feedback effects.

RESULTS: To test the spatial resolution of the haptic rendering engine, subjects were asked to locate the apex of several spheres placed in the haptic workspace in the absence of visual cues. The experiment was performed first in the virtual environment and subsequently in real space, using halved ping-pong balls. The error in locating the spheres' apexes in the real and virtual environments was 22.1% and 29.7% correspondingly (expressed as a percentage of the sphere radius). These results are promising since they indicate that the haptic models present enough information to the user to aid in spatial navigation tasks.

DISCUSSION & CONCLUSIONS: The process of haptic rendering, that is, applying localised haptic effects to an already existing graphical wire frame model, has been shown to be effective in the modelling of a virtual anatomical environment. This process is simple to apply and efficient in execution.

HANDS-FREE POWER WHEELCHAIR CONTROL USING A LINUX BASED PERSONAL DIGITAL ASSISTANT (PDA)

D. Craig and H. Nguyen

University of Technology, Sydney, NSW, Australia

INTRODUCTION: For a power wheelchair to be controlled by a severely disabled person, a control system needs to be developed whereby the user can operate the power wheelchair without the use of their hands. Two popular commercially available solutions are chin control and sip-'N'-puff control systems which are unintuitive and difficult to learn and use. In this paper, we describe the development of a real-time head-movement system and a Compaq Personal Digital Assistant (PDA) iPAQ H3870 for the control of a power wheelchair.
METHODS: The head movement transducer is an ADXL202EB, which is an evaluation board for the accelerometer ADXL202. Essentially, C++ has been used for the software upgrade, with QT Embedded as an additional graphical toolkit to allow user interface development, and the basic version of the Familiar Linux distribution for Embedded iPAQ development is incorporated. For this project, we built a customised RS232 to DAC Interface board which incorporated a microcontroller PIC18F2220 for interfacing between the iPAQ and the wheelchair. A state-machine has been developed for the design of the actual software. A key part of this project is the recognition of various head movement commands using a real-time neural network. This network was trained on data collected from ten different people. 32 samples were collected from each volunteer who participated in the data collection and the data recording window was chosen at 3 seconds. This data was separated into two sets: a training set and a validation set. We designed two neural networks for command classification: a Directional Recognition network (forward, backward, left, right) and an Emergency Stop network. The multi layer Directional Recognition neural network has 63 input nodes, 5 hidden nodes, and 4 output nodes. The Emergency Stop network has 63 input nodes, 5 hidden nodes, and 1 output node.
RESULTS: The test was carried out by having a person nod in random directions, on instruction. Each movement was observed, as was the success of the network. For the Directional Recognition neural network, the success rate of the first nod in any given direction was 97%, and the success rate of re-classifying on the second go was 100%. For the Emergency Stop neural network, the success rate of the first head shake was 93.75%, and the success rate of re-classifying on the second go was 100%.
DISCUSSION & CONCLUSIONS: The results showed that the project has successfully demonstrated the feasibility of Linux as an embedded operating system, and PDAs as architecture suitable for embedded control. A fully working prototype of a real-time head movement power wheelchair control has been developed that is easily extensible, and can be broaden to many other methods of hands-free control.
ACKNOWLEDGEMENTS: Part of this research was supported by an ARC LIEF grant LE0454081.

SMART CATHETER: DETERMINING CATHETER LOCATION WITHIN THE BILIARY AND PANCREATIC DUCTAL SYSTEMS

O. Pallotta[1], R. Woolford[1] and G. Saccone[2]

[1]*Department of Biomedical Engineering, Research and Development, Flinders Medical Centre, Bedford Park, SA, Australia*
[2]*Department of Gasteroenterology, Flinders Medical Centre, Bedford Park, SA, Australia*

INTRODUCTION: The smart catheter was developed to provide real-time information about the location of the catheter during pressure measurements within the ductal systems, without injecting dye, exposing the patient to radiation and altering the duct environment. Bile stones, pancreatitis, stenosis (narrowing of duct) and stricture (tightening of ducts) are common medical complications involving the pancreatic and biliary ductal systems. A manometry catheter is used to record the pressure measurements within the appropriate ductal system and diagnose the condition. The catheter is placed within the duct of interest via the opening in the duodenum. Anatomically this opening is a single tubular section of tissue, 5mm in length which is common to both systems and branches into the separate ducts. No visual information is available to the physician when the catheter is within this common section of the ducts, hence locating the correct ductal system is difficult. Currently, the physician places the catheter into the duct and takes pressure measurements. ERCP (Endoscopic Retrograde Cholangiopancreatography) is then used to determine the location of the catheter, involving the injection of a dye followed by a radiographic image. In 20% of cases the catheter is incorrectly placed. In which case it is removed and re-positioned. Pressure data is collected and imaging repeated with no guarantee it is correctly located.
METHODS: Optical techniques were employed to provide the necessary information regarding the location of the catheter in vivo. The manometry catheter was modified to incorporate optical components but still allow pressure measurements to be performed. Additional modifications to assist in optical measurements were added to the catheter tip. Two wavelengths of light were directed into the catheter and exposed to the fluid within the ductal system. Wavelength one is expected to behave in a known manner within the various environments the other is used as a reference. Using optoelectronic measurements and signal processing, the fluid within the vicinity of the catheter tip and hence the current location of the catheter can be determined.
RESULTS: Trials have been conducted with possum bile and pancreatic fluids in vitro. The system correctly identified bile presence or absence. In vivo trials have been conducted with animal models. Once again the system was able to distinguish between the pancreatic and bile ductal systems, hence determining the location of the catheter during the experiments.
DISCUSSION & CONCLUSIONS: The smart catheter in a clinical setting will remove the uncertainty in manometry catheter location by providing real time information about its position at all stages during the procedure. The smart catheter

will eliminate the need to perform radiographic imaging and reduce occurrence of re-entry and repetition of data collection due to incorrect placement. Additionally it will reduce procedure time, reduce perfusate in the ducts and reduce associated morbidity.

INTELLIGENT SHOULDER CONTROL OF AN UPPER LIMB PROSTHETIC HAND

I. Brown, M. Sanakiewicz, S. Mustafa and E. Track.

Centre for Biomedical Engineering, ECSE, Monash University, Clayton, Vic, Australia

INTRODUCTION: The literature on upper limb prosthetic hand control suggests only marginal improvement in its functionality over the past decade[1]. Hence a new prosthetic system has been developed using a combination of a body driven and power assisted telerobotic control concepts. The advantage of body control lies in the genesis of a control being an intact musculoskeletal system with its physiological proprioceptive feature being extended beyond the body into the prosthetic hand which leads to the skilled operability through Extended Physiological Proprioception (EPP)[2].
SYSTEM REQUIREMENTS: The prosthetic system design and the man/machine interface are specified and the intelligent prosthetic control structure concepts are analysed as outlined in Fig. 1. The shoulder position signals are linked to the Prosthetic Control Unit (PCU) that coordinates the controls of the power assisted prosthetic hand. The Prosthesis then provides its gripper position and force feedback signals to the controlling shoulder through the shoulder opposing force actuator in order to achieve EPP effect.

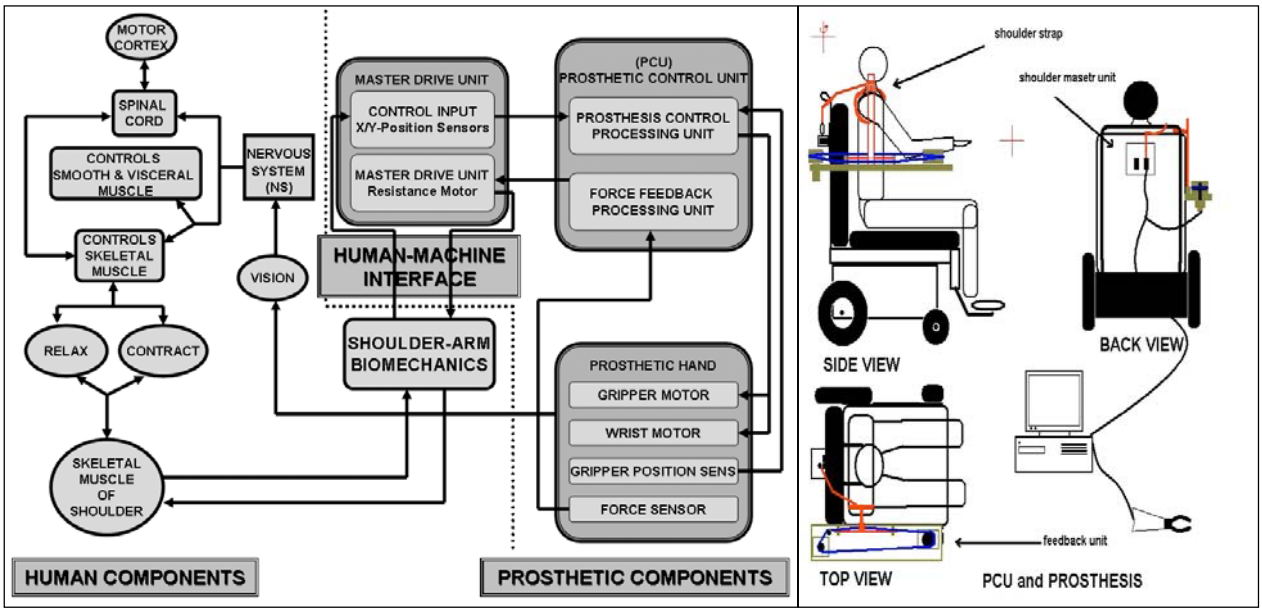

Figure 1. *Intelligent shoulder control of an upper limb prosthetic hand.*

RESEARCH AND CONCLUSIONS: Shoulder kinematics and physiology are examined and analysed in an input and output body control terms for the prosthetic system. In order to determine the advantage of our system control over other currently used prosthesis, the prosthetic hand operability improvement is examined and analysed across range of subjects. This research will enable amputees to achieve skilled prosthetic hand control through intelligent prosthetic control development.

THE APPLICATION OF WAVELET ANALYSIS TO ECG SIGNALS

A. Matsuyama[1], M. Jonkman[1] and T. Abdipranoto[2]

[1]*Charles Darwin University, Darwin, NT, Australia*
[2]*University of Wollongong, Wollongong, NSW, Australia*

INTRODUCTION: The *Electrocardiogram* (ECG) is one of the most commonly known biological signals. Traditionally ECG recordings are analysed in the time-domain by skilled physicians. However, pathological conditions may not always be obvious in the original time-domain signal. Fourier analysis provides frequency information but has the disadvantage that

time characteristics will be lost. Wavelet analysis, which provides both time and frequency information, can overcome this limitation. Here wavelet analysis is performed with the intent to investigate its suitability as a diagnostic tool.

METHODS: All ECG signals used for the research were obtained from the Physionet Database (*PhysioBank*) [2]. The types of ECG signals examined were: Normal Sinus Rhythm, Arrhythmia, Supraventricular Arrhythmia, and Malignant Ventricular Arrhythmia. The ECG signal examination was conducted over a complete signal, and then over the P wave and the QRS complex, which are the main features of ECG signals. Two steps of signal processing techniques were applied for ECG signals analysis: wavelet analysis and normalisation of energy.

RESULTS: The *besttree* command in Matlab, which employs the entropy criterion helped in eliminating inappropriate wavelets, though not in choosing a specific wavelet. The results from the normalised energy comparison showed a distinctive difference between a normal sinus rhythm signal and an arrhythmia signal. However, characterising ECG recordings can insufficiently distinguish the different arrhythmia signals from each other. The analysis of the P-waves showed that it is important to use fixed sized windows. This avoids the problem of having to locate the start of the P-wave, which is particularly difficult if the P-wave is absent. Inconsistent values for the normalised energy of the P-wave may be due to the inaccuracy of locating the P-wave. Wavelet analysis of the QRS complex shows some promising results. The premature ventricular contraction can be easily detected using the normalised energy of the QRS complex. Figure 1 shows the signal 800 from the supraventricular database and its respective continuous wavelet transform using Haar wavelets.

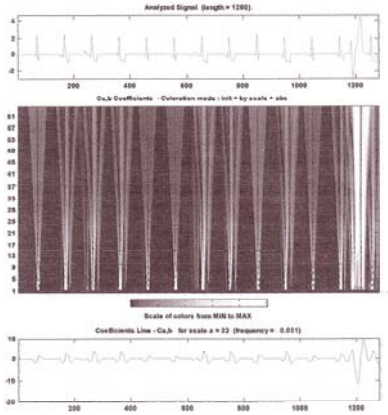

Figure 1. *QRS complex Analysis*

CONCLUSIONS: The results of normalised signals showed that localising specific features of an ECG signal was required for the accurate classification of abnormality. From the P wave analysis, normalised energy has demonstrated its sensitiveness to small changes in a signal. For the P wave analysis, it was found important to use fixed size windows in order to eliminate the impact from the average variation of the mean energy. The normalised energy of the QRS complex has demonstrated that it can accurately detect the abnormalities in the QRS complex.

REFERENCES:

[1]*PhysioBank*, Physionet, viewed 14th, May 2004, <http://www.physionet.org/physiobank/>.

[2]Valens, C 1999, *A Really Friendly Guide to Wavelets*, viewed 28/11 2003, <http://perso.wanadoo.fr/polyvalens/clemens/wavelets/wavelets.html>.

ADAPTIVE TRAINING OF NEURAL NETWORK CLASSIFIERS FOR POWER WHEELCHAIR CONTROL

P. Taylor[1] and H. Nguyen[1]

[1]*Key University Research Centre for Health Technologies, Faculty Of Engineering, UTS, Sydney, NSW, Australia*

INTRODUCTION: Head movement is used as a control interface for people with motor impairments in a range of applications. This paper outlines an adaptive training technique to improve the performance of a head movement classifier for use in a power wheelchair interface and the procedure and preliminary results of an experiment to compare the performance of the adaptive algorithm.

METHODS: The adaptive algorithm is comprised of two stages: pattern selection, and weight adjustment. Matched pairs of classifiers were used to compare the performance of the proposed adaptive training algorithm to the alternative of training using generic data. The performance metric used was the error rate for each class of movement, found on separate test sets for two disabled users.

RESULTS: Results obtained from preliminary data indicate a statistically and practically significant improvement in the error rate of classifiers trained using the adaptive algorithm for two classes of command movement for Subject 2.

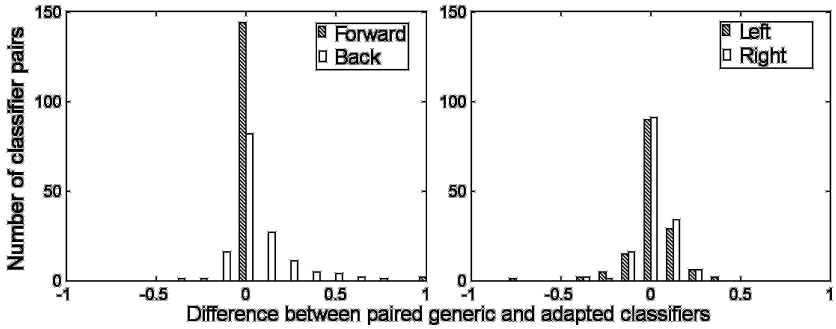

Figure 1. *Distribution of the difference in error rate between adapted and generic classifiers for Subject 1.*

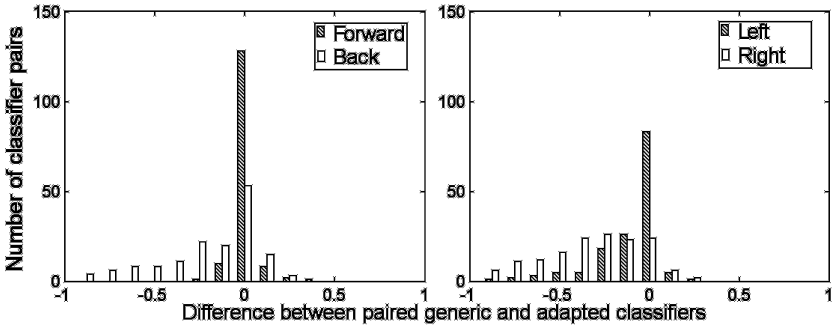

Figure 2. *Distribution of the difference in error rate between adapted and generic classifiers for Subject 2.*

DISCUSSION & CONCLUSIONS: It is suspected that the cause of the differing results is that Subject 2's level of injury was higher, resulting in a smaller range of lateral movement compared to the able-bodied subjects who provided the generic data. The method proposed includes further tests with larger data sets. These preliminary results indicate that when carrying out the experiment on the full sized data set, it will be important to collect data from people with a range of types of disability.

ACKNOWLEDGEMENTS: The authors acknowledge the staff and patients from the Moorong Spinal Unit of the Royal Rehabilitation Centre Sydney who assisted with the data collection for this paper.

HANDS-FREE CONTROL OF WHEELCHAIR USING EMBEDDED LINUX

L. King[1] and H. Nguyen[1]

[1]*University of Technology, Sydney, NSW, Australia*

INTRODUCTION: Head movement is a control technique used by people with limited abilities to control a conventional power wheelchair. Existing solutions such as chin operated joysticks have their positive aspects, however, they are generally difficult to operate and aesthetically unappealing. The system presented in this paper uses an artificial neural network (ANN) to classify head movement commands, and an embedded real-time system to improve the aesthetics.

METHODS: A 61 input, 6 hidden node and 5 output node artificial neural network has been developed to recognize and classify head movement commands made by a power wheelchair user. The embedded system has a size of 22.6cm x 28.5cm and provides wireless Bluetooth and control capabilities.

RESULTS: The cycle error plot in Fig 1. clearly shows the error of all commands approaching zero over the duration of the training cycle, with the stop command taking the longest time due to its relative complexity. The validation error plot in Fig 1. shows that the error in the validation set does not increase over during the training, showing that the network is not being over trained. Table 1 shows the real time results of real time testing both for the users' first attempt at a command, as well as their second attempt.

DISCUSSION & CONCLUSIONS: We have developed a network which we have proven successful in real time. In addition, an embedded system has been created which overcomes the significant barriers presented by existing hands free power wheelchair control systems, by the use of small embedded technology.

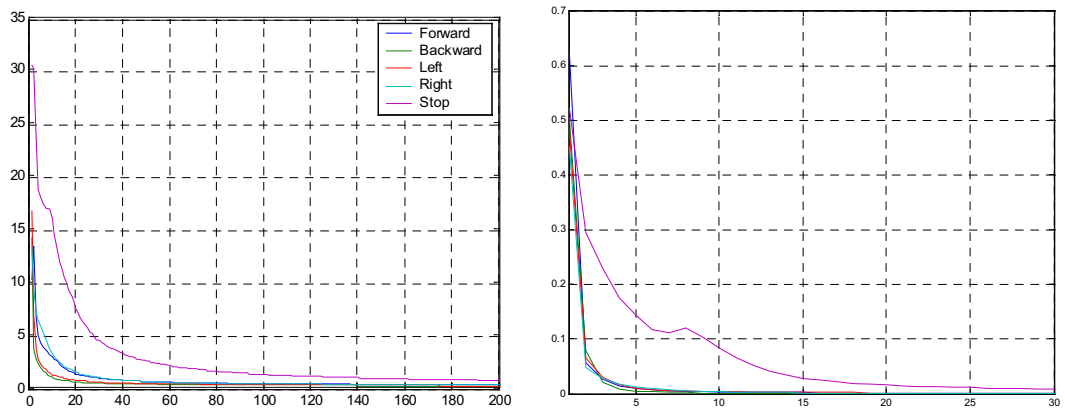

Figure 1. *Cycle Error and Validation Error.*

Command	First Command	Second Command
Forward	93.33%	96.66%
Backward	90.00%	96.66%
Left	93.33%	100.00%
Right	93.33%	100.00%
Stop	90.00%	96.66%
Average	92.00%	98.00%

Table 1. *Real-time network classification results, using the test set*

POSSIBLE FUNCTIONAL CLASSIFICATION OF ENZYMES USING THE RRM MULTIPLE-CROSS SPECTRAL FUNCTION

V. Vojisavljevic, E. Pirogova and I. Cosic

School of Electrical and Computer Engineering, RMIT University, Melbourne, Vic, Australia

INTRODUCTION: An important unsolved problem in the genome sequencing projects is how to determine function of proteins given only their primary sequences. Protein comparison and alignment still represent one of the most important and widely used methods of protein sequence analysis[1]. However two protein sequences with low sequential identity may show similarities in their physicochemical properties, tertiary structure, and biological function without having similarity in the primary structure[2,3] The Resonant Recognition Model[4] (RRM) multiple cross-spectral function can be regarded as a measurement of the similarity among different protein sequences in the frequency domain when each protein sequence is treated as a numerical series[6]. The most prominent peak shows the spectral similarity.

METHODS: Our collection of protein sequences was formed using the same strategy as Rost[3] from the SWISSPROT database version "*database-sprot40.dat*". At the following stage we have classified enzymes from the four major groups; (1) hydrolase, (2) lyases, (3) isomerases, and 4) lygases, into the sub-groups according to the criteria that enzymes belonging to the same sub-group are having the identical first, second and third EC number.

Resonant Recognition Model

The Resonant Recognition Model (RRM)[4] , is a physico-mathematical model based on the representation of the protein primary structure as a numerical series by assigning to each amino acid a physical parameter. An extensive number of numerical experiments[7] demonstrated that the best results can be obtained using the electron-ion potential value as an amino-acid parameters.

RESULTS: The "characteristic frequency" has been calculated for each group of enzymes having the same first three numbers in EC classification. Two main empirical conclusions can are reached from our investigations: 1) Different EC sub-sub classes are characterised by different "characteristic frequency". 2) The success of "characteristic frequency" to represent a hidden pattern common for a group of enzymes vary from group to group. The "relative occurrence" generally depends of number of subgroups inside the group with exception of some groups.

CONCLUSION: It should be noted that applications of "classical methods" in protein analysis that use alignment algorithms for measuring the level of the sequence similarity are successful only when a very high level of pairwise sequence identity is presented[3]. Therefore we suggest that additional measure of hidden similarity that can be calculated using the RRM methodology can improve classification efficiency

REFERENCES:
[1]Pearson, W. R. and Lipman, D. J., *Proc. Natl.Acad Sci USA*, 85 pp2444, 1988.
[2]Bairoch, A. & Apweiler, R., *The SWISS-PROT protein sequence database and its supplement TrEMBL in 2000*. Nucl. Acids Res 28, 45-48, 2000.
[3]Burkhard, R., *Enzyme Function Less Conserved Anticipated*, Journal Of Molecular Biology vol 318, 2, pp 596-608, 2002.
[4]Cosic, I., *The Resonant Recognition Model of macromolecular bioactivity,* Birkhouser. 1997.

RRM ANALYSIS OF PROTOPORPHYRINOGEN OXIDASE

M. Sauren, E. Pirogova and I. Cosic

School of Electrical & Computer Engineering, RMIT University, Melbourne, Vic, Australia

INTRODUCTION: Proteins are linear macromolecules made up of sequentially linked amino acids. The Resonant Recognition Model (RRM) is a novel physico-mathematical approach used to identify the selectivity of protein interactions by analysing amino acid sequences[1]. Here we use the RRM to analyse protoporphyrinogen oxidase (PpOI), an enzyme that catalyses the production of protoporphyrin IX (PpIX). This reaction is utilised in a cancer treatment known as photodynamic therapy. We have determined the characteristic frequencies and the "hot spot" amino acids, and predicted the location of proteins' active site(s). Several proteins that potentially belong to the PpOI functional group were also analysed to distinguish their viability in this role.
METHODS: RRM analysis involves representing the protein sequence as a series of discrete data by replacing each amino acid with its equivalent Electron-Ion Interaction Potential (EIIP). A multiple cross-spectral function is defined and calculated using Discrete Fourier Transform (DFT) to obtain the common frequency components from the spectra of a group of proteins. Peaks in such a function denote the common frequency components for all sequences analysed. The Inverse Fourier Transform (IFT) is used to identify the individual amino acids, i.e. "hot spots", which contribute most to the RRM characteristic frequency, and thus, to the observed protein's biological function[1]. Continuous Wavelet Transform (CWT) is used to determine the active sites along the protein sequence[2].
RESULTS: We found the PpOI protein group shares the activation frequency of f_1=0.3926± 0.0151 with S/N=375.46 with a less prominent frequency at f_2=0.1152±0.0151. The "Hot spots" and active sites were predicted for several proteins, two representative examples are provided. "Hot spots" for PpOI enzyme from *Salmonella typhimurium* were at residues 60:G, 69:F and 84:F, and one Wavelet predicted active site at f_2 but none at f_1. Predictions correspond with experimentally found active site (residues 3-172[3]).Predicted "hot spots" for PpOI from *Wolinella succinogene* were at residues 79:F, 84:F and 124:F. Several high-energy domains were visible in the Wavelet spectrum at f_1 and f_2. Experimental results are not available[4] so comparison cannot be made. Four potential PpOI proteins from various sources were analysed to determine their efficacy in the role by creating a multiple cross-spectral function of all the PpOI sequences in addition to one possible PpOI sequence. Proteins from *Escherichia coli, Lawsonia intracellularis* and *Rickettsia siberica* clearly showed the activation frequency f=0.3926±0.0151 with a high signal-to-noise ratio (286.08, 434.47 and 434.92 respectively). Analysis for a *Neisseria gonorrhoeae* protein displayed several peaks at various frequencies with a relatively low S/N of 82.44. Accordingly, we postulate that the PpOI frequency, and consequently the PpOI biological activity, is present in each of the first three proteins but that the *Neisseria gonorrhoeae* protein does not share the active frequency characteristic to the PpOI functional group nor the PpOI biological function.
DISCUSION & CONCLUSIONS: In this study we have used RRM analysis techniques to find the characteristic frequency and the "hot spot" amino acids of PpOI proteins, and predicted the location of proteins' active site(s). We also analysed several proteins that potentially belong to the PpOI functional group to distinguish their viability in this role.
REFERENCES:
[1]Cosic, I., The resonant recognition model of macromolecular bioactivity: Theory and applications. 1997, Melbourne: Springer & Verlag.
[2]Pirogova, E., Akay M., Cosic I., Investigation of the structural and functional relationship of oncogene proteins. Proceedings of the IEEE, 2002. 90(12): p. 1859-1867.
[3]ExPASy, http://kr.Expasy.Org/cgi-bin/niceprot.Pl?Q9l6l1
[4]ExPASy, http://kr.Expasy.Org/cgi-bin/niceprot.Pl?Q7mai5

HIGHER ORDER STATISTICAL ANALYSIS OF /X/ IN MALE SPEECH

M. C. Orr and B. Lithgow

Biosignal Processing Group, Department of Electrical and Computer Systems Engineering, Monash University, Clayton, Vic, Australia

INTRODUCTION: Annotation of speech to identify sounds is extremely difficult, requiring excellent listening, a moderate amount of phonetic training, and a lot of experience before a person could consider themselves highly component. Automated speech recognition software, in general terms, does not provide timing information, needs a significant amount of training, and is inflexible to environmental conditions[1]. A study of kurtosis and the analysis of /x/ (as in "ago") using

kurtosis in the time domain is presented. Using higher order statistics, in particular kurtosis, for analysis of small time features (less than 1000 milliseconds) is innovative and unique.

METHODS: The kurtosis analysis algorithm commences by segmenting the first window of data, and then the kurtosis is calculated. The kurtosis coefficient value is saved before the next window's kurtosis is calculated. Each window is independent however the data contained in the windows differs by one sample. In other words the windows slide across the signal one sample at a time.

RESULTS: The ANDOSL sentence used to extract the /x/ in "piano" is "Judith found the manuscripts waiting for her on the piano" (filename s017s041.wav). In the figure below, by inspection, 50% of the coefficients seem to be platykurtic (<3). In addition there are two leptokurtic (>3) spikes in the sound. The preceding sound to the /x/ is a highly nasal /n/ there is a chance that the /n/ has affected the following sound lifting its kurtosis value.

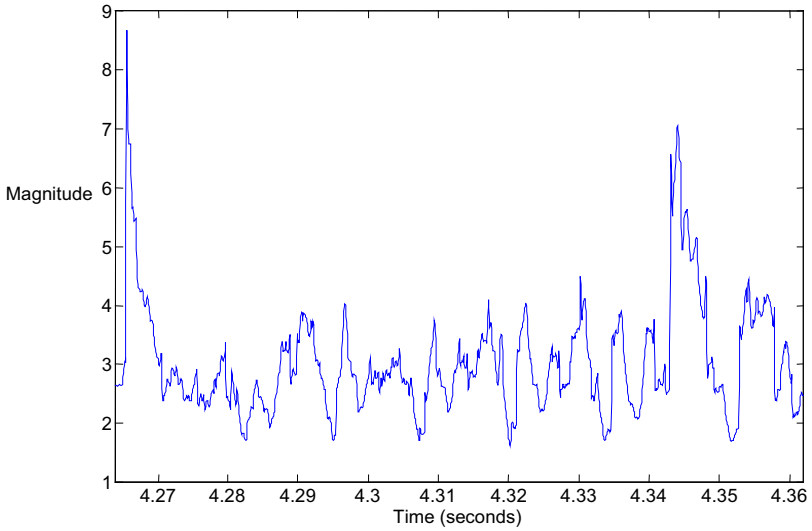

DISCUSSION & CONCLUSIONS: The major feature to be seen in all time plots e.g. figure 1 (a plot of kurtosis vs. time), is the inconsistent pattern of kurtosis coefficients. However in all five examples examined for this sound the majority of coefficients are still platykurtic. Figure 1 features a large leptokurtic spike at the end of the sound, due to a forced stopping of the sound. The forced stop makes the sound heard seem harsher. The work presented in this paper shows how kurtosis can be used with windows as short as 5 milliseconds to analysis speech phonemes. In the case of this paper the kurtosis analysis was used to investigate the vowel /x/ as in ago. It successfully showed that the majority of coefficients were platykurtic, as opposed to the expected leptokurtic value previous authors describe. The kurtosis results published here and similar ones in the author's thesis have lead to an investigation of speech production models in order to produce some understanding for why the kurtosis coefficients were so low.

REFERENCES:

[1]Deller, John R., Jr., Hansen, John H.L., and Proakis, John G. (2000) *Discrete-time processing of speech signals.*

CENTRAL SLEEP APNEA DETECTION: AN ALGORITHM BASED ON DETECTION OF CARDIOGENIC OSCILLATIONS ON AN AIRFLOW SIGNAL

C. W. Chan[1], C. S. Chan[2], K. Schindhelm[1,3] and S. Farrugia[3]

[1]*University of New South Wales, Sydney, NSW, Australia*
[2]*Sleep and Chest Disorders Centre, Sydney, NSW, Australia*
[3]*ResMed Corporation*

INTRODUCTION: Sometimes during a central sleep apnoea (CSA) and never an obstructive sleep apnoea (OSA), cardiogenic oscillations (COs) appear in the airflow signal.[0] An algorithm that differentiates between OSA, CSA and mixed apnoeas (MA) in an airflow signal is proposed, with CSA classification solely being dependent on the presence of COs during the apnoea. Heart rate is also extracted where COs are detected.

METHODS: Apnoea detection involved bandpass filtering the airflow signal in order to cancel DC offsets, minimise the effects of noise and improve the transmission of clear, regular COs. The root mean square and a reduction in amplitude to 75% for at least 10s were then calculated to detect the location of an apnoea. Parseval's theorem which calculates the energy in a signal was used to further classify the apnoeas based on the observation that the energy in an OSA signal would be significantly lower than a CSA with COs. Cross correlation was calculated on a suspected CSA event to confirm that the

extra energy on the signal was indeed due to the COs. If this was the case then the fast Fourier transform was used to extract the predominant frequency in the detected COs, that is, heart rate.

RESULTS: The algorithm was tested on 141 apnoeas collected from 9 patients, yielding a good overall performance of 72% with regard to its ability to accurately classify apnoeas. It was able to correctly detect the occurrence of apnoeas 99% of the time and was in particular robust in handling saturated signals. Also, where heart rate was extracted from the COs during a CSA event, the algorithm achieved a very high accuracy of 95% when compared to results obtained manually.

CONCLUSION: To the authors' knowledge, algorithms that classify apnoeas based on the presence of COs solely from an airflow signal and that extract heart rate from COs have not yet been developed. The implications of this may increase accuracy of automatic polysomnography scoring and also allow for further development of smart CPAP.

ACKNOWLEDGEMENTS: Permission was granted from the Sleep and Chest Disorders Centre, Sydney, to use their data.

REFERENCES:

[1]I.Ayappa, RG.Norman, DM.Rapoport. *Cardiogenic oscillations on the airflow signal during continuous positive airway pressure as a marker of central apnoea.* Chest 1999; 116:660-666. Available from: <http://www.chestjournal.org/ cgi/content/abstract/116/3/660> [3 August 2003]

MEETING CPD NEEDS OF RADIOLOGISTS IN RURAL & REMOTE AUSTRALIA

J. Shaw[1], A. Pitman[2] and K. Thomson[3]

[1]*RANZCR Victorian Branch, Melbourne, Vic, Australia*
[2]*Peter McCallum Cancer Centre, Melbourne, Vic, Australia*
[3]*The Alfred Hospital, Prahran, Vic, Australia*

INTRODUCTION: Radiologists differ significantly from other medical specialists in several respects. Typically they are very mobile professionals, working across public & private venues because of high demand for their services. Particularly in rural & remote areas, most Radiologists are generalists, called on to perform the full range of diagnostic imaging & in many cases, also involved in radiological interventions. In general terms, problems affecting RRs include: professional isolation, especially when in solo practice; lack of access to local CPD meetings & exposure to new equipment & techniques such as is available to city-based Radiologists; expectations from GPs & other medical specialists, that they will be all-round experts; commitment to frequent travel, as consultants working across a range of sites; high patient numbers & associated responsibilities. Since August 2003 the Royal Australian & New Zealand College of Radiologists (RANZCR) has been delivering Continuing Professional Development (CPD) programs by videoconference to Rural Radiologists (RRs) & associated staff across Australia & also, in New Zealand.

METHODS: Four programs are now under way using videoconferencing. In order of commencement they are: the Alfred Hospital Case Reviews (from August 2003); RANZCR Victorian Branch Monthly Scientific Meetings (from August 2003); meetings of the Interventional Radiologists Society of Australia (from June 2004); meetings of the Faculty of Radiation Oncologists (from July 2004). We briefly describe how the videoconferencing delivery system was developed, & discuss issues in determining needs, programming, content & evaluation across diverse settings. Videotaped material from sessions is shown to demonstrate that radiological images can be transmitted over vast distances with no loss of quality. We discuss strategies employed to meet the CPD needs of RRs including: providing information about current, state of the art & new Radiology techniques in a lively & interactive manner; offering complex cases with background information; encouraging Radiologists to share information & experiences; enabling the collection & storage of images & related videotaped content, for future webstreaming & for use in own time by Radiologists, Registrars & Overseas-trained Specialists.

RESULTS: Data is presented to show that uptake has been considerable (by RRs & also, Radiographers & Ultrasonographers), evaluations positive, & remote sites have begun to contribute presentations.

DISCUSSION & CONCLUSIONS: A brief discussion of pedagogical issues in developing CPD for RRs is provided.

ACKNOWLEDGMENTS: The RANZCR-SSRS projects are funded by the Support Scheme for Rural Specialists (Department of Health & Ageing). I-Med Ltd & Cook Australia have also sponsored specific parts of the program. We are very grateful for this support.

MODELING DEPRESSION THROUGH COUNTERACTIVE EFFECTS OF STRESS AND EXERCISE ON THE BRAIN

A. K. Saha[1], S. N. Sarbadhikari[2] and J. Mazumdar[1]

[1]*School of Electrical and Information Engineering, University of South Australia, Mawson Lakes, SA, Australia*
[2]*School of Medical Science and Technology, Indian Institute of Technology, Kharagpu, India*

INTRODUCTION: Mathematical modelling [1-3] is a useful tool for diagnosing and assessing the prognosis of depression. We also examine the role of exercise on depression in our model. Initially we divide the brain into four quadrants (left anterior: La; left posterior: Lp; right anterior: Ra and right posterior: Rp).

METHODS: The Mathematical Model based on the above assumption is:

$$\begin{aligned}
\frac{d}{dt}(Lp) &= \alpha_1(St) - \gamma_1(Lp) \\
\frac{d}{dt}(La) &= \frac{\alpha_2}{h^{n_2} + (St)^{n_2}} - \gamma_2(La) \\
\frac{d}{dt}(Rp) &= \frac{\alpha_3}{h^{n_3} + (St)^{n_3}} - \gamma_3(Rp) \\
\frac{d}{dt}(Ra) &= \alpha_4(St) - \gamma_4(Ra) \\
\frac{d}{dt}(St) &= f(St)
\end{aligned} \qquad (1)$$

RESULTS: Computer simulation results of the above dynamics are shown in the following graphs:

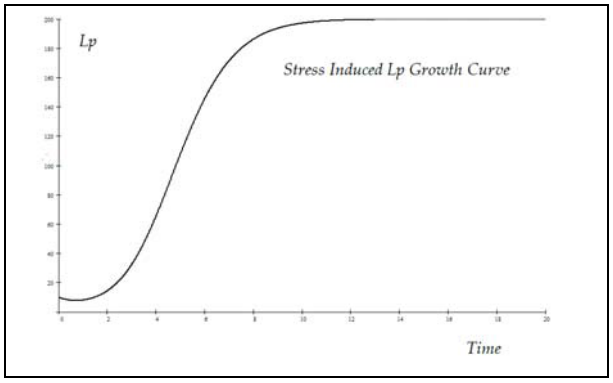

Figure 1. *Stress induced Lp (or Ra) growth curve with respect to time (in dimensionless form).*

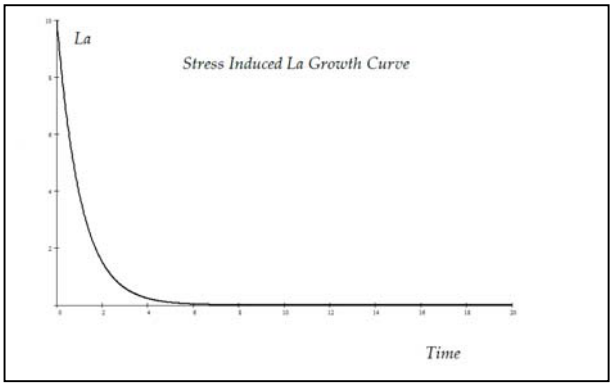

Figure 2. *Stress induced La (or Rp) growth curve with respect to time (in dimensionless form).*

DISCUSSION & CONCLUSIONS: By introducing exercise into the above dynamic, computer simulations of our model show that exercise and stress dynamics give rise to counteractive patterns which lead to a balancing harmony between the dynamics within the different quadrants of the brain.

REFERENCES:

[1]S. N. Sarbadhikari, K. Chakrabarty (2001) *Med. Eng. Phys,* 23**:** 445–455.
[2]S. N. Sarbadhikari, S.K. Pal (2002) *Handbook of Computational Methods in Biomaterials, Biotechnology and Biomedical systems*, Kluwer Academic Publishers, Boston, Vol. 4, Chapter 3: 51–81.
[3]S. N. Sarbadhikari (2004), *Depression and Dementia: Progress in Brain Research, Clinical Applications and Future Trends*, Nova Science Publishers, Inc., Hauppage, [In Press].

APPLICATION OF THE LATTICE BOLTZMANN MODEL TO ARTERIAL FLOW SIMULATION

J. Boyd[1], J.M. Buick[1], J.A. Cosgrove[2] and P. Stansell[2]

[1]Physics and Electronics, Biophysical and Biomedical Research Group, School of Biological, Biomedical and Molecular Sciences, University of New England, Armidale, NSW, Australia
[2]School of Physics, The University of Edinburgh, Edinburgh, Scotland, UK

INTRODUCTION: The dynamics of blood flow in arteries is an important topic. For example, there is a body of evidence to suggest that there is a correlation between the development of atherosclerosis and abnormal wall shear rate[1]. It is often difficult to make these measurements in vivo, thus numerical simulation becomes one of the main investigative tools of these phenomena.

METHODS: The Lattice Boltzmann model (LBM) is used to simulate arterial blood flow through the carotid artery with varying levels of stenosis using a D2Q9 lattice. Two boundary schemes are implemented: the traditional half-way bounce back method[2] and an extrapolation scheme[3], and the results are compared.

RESULTS: The extrapolation scheme is shown to give second order accurate resulted for oscillatory flows. Figure 1 shows the velocity magnitude in an artery with stenosis. The velocity along the cross-section lines A and B is shown in figure 2. The results differ increasingly as the artery width is decreased indicating the importance of the improved wall resolution provided by the extrapolation scheme.

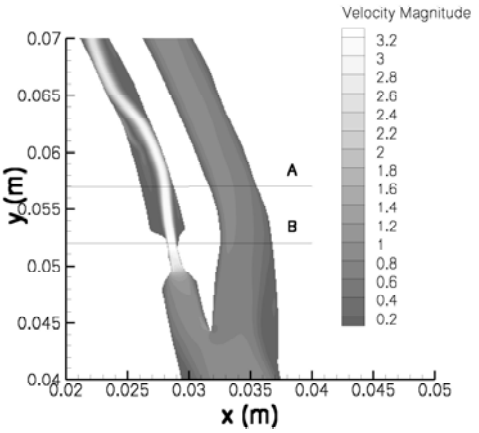

Figure 1. *Velocity field magnitude, Carotid artery.*

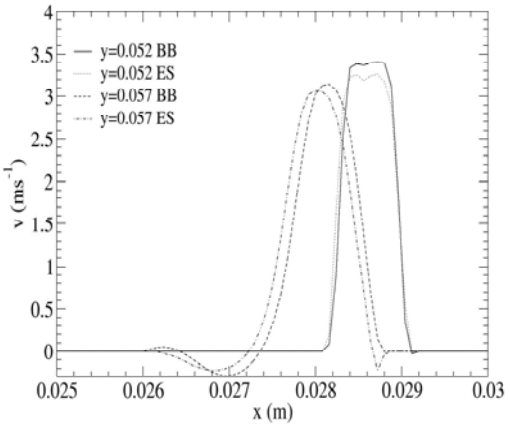

Figure 2. *Comparison of velocity profiles across A and B.*

DISCUSSION & CONCLUSIONS: The results demonstrate the need to use the improved accuracy of the extrapolation scheme when considering narrow arteries. The resolution of the lattice used in the simulations was 12.5 lattice sites per mm.

ACKNOWLEDGEMENTS: This work was partially supported by EPSRC (UK) under Grant No. GR/N16778 and this assistance is gratefully acknowledged.

REFERENCES:

[1]D.P. Giddens, *Role of fluid mechanics in localization and detection of atherosclerosis,* Journal of Biomechanical Engineering, 115:588-594, 1993.

[2]S. Succi, *The Lattice Boltzmann Equation for Fluid Dynamics and Beyond*, Oxford University Press, Oxford, 2001.

[3]Z. Guo, C. Zheng, and B. Shi, *An extrapolation method for boundary conditions in lattice Boltzmann method*, Physics of Fluids, 14:2007-2010, 2002.

SPECTRALLY RESOLVED FEMTOSECOND 2- COLOUR 3-PULSE PHOTON ECHOES: A NEW SPECTROSCOPIC TOOL TO STUDY MOLECULAR DYNAMICS

L. V. Dao, C. Lincoln, M. T. Do, P. Eckle, M. Lowe and P. Hannaford

Centre for Atom Optics and Ultrafast Spectroscopy, School of Biophysical Sciences and Electrical Engineering, Swinburne University of Technology, Hawthorn, Vic, Australia

The oxazine dye cresyl violet bonds strongly to DNA and RNA-rich cell compounds, e.g., in nerve tissues, and have been used for labelling and visualization of these tissues. The dye coumarin with different derivatives shows the basic structure of many natural substances and pharmaceutics. The physiological activity of coumarin derivatives is related to their reactivity toward DNA bases. The dye molecules are often distinguished by a relatively complex structure and in many cases this makes the assignment of vibrational modes, even by isotope substitution, or comparison with related structures quite difficult [1]. For studying the dynamics of proteins it is necessary to know the details of the vibrational structures and the structural dynamics of these molecules.

We present a new multidimensional spectroscopy technique based on spectrally resolved 2-colour 3-pulse photon echoes in the visible wavelength range for investigating vibrational and electronic dynamics [2,3] of the dye molecule cresyl violet and coumarin 485 in methanol. The use of this technique for the study of ultrafast transient processes that occur during the dissociation of carbonmonoxy myoglobin (MbCO) into myoglobin (Mb) and CO provides some valuable information.

The sample is illuminated by two femtosecond 'pump' pulses with wave vectors $\mathbf{k_1}$, $\mathbf{k_2}$ and wavelength λ_{pump} and a 'probe' pulse with wave vector $\mathbf{k_3}$ and wavelength λ_{probe}. For two-colour experiments with $\omega_1 = \omega_2 \neq \omega_3$, conservation of momentum and energy leads to the following phase-matching directions and signal frequencies: $\mathbf{k_4} = -\mathbf{k_1} + \mathbf{k_2} + \mathbf{k_3}$; $\mathbf{k_5} = -\mathbf{k_2} + \mathbf{k_1} + \mathbf{k_3}$; $\mathbf{k_6} = -\mathbf{k_3} + \mathbf{k_1} + \mathbf{k_2}$; $\omega_4 = \omega_3 + \delta\omega_4$; $\omega_5 = \omega_3 + \delta\omega_5$; $\omega_6 = -\omega_3 + 2\omega_1 + \delta\omega_6$, where the $\delta\omega$ represent frequency shifts associated with the transfer of optical coherence between transitions of different frequency. Thus, in 2-colour experiments in which $\omega_1 = \omega_2 \neq \omega_3$, the signal for $\mathbf{k_5}$ is the same as for $\mathbf{k_4}$ but with the sign of the coherence time t_{12} reversed, while the signal for $\mathbf{k_6}$ can yield additional information to that of $\mathbf{k_4}$ or $\mathbf{k_5}$. Our femtosecond laser system consists of a mode-locked Ti: sapphire oscillator and a regenerative amplifier which delivers 80 fs, 1mJ pulses at a wavelength of 800 nm and repetition rate 1 kHz. The laser pulses from the regenerative amplifier are split into two beams which pump two independently tuneable optical parametric amplifiers (OPAs), thus providing a two-colour source of femtosecond laser pulses. The OPAs have several options for frequency generation – second harmonic generation (SHG), fourth harmonic generation (FHG) or sum frequency generation (SFG) – allowing coverage of a broad range of wavelengths (250 – 2000 nm) with pulse duration of about 100 fs and high intensity. The output of the first OPA is split into two beams, which act as the pump pulses $\mathbf{k_1}$ and

$\mathbf{k_2}$, and the output of the second OPA acts as the probe pulse $\mathbf{k_3}$. The three pulsed beams with time delays t_{12} and t_{23} are aligned in a triangular configuration and focussed by a 15 cm focal length lens into the sample. The signal is measured in the phase-matching directions detected by one or more spectrometers with spectral resolution of about 1 nm.

REFERENCES:

[1]E. Vogel, A. Gbureck, W. Kiefer, *"Vibrational spectroscopic studies on the dyes cresyl violet and courmarin 152"*, J. of Molecular Structure 550-551, 177-190 (2000).

[2]L. V. Dao, C. Lincoln, M. Lowe and P. Hannaford *"Spectrally Resolved Femtosecond Two-Colour Three-Pulse Photon Echoes: Study of Ground and Excited State Dynamics in Molecules"*, J. Chem. Phys. 120, 8434- 8442 (2004).

[3]S. Mukamel, *Principles of Nonlinear Optical Spectroscopy* (Oxford University Press, New York, (1995).

BIOIMPEDANCE SPECTROMETER FOR TISSUE IMPEDANCE ANALYSIS

G. R. Poudel and H. T. Nguyen

Faculty of Engineering, University of Technology, Sydney, NSW, Australia

INTRODUCTION: Bioimpedance spectroscopy is a non-invasive method for determining the tissue characteristics and its characteristic frequency. Bioimpedance spectroscopy has been found to be able to repeatedly identify small tumours and tumour associated changes[1]. In this study we aim to design, implement and test a portable and cost effective bioimpedance spectrometer.

METHODS: The principle of data acquisition system is based on the conventional tetra polar impedance measurement system, represented in Fig. 1. A sinusoidal current with a frequency range 10 KHz to 500 KHz is applied between a pair of electrodes, which are called current electrodes. Current source is composed of cheap monolithic function generator XR – 2206 followed by current feedback amplifier used as voltage to current converter. Potential values are measured at two inner electrodes. Wideband instrumentation amplifier is used for amplification of the bioimpedance signal. Signal after filtering is rectified using precision rectifier to obtain the amplitude. Wide band four quadrant multiplier AD833 is used to obtain the phase component of the bioimpedance signal. Both amplitude and phase data are digitized and transferred to PC in real time for analysis.

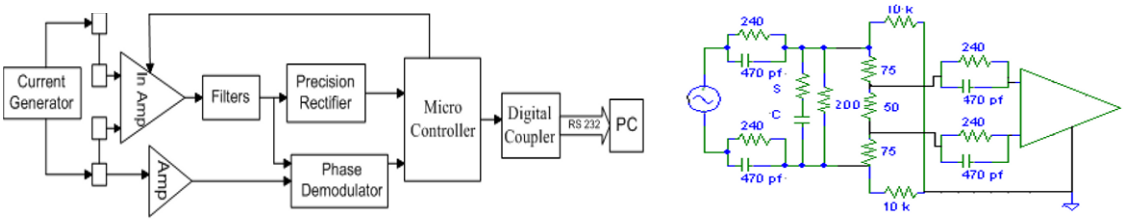

Figure1. *Block diagram of bioimpedance spectrometer and the test circuit used.*

RESULTS: Table 1 gives the result for the 100 Ω resistance. The absolute error of the system was found to be below 1%. To test the accuracy in measuring complex impedance, a model based on Cole-Cole equation was used[2]. Test circuit is shown in Fig. 1. The results of fitting measured data to Cole-Cole equation are shown in Table 1. Accuracy of the estimated parameters is found to be below 3%.

Frequency	Z	Error %
9.77	99.12	0.88
19.53	99.13	0.87
39.38	99.12	0.88
78.12	99.11	0.89
156.12	99.10	0.90
312.50	99.10	0.90
478.14	99.00	1.00

Tissue	Parameter	Tissue Value	Measured Fitted Values	
			Mean	Error %
Lung	R	99.91	102.1	2.19
	S	24.21	24.78	2.35
	C	10.37	10.12	-2.5
	Fc (kHz)	123.4	124.1	0.57

Table 1. *Measurement made on pure resistance and estimation accuracy using cole models.*

DISCUSSION & CONCLUSIONS: The device developed fulfils requirements for a bioimpedance spectrometer. Measurement on tissue model shows this can be used in tissue diagnostic applications.

REFERENCES:

[1]C. Skourou, P. J. Hoopes, R. R. Strawbridge, K. D. Paulsen (2004), *Physiological Measurement*, 25 :335-346.

[2]A. L. Nieto, D. Rezywowski, (1998), *Proceedings of the IEEE 24th ANBC*, 118-119.

ACTIVE TRANSPORT OF IGF-I THROUGH ARTICULAR CARTILAGE

B. S. Gardiner[1], D. W. Smith[1], P. Pivonka[1] and A. J. Grodzinsky[2]

[1]*Civil and Environmental Engineering, University of Melbourne, Parkville, Vic, Australia*
[2]*Center for Biomedical Engineering, Electrical Engineering and Computer Science, Mechanical Engineering, Massachusetts Institute of Technology, Cambridge, USA*

INTRODUCTION: When exposed to insulin-like growth factor (IGF-I), the rate of production of articular cartilage is enhanced by the application of a dynamic load e.g. [1]. Understanding the mechanobiological mechanisms involved may lead to better strategies for aiding matrix regeneration in diseased and damaged cartilage. Mauck et al. [2] have developed a mathematical model which predicts that the concentration of solutes in a poro-elastic material (e.g. cartilage) can be significantly increased (~x3) by applying a dynamic load. Moreover the final concentration is predicted to be well above the solute concentration in surrounding fluid. This result potentially provides an explanation for the synergy between IGF-I and dynamic loading. However, it is our opinion that Mauck et al's [2] results were sufficiently counter-intuitive as to warrant further investigation and verification.

METHODS: A three-phase poro-elastic model for neutral solute transport through articular cartilage is developed. Our approach differs from that of Mauck et al. [2] in only that our expression for the relative motion of the fluid and solid phases are given by Darcy's law, and the relative motion of solute and fluid by diffusion equations, rather than solute linear momentum balance expressions containing various dissipation constants. However we believe that the physics contained in the resulting equations are theoretically equivalent.

RESULTS: Unlike Mauck et al. [2], our model predicts no increase in IGF-I concentrations above the constant boundary concentration. However we do see that dynamic loading can increase the rate of transport of IGF-I into the cartilage (Figure 1a). This increased transport is due to the advective flow near the cartilage surface, and is recognized by the modification of the concentration profile from a typical simple diffusion (Figure 1b). This increased transport has been observed experimentally [1].

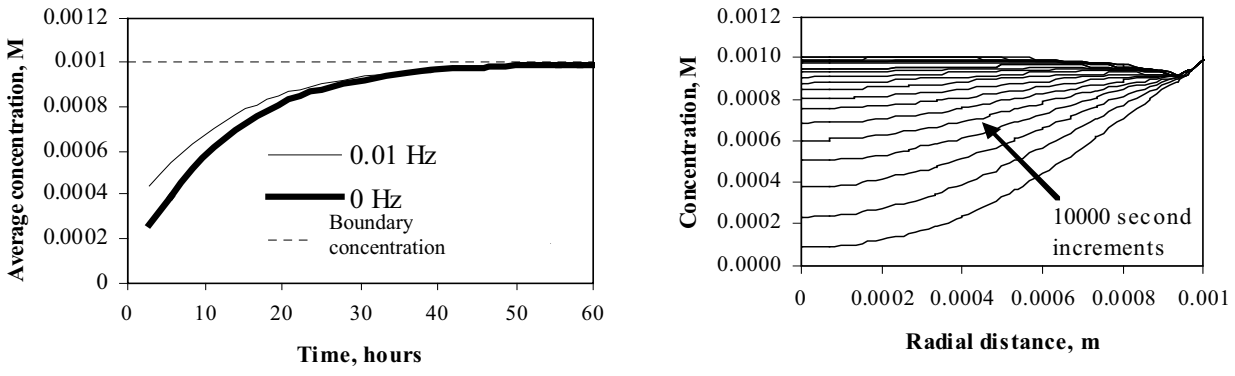

(a) *(b)*

Figure 1. *(a) The change in the spatially-averaged IGF-I concentration with time for the loaded and unloaded systems and (b) the radial change in IGF-I concentration for the loaded system.*

DISCUSSION & CONCLUSIONS: Transport models are beginning to predict enhanced transport of IGF-I under dynamically loading conditions. Further research needs to be conducted on the effects of matrix anisotropy, permeability and IGF-I adsorption.

REFERENCES:

[1]L. J. Bonassar, A. J. Grodzinsky, E. H. Frank, S. G. Davila, N. R. Bhaktav, S. B. Trippel (2001*) J. Orth. Res.*, 19:11-17.
[2]R. L. Mauck, C. T. Hung, G. A. Ateshian, (2003) *Trans. ASME*, 125:602-614.

PHYSIOLOGICALLY REALISTIC SIMULATION OF MULTIPLE LUNG GAS EXCHANGE DURING ANAESTHESIA BY SIMULTANEOUS GAS INFUSION AND EXTRACTION

P. Ramani[1], C. Stuart-Andrews[2] , G. Robinson[3], P. Peyton[4] and P. Junor[1]

[1]*Electronic Engineering, La Trobe University, Bundoora, Vic, Australia*
[2]*Electrical & Computer Systems Engineering, Monash University, Clayton, Vic, Australia*
[3]*The Alfred Hospital, Melbourne, Vic, Australia*
[4]*Austin Hospital, Melbourne, Vic, Australia*

INTRODUCTION: A lung gas exchange simulator was tested which produces simultaneous uptake and /or elimination of multiple gas species present during anaesthesia. The concept of the method more fully described here of simulating lung gas exchange was briefly outlined by Beams et al (1998), who used it in connection with their study of breathing circuits.
While measurement of gas exchange in a breathing system is routinely performed in some environments, such as intensive care, it is still not routinely performed during anaesthesia. However these measurements have potentially important anaesthetic applications such as the monitoring of O_2 uptake and CO_2 elimination, and the noninvasive measurement of pulmonary blood flow using lung exchange of either CO_2 or inert gas. Systems for gas exchange measurement require validation prior to use (Braun et al 1989). Lung simulators are an efficient way of achieving this, since they permit testing in a tightly controlled environment. They avoid many of the difficulties of in vivo testing, e.g. (1) the need for ethics approval with regard to either consent of human subjects or the logistical requirements of animal laboratory maintenance and (2) the numerous confounding physiological factors which can affect results and obscure their interpretation in live subjects.
METHODS: An artificial test lung was constructed with physiologically realistic expired and exhaust gas flows, using a combination of diluting/enriching gas infusion into the lung and lung gas extraction. An algorithm was devised for determination of gas infusion and extraction flow rates for any set of target gas exchange values with any given set of fresh gas flows and concentrations. Six different scenarios were simulated, comprising a range of gas exchange values for each gas species which lie within a physiologically realistic range for anaesthetised patients. For each of these experiments the system was tested for 15 consecutive measurements over 25 minutes.
RESULTS: Mean bias and standard deviation of the difference (SD in parentheses) relative to target value was: - 0.001 (0.008) L/min for oxygen uptake, -0.002 (0.005) L/min for carbon dioxide production,-0.008 (0.010) L/min for uptake of nitrous oxide and +0.5 (0.3) mL/min for uptake of a volatile anaesthetic agent (isoflurane). The mean bias was within 12% of the target value for all gases and scenarios. The limits of agreement lay within 25% of the target value in all cases, and within 12% of the target for oxygen and carbon dioxide.
DISCUSSION & CONCLUSIONS: Good accuracy and precision of this approach to lung gas exchange simulation were demonstrated, resulting in a versatile simulator.
REFERENCES:
Beams, D. M., Sasse, F. J., Webster, J. G., Radwi, R. G., 1998. *Model for the administration of low-flow anaesthesia*. Br. J. Anaesth.; 81: 161-70.
Braun, U., Zundel, J., Freiboth, K., Weyland, W., Turner, E., Heidelmeye,r C. F., Hellige, G., 1989. *Evaluation of methods for indirect calorimetry with a ventilated lung model*. Intensive Care Medicine. 15: 196-202.

APESM: TRENDS IN THE JOURNAL FROM 1993 TO 2003

M. Caon[1] and J. Pattison[2]

[1]*Flinders University, Bedford Park, SA, Australia*
[2]*University of South Australia, Mawson Lakes, SA, Australia*

INTRODUCTION: A brief historical overview of the journal "Australasian Physical & Engineering Sciences in Medicine" and significant happenings in its history since commencing publication in 1978 will be given. The number of subscribers, of articles published, size of each volume, country of residence of the author, type of article published and broad discipline area of the subject matter have been surveyed for the period 1993-2003 and will be discussed. In addition the roles of the members of the editorial team will be discussed.
SURVEY RESULTS: APESM has close to 500 subscribers, with the number of ACPSEM member subscribers increasing from 372 in 2000 to 426 in 2004. The journal has published between 20 and 36 articles per volume, with more than 30 articles in a volume being achieved in 3 years only. The number of pages in a volume has run from 170 to 284. It would be true to say that from 1999 to 2002 (volumes 22-25) the journal went through a difficult period where between 20 and 22 articles only were published annually. However the seeds for growth were sown as in 2002 and 2003, 48 and 36 manuscripts (respectively) were submitted. Consequently in 2003, 32 articles were published. It would also be true to say that prior to 2002, APESM was almost entirely an Australia and New Zealand journal with at least 85% of the articles coming from first authors who were resident in New Zealand & Australia. This is no longer the case. In 2003 only 50% of first authors were Australasian residents. The distribution between the professional disciplines, of the subject matter of articles published in APESM has not changed a great deal over the 11 years of this survey. However the percentage of articles on radiotherapy has been trending upwards from about 30% in 1993, currently they comprise about 50% of the total. It appears that the **proportions** of the 4 different types of article being published in the Journal have changed. In volumes 16 to 20 (1993-1997), "scientific papers" comprised 85% of the articles (there were always more than 20 per volume - usually 24 or more. In volumes 22 - 26 (1999 – 2003) "scientific papers" comprised 44% of articles (there were always less than 15 - sometimes 12 or less).
WEB PRESENCE: In 2002 the Journal published its own webpage for the first time. This was a significant development for the journal as prior to that, APESM's Web presence was through references to its articles, commercial abstract providers, or as a title on lists of scientific journals. The webpage considerably increases the exposure of the articles published in the

journal. From issue 27(1) the abstracts for published articles will be available on the unrestricted portion the website and will appear prior to the hard copy. Before the Journal had a webpage, Japan Society of Medical Physics (JSMP) was showing the flag for us by listing the contents pages of each issue of the journal. They were and still are the 1st hit when I *Google* for the Journal's full name (*Googling* "APESM" hits the journal first). After being contacted, JSMP have kindly added a link to the Journal's webpage.

We examined other significant hits that listed the journal **and** included a hotlink to the Journal. Unfortunately, the links (initially) all led to either the JSMP webpage; to a University of Wollongong site; or to a "page not found" window (the webmasters were advised and many hotlinks have now been corrected).

DISCUSSION & CONCLUSIONS: I would **encourage** you to consider getting more value from your presentation here at the conference and work your abstracts into manuscripts and submit them to APESM. I would further encourage you to consider publishing some non-conference articles in APESM and that when you publish in other journals, you cite your earlier work in APESM. Also cite other relevant articles in APESM written by other authors. Submission, review and printing are now handled entirely electronically. Corresponding authors are supplied with a .PDF file of their publication (a facsimile of the journal pages) to use in the same way as reprints would be used. The increasing web presence of the APESM journal and the reduction in processing time for submitted manuscripts that has occurred following the appointment of three assistant editors in 2003, are compelling reasons for publishing in APESM.

SUMMARY OF ISSUES ENCOUNTERED WHILE IMPLEMENTING A HOSPITAL WIDE PACS

L. Wilkinson[1], N. Liddell[1] and J. Heggie[2]

[1]*Medical Imaging Department, St. Vincent's Hospital, Fitzroy, Vic, Australia*
[2]*Medical Engineering and Physics, St. Vincent's Hospital, Fitzroy, Vic, Australia*

A hospital wide PACS is more than an archive and distribution system for medical images. It must be successfully integrated to other hospital systems, in particular a Radiology Information System (RIS). The PACS solution implemented at St. Vincent's Hospital Melbourne in 2003 has 3 TB of RAID in a SAN to provide 3 years of on-line data to 10 diagnostic workstations and includes web distribution to the clinical users, including A&E, ICU and Theatres. The PACS was integrated to a Kestral RIS and the webviewer for images was integrated to a Clinical Information System used to distributed radiology/pathology results around the hospital.

A lot of attention was applied to trying to identify and rectify potential issues with implementing PACS before they occurred. The issues that were anticipated related to transmission speeds of image data across the hospital network, integration of all imaging modalities to the PACS and clinical acceptance, in particular in the operating theatres. In practice none of these items were a major problem.

Other issues, which were more significant than anticipated and were resolved during the implementation, include:

(1) Developing an efficient process for handling of external films / images.
(2) Image Quality on PACS workstations for nuclear medicine images.
(3) Developing a precise workflow to allow successful use of the combined RIS/PACS and issues relating to scanning in referrals.
(4) Restructuring of RIS exam codes
(5) RIS/PACS integration at the system level – routine messaging was planned and worked well but a number of unexpected issues arose.
(6) Integrating the web distribution of images to the existing Clinical Information System.
(7) Dictation system integration.
(8) Education of staff within the Medical Imaging Department, particularly in relation to workflow changes.
(9) Managing duplicate systems during a transition phase.
(10) A process for printing film for use outside the hospital, i.e. patient transfers to another hospital. Also issues with exporting data on CD.
(11) Local support in Australia can be compromised by dependency on the expertise of a few individuals.
(12) Patch Management/Virus Protection of critical servers
(13) Facilities for clinical meetings/presentations

CLINICAL APPLICATIONS OF A WIDE AREA NETWORK IN RURAL HEALTH

D. Stewart[1], M. Johnstone[2] and G. Druitt[2]

[1]*Biomedical Engineering Services, South West Healthcare, Warrnambool, Vic, Australia*
[2]*South West Alliance of Rural Health, Warrnambool, Vic, Australia*

INTRODUCTION: Established in June 1998, the South West Alliance of Rural Health (Vic) (SWARH), is an Alliance of public health agencies in the South West of Victoria covering an area of approximately 60,000 sq. kilometres connecting all

public acute hospitals and associated health services in a region extending from west of Melbourne to the South Australian Border. The basis of the SWARH is a high speed multi-star converged telecommunications network connecting all member sites to each other and to Melbourne in a unique regional infrastructure. This paper will discuss clinical applications and technology that utilises this network.

METHODS: Through consultation with SWARH members, a number of clinical applications were proposed. Projects that have been implemented thus far include : Web based cardiac monitoring overview, cross campus transfer of patient monitoring data (trends etc), IP based Video Conferencing Integration for remote clinical management and assessment (Breast Screening, ED etc), Emergency Department Point of Care Triage Pilot. A number of other projects are also proposed or under development.

DISCUSSION & CONCLUSIONS: The clinical applications presented represent the 'tip of the iceberg" of possibilities and potential for this type of network. With ever increasing healthcare costs, an aging rural population and the difficulty in recruiting health professionals in rural areas, the need to link smaller rural health facilities with larger specialist centres will become more and more important. Telemedicine, teleradiology and many other applications requiring hi speed wide area networks are destined to play a major role in healthcare delivery in rural areas. SWARH hopes to continue as a leader in this area.

REFERENCES:

[1]M. Johnstone, South West Alliance of Rural Health (SWARH)/Barwon Health *Change Management Report*, July 2003.
[2]G. Druitt, South West Alliance of Rural Health (Vic), *Overview* 2004.

MEDICAL TECHNOLOGY AND DEVELOPING COUNTRIES - THE REALITIES AND CHALLENGES

D. A. W. Smith

PNG HSSP Pty. Ltd,. Port Moresby, Papua New Guinea

THE ENVIRONMENT AND CONTEXT

The Pacific Islands are often depicted as tropical paradises with idyllic beaches, crystal clear lagoons and oceans teaming with fish and offering endless coral reefs to explore. The people are shown as healthy, happy and living in quaint bush material houses and eating fish and tropical fruit. The truth is often quite different. Diseases that are history in Australia are common place, health systems are basic and life spans are short. The country is unlikely to have substantial natural resources to maintain a growth economy and is likely to be partly or largely dependent on external donor aid.

AID FUNDING – APPROACHES AND EXPECTATIONS

The governments of the developed countries provide donor funds through various agencies to assist developing countries. Substantial funds are provided to government health departments to improve the standard of health care through sector wide programs which work towards building capacity in the health care delivery system through mentoring and encouraging the partner.

A HEALTH SYSTEM APPROACH TO MEDICAL TECHNOLOGY APPLICATIONS

The approach to capacity building has a number of key elements described in this paper. Particular recognition must be given to the need to improve planning, management and resource utilisation related to medical equipment management in the context of limited health dollars, the priorities of the National Health Plan and the current level of development of technical support skills.

THE CHALLENGES OF MANAGING AND MAINTAINING MEDICAL TECHNOLOGY

Many Pacific nations have had their political independence for some years but little has been done to maintain or develop infrastructure systems established prior to independence. Health is often a casualty of insufficient in-country resources and priority and is nearly always a target of donor assistance programs. This assistance always contains capital investment in buildings, static plant and medical equipment and can amount to millions of dollars.

When technology is transferred to developing countries by donors, the infrastructure required to support the technology may not exist. It may be lack of clinical services but it also can be unreliable electricity supply or poor water quality. The high cost of spare parts for medical equipment is accepted in developed countries as an overhead which comes with the new technology. The same spare parts when required in developing countries cost substantially more yet the country has no foreign reserves and little income to afford them. Then there is the problem of well-meaning donors assembling a patchwork collection of redundant equipment without operating instructions or installation information.

It has been demonstrated by successful donor development projects that increased capacity to manage and maintain medical technology can be sustained and with the support of the country's government, developed to be self-sufficient in all aspects of the discipline.

REFERENCES:

The Australian Agency for International Development http://www.ausaid.gov.au/

ASPECT OF PLANNING A MEDICAL DIAGNOSTIC CLINIC IN THE MEKONG DELTA

T. C. Nguyen[1] and Q. Tran[2]

[1]*Gait Laboratory, Royal Children's Hospital, Melbourne Vic, Australia*
[2]*Mayne Health, Imaging Division, Melbourne Vic, Australia*

INTRODUCTION: The health of a population is an important precondition for economic and social development. The Mekong Delta Region is situated on the Mekong River and accounts for 12% of the area and 22% of population in Vietnam. The region has been identified as an economically disadvantaged area where investment should be focused to alleviate poverty and stimulate economic activity [1]. Diagnostic imaging plays an important role in today's medical treatment and management as it enables physicians to look inside the body without surgery and view its structures and functions. Consequently, diseases are detected earlier, more appropriate treatments are selected and health care cost is reduced. Currently there is one major specialize centre providing clinical diagnostic services in Vietnam with its headquarter located in Ho Chi Minh City (HCMC) while adequate imaging and radiology department are only attached to a limited number of major hospitals in Hanoi and HCMC. With a population of about 20 million people, the Mekong Delta remains one of the poorest regions in the country; hence essential medical diagnostic services are inaccessible to many people. This paper gives a brief review of the healthcare system in Vietnam and explores all aspects of setting up a medical diagnostic clinic including: model of operation, equipment, human resources required and the type services provided.

METHODS: An extensive literature review of Vietnam's current healthcare sector was conducted. This involved reviewing reports from various agencies such as WHO, ADB, AusAID and World Bank and extracting information relating to the Mekong Delta. Personal communication with numerous healthcare professionals who are currently working in Vietnam and experts in the area of healthcare management were used in the feasibility report.

RESULTS: A report on setting up a medical diagnostic clinic in the Mekong Delta was drafted which includes vigorous analysis of the healthcare market and recommendations.

DISCUSSION & CONCLUSIONS: The issues of affordability and accessibility were addressed previously [3] . This paper attempts to address the issue of equality in health care services currently in Vietnam. While the GDP per capita in Vietnam remains low at US$420 (March 2003) and may be up to 5% of this is spent on health care, a basic general check up could cost somewhere between US$5-10 with a more thorough assessment costing between US$80-120. This is clearly out of reach for the majority of the population. In the context of setting up a medical diagnostic clinic in an area like the Mekong delta in Vietnam, one must ask whether this is feasible and sustainable?

REFERENCES:

[1]AusAID (2003), *Report: Mekong Delta Poverty Analysis*.
[2]World Bank, (2001), *Vietnam Growing Healthy: A Review of Vietnam's Health Sector*.
[3]T. Nguyen & Q. Tran (2004) *VPS-Australia 11th National Conference, Brisbane.*

Abstracts of poster presentations

MAXIMIZATION OF THE MUTUAL INFORMATION INDEX FOR CT-CT IMAGE FUSION

M. Bailey, M. West, V. Nelson, L. Holloway, G. Cho, O. Collins, G. Song, J. Lees and J. Arts

Department of Medical Physics, Macarthur & Liverpool Cancer Therapy Centres, South Western Sydney Cancer Services, Campbelltown, NSW, Australia

INTRODUCTION: The accuracy with which two different image sets are co-registered is vital to the delineation of tumour volumes in radiotherapy. In order to obtain a confidence level in the ability of CMS FOCAL V4.1.1 (St. Lois, USA) to co-register CT study sets for radiotherapy treatment planning a phantom study was undertaken. The image registration algorithm used by CMS is the maximization of mutual information [1,2,3].
METHODS: A Siemens Sensation 4 CT Scanner (Forchheim, Germany) was used to scan the phantoms for the study. The CMS FOCALSim application was used to co-register the different data sets. The co registration of two CT data sets was examined using two separate phantoms [4]. The maximization of mutual information index (MMII) when different parameters were varied was examined. The CT slice thickness was varied from 1mm up to 5mm as used in clinical CT Simulation protocols. The CT image field of view (FOV) was varied from 20cm to 50cm. The angle rotation of the phantom was varied. The various geometries within the phantom were rotated by known angles for co-registration with the default position. The inserts of different relative electron densities were removed for co-registration with the default position. The influence of these changes on the MMII was examined as an indication of the "goodness" of the image co registration.
RESULTS: The accuracy of the CT-CT registration was determined. The MMII ranged from 1.36 to 0.92 for the combination of CT slice thickness investigated. For the angle offset of the phantom the MMII ranged from 0.63 to 0.90. For the range of field of views investigated for the phantom the MMII ranged from 0.49 to 1.01. For angle offset of only a single geometric component the MMII remained fairly uniform ranging from 0.686 to 0.690. For the removal of the various relative electron density inserts the bone inserts were found to have the most significant impact on the MMI. These results are clinically significant for patients that are scanned with contrast or require a re-plan.
DISCUSSION & CONCLUSIONS: The co registration of two different CT study sets using the maximization of mutual information is greatly dependent on the amount of information contained in each. The "goodness" of an image registration can be obtained by evaluating the MMII. Partial volume effects due to CT slice thickness will affect the registration and may lead to significant differences in the volumes contoured by the radiation oncologist. Similarly the FOV dependence highlights the need for corresponding mutual information, more data is better! The relative electron densities play an important role in image registration with the more dense materials given a greater weighting by the algorithm. – i.e. a greater difference in mutual information of corresponding voxels. Geometric differences are significant depending upon the size of the difference and amount of unchanged information, which is particularly important for pre & post operative CT images. The work undertaken demonstrates the need to accurately determine the confidence with which image sets are co-registered. Further work will include MRI and PET images.
REFERENCES:
[1]Maes et al, *Multi-Modality Image Registration by Maximization of Mutual Information*, Proceedings of MMBIA '96, IEEE, 1996.
[2]Hibbard, L., *Maximum a posteriori Segmentation for Medical Visualization*, IEEE Workshop on Biomedical Image Analysis, 93-102, 1998.
[3]Hanjai, J.V. et.al. (eds.) *Medical Image Registration*, CRC Publishing, 2001.
[4]*QUASAR Phantom Manuals*, MODUS Inc, Ontario, Canada.

EVALUATION OF THE VARIANCE REDUCTION OPTIONS AVAILABLE WITH THE NEW BEAM CODE DISTRIBUTION

P. Vial[1,2], L. Oliver[1,2] and C. Baldock[2]

[1]*Royal North Shore Hospital, Sydney, NSW, Australia.*
[2]*Institute of Medical Physics, University of Sydney, Sydney, NSW, Australia*

INTRODUCTION: The BEAM Monte Carlo code has been widely benchmarked for dosimetry calculations with medical linear accelerators. The computational time required to run simulations on BEAM remains a limitation to its use in the clinic. The computational time can be reduced by increasing a) computing power and/or b) calculation efficiency. Computing power may be increased by the use of PC clusters which require significant resources and expertise that may not be available in most small radiotherapy clinics. Calculation efficiency is improved by variance reduction and approximation techniques.

The latest distribution, BEAMnrc04 contains new variance reduction options that are claimed to improve photon fluence efficiency by a factor of 8 over the previous distribution[1]. This work investigates the efficiency gains available with BEAMnrc04 for simulations of megavoltage photon beams.

METHODS: A model of a high energy (16 MV) and a low energy (6 MV) linear accelerator were investigated. The 16 MV model is a simplistic example provided by the BEAM developers. The 6MV model was created for this work from Varian's specifications of a Clinac 600C. The efficiency was calculated for each case using the following equation: $\varepsilon = 1/(Ts^2)$. Where ε is the efficiency, T is computer processing time and s is the estimated uncertainty in fluence in a 2 cm square scoring region on the central axis at 100 cm distance. The uncertainty was calculated by the BEAM code system. The new bremsstrahlung splitting technique called Directional Bremsstrahlung Splitting (DBS) is compared for efficiency with the older Uniform Bremsstrahlung Splitting (UBS) method. Photon Forcing, Russian Roulette (RR) and Range Rejection were also tested for their impact on efficiency. The same simulations were run on two desktop computers, one with a 1.7 GHz processor and one with a dual processor (2 x 3.06 GHz) for comparison. All efficiencies are quoted relative to a reference simulation with default settings and no bremsstrahlung splitting.

RESULTS: Changing Range Rejection (Global electron cut-off energy) from 1 MeV to 3 MeV increased photon efficiency by a factor of 1.41. No effect on electron efficiency was observed. Photon forcing made no significant difference in photon fluence efficiency with photon forcing turned on. A decrease in electron fluence uncertainty was observed but not enough to significantly improve electron efficiency when using DBS with esplitting. Maximum photon efficiency with DBS (no e-splitting) was 13.5 times greater than with UBS (no Russian Roulette) and 176 times greater than with no bremsstrahlung splitting at all. With e-splitting and RR enabled the gain with DBS over UBS was reduced to 8.7 times. No significant difference in electron efficiency was observed. The effect of e-splitting when using DBS is to decrease photon efficiency by a factor of about 0.9. No significant difference in electron efficiency was observed. The effect of moving the RR plain relative to the splitting plane with DBS was not significant. The largest efficiency was achieved with the splitting plain on the bottom surface of the flattening filter and the RR plane 1mm above it. The dual processor computer was on average a factor of 2 times more efficient than the 1.7 GHz computer.

DISCUSSION & CONCLUSION: Efficiency gains of about two orders of magnitude can be achieved with the use of DBS. A gain of approximately 9 times was achieved with the DBS technique over UBS. Continued improvement of variance reduction techniques with BEAM will significantly improve the efficiency of phase space and ultimately dose calculations.

REFERENCES:

[1]Rogers, D. W. O., Walters, B., Kawrakov, I, *BEAMnrc Users Manual*, NRCC Report PIRS-0509(A) rev H, 2004.

COMMISSIONING OF THE BRAINLAB M3 MICRO-MLC AND PLANNING SYSTEM FOR STEREOTACTIC RADIOSURGERY – EXPERIENCE OF FIRST AUSTRALIAN SITE

J. Crosbie, R. Smith, S. Elliott, F. Gagliardi, C. Lancaster, J. Droege, R.M. Millar and M. Dally

William Buckland Radiotherapy Centre, The Alfred Hospital, Melbourne, Vic, Australia

INTRODUCTION: Stereotactic radiosurgery demands that the dose to the tumour be delivered with a high degree of conformality and precision. The BrainLAB m3 is a computer-controlled, automated multi-leaf collimator (MLC) system that attaches to the linear accelerator [1]. The small leaf width allows the radiation dose to tightly conform to the tumour volume in three dimensions. The William Buckland Radiotherapy Centre in Melbourne is the first site in Australia to use the micro MLC clinically. We present our experiences with the commissioning process.

MATERIALS & METHODS: The mechanical isocentre was verified using the so-called Winston-Lutz test [2]. Leaf transmission and leakage was measured using radiographic film. The system's ability to accurately produce planned conformal field shapes as well as light-field to radiation field coincidence was extensively tested. Beam data (PDDs, OARs and output factors) for the BrainSCAN planning system were acquired in a scanning water tank phantom using small volume ionisation chambers (IC3) and semiconductor diodes. Output factors for very small field shapes (6 to 18 square mm) were measured using microchip LiF TLDs (12 measurements per field) in a solid water phantom. The planned dose (monitor units) for basic and complex clinical field shapes was verified using a calibrated ionisation chamber in a miniature water phantom. An independent monitor unit calculation program using curve fitting techniques has also been developed in which all PDD curves have been converted to tissue phantom ratios.

RESULTS: The linac's mechanical isocentre was not affected by the addition of the m3 micro-MLC and field displacement measurements were within manufacturer's specifications. The mean transmission through closed leaves was 0.6 % and the leakage between leaves was 1.7 %. Analysis of the initial light field to radiation field coincidence films showed that the entire m3 carriage required an inplane shift of approximately 1 mm. Subsequent films have shown the fields to be within our own and the manufacturer's tolerance. Nine TLD readings per small square field had a reproducibility of $\leq 3\%$ and were used in the construction of the output factor table. The measured dose, for basic and complex fields, in the miniature water phantom agreed with the planned dose to within 2.5%, even for very small field sizes. The independent MU program displays good agreement with the BrainSCAN planning system, typically within 2% for the majority of clinical treatment

fields. Collisions between the m3 micro-MLC and the treatment couch have occurred at our centre and a collision table would be a very useful tool for planners.

CONCLUSIONS: The BrainLAB m3 micro multi-leaf collimator system is capable of delivering precise field shapes which make it very suitable for the rigours of stereotactic radiosurgery. Dose distributions can be calculated on the planning system and can be delivered accurately to very small fields. We hope that our experiences as outlined in this paper, will prove helpful to other centres who are considering purchasing such a system for stereotactic radiosurgery.

REFERENCES:

[1]Cosgrove V. et al., *Commissioning of a micro multi-leaf collimator and planning system for stereotactic radiosurgery*, Radiotherapy and Oncology, 50:325-326, 1999.

[2]Winston K and Lutz W., *Linear accelerators as a neurosurgical tool for stereotactic radiosurgery*, *Neurosurgery*; 22: 454-464, 1988.

RESPONSE VARIATION IN A BATCH OF TLDS

J. Burrage and A. Campbell

Department of Medical Engineering and Physics, Royal Perth Hospital, Perth, WA, Australia

INTRODUCTION: At Royal Perth Hospital, LiF thermoluminescent dosimeter rods (TLDs) are handled in batches of 50. Rods in each batch are always annealed together to ensure the same thermal history and an individual batch is used with the same type and energy of radiation. A subset of a batch is used for calibration purposes by exposing them to a range of known doses and their output is used to calculate the dose received by other rods used for a dose measurement. Variation in TLD response is addressed by calculating 95% certainty levels from the calibration rods and applying this to the dose measurement rods. This approach relies on the sensitivity of rods within each batch being similar. This work investigates the validity of this assumption and considers possible benefits of applying individual rod sensitivities.

METHODS: The variation in response of TLD rods was assessed using 25 TLD-100 rods (Harshaw/Bicron) which were uniformly exposed to 1 Gy using 6 MeV photons in a linear accelerator on 5 separate occasions. Rods were read with a Harshaw 5500 reader. During the read process the Harshaw reader periodically checks for noise and PMT gain drift and the data were corrected for these parameters. Replicate exposure data were analysed using 1-way Analysis of Variance (ANOVA) to determine whether the between rod variations were significantly different to the variations within a single rod. A batch of 50 rods was also exposed on three occasions using the above technique. Individual TLD rod sensitivity values were determined using the rod responses from 2 exposures and these values were applied to correct charges on a rod-by-rod basis for the third exposure.

RESULTS: ANOVA results on the 5 exposures of 25 rods showed the variance between rods was significantly greater than the within rod variance ($p < 0.001$). The precision of an individual rod was estimated to have a standard deviation of 2.8%. This suggests that the 95% confidence limits for repeated measurements using the same dose and rod would be approximately ±5.5%. For a typical run, we observed the response of a single rod could differ by as much as 17% from the overall run mean. This suggested the precision of TLD dose measurements could be improved by using individual rod correction factors. Application of individual rod sensitivity factors calculated from 2 exposures for the batch of 50 rods reduced the variance of readings in the third run by a factor of 10. This would reduce the 95% confidence intervals of dose estimates by a factor of 3.

DISCUSSION & CONCLUSIONS: This study demonstrates that individual sensitivity correction factors for TLD rods will significantly improve the precision of dose estimations. However, the use of individual correction factors requires strict care to be taken to ensure that the correct identification of rods is maintained.

ACKNOWLEDGEMENTS: The authors thank Livio Mina for helpful discussions about statistical analysis and Kathy Woolley and Peter Rampant for their work with the TLD preparation, exposure and readout.

PHANTOM COMPARISON FOR KILOVOLTAGE X-RAY DOSIMETRY

R. Hill[1,2], L.Holloway[1,2] and C.Baldock[2]

[1]*Cancer Therapy Centre, Liverpool Hospital, Sydney, NSW, Australia*
[2]*Institute of Medical Physics, School of Physics, University of Sydney, Sydney, NSW, Australia*

INTRODUCTION: Kilovoltage x-ray beams are used for treatment of superficial cancers. The IPEMB Code of practice[1] and the IAEA TRS398 dosimetry protocol[2] recommend that in-phantom absolute dose calibrations be performed in water. In addition, both state that relative dosimetry measurements can be performed in a solid phantom provided a comparison with water is made. This study investigated the use of two solid phantoms in relative and absolute dosimetry of kilovoltage x-ray beams.

METHODS: A Pantak DXT300 Orthovoltage X-ray unit (Pantak Inc., Branford, USA) was used to generate x-ray beams with accelerating potentials ranging from 75 to 300kVp. Three phantom materials were used: Solid Water RMI-457 (RMI

Gammex, Middleton, Wisconsin), Plastic Water (Computerized Imaging Reference Systems Inc., Norfolk, Virginia) and water. Percentage depth dose curves and relative output factors for x-ray beams with energies 75kVp to 300kVp were measured in all three phantoms using a PTW Markus parallel plate chamber. The absolute dose per monitor unit was determined for x-rays beams of energies 180kVp to 300kVp using the IPEMB code of practice[1]. The dose was measured with an NE 2571 Farmer type ionisation chamber placed at 2cm depth in all phantoms.

RESULTS: The depth doses measured in Solid Water gave a good dosimetric match with water. The maximum deviation of 2.4% occurred for the beam with energy of 75kVp at a depth of 40mm. The results for the Plastic Water indicate a greater dosimetric difference compared to water. For the beam with energy of 75kVp, the maximum deviation was 23.2%. For the 300kVp energy beam, the maximum dose deviation was 2.2%. The results of the output factors indicate that Solid Water provides excellent dosimetric match with water over all energies with a maximum deviation of 0.6%. The Plastic Water gives a greater difference in output factor. The maximum difference is 8.4% and occurs for the beam with energy of 75kVp, while the output factors are within 1% for the 300kVp energy beam. The absolute doses measured in Solid Water and water differed from 3.1 to 1.2% with increasing energy and for Plastic Water, the absolute doses varied from 12.8 to 3.4% with increasing beam energy.

DISCUSSION: The ICRU recommends that the dosimetric match of the solid phantom with water be within 1%[3]. This criterion is only met for the measurements of a limited subset of relative dosimetric data and is not met for absolute dose calibrations. A comparison of the mass attenuation coefficients of the three phantoms indicates Solid Water has a closer match to water compared to Plastic Water.

CONCLUSION: Using the ICRU recommendation of a 1% dosimetric match to ensure water equivalence, the results indicate that the Solid Water was found to provide acceptable dosimetric accuracy for relative dosimetry of the higher energy beams. The results indicate that any water equivalent material should be tested before use with kilovoltage x-ray beams.

REFERENCES:

[1]Klevenhagen S *et al*., *The IPEMB code of practice for the determination of absorbed dose for x-rays below 300 kV generating potential*, Phys. Med. Biol., 41(12): 2605-2625, 1996.

[2]IAEA Technical Report Series No. 398, *Absorbed Dose Determination in External Beam Radiotherapy, An International Code of Practice for Dosimetry Based on Standards of Absorbed Dose to Water*, International Atomic Energy Agency, Vienna, 2000.

[3]ICRU Report 44, *Tissue Substitutes in Radiation Dosimetry and Measurement*, ICRU, Bethesda, MD, 1989.

COMPARISON OF DOSIMETRIC METHODS FOR VIRTUAL WEDGE ANALYSIS

M. Bailey, V. Nelson, O. Collins, M. West, L. Holloway, S. Rajapaske, J. Arts, J.Varas, G. Cho and R. Hill

Department of Medical Physics, Macarthur & Liverpool Cancer Therapy Centres, South Western Sydney Cancer Services, Campbelltown, NSW, Australia

INTRODUCTION: The Siemens Virtual Wedge (Concord, USA) creates wedged beam profile by moving a single collimator jaw across the specified field size whilst varying the dose rate and jaw speed for use in the delivery of radiotherapy treatments. The measurement of the dosimetric characteristics of the Siemens Virtual Wedge poses significant challenges to medical physicists[1-4]. This study investigates several different methods for measuring and analysing the virtual wedge for data collection for treatment planning systems and ongoing quality assurance.

METHODS: The beam profiles of the Virtual Wedge (VW) were compared using several different dosimetric methods. Open field profiles were measured with Kodak X-Omat V (Rochester, NY, USA) radiographic film and compared with measurements made using the Sun Nuclear Profiler with a Motorized Drive Assembly (MDA) (Melbourne, FL, USA) and the Scanditronix Wellhofer CC13 ionisation chamber and 24 ion Chamber Array (CA24) (Schwarzenbruck, Germany). The resolution of each dosimetric method for open field profiles was determined. The Virtual Wedge profiles were measured with radiographic film the Profiler and the Scanditronix Wellhofer CA 24 ion Chamber Array at 5 different depths. The ease of setup, time taken, analysis and accuracy of measurement were all evaluated to determine the method that would be both appropriate and practical for routine quality assurance of the Virtual Wedge.

RESULTS: The open field profiles agreed within ±2% or 2mm for all dosimetric methods. The accuracy of the Profiler and CA24 are limited to half of the step size selected for each of these detectors. For the VW measurements a step size of 2mm was selected for the Profiler and the CA24. The VW profiles for all dosimetric methods agreed within ±2% or 2mm for the main wedged section of the profile. The toe and heel ends of the wedges showed the significant discrepancies dependent upon the dosimetry method used, up to 7% for the toe end with the CA24.

DISCUSSION & CONCLUSIONS: The dosimetry of the Virtual Wedge is difficult even with the range of dosimetric methods available. Film dosimetry has the highest available resolution but require the development of film and analysis. The CA24 requires a water phantom setup, which is time consuming, and the accuracy (step size) and time are inversely proportional. The Profiler is much more simple to setup and provides a real time analysis that can prove useful for tuning beam characteristics.

REFERENCES:

[1]Walker, C. P., Richmond, N. D. and Lambert, G. D., *Optimal clinical implementation of the Siemens virtual wedge*. Med. Dosim., 28(3): 149-54, 2003.

[2]Zhu, X. R., et al., *Dependence of virtual wedge factor on dose calibration and monitor units*. Med. Phys., 28(2): 174-177, 2001.
[3]Zhu, X. R. et al., Comparison of dosimetric characteristics of Siemens virtual and physical wedges. Med. Phys., 27(10): 2267-2277, 2000.
[4]van Santvoort, J., *Dosimetric evaluation of the Siemens Virtual Wedge*. Phys. Med. Biol., 43(9): 2651-2663, 1998.

A NOVEL SYSTEM FOR THE PRODUCTION OF IMMOBILISATION FACE MASKS FOR RADIOTHERAPY

T. Deans[1] and B. McKernan[2]

[1]*Department of Medical Technology & Physics, Sir Charles Gairdner Hospital, Perth, WA, Australia*
[2]*Department of Radiation Oncology, Sir Charles Gairdner Hospital, Perth, WA, Australia*

INTRODUCTION: Patient immobilisation is critically important for the radiation treatment of Head and Neck cancers. Immobilisation masks can be made from either thermoplastics or vacuumed polycarbonate taken from a plaster "positive" mould. To create the positive mould, our Radiation Oncology Department has traditionally used Plaster of Paris impressions. This process is time consuming, messy and stressful for the patient. This presentation describes an alternative method for the creation of the positive mould which was developed at this hospital, which is much quicker than previous methods and which obviates all stress to the patient.
METHODS: The patient's face is scanned in the Department of Radiation Oncology using one of a new generation of lightweight, hand-held, laser surface scanners. This process takes a few seconds. The digital information captured by the scanner characterising the patient's face is then emailed to the Department of Medical Technology & Physics (MTP), where a software package is used to manipulate the information into a form suitable for use as input to a Computerised Numerical Control Vertical Machining Centre (CNC-VMC). The CNC-VMC then automatically mills a mould of the patient's face from a block of machineable Plaster of Paris. Two mechanical technicians have undergone specialised training in the manipulation of the data supplied by the scanner into the CNC-VMC format.
RESULTS AND DISCUSSION: Proof of principle of this method was established nearly four years ago, with the first patient face mould being produced in February 2004. Since that time more than 100 moulds for face masks have been produced. Typically moulds are delivered to Radiation Oncology within ninety minutes of an email containing patient face data being received in MTP. Approximately half of this time is used for the manipulation of the data provided, while the remaining time is used for the actual automated milling of the mould. This compares with an average time of in excess of 40 hours for producing such a mould by the previous method, during which time it was possible for the shape of the patient's face to alter significantly. The savings in labour costs when using this method compared with the old method are also a significant consideration in its implementation. We have been producing 5 masks per week on average for the past 6 months, and have the capacity to produce up to four masks in any one day. This method of producing radiotherapy immobilisation face masks has not been used previously to our knowledge.
CONCLUSION: A novel method for the production of radiotherapy face immobilisation masks has been developed which is accurate, much faster than previous methods, and which is less stressful to patients. This technology can be used in any hospital that has access to an appropriate laser scanner and Numerical Milling facilities.

COMPARISON OF EYE SHIELDS IN RADIOTHERAPEUTIC BEAMS

B. E. Currie[1,2] and A. D. Johnson[2]

[1]*Department of Physics and Astronomy, University of Canterbury, Christchurch, New Zealand*
[2]*Wellington Cancer Centre, Wellington Hospital, Wellington, New Zealand*

INTRODUCTION: Both MeV electrons and kV photons are used in the treatment of superficial cancers. The advantages and disadvantages for each of these modalities have been widely reported in the literature (See for example [1-2]). Of particular note in the literature is the use of lead and tungsten eye shields to protect ocular structures during radiotherapy. An investigation addressing issues raised in the literature that are relevant to the Wellington Cancer Centre method of treatment of lesions near the eye shall be summarised. Various small sized fields were irradiated to determine depth dose and profile curves in a water phantom shielded by various commercially available eye shields. Transmission factors relevant to critical ocular structures and particle distribution theories are used to further elucidate the comparison between the use of MeV electrons and kV photons in the treatment of superficial cancers.
MATERIALS: Superficial X-rays from a Pantak Therapax unit SXT 150 model of HVL 4.90mm Al were used for the lead eye shield measurements and electrons from a Varian Clinac 2100C nominal energies 6MeV and 9MeV (R_p 3.00cm and 4.34cm respectively) were used for the tungsten eye shield measurements. For the photon measurements circular applicators of 3cm, 4cm and 5cm diameter were used and for the electrons standard 6×6cm and 10×10cm applicators were used, with no custom inserts. A Scanditronix RFA-300 water phantom and Scanditronix RFAplus version 5.3 software application were

used to collect and collate all data. The eye shields were the Radiation Products Design Inc. medium lead eye shield (item # 934-014) and the MED-TEC tungsten eye shields MT-T-45 M and MT-T-45 S.

RESULTS: It is demonstrated that electron fields have appreciably greater scatter into the area directly under the eye shields than the photon fields. Similarly at the region of d_{max} for the electron fields the relative dose is appreciably greater than the photon fields at similar depth.

DISCUSSION & CONCLUSION: The relative merits for electron and photon treatments are discussed with respect to the investigations findings and reference to the literature. When comparing electrons and photons it is usually the definite range of electrons within tissue that recommends electron treatments. However, one should weigh this consideration against some of the salient features of a well-constructed superficial photon treatment, for example the effective blocking of kilovoltage photons by lead and the sharp edges of the kilovoltage photon fields.

ACKNOWLEDGEMENTS: The authors would like to acknowledge the support of the medical physics group at Wellington Cancer Centre.

REFERENCES:

[1]Shiu, A. S., Tung, S. S., Gastrof, R. J., Hogstrom, K. R., Morrison, W. H. and Peters, L. J., *Dosimetric evaluation of lead and tungsten eye shields in electron beam treatment*, Int. J. Radiation Oncology Biol. Phys., 35(3): 599 – 604, 1996.

[2]Amdur, R. J., Kalbaugh, K. J., Ewald, L. M., Parsons, J. T., Mendenhall, W. M., Bova, F. J. and Million, R. R., *Radiation therapy for skin cancers near the eye: kilovoltage x-rays versus electrons*, Int. J. Radiation Oncology Biol. Phys., 23(4): 769 – 779, 1992.

MONTE CARLO MODELLING OF A VARIAN 21EX CLINAC 6 MEV ELECTRON BEAM WITH EGS4/BEAMNRC

J. Kenny[1,2,] M. Ebert[1,3] and B. Aldrich[1]

[1]*Newcastle Mater Hospital, Newcastle, NSW, Australia*
[2]*Queensland University of Technology, Brisbane, Qld, Australia*
[3]*University of Newcastle, Newcastle, NSW, Australia*

INTRODUCTION: The beam model created was primarily intended for use in a larger study investigating low kV imaging methods that utilise mega-voltage electron beams. However mega-voltage electron beams continue to fulfil a niche role in radiation therapy treatments and a flexible, well established Monte Carlo code is also a useful tool for evaluating new electron treatment techniques and clinical Monte Carlo treatment planning systems.

METHODS: The EGS4/BEAMnrc[1] User Code (BEAMnrc, BEAMDP and DOSxyz) was used to model a Varian 21EX Linear Accelerator 6 MeV electron beam. The code was run under the Red Hat Linux 9 Operating System on an HP XW6000 Workstation (3GHz Xeon CPU, 1GB RAM, 80GB Hard Drive). Analysis of the DOSxyz files was primarily done with purpose written MATLAB code. All major components of the linac treatment head were included in the model using manufacturer-supplied specifications. The simulation was initiated with a mono-energetic pencil beam of 15 million electrons incident on the primary collimator. This resulted in ~2.3 million particles (includes electrons, positrons and photons) at the isocentre plane. Dose distribution was simulated in DOSxyz by constructing a water phantom and recycling the particle information 14 times so that effectively 30 million particles were incident on the phantom surface. The simulated dose distributions in DOSxyz were compared to data measured with a Wellhoffer CC13 ion chamber and water tank scan system during linac commissioning. The energy spectrum of the electrons and photons at the isocentre plane and their spatial distribution, derived from the BEAMDP program, were also used as tools to ascertain the accuracy of the model. This was an iterative procedure repeated multiple times, making small model adjustments to increase the accuracy of the match.

RESULTS: Simulations of the linac head were completed in less then 24hrs, with the applicator simulated separately in a further 1hr. The simulated dose profiles matched measured data to within 5% in most cases, the exceptions being on the depth dose curve from surface to 0.5cm deep and also at 3cm deep, which was around Rp. Initial simulations used a simple applicator design incorporating only the central cut-out region. This proved unsatisfactory, as sufficient electrons were able to escape the applicator, but still be scored at the isocentre plane, evident as an increased penumbra of several centimetres and increased surface dose. The applicator was re-modelled using a closer approximation of the actual measured geometry that included the tapered scrapers. Also observed in the initial simulations was a double peak in the high end of the electron energy spectrum, when the beam emerged from the lower scattering foil. This was probably due to scattered electrons from the upper foil that missed the lower foil but were scattered back into the main beam below it. This is supported by the fact that surrounding the lower scattering foil with lead of thickness equal to that of the foil removed the double peak. The inclusion of shielding in this region is typically not considered necessary for the purposes of Monte Carlo modelling

DISCUSSION & CONCLUSIONS: A 6 MeV electron beam was successfully modelled using BEAM. The simulated dose distributions matched measurements to within 5%. Extensive modelling of the electron applicators was required to obtain a beam with correct spatial distribution. Additional shielding around the lower scattering foil needed to be included in the model in order to obtain a correct energy spectrum

REFERENCES:

[1]Rogers, D. W. O. et al, *BEAM: A Monte Carlo code to simulate radiotherapy treatment units.* Med. Phys., 22(5): 503-524, 1995.

COMMISSIONING OF THE MULITPLE SOURCE MODEL FOR MONTE CARLO SIMULATION

K. Chan

Prince of Wales Hospital, Randwick, NSW, Australia

INTRODUCTION: Measurement based treatment planning algorithms have problems under electron disequilibrium conditions (for example, in small field size and inhomogenity). The Convolution Method is considered a short cut for Monte Carlo Simulation (MCS) and it has solved some of the problems but not all. MCS is regarded as the most accurate treatment planning algorithm available. The traditional MCS uses a 2 steps approach for treatment planning. The first step is to obtain a Phase Space File which contains all the information of the particles above the phantom surface. The second step is to run MCS on a CT image by using the Phase Space File to get isodose distributions. A Phase Space File is derived from details of a Linear Accelerator's structure. The Fox Chase Cancer Centre in US has proposed a Multiple Source Model method to replace the Phase Space File. This method based on profiles and central depth dose measurement and hence do not require details of the head structure. This poster will show the results of the Multiple Source Model of the 6MV photon beam on our Siemens Primus Machine. This method will speed up the simulation process and retain the accuracy of 1%. Thus making it more practical for the use of Monte Carlo Simulation for treatment planning.
METHODS: The Linear Accelerator's head is modelled by placing different sources with different spectrum.

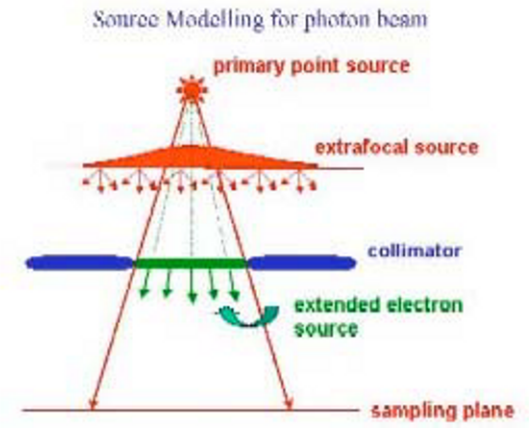

RESULTS: The MCS results are expected to be within 1% of the results of measurement. I have obtained central depth doses for field size 5 cm x 5 cm and 10 cm x 10 cm. The results are within 1% when compared with measurement. I will get more information for different field sizes and also do a comparison of a Monte Carlo Plan with a plan from the CMS Focus planning computer.
DISCUSSION & CONCLUSIONS: The source modelling method is a fast and accurate way for Monte Carlo Simulation and retains an acceptable accuracy.
ACKNOWLEDGEMENTS: Medical Physics Dept of Prince of Wales Hospital, Sydney.
REFERENCES:
[1]Ma, C. M. et al, *Clinical implementation of a Monte Carlo treatment planning system* Med. Phys, 26: 2133-2143, 1999.
[2]Rogers, D. W. O. et al, *A Monte Carlo code to simulate radiotherapy treatment units*. Med Phys, 22: 503-524, 1995.

VERIFICATION OF A TABLE OF PHANTOM SCATTER FACTORS FOR RADIOTHERAPY TREATMENT PLANNING

J. K. Arts, M. J. Bailey and R. Hill

Department of Medical Physics, Macarthur & Liverpool Cancer Therapy Centres, South Western Sydney Cancer Services, Campbelltown, NSW, Australia

INTRODUCTION: Many commercially available treatment planning systems require the medical physicist to measure and enter significant quantities of data for the verification of physics based algorithms. The CMS XiO (St. Louis, USA) treatment planning system requires a table of phantom scatter factors amongst other data. In a previous paper by Storchi et al[1], a table of phantom scatter factors is described. This table gives the phantom scatter factor as a function of field size and quality index determined from a collection of measured data for the total scatter factor and the collimator scatter factor from 25 different beam qualities ranging from 4MV up to 25MV. These factors have been determined at a fixed reference depth of 10cm for square fields of various sizes. This work investigates the claim that this table can be used as an alternative to calculated phantom scatter curve from measured data of a particular treatment unit.

METHODS: According to definition, it is difficult to directly measure the phantom scatter correction factor (Sp). This problem can be solved using the relation;

$$S_{c,p}(A) = S_c(A)S_p(A) \qquad (1)$$

where $S_{c,p}(A)$ is the measured total scatter factor for a field size of square side dimension, A and $S_c(A)$ is the measured collimator scatter factor for a field size of square side dimension, A (Khan et al 1980, van Gasteren et al 1991). The total scatter correction factor (Sc,p) was measured in a full phantom, and the collimator scatter factor (Sc) measured using an ESTRO mini-phantom. These factors were measured on three Siemens linear accelerators (Concord, USA) with energies 6MV and 18MV and square field sizes ranging from 4x4cm to 40x40cm. The Primus and KD Mevatron produced 6 and 18MV X-rays and the MXE Mevatron produced 6Mv X-rays only. The values for Sp were calculated by rearranging equation (1). Phantom scatter factors were calculated from the data provided by Storchi *et al* using the quality index of each beam. For comparison, a set of Sp values was referenced from the XiO training guide manual[2].

RESULTS:. Comparison of the phantom scatter factors results show agreement within ± 1.2% for the Primus machine for both 6MV and 18MV X-rays. For the KD Mevatron linear accelerator, the 18MV data matched within 1.3% except at the 4x4cm field size. For the 6MV X-rays, the match was and within ± 2.5% for the KD and MX machines at the largest field sizes.

CONCLUSION: The results of these comparisons indicate that the table of phantom scatter factors as described by Storchi *et al* is a useful QA tool for checking of beam data. These results suggest that it would not be recommended to rely upon the published data alone when calculating phantom scatter factors for treatment planning in radiotherapy.

REFERENCES:

[1]Storchi, P., and van Gasteren, J.J.M. *A table of phantom scatter factors of photon beams as a function of the quality index and field size*. Phys. Med. Biol. 41: 563-571, 1996.

[2]*CMS Xio Training Guide*, CMS Inc, St. Louis, MI, USA, 2004.

MATCHING BEAMS ON PHOTON/ELECTRON LINEAR ACCELERATORS

L. Oliver[1], P. Vial[1] and P. Hunt[1]

[1]*Radiation Oncology, Royal North Shore Hospital, St Leonards, NSW, Australia*

INTRODUCTION: There are a number of obvious reasons to match megavoltage X-ray and electron beams for clinical purposes. If two dual-purpose X-ray/electron linear accelerators are of the same design and manufacturer, then this might be possible. The issue is however whether the beams can be matched sufficiently close to be considered the same for patient treatments and planning data for dose calculation purposes. If successfully achieved, there are significant advantages in reduced commissioning time, less work in planning and flexibility in the treatment of patients between the two treatment machines. We have investigated matching a new Varian Clinac 21EX with our 1993 Varian Clinac 2100 C/D. A Varian Clinac 1800 was the first linear accelerator installed at RNSH in 1987. When the Clinac 2100 C/D was installed in 1993, we attempted to match all the X-ray and electron beams with the original Clinac 1800 physical data. The X-ray beam characteristics were satisfactory but the electron beams were not sufficiently compatible for planning or patient treatment purposes. A different designed scattering foil and electron applicator were the cause of the different electron beam physical characteristics between the two models.

METHODS: In replacing the Clinac 1800 with the Clinac 21EX, we have used the original 1993 data of the Clinac 2100 C/D as the gold standard to aim for. Initial measurements during acceptance tests showed that all beams satisfied the manufacturer's specification. The energy was then matched to the existing clinical physics data by adjusting the bending magnet power supply and re-tuning the accelerator. This involved matching % depth dose and the corresponding ratio of 10 and 20 cm % depth dose ratio for 6MV and 18 MV X-ray beams. For 6, 9, 12, 16 and 20 MeV electron beams the normal physical parameters of depth of maximum (R_{max}), the practical range (R_p), the depth of 50% (R_{50}), the slope (G), the average energy at the surface (E_0) and the % photon contamination (Dx) were matched as near as possible with an emphasis on R_p and G.

RESULTS: As was the case for the 1993 work, a spot check of the 6 and 18 MV X-ray beam planning data (e.g. % depth dose, tissue-maximum-ratios, collimator factors, area factors, wedge factors, enhanced dynamic wedge data and transmission factors) was found to be the same to within 1%. The new Millennium 120 multileaf collimator required additional physics measurements for IMRT purposes. A comparative study of the Clinac 21 EX electron beams indicated a very high degree of coincidence between the two linear accelerators. The % depth dose agreed at maximum, to within 1.5% in all energies except 6MeV (+4%) between the surface and maximum but tended to be more in the order of +5% at the falling 'tail end'. Applicator factors averaged the same to within ±1% and the dose measured across a distance range of 97 to 115 cm ranged from –1% at the short distance to a maximum dose error of +1.9% at 16 – 20 MeV for the longest extended distance.

DISCUSSION & CONCLUSIONS: We believe the data matches sufficiently to use the 1993 data for the 2004 new linear accelerator. Physics data for the computer treatment planning system and manual dose calculations are now essentially common for these two machines and patients may be transferred without correction during any downtime. We are

monitoring any practical differences that may arise from the use of the newer accessories, particularly the Millennium MLC. Investment in time to match the beams significantly shortens the commissioning and clinical measurement period to be around one month on top of one month installation and acceptance period. As well as departmental data compatibility, this method enables the same data to be established on other linear accelerators at rural sites or even at other hospitals. The transfer or remote monitoring of patient treatments between centres would therefore be a very real possibility.

ACKNOWLEDGEMENTS: We are grateful for the assistance of Mr W. Morrison, Varian Medical Systems Australasia for his part in tuning the required linear accelerator beam parameters.

DOSE AND DOSE RATE MEASUREMENTS USING ELECTRONIC PORTAL IMAGING DEVICES (EPIDS)

M. Mohammadi[1,2,3] and E. Bezak[1,2]

[1]*School of Chemistry and Physics, the University of Adelaide, Adelaide, SA, Australia*
[2]*Dept. of Medical Physics, Royal Adelaide Hospital, Adelaide, SA, Australia*
[3]*Dept of Medical Physics, Faculty of Medicine, Hamadan University of Medical Sciences, Hamadan, Iran*

INTRODUCTION: Electronic Portal Imaging Devices (EPIDs) have an outstanding position for treatment verification in Radiation Therapy. The produced Electronic Portal Images (EPIs) can be used for verification of patient position, dose as well as for linac quality assurance[1,2]. The pixel values of EPID can be converted to the dose rate and dose values when calibrated with measured ionization chamber data. As result, one can verify the transmitted dose rate and dose distribution at the EPID layer[3]. The assessment of uniformity and reproducibility of EPIs during image acquisition for dosimetric purposes was performed in this study. Moreover the relationship between acquired pixel values, dose and dose rate was identified for various linac output repetition modes.

METHODS: Varian 600CD linac, producing 6 MV X-ray beams, equipped with SLIC-EPID was used in the measurements. In order to perform the measurements with the EPID layer in electronic equilibrium region, 1 to 30 mm of RW3 material was placed on the EPID, images acquired and dependence of pixel values on build-up thickness was assessed. The reproducibility (short-term and long-term) was evaluated using 7 series (collected over 2 weeks) of 10 consecutively acquired images using 300 MU/min dose rate at SSD=140 cm and field size of 24×24 cm^2. The variation of pixel values was then investigated in 9 areas within irradiated field using MATLAB software to evaluate the reproducibility of mean pixel values and image uniformity. The radiation dose rate incident on the EPID surface was varied by moving the EPID to various distances from 10 to 60 cm below the isocentre with a 5 mm RW3 placed on top of the EPID using 10×10 cm^2 field size. The relationship between dose rate and acquired EPID pixel values was assessed. Using EPID acquisition time, the relationship between dose and EPID pixel values was evaluated. The obtained data were then compared with dose values measured by calibrated ionization chamber. The average acquired pixel values were plotted against the dose and dose rate values and a fitted with functions to define the dependence.

RESULTS: A 5 mm of RW3 placed on top of the EPID surface increases the pixel values to the maximum, reaching thus the electronic equilibrium. There was no significant variation between maximum build-up layer for the central axis and other peripheral areas. The average uniformity factor in 70 acquired images was 2.59%. The maximum variation of pixel values in the 10 consecutive images and in all 70 acquired images were 0.68% and 1.28% respectively. The maximum standard deviation and the average relative error was 0.295 and 0.59% respectively. The relationship between dose, dose rate and EPIs pixel values for various repetition modes was quantified. Introducing an equation, the calculated dose values were then compared with measured dose values using ion chamber. The percentage of average relative error was within 0.56%.

DISCUSSION & CONCLUSIONS: EPIDs can be used for dosimetric purposes without daily calibration (fortnightly calibration is sufficient) using an appropriate extra-build-up layer. EPID can also be used to calculate the transmitted dose through the patient with an acceptable accuracy.

REFERENCES:

[1]Boellard, R., van Herk, M. and Mijnheer, B., *The dose response relationship of a liquid-filled electronic portal imaging device*, Med. Phys. 23(9): 1601-1611, 1996.

[2]Essers, M., Boellard, R., van Herk, M., Lanson, H., and Mijnheer, B., *Transmission dosimetry with a liquid-filled electronic portal imaging device,* Int. J. Radiat. Oncol. Biol. Phys., 34: 931-941, 1996.

[3]Chang, J., Mageras, G., Chui C., Ling C. and Lutz W., *Relative profile and dose verification of intensity-modulated radiation therapy*." Int. J. Radiat. Oncol. Biol. Phys. 47(1): 231-240, 2000.

THE COMPARISON OF RADIATION FIELD CHARACTERISTICS OBTAINED BY ELECTRONIC PORTAL IMAGING DEVICES (EPIDS), FILM AND ION CHAMBER

M. Mohammadi[1,2,3] and E. Bezak[1,2]

[1]*School of Chemistry and Physics, the University of Adelaide, Adelaide, SA, Australia*
[2]*Dept. of Medical Physics, Royal Adelaide Hospital, Adelaide, SA, Australia*
[3]*Dept. of Medical Physics, Faculty of Medicine, Hamadan University of Medical Sciences, Hamadan, Iran*

INTRODUCTION: Electronic Portal Imaging Devices (EPIDs) can be used for verification of two-dimensional (2D) dose distribution provided that they are calibrated[1-2]. To perform the calibration in 2D can be quite consuming when using ion chamber scanning. This study therefore concentrates on using the Kodak EDR2 film for this purpose, as its response is close to that of ion chamber measurements[3]. The comparison of transmitted fluence maps obtained by EPID and films was performed to calibrate EPID for dosimetric purposes. In addition, ionization chamber was used to measure inplane and crossplane profiles for the same experimental setup and to compare with film and EPID data.

METHODS: After labelling, the films were irradiated in the same experimental conditions as for EPID image acquisition. The irradiated films were processed and scanned with using Agfa Curis 160 processor and Vidar scanner respectively. The measurements were performed using a 6 MV photon beam (Varian 600CD linac) for 20×20 cm^2 and 15×15 cm^2 nominal field sizes at the 10, 30 and 60 cm below the isocentre. Both EPID images and films were analysed using MATLAB software (Mathworks Inc.) to identify the Region Of Interest (ROI) and compare corresponding pixel values. After normalization to the central axis pixel value, a correction (calibration) matrix was then defined to relate EPID pixel values to corresponding film pixel values. To verify the use of EDR2 for EPID calibration, the crossplane and inplane profiles were also measured with ion chamber in water at the isocentre as well as at 10 and 30 cm below the isocentre. The achieved data were then compared with film and EPID profiles.

RESULTS: The differences observed within the 2D fluence map, inplanes and crossplanes for EPID and film were between 0-3.5%. With the increasing field size, an increase in difference was observed between the compared data. There were no significant differences between corresponding inplane and crossplane profiles measured with film and ion chamber.

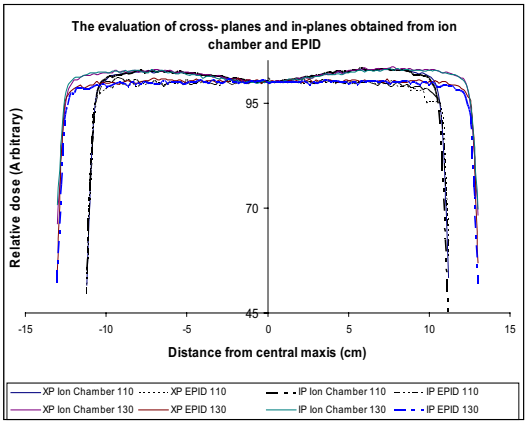

Figure 1. *In planes and Cross planes of Ion chamber and EPID.*

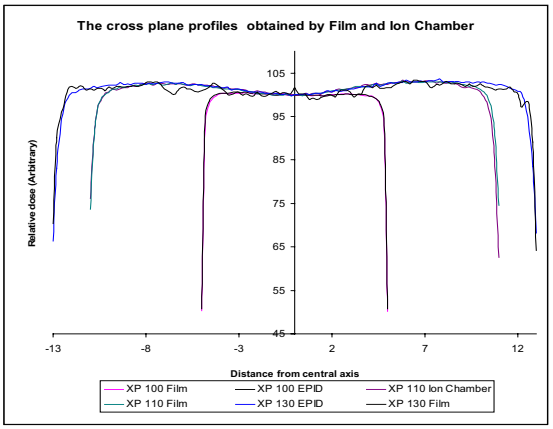

Figure 2. *Inplanes and cross planes of Ion chamber and film.*

DISCUSSION & CONCLUSIONS: For two-dimensional dosimetric purposes, EPID must be calibrated with appropriate correction factors. These can be obtained reliably using Kodak EDR2 film.

REFERENCES:

[1]Boellard, R., van Herk, M. and Mijnheer, B., *The dose response relationship of a liquid-filled electronic portal imaging device*, Med. Phys. 23(9): 1601-1611, 1996.

[2]Parsaei, H., el-Khatib, E., Rajapakshe, E. R., *The use of an electronic portal imaging system to measure portal dose and portal dose profiles.*" Med. Phys. 25(10): 1903-1909, 1998.

[3]Dogan, N., Leybovich, L. and Sethi, A., *Comparative evaluation of Kodak EDR2 and XV2 films for verification of intensity modulated radiation therapy*, Phys. Med. Biol., 47(22): 4121- 4130, 2002.

RADIOGRAPHIC FILM DOSIMETRY : POLARIZATION EFFECTS

M.J. Butson[1,2], T. Cheung[1] and P.K.N. Yu[1]

[1]*City University of Hong Kong Dept. of Physics and Materials Science Kowloon Tong, Hong Kong*
[2]*Dept. of Medical Physics, Cancer Services, Crown St, Wollongong, NSW, Australia*

Kodak X-omat V radiographic film has been tested for its polarization properties when using polarized and non-polarized light sources and detectors. The radiographic film has been shown to produce a relatively small but not negligible (less than 5%) variation in 90° cycles in measured optical density within the visible spectrum when the light source is fully linear polarized and the film is rotated through 360º angle. Negligible variations are seen when the detector is linearly polarized. If both light source and detector is linearly polarized variations in measured optical density can reach 35% when the film is rotated through 360º angle. This seems to be due to variations in the degree and axis of rotation in polarized light caused by the radiographic film and is independent of exposure level as the intensity of variation in absolute optical density is relatively

the same for all film exposures. We recommend that a polarization test be performed on a densitometry system to establish the extent of its polarization properties before accurate dosimetry is performed with radiographic film.
ACKNOWLEDGEMENTS: This work has been fully supported by a grant from the Research Grants Council of HKSAR, China (Project No. City U 100603).

ASSESSMENT OF LOW ABSORBED DOSE WITH A MOSFET DETECTOR

M. J. Butson[1,2], T. Cheung[1] and P. K. N. Yu[1]

[1]*City University of Hong Kong, Dept. of Physics and Materials Science, Kowloon Tong, Hong Kong*
[2]*Department of Medical Physics, Cancer Services, Crown St, Wollongong, NSW, Australia*

The ability of a MOSFET dosimetry system to measure low therapeutic doses has been evaluated for accuracy for high energy x-ray radiotherapy applications. The MOSFET system in high sensitivity mode produces a dose measurement reproducibility of within 10%, 4% and 2.5% for 2 cGy, 5 cGy and 10cGy dose assessment respectively. This is compared to 7%, 4% and 2% for an Attix parallel plate ionisation chamber and 20%, 7% and 3.5% for a Wellhofer IC4 small volume ionisation chamber. Results for our dose standard thimble ionisation chamber and low noise farmer dosemeter were 2%, 0.5% and 0.25% respectively for these measurements. The quoted accuracy of the MOSFET dosimetry system is partially due to the slight non linear dose response (reduced response) with age of the detector but mainly due to the intrinsic variations in measured voltage differential per applied dose. Results have shown that the MOSFET dosimetry system provides an adequate measure of dose at low dose levels and is comparable in accuracy to the Attix parallel plate ionisation chambers for relative dose assessment at levels of 2cGy to 10cGy. The use of the MOSFET dosimeter at low doses can extend the life expectancy of the device and may provide useful information for areas where low dose assessment is required.
ACKNOWLEDGEMENTS: This work has been fully supported by a grant from the Research Grants Council of HKSAR, China (Project No. CityU 100603).

RADIOCHROMIC FILM AND POLARIZATION EFFECTS

P. K. N. Yu[1], T. Cheung[1], M. J. Butson[1,2] and D. Inwood[2]

[1]*City University of Hong Kong , Dept. of Physics and Materials Science, Kowloon Tong, Hong Kong*
[2]*Dept. of Medical Physics, Cancer Services, Crown St, Wollongong, NSW, Australia*

A new high sensitivity radiochromic film has been tested for its polarization properties. Gafchromic HS film has been shown to produce a relatively small (less than 3%) variation in measured optical density measured at 660nm wavelength when the light source is fully linear polarized and the film is rotated through 360º angle. Similar variations are seen when the detector is linearly polarized. If both light source and detector is linearly polarised variations in measured optical density can reach 15% when the film is rotated through 360º angle. This seems to be due to a phase shift in polarised light caused by the radiochromic film resulting in the polarised light source becoming out of phase with the polarised detector. Gafchromic HS radiochromic film produces a minimal polarization response with varying angle of rotation however we recommend that a polarization test be performed on a densitometry system to establish the extent of its polarization properties before accuracy dosimetry is performed with radiochromic HS film.
ACKNOWLEDGEMENTS: This work has been fully supported by a grant from the Research Grants Council of HKSAR, China (Project No. CityU 100603).

MOSFET DOSIMETRY: TEMPERATURE EFFECTS IN-VIVO

P. K. N. Yu[1], T. Cheung[1] and M. J. Butson[1,2]

[1]*City University of Hong Kong, Dept. of Physics and Materials Science , Kowloon Tong, Hong Kong*
[2]*Dept. of Medical Physics, Cancer Services, Crown St, Wollongong, NSW, Australia*

This note investigates temperature effects on dosimetry using a Metal Oxide Semiconductor Field Effect Transistor (MOSFET) for radiotherapy x-ray treatment. This was performed by analysing the dose response and threshold voltage outputs for MOSFET dosimeters as a function of ambient temperature. Results have shown the clinical semiconductor dosimetry system (CSDS) MOSFET provides stable dose measurements with temperatures varying from 15°C up to 40°C. Thus standard irradiations performed at room temperature can be directly compared to *in-vivo* dose assessments performed at near body temperature without a temperature correction function. The MOSFET dosimeter threshold voltage varies with temperature and this level is dependant on the dose history of the MOSFET dosimeter. However the variation can be

accounted for in the measurement method. For accurate dosimetry the detector should be placed for approximately 60 seconds on a patient to allow thermal equilibrium before measurements are taken with the final reading performed whilst still attached to the patient or conversely left for approximately 120 seconds after removal from the patient if initial readout was measured at room temperature to allow temperature equilibrium to be established.
ACKNOWLEDGEMENTS: This work has been fully supported by a grant from the Research Grants Council of HKSAR, China (Project No. CityU 100603).

RADIOCHROMIC FILM MEASUREMENTS OF ROUNDED END MULTI LEAF PENUMBRA

T. Cheung[1], M. J. Butson[1,2] and P. K. N. Yu[1]

[1]*City University of Hong Kong , Dept. of Physics and Materials Science, Kowloon Tong, Hong Kong*
[2]*Department of Medical Physics, Cancer Services, Crown St, Wollongong, NSW, Australia*

Multi-leaf penumbral doses have been investigated for 6MV x-rays and a Varian millennium Multi Leaf Collimator (MLC) using Gafchromic MD-55-2, radiochromic film and X-omat V radiographic film. An advantage of Gafchromic film for multi-leaf penumbral dose measurement is the relatively low energy dependence of the film. A comparison of penumbral dose measurements has also ascertained the effects of energy response on radiographic film in this region. Similar 80%/20% penumbral doses have been measured with both types of films. Thus there is a relatively low energy effect on penumbral dose measurements in film dosimetry. The 80% / 20% dose penumbral distances for rounded leaf end multi-leafs for a 10cm x 10cm field at D_{max} was found to be 4.6mm and 4.3mm for radiochromic and radiographic film accordingly. This is compared to 2.6mm and 2.6mm for the leaf edge penumbra. Radiochromic film also measured leaf end/interleaf leakage doses in the penumbral region, which was showed to produce an approximate 4% of maximum dose wave across the penumbral region with maximum doses delivered at the MLC leaf interfaces.
ACKNOWLEDGEMENTS: This work has been fully supported by a grant from the Research Grants Council of HKSAR, China (Project No. CityU 100603).

SUPERFICIAL X-RAY IN-VIVO DOSIMETRY WITH MOSFET DETECTORS

T. Cheung[1], P. K. N. Yu[1] and M. J. Butson[1,2]

[1]*City University of Hong Kong, Dept. of Physics and Materials Science , Kowloon Tong, Hong Kong*
[2]*Dept. of Medical Physics, Cancer Services, Crown St, Wollongong, NSW, Australia*

This note investigates in-vivo dosimetry using a Metal Oxide Semiconductor Field Effect Transistor (MOSFET) for radiotherapy treatment at superficial and orthovoltage x-ray energies. This was performed within one fraction of the patient's treatment. Standard measurements along with energy response of the detector are given. Results showed that the MOSFET measurements in-vivo agreed with calculated results on average within ± 5.6% over all superficial and orthovoltage energies. These variations were slightly larger than TLD results with variations between measured and calculated results being ± 5.0% for the same patient measurements. The MOSFET device provides adequate in-vivo dosimetry for superficial and orthovoltage energy treatments with the accuracy of the measurements seeming to be relatively on par with TLD in our case. The MOSFET does have the advantage of returning a relatively immediate dosimetric result after irradiation.
ACKNOWLEDGEMENTS: This work has been fully supported by a grant from the Research Grants Council of HKSAR, China (Project No. CityU 100603).

SSD EFFECTS ON HIGH ENERGY X-RAY SURFACE AND BUILD UP DOSE

T. Cheung[1], M. J. Butson[1,2] and P. K. N. Yu[1]

[1]*City University of Hong Kong, Dept. of Physics and Materials Science , Kowloon Tong, Hong Kong*
[2]*Dept. of Medical Physics, Cancer Services, Crown St, Wollongong, NSW, Australia*

Dose in the build up region for high energy x-rays produced by a medical linear accelerator is affected by the x-ray source to patient surface distance (SSD). The use of isocentric treatments whereby the tumour is positions 100cm from the source means that depending of the depth of the tumour and the size of the patient, the SSD can vary from distances of 80cm to 100cm. To achieve larger field sizes, the SSD can also be extended out to 120cm at times. Results have shown that open fields are not significantly affected by SSD changes with deviations in percentage dose being less than 4% of maximum dose for SSD's from 80cm to 120cm SSD. With the introduction of beam modifying devices such as Perspex blocking trays, the effects are significant with a deviation of up to 22% measured at 6MV energy with a 6mm Perspex tray for SSD's from

80cm to 120cm. These variations are largest at the skin surface and reduce with depth. The use of a multi leaf collimator for blocking removes extra skin dose caused by the Perspex block trays with decreasing SSD.
Acknowledgements: This work has been fully supported by a grant from the Research Grants Council of HKSAR, China (Project No. CityU 100603).

SKIN DOSE VARIATION: INFLUENCE OF ENERGY

T. Cheung [1], P. K. N. Yu[1] and M. J. Butson[1,2]

[1]*City University of Hong Kong, Dept. of Physics and Materials Science , Kowloon Tong, Hong Kong*
[2]*Dept. of Medical Physics, Cancer Services, Crown St, Wollongong, NSW, Australia*

This research aimed to quantitatively evaluate the differences in percentage dose of maximum for 6MV and 18MV x-ray beams within the first 1cm of interactions. Thus provide quantitative information regarding the basal, dermal and subcutaneous dose differences achievable with these two types of high-energy x-ray beams. Percentage dose of maximum build up curves are measured for most clinical field sizes using 6MV and 18MV x-ray beams. Calculations are performed to produce quantitative results highlighting the percentage dose of maximum differences delivered to various depths within the skin and subcutaneous tissue region by these two beams. Results have shown that basal cell layer doses are not significantly different for 6MV and 18Mv x-ray beams. At depths beyond the surface and basal cell layer there is a measurable and significant difference in delivered dose. This variation increases to 20% of maximum and 22% of maximum at 1mm and 1cm depths respectively. The percentage variations are larger for smaller field sizes where the photon in phantom component of the delivered dose is the most significant contributor to dose. By producing graphs or tables of % dose differences in the build up region we can provide quantitative information to the oncologist for consideration (if skin and subcutaneous tissue doses are of importance) during the beam energy selection process for treatment.
ACKNOWLEDGEMENTS: This work has been fully supported by a grant from the Research Grants Council of HKSAR, China (Project No. CityU 100603).

RADIOGRAPHIC FILM: SURFACE DOSE EXTRAPOLATION TECHNIQUES

T. Cheung[1], M. J. Butson[1,2], P. K. N. Yu[1] and M. Currie[2]

[1]*City University of Hong Kong, Dept. of Physics and Materials Science , Kowloon Tong, Hong Kong*
[2]*Dept. of Medical Physics, Cancer Services, Crown St, Wollongong, NSW, Australia*

Assessment of surface dose delivered from radiotherapy x-ray beams for optimal results should be performed both inside and outside the prescribed treatment fields. An extrapolation technique can be used with radiographic film to perform surface dose assessment for open field high energy x-ray beams. This can produce an accurate 2 dimensional map of surface dose if required. Results have shown that surface % dose can be estimated within ±3% of parallel plate ionisation chamber results with radiographic film using a series of film layers to produce an extrapolated result. Extrapolated percentage dose assessment for 10cm, 20cmand 30cm square fields was estimated to be 15% ± 2%, 29% ± 3% and 38% ± 3% at the central axis and relatively uniform across the treatment field. Corresponding parallel plate ionisation chamber measurement are 16%, 27% and 37% respectively. Surface doses are also measured outside the treatment field which are mainly due to scattered electron contamination. To achieve this result, film calibration curves must be irradiated to similar x-ray field sizes as the experimental film to minimize quantitative variations in film optical density caused by varying x-ray spectrum with field size.
ACKNOWLEDGEMENTS: This work has been fully supported by a grant from the Research Grants Council of HKSAR, China (Project No. CityU 100603).

RADIOTHERAPY HIGH ENERGY SURFACE DOSE MEASUREMENTS: EFFECTS OF CHAMBER POLARITY

T. Cheung[1], M. J. Butson[1,2] and P. K. N. Yu[1]

[1]*City University of Hong Kong, Dept. of Physics and Materials Science , Kowloon Tong, Hong Kong*
[2]*Dept. of Medical Physics, Cancer Services, Crown St, Wollongong, NSW, Australia*

The effects of chamber polarity have been investigated for the measurement of 6MV and 18MV x-ray surface dose using a parallel plate ionization chamber. Results have shown that a significant difference in measured ionization is recorded between to polarities at 6MV and 18MV at the phantom surface. A polarity ratio ranging from 1.062 to 1.005 is seen for 6MV x-rays at the phantom surface for field sizes 5cm x 5cm to 40cm x 40cm when comparing positive to negative polarity. These ratios range from 1.024 to 1.004 for 18MV x-rays with the same field sizes. When these charge reading are compared

to the D_{max} readings of the same polarity it is found that these polarity effects are minimal for the calculation of percentage dose results with variations being less than 1% of maximum.

ACKNOWLEDGEMENTS: This work has been fully supported by a grant from the Research Grants Council of HKSAR, China (Project No. CityU 100603).

PRODUCTIVITY IMPROVEMENTS SINCE THE ADVENT OF ISO9001:2000

A. Thomas, R. Price and J. DeRoach

Department of Medical Technology & Physics, Sir Charles Gairdner Hospital, Perth, WA, Australia

INTRODUCTION: The subject of this abstract is the demonstration of the benefits to our department and its customers that have been achieved by following the processes and methods prescribed in AS/NZS 9001:2000. With a staff of 45 people, the Department of Medical Technology and Physics provides services in medical and scientific equipment, medical physics, radiation health, project development group, diagnostic services to patients, PET radio pharmaceutical production and teaching in medical physics and electrical safety. Following the recent upgrading of our Quality Management System from ISO9001:1994 to ISO9001:2000 a number of improvements have been incorporated into the department's management practices. Over the past two years the department has also taken on additional functions with the production of radiopharmaceutical products for the WA PET Centre and the manufacture of facial moulds from scanned images on a CNC milling machine for the Radiation Oncology Department. These two major changes to our work practices have been moulded seamlessly into our management system.

METHODS: A decision was made to operate the entire department under one quality management system, and therefore all of the department's functions are incorporated in one ISO9001:2000 'Scope of Certification'. This abstract examines the benefits derived from focusing on Customer Satisfaction and Client Feedback for all groups within the department, continuously reviewing our Key Performance Indicators (KPIs), and addressing issues identified in Service Improvement Forms (SIFs). The resulting information forms the basis of our management review meetings, which have identified and put in place many improvement opportunities, which have then been embraced and the outcomes of which have been subsequently measured, analysed, documented and fed back into the system. We believe that five years operating under ISO accreditation has caused us to greatly improve our collective management skills. One of the important lessons learnt is how to use KPIs to provide us with a clear view of our performance, provide us with incentives to improve and to provide a platform from which to make decisions that will produce positive outcomes for the benefit of the hospital. The most important feature is not just the collection of statistical information, but rather the examination of what is being collected, analysis of any distorting factors, and the use of the information to constantly monitor the results of our strategies in order to inform us whether or not those strategies require modification. Each group in the department must conduct regular management review meetings to evaluate its services, processes and performance. The KPIs are derived from the Medical Technology & Physics Maintenance Management System (MMS), Client Feedback reports and the Quality Management System. The department has a number of in-house programs to manage the different facilities within the department. This includes the management of all equipment for which we are responsible, including an asset register, work order system, quality assurance program, compliance testing, customer satisfaction, clinical services, purchasing, budgeting and accounting.

RESULTS AND DISCUSSION: We have identified 25 key performance indicators for the analysis of our management practices. Some examples are:

- Correlation between equipment maintained, work orders and staff resources.
- Items overdue for Quality Assurance are reported and discussed at regular departmental meetings. Introduction of the use of this KPI has greatly improved our performance in this area.
- Resolution of issues identified by Service Improvement Forms is now done in a more timely manner, owing to the routine analysis of the related KPIs.
- The analysis of customer feedback in the project development group has heightened the awareness of staff in relation to meeting deadlines and keeping customers informed of progress, resulting in a demonstrably improved service to our customers.
- The monthly reports from the MMS has enabled us to examine the relationships between work groups and the differences in the nature of the different tasks undertaken within the group.
- The measurement and analysis of the average 'Turn-a round time' and 'Mean time between failures' for individual items of equipment for maintenance work has been useful in identifying equipment that is particularly problematic, and that may need special attention, including replacement.

It is not always possible to improve the trend of our key performance indicators for reasons outside our control, but their measurement and analysis has allowed us to improve the efficiency and quality of our services, and to document those improvements.

AN IMAGING APPLICATION FOR CELL BIOLOGY RESEARCH

P. Hunt[1], R. Bromely[1], R. Harvie[2] and R. Davey[2]

[1]*The Northern Sydney Cancer Centre, The Royal North Shore Hospital, Sydney, NSW, Australia*
[2]*The Bill Walsh Cancer Research Laboratories, The Royal North Shore Hospital, Sydney, NSW, Australia*

INTRODUCTION: Image segmentation is commonly used to provide cell statistics for cell biology research. While there are commercial packages that perform general segmentation tasks, specific image analysis often requires an ad-hoc amalgamation of image processing procedures to accomplish the given task. Ideally the development of specific image processing applications would be done with a suitable image-processing interpreter (MATLAB). In the absence of such a tool we have found the C# programming language operating in the Visual Studio (Microsoft TM) environment as an acceptable alternative for developing research software. This paper summarizes an image processing application for measuring cell growth and cell migration in a classical wound recovery experiment. A "wound" is produced in a plate of cultured attached cells by scraping off a narrow strip of cells and the rate at which the cells re-populate this narrow strip (wound) is measured.
METHODS: A program (CellLab) was developed using the C# programming language, using the integrated development environment (IDE) Visual Studio (Microsoft TM). CellLab includes a number of small libraries to handle the essential image processing and visual display tasks. The wound region is segmented semi-automatically, requiring a minimum of interaction. This identifies a region of interest within which the re-growth of cells can be tracked over a given time period. The ROI is used as a mask within which to automatically detect cells in subsequent image frames.
RESULTS: The success rate of cell identification is approximately 95%, depending upon image quality and cell density. Examples are given in the text, and below

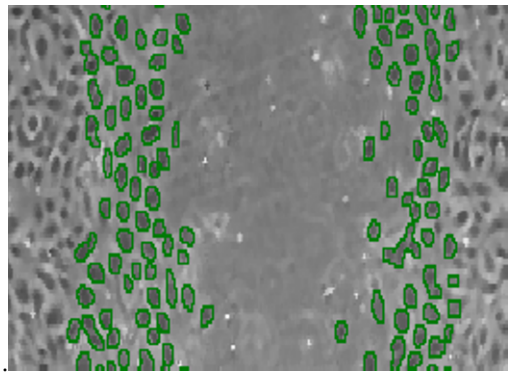

Figure 1. *A portion of a wound in which there is cell re-growth. White regions are dead cells. Some cell fusion can be seen.*

DISCUSSION & CONCLUSIONS: CellLab has been found to be a feasible solution for non-destructive monitoring of cell populations, as in wound recovery experiments. The counting accuracy depends upon the cell density within the wound region, thereby limiting the follow-up investigation time.

DICHOTOMOUS ASTHMATIC RESPONSES IN SHEEP CHALLENGED WITH HOUSE DUST MITE

E. Koumoundouros[1,2], R. Bischof[2], I.M.Y. Mareels[1] and K. Snibson[2]

[1]*Department of Electrical and Electronic Engineering, The University of Melbourne, Melbourne, Vic, Australia*
[2]*Centre for Animal Biotechnology (CAB), The University of Melbourne, Melbourne, Vic, Australia*

INTRODUCTION: House dust mite (HDM) is a common allergen that triggers allergic bronchoconstriction in the airways of asthmatics. The onset of bronchoconstriction can be monitored by measuring airway resistance (R_{aw}). We have developed a sheep model for chronic asthma based on repeated exposure to HDM. We now present data showing dichotomous physiological responses to HDM in this model.
METHODS: The sheep were sensitised to HDM and analysed for levels of HDM-specific IgE, an antibody indicator of allergy. Six allergic sheep (i.e. high levels of serum IgE) were selected for weekly challenges of either HDM (challenged group, n=4) or Saline (control group, n=2) to mimic the pathophysiological conditions of chronic asthma. During aerosol challenges the HDM or Saline was administered via a jet nebulizer connected to a BEAR 2 ventilator which mechanically ventilated the sheep for the duration of the challenge. A LabView based system was developed to monitor the lung mechanics using lumped sum modelling. Respiratory Rate (RR), Tidal Volume (TV), Inertance (I), Compliance (C) and R_{aw} were determined per breath.

RESULTS: The mean peak resistance reached by the responding sheep during the early phase response (EPR) was 7.8 ± 0.4 cmH2O/l/s (mean ± SD) with RR of 45 ± 5 BPM, TV of 0.23 ± 0.02 l, I of 0.08 ± 0.01 cmH2O/l/s^2, and C of 0.34 ± 0.25 l/cmH2O for #4 and #6 collectively. The EPR occurs within one hour of the HDM challenge. Sheep #4 was the only sheep which displayed a late phase response (i.e. an increase in resistance 5-8 hours after challenge) The non-responding sheep recorded significantly lower values and developed no early or late phases responses.

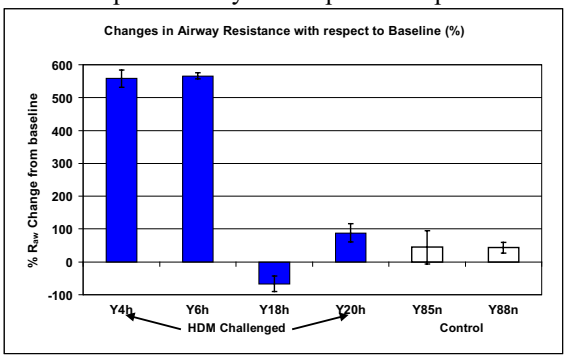

Figure 1. *Maximum R_{aw} changes during the first hour after a single HDM or saline aerosol challenge. The results reflect percentage change from baseline prechallenge resistance. This experiment was performed on sheep repeatedly challenged for 11 weeks.(mean ± SD of 5 consistent and consecutive breaths)*

DISCUSSION & CONCLUSIONS: Fig. 1 shows that R_{aw} increases markedly in sheep #4 and #6 after a single HDM challenge. In contrast, Sheep #18 and #20 do not show significant increases in resistance after a HDM challenge, and have responses similar to saline challenged (control) sheep. The results are interesting in that they suggest that allergic sheep have variable physiological responses to HDM. This variability is consistent with the varying physiological responses observed in mild and severe asthmatics. The sheep asthma model is thus well suited for the study of the underlying mechanisms involved in the severity of asthma.

EVOLUTION OF CEREBRAL BIOELECTRICAL RESISTANCE AT VARIOUS FREQUENCIES DURING HYPOXIA IN FETAL SHEEP

F. Seoane[1,2], K. Lindecrantz[1], T. Olsson[2], I. Kjellmer[3] and C. Mallard[4]

[1]*School of Engineering, University College of Borås, Borås, Sweden*
[2]*Department of Signal and Systems, Chalmers University of Technology, Gothenburg, Sweden*
[3]*Department of Paediatrics, Göteborg University, Gothenburg, Sweden*
[4]*Department of Physiology and Pharmacology, Göteborg University, Gothenburg, Sweden*

INTRODUCTION: Perinatal asphyxia is a significant cause of mortality, neuro-developmental disability and long-term neurological morbidity in term newborn infants. Neural rescue therapies have been tested in animal with satisfactory results [1] and clinical trials on human population are in progress. A quick and reliable detection of the hypoxia would allow an earlier initiation of the rescue therapy. Cerebral electrical bioimpedance can detect cytotoxic oedema caused by hypoxic cell swelling [2].

METHODS: A group (n = 4) of foetal sheep at 93-96 days of gestation was subjected to 25 minutes of induced hypoxia by occlusion of the umbilical cord with a vascular occluder. Through surgically implanted electrodes, brain electrical bioimpedance (only the real part, the resistance, not the reactance) was measured at 30 kHz and 200 kHz using a 4-electrode method custom-made impedance meter.

RESULTS: In fig. 1 we can see the changes in the bioelectrical resistance of the brain measured at two different frequencies during induced hypoxia. Initially there is a stabile baseline. At onset of hypoxia there is a period of latency, followed by a phase of increasing resistance at both frequencies. Resistance keeps increasing throughout the hypoxic period and even a while after reoxygenation. Resistance measured at 30 kHz shows quicker and more noticeable changes than measured at 200 kHz, see table 1.

kHz	Mean latency before noticeable changes (mm:ss)	Mean time to 10% over baseline (mm:ss)	Mean peak (%)
30	07:47	16:37	35
200	08:38	17:51	30

Table 1. *Mean values of the evolution of brain electrical resistance in foetal sheep during induced hypoxia at 30 kHz and 200 kHz.*

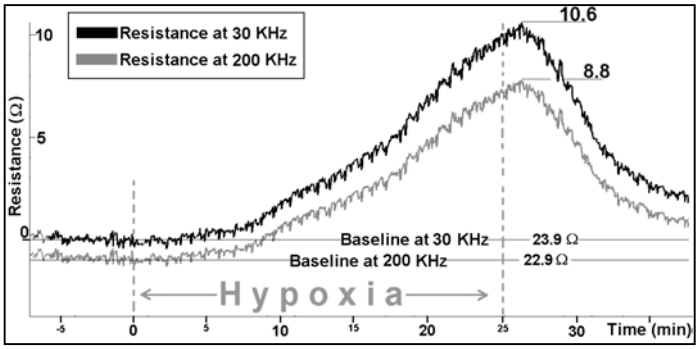

Figure 1. *Evolution of transencephalic electrical resistance in a foetal sheep during induced hypoxia, at 30 kHz and 200 kHz.*

DISCUSSION & CONCLUSIONS: Resistance measured at 30 kHz starts to increase earlier and increases more, proportionally and in absolute terms, than resistance measured at 200 kHz. These observations confirm that measurements at low frequencies are a better indicator of cell swelling, in time and magnitude, than measurements at higher frequencies.
Although bioelectrical resistance indicates fairly well the evolution of cell swelling, the results show that measurements of resistance at a single-frequency have certain limitations in early detection of hypoxia. For this purpose multi-frequency measurements of complex bioimpedance, resistance and reactance, may be a quicker and better indicator [3].

REFERENCES:

[1]Gunn, A. J. *et al*, *Pediatrics ,* 102(5): 1098-106. 1998.
[2]Williams, C. E., Gunn, A., Gluckman, P.D. *Stroke*, 22(4): 516-21, 1991.
[3]Seoane, F., Lindecrantz, K., Olsson, T., Kjellmer, I., *XII ICEBI Conference Proceedings,* 1: 73-76, 2004.

DETERMINATION OF PARAMETERS OF SYSTEMIC ARTERIAL TREE OF HUMAN BODY

M. Jelinek[1, 2], J. Dobes[1], L. Pousek[2] and K. Hana[2]

[1]*Department of Radio Electronics, Faculty of Electrical Engineering, Czech Technical University in Prague , Prague, Czech Republic*
[2]*Institute of Biomedical Engineering, Czech Technical University in Prague, Prague, Czech Republic*

INTRODUCTION: Nowadays a risk of a cardiovascular system disorder is increasingly frequent, as is generally known. This is reason why a simple method of an estimation of the selected parts of arterial system condition is developed. A main goal of this work is to provide a simple and cheap way to make early interception of some problems in selected parts of a systemic arterial circulation, utilizable namely by general practitioners.

METHODS: Whole experiment can be divided to the three separated parts as shown in Fig. 1. At first, phonocardiographic (PCG) signals supplemented by a three lead electrocardiography (ECG) were recorded. Two electronic phonendoscopes were used as PCG signal transducers. The PCG signals were taken at three locations (heart, left and right carotid artery, as shown in Fig. 1). A pair of PCG signals was recorded simultaneously (heart – left carotid a., heart – right carotid a.). After a signal processing and analysing, the PCG signals were used as input data of an arterial wave model of examinant parts of the systemic circulation. The wave model of systemic arterial circulation is based on Windkessel linear model at this time. A time-domain identification method is applied to identify the model parameters (e.g. arterial compliance).

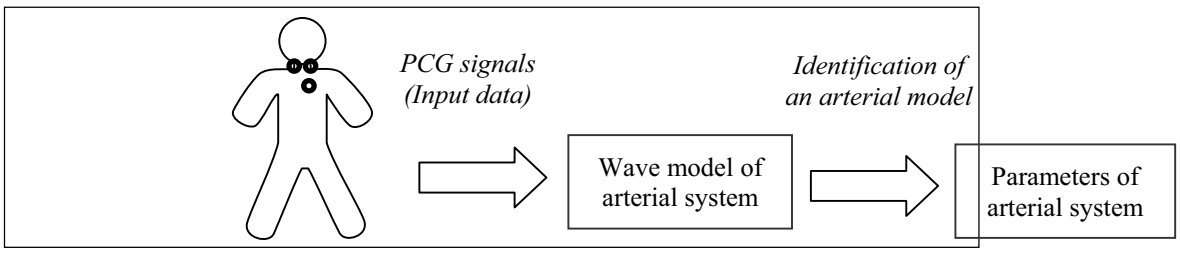

Figure 1. *Diagram of experimental setup.*

The input data were obtained in clinical experiments in conjunction with general practitioner. In the measurements a mobile autonomous device was used, developed specially for this purpose.

DISCUSSION & CONCLUSIONS: This method of the arterial system condition detection does not provide detailed view to each and every segments of human arterial system. The method is dedicated to make an overview of the systemic arterial circulation and its selected parts especially. Signals are measured using common medical instrumentation, i.e., electronic

phonendoscopes and PC with digital data processing equipment. This could provide an easy and relatively cheap tool to find out main features of arterial tree.

ACKNOWLEDGEMENTS: This work was supported by the Czech Grant Agency under grant No. 102/03/H086, by the grant No. 10/83086/13137 of the Czech Technical University in Prague, and by the research program MSM 210000012.

REFERENCES:

[1]Jelinek, M., Dobes, J., Pousek, L., Hana, K., *Using a Phonocardiography in a Pulse Wave Velocity Measurement*, In: ISSPIT 2003 [CD-ROM], p. 5/TP3, 2003.
[2]Stergiopulos, N., Young, D.F., Rogge, T.R., *Computer Simulation of Arterial Flow with Applications to Arterial and Aortic Stenoses*, Journal of Biomechanics, 25: 1477-88, 1992.
[3]Geipel, P. S. and Li, J.K.J. *Time and Frequency Domain identification of Arterial System Model Parameters*, In: 16th NE Bioeng. Conf., 75-76, 1990.
[4]Li, J. K. J., *Arterial Circulation – Physical Principles and Clinical Applications*, Humana Press, New Jersey, 2000.

USING PULSE TRANSIT TIME TO ESTIMATE CHANGES IN INSPIRATORY EFFORTS IN CHILDREN

J. Y. A. Foo[1], S. J. Wilson[1], G. Williams[2], S. Burgess[2], M. Harris[2] and D. Cooper[2]

[1]*School of ITEE, University of Queensland, Brisbane, Qld, Australia*
[2]*Dept. of Respiratory & Sleep Medicine, Mater Children's Hospital, South Brisbane, Qld, Australia*

INTRODUCTION: Current practice recommends that oesophageal pressuring (Pes) monitoring as the best measure of respiratory efforts. However, this technique is an invasive procedure that subjects may find intolerable, especially for children[1]. Moreover, studies have suggested that Pes monitoring may alter normal respiratory patterns and sleep architectures. A cardiorespiratory measure known as pulse transit time (PTT) has been proposed as it shows promises to be practical and efficient for such purposes in adults[2]. Studies have validated the use of vascular resistance change observed in response to externally applied inspiratory resistive loading (IRL) to estimate changes in respiratory efforts[3].

METHODS: A standard handheld paediatric flexible silicon nasal and oral facemask is used. The valve port is fitted with a customised adaptor with two valved airflow openings are used in this study. On the inspiratory arm, one of three different IRL's can be inserted at any time. While the other acts as the expiratory end, a unidirectional valve is fitted to ensure that inspiration cannot occur there. A differential piezoresistive pressure transducer is used to measure changes in air pressure within the facemask via an outlet during the respiration cycle.

RESULTS: PTT measurements are evaluated with four different inspiratory load setting. With no load, PTT is measured at a mean and standard deviation (SD) of 222.1±7.5 ms, the 6.9 $cmH_2O/L/s$ load measured 223.2±8.6 ms, the 26.7 $cmH_2O/L/s$ load measured 227.8±10.7 ms and the 36.1 $cmH_2O/L/s$ load measured 233.3±13.2 ms.

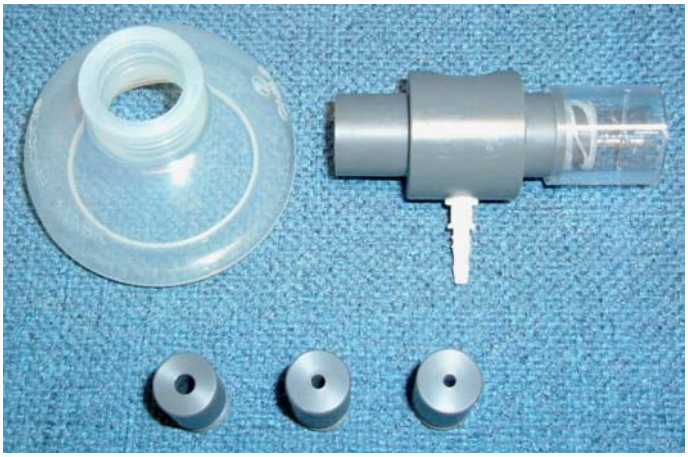

Figure 1. *Adopted facemask, customised adaptor and three different IRL*

DISCUSSION & CONCLUSIONS: PTT technique can be a suitable candidature for such measure and is able to estimate the changes in respiratory efforts of children. By observing the magnitude of mean PTT and variations, the amount of inspiratory resistance experienced during breathing can be deduced. Even though PTT measure is only semi-quantitative, this is more tolerable for children and has shown its sensitivity to changes in respiratory efforts. This technique may also be useful to monitor obstructive sleep apnoeic events in children. The use of this simple yet reliable technique can be extended beyond medical institutions and may land itself in screening studies in the future.

REFERENCES:

[1]Chervin, R. D. and Aldrich, M. S., *Am J Respir Crit Care Med*, 156:881-885, 1997.
[2]Pitson, D. J., Sandell, A., van den Hout, R. and Stradling J. R., *Eur Respir J*, 8: 1669-1674, 1995.
[3]Marcus, C. L., Moreira, G. A., Bamford, O. and Lutz, J., *J Appl Physiol*, 87:1448-1454, 1999.

MOTION ARTEFACT REDUCTION OF THE PHOTOPLETHYSMOGRAPHIC SIGNAL IN PULSE TRANSIT TIME MEASUREMENT

J. Y. A. Foo[1], S. J. Wilson[1], G. Williams[2], M. Harris[2] and D. Cooper[2]

[1]*School of ITEE, University of Queensland, Brisbane, Qld, Australia*
[2]*Dept. of Respiratory & Sleep Medicine, Mater Children's Hospital, South Brisbane, Qld, Australia*

INTRODUCTION: Motion artefact can be a common occurrence that contaminates non-invasive physiological measurements. To extract interested timing information from signals during artefact is challenging. Photoplethysmographic (PPG) signal is very sensitive to such artifacts and can be used in applications like, pulse transit time (PTT) as part of polysomnographic studies[1]. However, most present commercial efforts are focused on artefact reduction in the measurement of oxygen saturation.
METHODS: A correlation cancellation and signal processing solution is implemented with the adaptive cancelling filter concept[2] and a triaxial accelerometry. PPG signals obtained from a Masimo pulse oximeter is used as a reference to compare with the reconstructed PPG signals. The latter is obtained from a custom-made system with no signal processing capability. Different hands are used for each PPG source, one stationary while the other involves in unregulated movements. A second Masimo pulse oximeter is used to illustrate the intensity of timing errors the artifacts have on commercial PPG signals.
RESULTS: A total of 108 PTT readings are recorded in three different unregulated movements. Reference PPG shows a mean with standard deviation of 253.4±21.4 ms, commercial Masimo registers 174.6±104.9 ms, custom-made system records 189.4±68.8 ms and the filtered displays 254.3±14.1 ms.

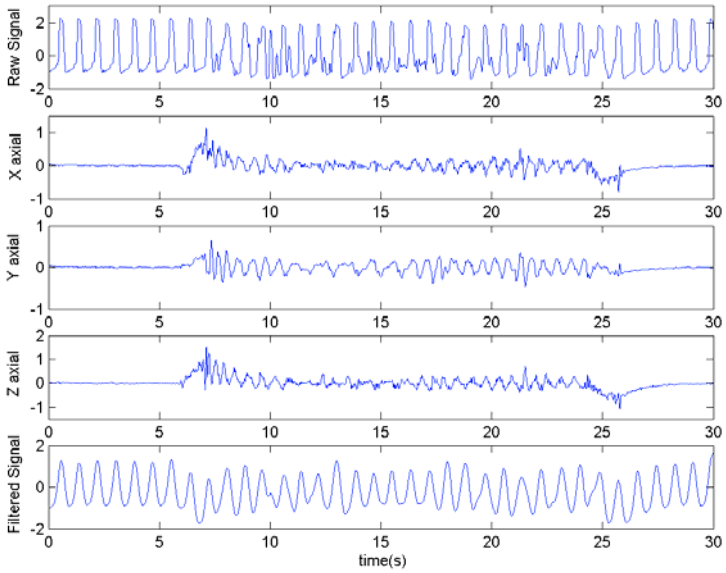

Figure 1. *Reconstructed PPG signals with their raw and artefact inputs.*

DISCUSSION & CONCLUSIONS: Triaxial accelerometry implemented on or near a PPG probe site can be a valid tool for detecting timing errors caused by motion artifacts. Detection of such errors may be useful in its PTT application when periods with artifacts are required for further analysis. The suggested adaptive cancelling filter model can then reconstruct these PPG signals and may be time shifted slightly. Further studies on more advanced adaptive filter algorithms can be examined to provide better motion artifacts detection and reduction in timing characteristics of PPG signals in respiratory sleep studies.
REFERENCES:
[1]Smith, R. P., Argod, J., Pepin, J. L. and Levy, P.A., *Thorax*, 54: 452-458, 1999.
[2]Haykin, S., *Adaptive Filter Theory*, Prentice-Hall Inc., New Jersey, USA, 1991.

TIMING VARIATIONS IN PHOTOPLETHYSMOGRAPHIC SIGNALS FROM DIFFERENT PULSE OXIMETERS

J. Y. A. Foo[1], S. J. Wilson[1], G. Williams[2], M. Harris[2] and D. Cooper[2]

[1]*School of ITEE, University of Queensland, Brisbane, Qld, Australia*
[2]*Dept. of Respiratory & Sleep Medicine, Mater Children's Hospital, South Brisbane, Qld, Australia*

INTRODUCTION: Since its introduction, pulse oximetry has become a conventional clinical measurement. Besides its primary role as a measure of arterial blood oxygen saturation (SpO_2) [1], pulse oximeters can be used for other

cardiovascular measurements. These include heart rate (HR) and pulse transit time (PTT) estimations, both using the photoplethysmographic (PPG) signal derived from the oximeter. The temporal coherence of the PPG signals and thereby PTT estimates are heavily dependent on minimal phase variability. Three different signal sources were investigated for relative phase variation.

METHODS: A Masimo SET® Rad-9™ oximeter, Novametrix Oxypleth oximeter and a custom designed, analogue filter based PPG system were selected. PPG timing characteristics obtained from the three devices were assessed during a static test with probes applied to the 2nd, 3rd and 4th fingers of the dominant hand resting on a table for 60 seconds. Concurrently, a single lead electrocardiograph (ECG) was recorded and R-R intervals calculated for each beat.

RESULTS: The PPG signals obtained from the three systems were evaluated by comparing their respective beat-to-beat intervals with the R-R estimates from the ECG. The results show that the Masimo device introduces timing variations in the PPG output. For relative beat-to-beat comparison, Novametrix system achieved 100±0.87% ($p<0.05$), custom device 99.99±2.05% ($p>0.05$) and Masimo device 100.06±5.63% ($p>0.05$). In PTT estimate comparison, Masimo and Novametrix system differed by -7.2±48.5%, Masimo and custom system -19.8±49.6% while Novametrix and customised system varied by 11.2±5.2%.

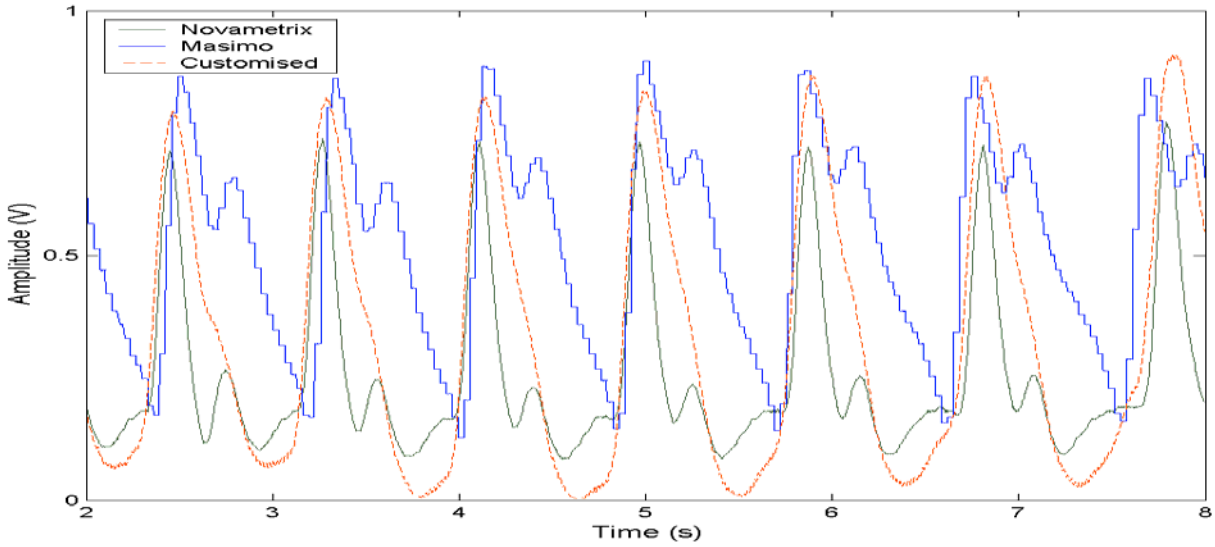

Figure 1. *PPG signals from three different sources show phase variability.*

DISCUSSION & CONCLUSIONS: Recent advanced signal processing approach has shown promising results pertaining to the accuracy and noise immunity of the SpO_2 measure. However, one consequence may be the variability introduced into the phase characteristics of the PPG signal. Clinical interpretation of measures other than SpO_2, such as PTT and HR variability may be compromised by these findings. Further studies at varying HR and PPG signal quality are indicated by this result.

REFERENCES:

[1]van Oostrom, J. H. and Melker, R. J. *Anesthesia and Analgesia*, 98:1354-1358, 2004.

USE OF PULSE TRANSIT TIME TO DIFFERENTIATE CENTRAL FROM OBSTRUCTIVE RESPIRATORY EVENTS IN SLEEPING INFANTS

J. Y. A. Foo[1], S. J. Wilson[1], G. Williams[2], M. Harris[2] and D. Cooper[2]

[1]*School of ITEE, University of Queensland, Brisbane, Qld, Australia*
[2]*Dept. of Respiratory & Sleep Medicine, Mater Children's Hospital, South Brisbane, Qld, Australia*

INTRODUCTION: There is a current need for a non-invasive alternative to oesophageal pressure measure to monitor sleep disordered breathing, including for infants. Pulse transit time (PTT) shows potential to estimate breathing efforts in response to upper airway obstruction that can cause transient blood pressure (BP) changes. The principle determinant of PTT is the change in compliance of the arterial wall [1]. The objectives of this study were to assess the capability of PTT to differentiate central from obstructive sleeping respiratory events.

METHODS: To investigate the use of PTT, overnight sleep studies were conducted in parallel with conventional polysomnography (PSG). The subjects were 4 infants (3 male and 1 female) mean age of 7.8 months (ranged 5-9 months). The fundamental detection of apnoea and hypopnoea was based upon respiratory inductance plethysmography and oronasal

airflow measure. From these parameters, respiratory events were categorised as being obstructive or central in nature by blinded observers. Institutional ethical approval and informed consent were obtained for these studies.

RESULTS: 58 respiratory events free from motion artifacts occurred in the 4 selected routine overnight PSG studies. PTT measurements were then evaluated against the corresponding PSG scorings. Tidal breathing varied with standard deviation (SD) of 5.13ms and maximal decrease of 3.57% from baseline. Obstructive events showed a mean change of 4.95% ($p<0.05$), with 13.10ms SD ($p<0.05$) and maximal decrease of 14.92% ($p<0.05$) from tidal breathing. Central events showed a mean 1.72% ($p<0.05$) change, with 2.47ms SD ($p<0.05$) and maximal decrease of 2.90% ($p<0.05$) in PTT value. 0

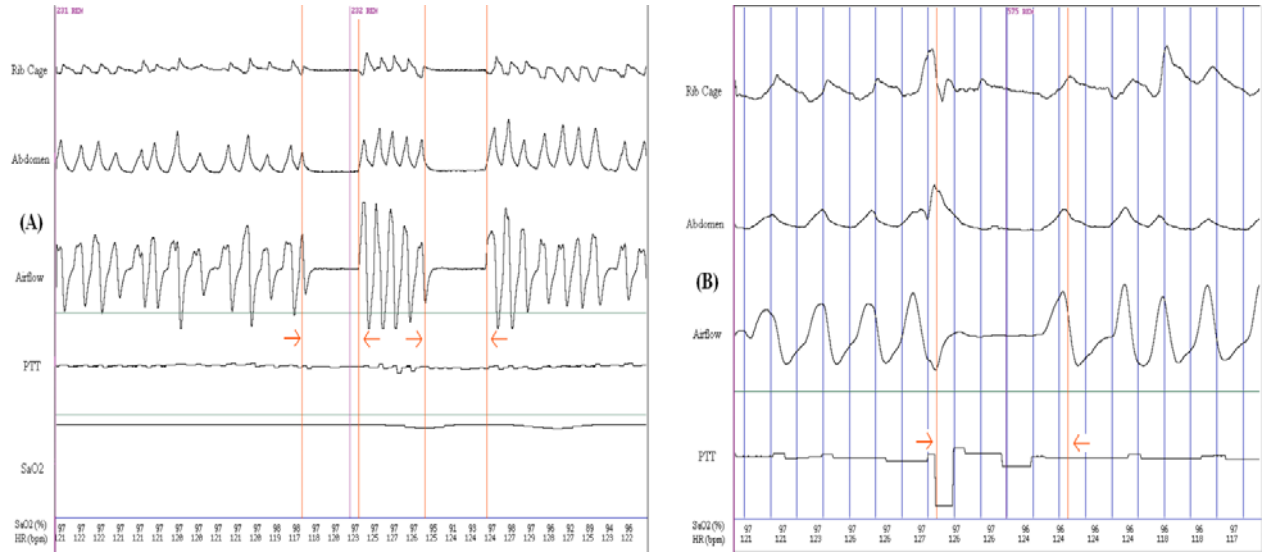

Figure 1. *(A) Central apnoeas and (B) obstructive apnoea in a 9-month-old male.*

DISCUSSION & CONCLUSIONS: PTT was able to categorise central and obstructive respiratory events. Furthermore, PTT has showed its sensitivity to monitor marginal BP fluctuations during tidal breathing. Hence, PTT shows promises to differentiate respiratory events accordingly and can be an important tool for sleep disordered breathing in infants. Further investigation will be required to validate the preliminary results obtained in this study.

REFERENCES:

[1]Katz, E. S., Lutz, J., Black, C. and Marcus, C. L., *Pediatric Research*, 53:580-588, 2003.

PULSE TRANSIT TIME TO MONITOR CHANGES IN PERIPHERAL PULSE TIMING CHARACTERISTICS OF CHILDREN

J. Y. A. Foo[1], S. J. Wilson[1], G. Williams[2], M. Harris[2] and D. Cooper[2]

[1]*School of ITEE, University of Queensland, Brisbane, Qld, Australia*
[2]*Dept. of Respiratory & Sleep Medicine, Mater Children's Hospital, South Brisbane, Qld, Australia*

INTRODUCTION: Besides being a non-invasive measure of arterial compliance, pulse transit time (PTT) can be a non-invasive indicator of instantaneous blood pressure (BP) changes. PTT is the time difference between the origin of a pulse wave in the left ventricle to the detection at a periphery, usually a finger or toe for children [1]. Two common postures used in such studies are sitting (SIT) and supine (SUP). However, the relationship between PTT and these postures in children has yet to be investigated. The objective of this study was to evaluate the relative differences in PTT between the recording postures and sites in normal children.

METHODS: This was a prospective study that included 11 children (9 male and 2 female) mean age of 6.5 years (ranged 5-8 years). All subjects were asked to rest for 5 minutes prior to any measurements. Photoplethysmography (PPG) was first measured on an index finger and then on a toe. The PPG recordings were measured in conjunction with electrocardiogram (ECG) signals. A minimum of 30 pulses free from motion artifacts was obtained from each examination. After these examinations, the subject was placed in the SUP posture on a bed and rest for 1 minute. Similarly, at least 30 motion artifacts-free PTT readings were then recorded with the same finger and toe as the previous examinations.

RESULTS: SIT posture showed a mean relative difference of 23.9±3.6% ($p<0.01$) between the two peripheral sites while SUP posture was 44.0±3.4% ($p<0.01$) of PTT change. The principal contributor to the discrepancy was the lower limb (LL) where PTT variation was 14.6±2.4% ($p<0.01$) between the two postures. Upper limb (UL) showed insignificant difference of -1.5±1.0% ($p>0.05$).

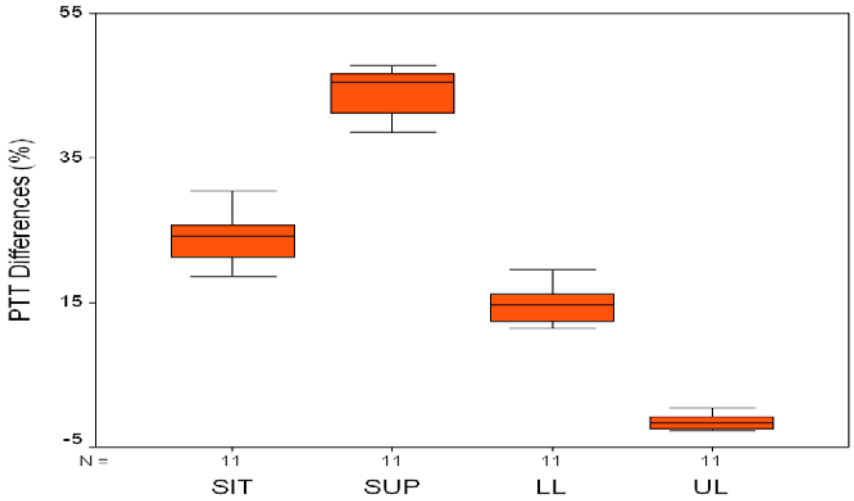

Figure 1. *Boxplot of postural and peripheral differences in finger and toe PTT.*

DISCUSSION & CONCLUSIONS: The present study was conducted to corroborate evidence that PTT has the capability to correlate with cardiovascular responses due to postural and peripheral changes. Postural change caused a distinctive PTT differences in children at the LL only due to the hydrostatic pressure changes at these peripheries. Hence, PTT measure can be useful for continuous non-invasive BP monitoring in children.

REFERENCES:

[1]Foo, J. Y. A, Wilson, S. J., Williams, G., Harris, M. and Cooper, D., *Internal Medicine Journal,* 34:A27, 2004.

THE FIRST SYNCHROTRON IMAGES OF TAMAR WALLABY LUNGS

I. Williams[1], R. Lewis[1], J. Whitley[2], et al.

[1]*School of Physics and Materials Engineering, Monash University Clayton,, Vic, Australia*
[2]*Department of Primary Industries, Molecular Genetics, Attwood, Vic, Australia*

INTRODUCTION: The resuscitation, ventilation and transition to extra-uterine life of infants that are born preterm is complicated by the failure of the lungs to clear liquid from the airways. The tammar wallaby (Marcopus eugenii) can be used as a model to elucidate lung development in eutherian mammals (animals which nourish their young through a placenta) including humans. We have applied high resolution x-ray refraction enhanced imaging (REI) for imaging aerated neonatal wallaby lung. This, the first attempt to image neonatal wallaby lung using REI, tested the technique and the sample preparation method to investigate the fluid clearance and lung aeration of newborn animals.

METHODS: Conventional radiographic imaging exploits differences in the attenuation of adjacent media to distinguish between them. REI in contrast exploits the differences in refractive index.

We have imaged neonatal wallabies using REI conditions on the BL20XU beamline at 17.1 keV at the SPring-8 Synchrotron in Japan. The images were obtained with a CCD camera with a pixel size of 3.14 μm^2.

RESULTS: Wallabies with ages ranging from 2 to 28 days were imaged. A number of high resolution images were obtained which proved that the technique could be used to investigate lung clearance. The images are to be correlated with existing and ongoing studies employing electron microscopy, gas-exchange analysis and high throughput gene expression analysis.

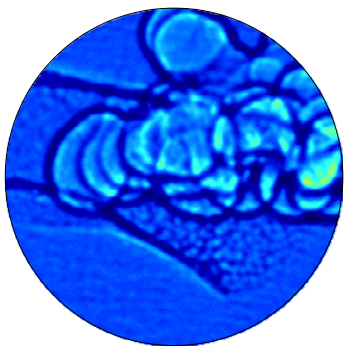

Figure 1. *The edge of the lung detailing individual air sacs. The image sample is 1mm across. The rounded nature of the sacs is apparent and the overlapping air sacs increases the complexity of the image.*

DISCUSSION & CONCLUSIONS: The experiment at SPring-8 was designed to determine whether REI could image the structure of the lung and its formation and development in neonatal wallabies.

- This experiment produced the first REI wallaby lung images.
- The analysis of all the data obtained during the experiment is ongoing.
- We aim to calculate the change in lung volume of the neonatal wallaby.

Further experiments are planned to image animals minutes to hours old. These very young animals will give the best information applicable to the survival of newborn human babies and the mechanisms for fluid clearance of the lungs.

ACKNOWLEDGEMENTS: The work described here was performed with grants from The State of Victoria Department of Innovation, Industry and Regional Development and the Access to Major Research Facilities program of Australian Nuclear Science and Technology Organisation.

PERFORMANCE EVALUATION OF FLAT PANEL DETECTOR IN X-RAY FLUOROSCOPY

R. K. Grewal and I. D. Mclean

Medical Physics Department, Westmead Hospital, Westmead, NSW, Australia

INTRODUCTION: Flat panel detectors are currently replacing the conventional image intensifiers in R-F imaging. We evaluated the performance of a biplane cardiac imaging system (Siemens Axiom Artis dBC), the image acquisition was based on a 25 cm diagonal digital flat panel detector. Performance characteristics included image quality, typical patient entrance dose and measurement of input to the surface of flat detector. The results were compared with conventional image intensifier systems (Siemens Hicor Unit and Toshiba DPF 2000 A Biplane Unit) used in cardiac imaging at Westmead.

METHOD: Image quality and dose measurements were performed following standard protocols[1] using Westmead test object[2] and 20 cm solid water as absorber in the beam. For measurement of input to the surface of flat detector, 2 mm copper was placed on the collimator. Radcal 3cc and 180 cc ion chambers were used for dose measurements.

RESULTS: *Image quality*: Our measurements on flat panel system indicate that high contrast resolution and threshold contrast is not affected by changing field size. This is expected due to minimum loss of signal in the imaging chain of digital systems and the independence of detector pixel size with change in field of view.

While low contrast resolution was found to be similar to conventional systems, high contrast resolution was significantly superior using flat detector system for large and intermediate field of view (25-28 lp/cm against 18-20).

Typical patient dose as measured using flat detector system was similar to the conventional Toshiba pulsed fluoroscopy system(~ 3 – 8 mGy/min depending on the field size). This was 40-50 % lower than our old Siemens hicore unit.

Input to the surface of flat detector was found to vary with field size as is the case with a conventional II system. As described elsewhere[3], although there is no necessity to increase exposure or video gain in a digital magnification, digital data interpolation process introduces noise. As a result system increases the input dose during magnification to maintain image quality in much the same way as in a conventional fluoro system.

DISCUSSION AND CONCLUSIONS: Flat panel detectors in x-ray fluoroscopy systems can provide similar or better images than achievable with conventional II's. There is no obvious distortion, typical patient dose is low and image quality is good.

REFERENCES:

[1]NSW EPA 2004, *EPA Radiation Guideline 6: Registration requirements & industry best practice for ionising radiation apparatus used in diagnostic imaging - Testing Protocols*, 2004.

[2]Ricciardello, M. and Mclean, D., *Aust. Phy. and Eng. Sci. in Med.* 18(2): 104-112, 1995.

[3]Srinivas, Y. and Wilson, D. L., *Med. Phys.* 29(7): 1611-23, 2002.

DEVELOPMENT OF CYCLOTRON SOLID TARGETRY

J. D'Souza, T. Deans, D. Cryer and R. Price

Department of Medical Technology & Physics, Sir Charles Gairdner Hospital, Perth, WA, Australia

INTRODUCTION: Western Australia's first medical cyclotron was recently installed in the Department of Medical Technology & Physics at Sir Charles Gairdner Hospital. The cyclotron is routinely used for ^{18}F production using a liquid target, and now research is being undertaken into solid target bombardment for production of novel isotopes such as ^{124}I, ^{64}Cu & ^{96}Tc. The IBA Cyclone 18/9 has a maximum proton beam energy of 18MeV and maximum beam current of 80μA. A proton beam is generated by the acceleration of H- ions in the evacuated cyclotron (10^{-6}bar) which are then stripped of 2 electrons just prior to exiting a target port. Each port has two strippers which are made of 10μm thick carbon with dimensions 12mmx13mm. Due to their thinness, the strippers are easily ruptured. The Cyclone 18/9 has 8 target ports. In order to fit a target onto the cyclotron when the cyclotron is already evacuated the target is first evacuated to 10^{-3}bar by a roughing pump before an isolation valve at the port is opened. This stops any damage that may occur by the flow of air from

the target reservoir to the cyclotron eg to the strippers. The first step in the project to develop solid targetry is to build a beam line in order to measure the beam profile. If successful, this design will be improved in order to have a beam line and target holder that are suitable for use in solid target bombardment.
METHODS: A 40cm beam line with an internal diameter of 3.6cm was built to fit onto the IBA Cyclone 18/9. The beam line, made out of aluminium, incorporates a step 5cm from the end at which a target material can be fitted. A cover fits onto the beam line, behind the target in order to maintain vacuum. The cover is held in place by the vacuum within the beam line. At the end of bombardment, the beam line can be isolated from the vacuum of the target and normal air pressure restored. In doing so the cover plate falls open and the target falls into a lead pot, ready for removal from the cyclotron bunker. Electrometers were attached to measure beam current obtained on the target and on the beam line. This was to ensure that the ratio of current hitting the target position is optimised compared to the current hitting the beam line. Teflon (mp: 285-295^{o}C) was used in order to electrically isolate the target from the beam line. The cyclotron roughing pump was used to pull the beam line down to 10^{-3} bar. The isolation valve between the beam line and the cyclotron was opened. The cyclotron was run for 10 minutes at a low current
RESULTS & DISCUSSION: During the first trial of the beam line two main problems arose:

- Although the beam line was brought down to 10^{-3} bar prior to the isolation valve being opened, the large volume within the beam line (compared with that in the regularly used liquid targets) contained enough air to cause flow into the cyclotron, sufficient to rupture the strippers.
- The bombardment melted the Teflon insulator.

Due to these faults the design of the beam line was changed. A diffusion pump was fitted to the beam line which evacuated the beam line to 10^{-7}bar. The beam line was fitted onto the cyclotron and the port isolation valve opened. There was no loss of stripper integrity. This design improvement of including the diffusion pump on the beam line was therefore successful. The target body was electrically isolated from the beam line further away from the target and also incorporated water cooling via a water flow system, therefore the temperature of this component will not reach its melting point. The next step is to bombard the target to verify that the new cooling system is successful. Once this bombardment has been conducted successfully, the next step in the project is to irradiate a disc of known substance and get a profile of the beam at the target position by measuring the emissions from the disc using radiographic film.
CONCLUSION: Considerable progress has been achieved in the design of a facility for bombarding solid targets, using the medical cyclotron at Sir Charles Gairdner Hospital.

A STUDY OF REQUESTED CT HEAD EXAMINATIONS AND THEIR POSITIVE YIELD RATE

K. S. Coakley

Biomedical Technology Services, Queensland, Australia

INTRODUCTION: Requests for CT examinations are ever increasing, partly due to the excellent clinical information they can provide for patient management and partly due to a perceived need for "evidence" that everything has been done to diagnose a patient correctly. This has led to many CT examinations being done on patients where many of the radiology community does not necessarily feel CT will yield a positive finding, i.e. in their eyes – a possible unjustified use of radiation. To determine whether this was in fact true, or merely a perception, a study was performed by medical imaging and physics staff at the Royal Brisbane Hospital to determine statistics of positive yield for CT head exams.
METHODS: 600 CT head examinations from the Emergency Department at the Royal Brisbane Hospital were retrospectively examined and their findings were tabulated under various clinical categories to determine positive yield statistics. These categories were also tabulated with the radiologists advice as to whether they would have expected a positive finding.
RESULTS: For several categories the positive yield for CT head exams was so low as to be considered negligible. Other categories, although low were still considered significant. These will be presented to the emergency department along with a suggested protocol for requesting CT head exams.
DISCUSSION & CONCLUSIONS: It was unfortunate that this study had to be performed to prove to clinical staff that medical imaging staff members do in general have an excellent idea of what will show up in an x-ray and what will not! However, it was useful to be able to categorise "positive yield" statistics into such specific classes. The next step is to try and communicate these findings to staff to create more trust and better communication between departments.

DOSE MODULATED COMPUTED TOMOGRAPHY AUTOMATED DOSIMETRY

J. Atkinson and M. Bottomley

Sir Charles Gairdner Hospital, Perth, WA, Australia

INTRODUCTION: Computed Tomography (CT) scans contribute a significant portion of the effective radiation dose from medical procedures and generally large effective radiation doses per diagnostic examination [1]. With the advent of

Multislice CT, the potential for large radiation exposures increased. This combined with the appeal of the resultant isotropic imaging and the increasing number of applications for which CT could be utilised (including screening procedures) has further increased the need for vigilant monitoring of CT protocols and use with respect to radiation dose. The introduction of dose modulated Computed Tomography has proven an effective method for reducing patient dose and is now widely used by CT manufacturers [2]. This involves lowering the mA when scanning through anatomical regions which do not require a large mA. Many CT investigations now utilise dose modulation. Some of these studies will include over 900 images for which the mA and occasionally other factors could vary. In order to utilise the existing software to perform CT dosimetry a program has been written to automatically extract scan parameters from CT dicom image files and apply the ImPACT CT Patient Dosimetry Calculator, for slices with differing factors.

METHODS: Matlab has been used to write and compile a program which sorts through a folder of dicom images and extracts the appropriate dicom header information. Some manufacturers store different series and reformatted images all within the same folder. The images of the CT study for which the dosimetry is to be performed must be stored within the one folder and must be in a dicom format. The program has been written to accommodate several manufacturers, which all contain different information in their dicom headers. The Matlab program groups the various study/image types, extracting the relevant dicom header information, which is written to an Excel worksheet. An Excel file uses this information to run the ImPACT CT Patient Dosimetry Calculator with the appropriate factors as they vary with position scanned through the patient. The ImPACT CT Patient Dosimetry Calculator program is called on a minimum number of times to reduce the time required to perform a dosimetry study. The results are presented in a similar format to the ImPACT CT Patient Dosimetry Calculator worksheet to enable comparisons and to assist use.

DISCUSSION & CONCLUSIONS: This automated dose modulated CT dosimetry program has been successfully implemented to perform calculations which would otherwise be too onerous to attempt and has been used in the comparison of patient dose from CT studies submitted as part of a tender evaluation process. It is reliant on the use of the ImPACT CT Patient Dosimetry Calculator, which also utilises Excel. The program requires images to be within a single folder and in dicom format. This program has become an essential tool for performing CT dosimetry, required on scanners capable of dose modulation, in a time effective manner.

REFERENCES:

[1]McNitt-Gray, M. F., *Radiographics*, 22:1541 – 1553, 2002.

[2]H.Greess, H., Wolf, H., Baum, U., Lell, M., Pirkl, M., Kalender, W. and Bautz, W. A., *European Radiology*, 10(2): 391-394, 2000.